Titre: Title:	Evaluating Hydro-Mechanical Properties of Waste Rocks by Considering Scale Effect
Auteur: Author:	Akram Deiminiat
Date:	2022
Type:	Mémoire ou thèse / Dissertation or Thesis
Référence: Citation:	Deiminiat, A. (2022). Evaluating Hydro-Mechanical Properties of Waste Rocks by Considering Scale Effect [Thèse de doctorat, Polytechnique Montréal]. PolyPublie. https://publications.polymtl.ca/10263/

URL de PolyPublie: PolyPublie URL:	https://publications.polymtl.ca/10263/
Directeurs de recherche: Advisors:	Li Li, Robert P. Chapuis, & Thomas Pabst
Programme: Program:	Génie minéral

POLYTECHNIQUE MONTRÉAL

affiliée à l'Université de Montréal

Evaluating hydro-mechanical properties of waste rocks by considering scale effect

AKRAM DEIMINIAT

Département de génies civil, géologique et des mines

Thèse présentée en vue de l'obtention du diplôme de *Philosophiæ Doctor*

Génie minéral

Février 2022

POLYTECHNIQUE MONTRÉAL

affiliée à l'Université de Montréal

Cette thèse intitulée:

Evaluating hydro-mechanical properties of waste rocks by considering scale effect

Présentée par **Akram DEIMINIAT**

en vue de l'obtention du diplôme de *Philosophiæ Doctor*

a été dûment acceptée par le jury d'examen constitué de:

Ahmad SHAKIBAEINIA, président

Li LI, membre et directeur de recherche

Robert CHAPUIS, membre et codirecteur de recherche

Thomas PABST, membre et codirecteur de recherche

Carlos OVALLE, membre

Jonathan AUBERTIN, membre externe

DEDICATION

To my supervisors

To whom seeking knowledge

ACKNOWLEDGEMENTS

I would like to express my appreciation to my supervisor, Prof. Li Li, for his constant support and guidance in all times. His encouragement, advice and patience helped me throughout this process. I appreciate all that I have learned from him, things that are beyond words. I will always be grateful for the opportunity he gave me to begin and end a journey that was full of learning. I appreciate Prof. Robert Chapuis and Prof. Thomas Pabst for advising me during my research work. Prof. Thomas Pabst and Dr. Feitao Zeng are gratefully acknowledged for their valuable comments on my pre-doctoral proposal during the comprehensive examination and article(s).

I am very grateful to Prof. Ahmad Shakibaeinia, Prof. Jonathan Aubertin and Prof. Carlos Ovalle for their time and acceptance as jury members of my Ph.D thesis. Prof. Vincenzo Silvestri is acknowledged for being the representative of directeur d'études supérieures.

I appreciate Prof. Paul Chiasson and Dr. Feitao Zeng for their time, comments and discussion on my article(s) and Dr. Abtin Jahanbakhshzadeh for his time and advices. Samuel Chénier, Eric Turgeon, Noura EI-Harrak and Patrick Berneche are gratefully acknowledged for their kind help in my laboratory work. I appreciate my colleagues specifically Alireza Zafarani, Peiyong Qiu and Yulong Zhai for their presence and their advices.

Sooraya Balgobin is also appreciated for her service, constant presence and kind responses.

The financial support from the Natural Sciences and Engineering Research Council of Canada (NSERC RGPIN-2018-06902), Fonds de recherche du Québec—Nature et Technologies (FRQNT 2017-MI-202860), industrial partners of the Research Institute on Mines and the Environment (RIME UQAT-Polytechnique) is also acknowledged.

Finally, I want to thank and express my appreciation to my family and close friends for their unconditional love and support.

RÉSUMÉ

Les roches stériles extraites des mines sont généralement entreposées en surface sous forme de haldes à roches stériles. Elles sont utilisées de plus en plus comme matériaux de construction pour des constructions sur site ou hors site minier. La détermination de leurs propriétés hydromécaniques est cruciale pour assurer une conception et construction économique et stable des infrastructures faites de roches stériles, qui constitue l'objectif final de cette thèse. Il s'agit cependant d'une tâche difficile car les stériles ont généralement une gradation largement étalée avec des particules aussi petites que des silts et aussi grandes que des blocs en mètres.

La revue de la littérature montre qu'il existe un grand nombre de publications sur la détermination de la résistance au cisaillement des remblais rocheux, mais très peu sur les stériles. La revue de la littérature montre également que la majorité des travaux publiés sur les stériles ont été réalisés en suivant des méthodes d'essai développées en génie civil. Par conséquent, la norme ASTM D3080/D3080M-11 a été largement utilisée dans les essais de cisaillement direct sur des roches stériles alors que la norme ASTM D2434-19 a été largement utilisée pour les essais de perméabilité à charge hydraulique constante. La première stipule que le ratio de la largeur d'un échantillon (W) par rapport à la taille minimum des particules (d_{max}) ne doit pas être inférieur à 10, tandis que la seconde exige que le ratio du diamètre d'un échantillon (D) par rapport au rapport à la d_{max} soit égal ou supérieur à 8 ou 12, dépendamment du pourcentage des particules grossières. Ces exigences peuvent être atteintes facilement pour les matériaux à particules fines. Mais elles constituent des obstacles considérables pour les matériaux granulaires grossiers comme le gravier, les remblais rocheux et les roches stériles lors des essais en laboratoire.

Pour surmonter ces difficultés, plusieurs techniques en échelle réduite ont été proposées et largement utilisées en éliminant les particules trop grandes. En plus, le ratio minimum requis de 10 pour le W/d_{max} donné par l'ASTM D3080/D3080M-11 a été utilisé dans presque tous les essais de cisaillement direct, tandis que le rapport minimum requis de 10 ou de 12 pour le D/d_{max} stipulé par l'ASTM D2434-19 a été largement utilisé dans les essais de perméabilité à charge hydraulique constante, même si la validité de ces rapports minimum requis n'est jamais clairement démontrée. Le premier objectif spécifique (OS) de cette thèse est d'identifier une fiable technique en échelle réduite qui peut être utilisée pour déterminer correctement la

résistance au cisaillement des matériaux à particules grossières, tels que le gravier, les remblais rocheux et les roches stériles. Le deuxième OS est de vérifier la validité du rapport minimum requis de la norme ASTM D2434-19 pour les échantillons et d'identifier un rapport minimum requis suffisamment grand qui peut être utilisé pour obtenir une mesure fiable de la conductivité hydraulique saturée.

Pour atteindre ces OSs, une revue de littérature a d'abord été réalisée sur les résultats publiés et obtenus par des essais de cisaillement direct sur des matériaux granulaires grossiers. On a constaté que la méthodologie utilisée antérieurement par les chercheurs pour vérifier la validité ou invalidité des techniques en échelle réduite dans l'estimation de la résistance au cisaillement des matériaux de terrain est inappropriée. La fiabilité de toutes les techniques en échelle réduite reste inconnue, même si la technique en échelle réduite parallèle est la plus populaire et la plus utilisée. En plus, le rapport minimum requis de 10 pour le W/d_{max} stipulé dans la norme ASTM D3080/D3080M-11 pour les essais de cisaillement direct n'est pas assez grand pour éliminer l'effet de taille d'échantillon (ETE). La fiabilité de tous les résultats publiés précédemment et obtenus en utilisant ce rapport minimum requis devient discutable.

Afin de savoir quel est le rapport minimum requis de W/d_{max} pour éliminer l'ETE, une série d'essais de cisaillement direct a été réalisée en utilisant trois boîtes de cisaillement direct de tailles différentes. De nouveau, les résultats montrent que le rapport minimum requis de 10 pour le W/d_{max} n'est pas assez grand pour éliminer l'ETE. En revanche, un rapport de W/d_{max} égal ou supérieur à 60 semble être suffisamment grand pour éviter l'ETE dans les essais de cisaillement direct. Ce rapport a été appliqué ensuite pour évaluer la fiabilité des techniques en échelle réduite par une série d'essais de cisaillement direct réalisés sur des échantillons de « terrain » et des échantillons d'échelle réduite avec différentes d_{max}, préparés en appliquant les techniques en échelle réduite tronquée et parallèle. Les angles de frottement des échantillons d'échelle réduite ayant des valeurs de d_{max} inférieures à celles des échantillons de terrain ont été utilisés pour établir des équations prédictives entre l'angle de frottement et la d_{max} pour chaque technique en échelle réduite. Ces équations ont ensuite été utilisées pour prédire les angles de frottement des échantillons de terrain. Les comparaisons entre les angles de frottement mesurés et prédits des échantillons de terrain indiquent que la technique en échelle réduite tronquée peut être utilisée

pour prédire les angles de frottement des échantillons de terrain, et que la technique en échelle réduite parallèle ne permet pas de prédire les angles de frottement des échantillons de terrain.

Bien que les résultats précédents montrent un aperçu intéressant de la validité ou de 'invalidité des techniques en échelle réduite, on constate que les échantillons de terrain ont été limités à une valeur de 5 mm pour la d_{max} afin de respecter le rapport minimum requis de 60 pour le W/d_{max} avec la grande boîte de cisaillement direct spéciale de 30 cm de largeur. La question qui se pose est comment obtenir l'angle de frottement des échantillons de terrain dont la valeur de d_{max} est supérieure à 5 mm sans appliquer les techniques en échelle réduite. Pour répondre à cette question, une équation basée sur les résultats expérimentaux disponibles a été proposée entre les angles de frottement normalisés par l'angle de frottement des échantillons suffisamment grands et le ratio de W/d_{max}. Avec cette équation et l'angle de frottement mesuré avec un échantillon ayant un $W/d_{max} < 60$, l'angle de frottement du même échantillon à $W/d_{max} = 60$ peut être prédit. Afin de tester la validité de cette méthode proposée, on a profité de théorie selon laquelle l'angle de repos d'un matériau correspond à l'angle de frottement interne du même matériau à l'état le plus lâche. Une série d'essais de cisaillement direct a donc été réalisée en plaçant lentement les matériaux dans des boîtes de cisaillement pour obtenir un échantillon à l'état le plus lâche. Une autre série d'essais en tas a été réalisée pour obtenir l'angle de repos des différents échantillons. Les comparaisons entre les angles de frottement mesurés et prédits indiquent que la méthode proposée peut être utilisée pour prédire les angles de frottement des matériaux granulaires grossiers ayant une valeur d_{max} supérieure à 5 mm.

Tout comme l'analyse des propriétés mécaniques des matériaux granulaires grossiers, une analyse a également été faite sur les mesures existantes de conductivité hydraulique saturée. Presque toutes les études antérieures ont été réalisées en utilisant le rapport minimum requis de 8 ou 12 pour le D/d_{max} spécifié par l'ASTM D2434-19 pour les essais de perméabilité à charge hydraulique constante des matériaux granulaires, même si la fiabilité du rapport minimum requis de 8 ou 12 pour le D/d_{max} n'a jamais été testée.

Pour étudier si le rapport minimum requis de 8 ou 12 est suffisamment grand pour éviter tout ETE et pour identifier le rapport minimum requis de D/d_{max} pour éviter tout ETE, des essais de perméabilité à charge constante ont été réalisés en utilisant quatre colonnes de dimensions différentes sur quatre échantillons avec différentes valeurs de d_{max}. Les rapports de D/d_{max} des

échantillons testés varient entre 13 et 252. Les résultats montrent de nouveau que le rapport minimum requis de 12 est trop petit pour éviter l'ETE dans les essais de perméabilité à charge hydraulique constante. Les résultats expérimentaux montrent plutôt qu'une valeur de D/d_{max} comprise entre 170 et 252 devrait être suffisamment grande pour éliminer l'ETE.

ABSTRACT

Waste rocks extracted from mines are commonly dumped on the ground surface and stored as waste rock piles. They have also been increasingly used as building materials for in site or off site constructions. Determining their hydro-mechanical properties is a critical issue to ensure economic and stable design and construction of infrastructures made from waste rocks. This is also the end objective of this thesis. It is however a challenging task because waste rocks typically have a wide gradation with particles as small as silt and as large as boulders of meters.

The literature review shows that there are a large number of publications on the determination of shear strength of rockfill, very few on waste rocks. The literature review also shows that the most published works on waste rocks were mainly realized by following the testing methods developed for and used in civil engineering. Subsequently, ASTM D3080/D3080M-11 has been largely used for direct shear tests, while ASTM D2434-19 largely used for constant head permeability tests of waste rocks. The former stipulates that the specimen width (W) over the minimum particle size (d_{max}) ratio should not be smaller than 10 while the latter requires that the specimen diameter (D) over d_{max} ratio must be equal to or larger than 8 or 12, depending on the percentage of coarse particles. These requirements can be easily reached for fine particle materials. But they constitute considerable obstacles for coarse granular materials like gravel, rockfill and waste rocks in laboratory tests.

To overcome these difficulties, several scaling down techniques have been proposed and largely used to eliminate the oversized particles. In addition, the minimum required W/d_{max} ratio of 10 given by ASTM D3080/D3080M-11 has been universally used for direct shear tests, while the minimum required D/d_{max} ratio of 8 or 12 stipulated by ASTM D2434-19 largely employed for constant head permeability tests even though the validities of these minimum required specimen size over d_{max} ratios have never been clearly shown. The first specific objective (SO) is to identify a reliable scaling down technique that can be used to correctly determine the shear strength of coarse particle materials, such as gravel, rockfill and waste rocks. The second SO is to validate the minimum required specimen size ratio of ASTM D2434-19 and to identify large enough ratios that can be used to determine reliable saturated hydraulic conductivity.

To reach these SOs, a literature review was first performed on published data obtained by direct shear tests on coarse granular materials. It is found that the methodology used by previous researchers to validate or invalidate the scaling down techniques in estimating the shear strength of field materials is inappropriate. The reliability of all the scaling down techniques remains unknown even though the parallel scaling down technique has been the most popular and the most used one. In addition, the minimum required W/d_{max} ratio of 10 stipulated in ASTM D3080/D3080M-11 for direct shear tests is not large enough to eliminate specimen size effect (SSE). The reliability of all the previously published results obtained by using this ratio can become questionable.

In order to know what is the minimum required W/d_{max} ratio to eliminate the SSE, a series of direct shear tests have been conducted using three shear boxes of different sizes. The results show once again that the minimum required W/d_{max} ratio of 10 is not large enough to eliminate SSE. Rather, a $W/d_{\max}$ ratio equal to or larger than 60 seems to be large enough to avoid SSE in the direct shear tests. This ratio was then applied to evaluate the reliability of scaling down techniques through a series of direct shear tests performed on "field" samples and scaled down samples with different d_{max}, prepared by applying scalping and parallel scaling down techniques. The friction angles of scaled down samples having d_{max} values smaller than that of field samples were used to establish predictive equations between the friction angle and d_{max} for each scaling down technique. The equations were later used to predict the friction angles of the field samples. The comparisons between the measured and predicted friction angles of field samples indicate that scalping scaling down technique can be used to predict the friction angles of field samples, and the parallel scaling down technique fails to predict the friction angles of field samples.

While the previous results showed interesting insight to the validity or invalidity of the scaling down techniques, one notes that the field samples were limited to have a $d_{\max}$ value of 5 mm in order to meet the minimum required $W/d_{\max}$ ratio of 60 with the special large direct shear box of 30 cm wide. A raised question is how obtain the friction angle of field samples with a $d_{\max}$ value larger than 5 mm. To answer this question, an equation based on available experimental results was proposed between the friction angles normalized by the friction angle of large enough specimens and $W/d_{\max}$ ratio. This equation along with the friction angle obtained with a specimen having a $W/d_{\max} < 60$ can then be used to give a prediction to the friction angle of the same

samples having $W/d_{max} = 60$. In order to test if the proposed method works, one took use of the theory in which the repos angle of a material corresponds to the internal friction angle of the same material in the loosest state. A series of direct shear tests were thus performed by slowly placing the samples in shear boxes. Another series of pile tests were conducted to obtain the repos angle of the same samples. The comparisons between the measured and predicted friction angles indicate that the proposed method can be used to predict the friction angles of coarse granular materials having a d_{max} value larger than 5 mm.

Similarly to the analysis of mechanical properties of coarse granular materials, an analysis was also made on existing data of saturated hydraulic conductivity. It is noted that almost all the previous investigations were made by using the minimum required D/d_{max} ratio of 8 or 12 specified by ASTM D2434-19 for constant head permeability tests of granular materials even though the reliability of the minimum required D/d_{max} ratio of 8 or 12 has never been tested.

To further study if the minimum required D/d_{max} ratio of 12 is large enough to avoid any SSE and to identify the minimum required D/d_{max} ratio to avoid any SSE, constant head permeability tests were performed by using four columns of different sizes on four samples with different d_{max} values. The D/d_{max} ratios of tested specimens vary between 13 and 252. The results showed again that the minimum required D/d_{max} ratio of 8 or 12 is too small to avoid SSE in constant head permeability tests. Rather, the experimental results tend to show that a value of D/d_{max} between 170 and 252 should be large enough to eliminate the SSE.

TABLE OF CONTENTS

LIST OF TABLES

LIST OF FIGURES

LIST OF SYMBOLS AND ABBREVIATIONS

Symbols

A	Cross section area of soil [L^2]
C	Cohesion
C	Constant related to material type
C_1	Constant parameter
C_0	= 8 for smooth, rounded grains and 4.6 for grains of irregular shape
C_G	Specific surface
C_u	Coefficient of uniformity
d	Particle size [L]
d_5	Particle size that 5% by weight of particles pass [L]
d_{10}	Particle size that 10% by weight of particles pass [L]
d_{50}	Mean particle size [L]
d_{60}	Particle size that 60% by weight of particles pass [L]
d_{max}	Maximum particle size [L]
$d_{max.f}$	d_{max} of field material [L]
$d_{max.p}$	d_{max} of scaled down sample [L]
$d_{p.m}$	Particle sizes of modeled sample [L]
$d_{p.f}$	Particle sizes of field material [L]
D	Specimen diameter [L]
D/d_{max}	Specimen diameter to d_{max} ratio [-]
d_p	Bottom diameter of the pile [L]
dh/dl	Hydraulic head
d_{pmax}	d_{max} of reference rockfill [L]

D_r	Relative density
e	Void ratio
e_{max}	Maximum void ratio
f_s	Grain shape factor
f_a	Porosity factor
G_s	Specific gravity
g	Acceleration gravity [LT^{-2}]
H	Specimen height [L]
h	Difference in head on piezometers [L]
h_1	Water height in the piezometer 1 [L]
h_2	Water height in the piezometer 2 [L]
h_p	Vertical height of pile [L]
h	Water head in piezometer [L]
H	Head loss [L]
i	Hydraulic gradient
i_{cr}	Critical hydraulic gradient
K_{sat}	Saturated hydraulic conductivity [LT^{-1}]
L	Specimen lenght [L]
L_s	Length of soil sample [L]
L	Distance between piezometers [L]
M_1	Mass of the dry permeameter alone [M]
M_2	Mass of the dry permeameter filled with dry soil [M]
M_s	Mass of dry soil [M]
M_{ms}	Mass of moist soil [M]

M_{tot}	Total mass of the permeameter system [M]
M_e	Mass of the permeameter filled with de-aired water [M]
M_w	Mass of water in the soil specimen [M]
n	Porosity
N	Parallel scaled down ratio
N_e	Effective porosity of geological units
P_i	Percentage by weight of the specimen that is retained on sieve *i*
P_{oi}	Percentage by weight of the field material retained on sieve *i*
P_5	Percentage by weight of the field material retained on sieve 5 mm
P_{dmax}	Percentage by weight of the field material coarser than dmax
P	Percentage by weight of the modeled particle size
$P_{ij,a}$	Percentage by mass of added particles passing sieve having size *j* ($\leq d_{max}$) and retained on the neighbor sieve having size *i* ($\geq$ 4.75 mm)
$P_{ij,f}$	Percentage by mass of field material particles passing sieve size *j* ($\leq d_{max}$) and retained on the sieve size *i* ($\geq$ 4.75 mm)
$P_{No.4}$	Percentage of field material particles passing the sieve of 4.75 mm (i.e., sieve No. 4)
P_o	Percentage by mass of field material particles retained on the sieve having a size of the targeted d_{max}
P_Q	Percentage by mass of the particles smaller than *d* of the modeled sample [%]
P_{20}	Percolation rate at $20^{\circ c}$ [LT^{-1}]
Q	Water discharge [L^3T^{-1}]
q	Quantity of flow per time [L^2T^{-1}]
R	Equivalent roughness factor
r	Radial distance [L]
S	Shear strength [$ML^{-1}T^{-2}$]

S_r	Saturation degree
S_s	Specific surface
T	Specimen thickness
T/d_{max}	Specimen width to maximum particle size ratio
T	Temperature
t	Time of discharge [T]
v	Water velocity [LT^{-1}]
V	Volume [L^{-3}]
V_{mini}	Volume of mini shear box [L^3]
V_{small}	Volume of small shear box [L^3]
V_{tot}	Total volume [L^3]
V_{large}	Volume of large shear box [L^3]
Vv	Void volume [L^3]
V_s	Volume of the rock or sediment sample [L^3]
V_w	Volume of the water introduced or removed during recorded time interval [L^3]
V_p	Volume of water removed from the pumped well [L^3]
V_{Darcy}	Water velocity [LT^{-1}]
W	Specimen width [L]
W/d_{max}	Specimen width to maximum particle size ratio
W/T	Scale ratio
x	Model parameter ≈ 2
z	Depth [L]
α	Tilt angle or angle of repose

ρ_s	Soil density [ML^{-3}]
ρ_w	Water density [ML^{-3}]
ρ	Density [ML^{-3}]
γ_w	Water unit weight [$MT^{-2}L^{-2}$]
σ	Vertical (normal) stress [$ML^{-1}T^{-2}$]
σ'	Effective stress [$ML^{-1}T^{-2}$]
σ_3	Minimum principal stress [$ML^{-1}T^{-2}$]
σ_n	Normal vertical stress [$ML^{-1}T^{-2}$]
τ	Shear stress [$ML^{-1}T^{-2}$]
ϕ	Friction angle
ϕ_{peak}	Peak friction angle
ϕ_b	Base friction angle
ϕ_{pt}	Repose angle measured by the pile test
$\phi_{W/dmax}$	Friction angle of the specimen measured by direct shear test
ϕ_{60}	Friction angle of the specimen exempt of specimen size effect
μ_T	Water dynamic viscosity at t °C [$ML^{-1}T^{-1}$]
μ_w	Dynamic viscosity of water [$ML^{-1}T^{-1}$]
μ_{10}	Water viscosities at 10 °C [$ML^{-1}T^{-1}$]
ϑ	Kinematic viscosity [M^2T^{-1}]

Abbreviations

ASTM	American society for testing and materials
A-S	Alyamani and Sen

KC	Kozeny-Carman
KCM	Modified Kozeny-Carman
NAVFAC	Naval Facilities Engineering Command
PSD	Particle size distribution
PSDC	Particle size distribution curve
SSE	Specimen size effect
UFC	Unified Facilities Criteria
USBR	US Bureau of Reclamation
USACE	United States of Army Corps of Engineers
WR	Waste rock

LIST OF APPENDICES

CHAPTER 1 INTRODUCTION

1.1 Statement of the problem

While producing a small quantity of precious minerals, mines have also to produce each year a large amount of waste rocks, generated during the development working to obtain access to the target ore bodies. This large amount of mine wastes in terms of tailings and waste rocks needs to be appropriately managed. The latter, which lack sufficient value for treatment (Tachie-Menson, 2006), are typically stored on the ground surface as waste rock piles (Wilson, 2000; Aubertin et al., 2002), accompanied with several geotechnical or/and geochemical problems. They can also be used in and off mine sites as a good building material for the construction of diverse infrastructures (Tardif-Drolet et al., 2020), such as waste rock inclusions in tailings storage facilities to accelerate the drainage and consolidation process (Bolduc & Aubertin, 2014; Ferdosi et al., 2015; Saleh-Mbemba et al., 2019) and barricades to retain backfill slurry in underground mine stopes (Li et al., 2009; Li & Aubertin, 2011; Yang et al., 2017; Zhai et al. 2021a). The design of such infrastructures needs the knowledge of the hydro-mechanical properties of waste rocks to ensure an economic and safe design of the infrastructures.

To determine the shear strength and hydraulic conductivity of waste rocks, ASTM D3080/D3080M-11 requires the specimen width to be at least 10 times the maximum particle size (d_{max}) of materials for direct shear tests, and ASTM D2434-19 stipulates the specimen diameter to be at least 12 times d_{max} for constant head permeability tests. Following the requirements of these standards for waste rocks having large particle sizes or boulders is a challenging task if not impossible. This challenge was removed since the scaling down techniques were proposed and they have been actively used by many researchers to eliminate the oversized particles of coarse granular materials and to obtain test samples with smaller particle sizes. However, the literature review shows that almost all the previous studies used parallel scaling down technique to determine the friction angle of test samples (i.e., Vallerga et al., 1957; Marachi et al., 1972; Lowe, 1964; Verdugo & De la Hoz, 2006; Abbas, 2011; Ovalle et al., 2014; Kouakou et al., 2020; Dorador & Villalobos, 2020b), and scalping technique to determine the hydraulic conductivity of coarse granular materials (i.e., Mavis & Wilsey, 1937; Rowe et al.

2000; Peregoedova, 2012; Duhaime et al., 2012; Cabalar & Akbulut, 2016; Essayad et al., 2018; Gan et al. 2019). The validity or invalidity of the scaling down techniques has never been correctly shown or the reported results are contradictory (Bagherzadeh & Mirghasemi, 2009; Hamidi et al., 2012; Dorador & Villalobos, 2020b; Deiminiat et al., 2020; MotahariTabari & Shooshpasha, 2021; Deiminiat and Li, 2022).

Analyses on the available experimental data further indicate that all the previous studies used the minimum specimen width to d_{max} ratio of 10 specified by ASTM D3080/D3080M-11 to conduct direct shear tests on coarse granular materials (Rathee 1981; Scarpelli & Wood 1982; Amirpour Harehdasht et al. 2018; Cai et al. 2020; Zahran & Naggar 2020; Yaghoubi et al. 2020; Nicks et al. 2021; Saberian et al. 2021), while this ratio seems to be invalidated for these materials and not validated for fine particle materials with $d_{max} \leq 1$ mm (Rathee, 1981; Cerato & Lutenegger, 2006; Mirzaeifar et al., 2013; Ziaie Moayed et al., 2017). The minimum specimen width to d_{max} ratio of ASTM D3080/D3080M-11 must be revised for coarse granular materials and validated for fine particle materials.

The specimen diameter over d_{max} ratio of 12 stipulated by ASTM D2434-19 has also been used widely by previous studies to prepare the test specimens of constant head permeability tests, despite the fact that the validity of the required ratio has never been thoroughly studied for coarse granular materials such as waste rocks. The reliability of the test results remains unclear.

Apart from the findings of previous studies, scaling down techniques have been used continually by researchers to prepare the specimens of coarse granular materials in the laboratory without validating the scaling down techniques. In addition, the specimen size effect and the validation of the specimen size ratios specified by the ASTM standards have never been well studied in direct shear tests and constant head permeability tests. The problems associated with determining reliable shear strength and saturated hydraulic conductivity of coarse granular materials has remained unsolved. Finding the good methods to evaluate shear strength and saturated hydraulic conductivity of waste rocks thus constitute the main scope of this thesis.

1.2 Thesis objectives and methodology

This thesis aims to fine the good methods to determine the hydro-mechanical properties of waste rocks. The investigations take in to account the specimen size effect in direct shear tests and constant head permeability tests to enhance the reliability of test results.

The main objective has been achieved through the realization of the following specific objectives:

1) Identify a reliable scaling down technique that can be used to correctly determine the shear strength of coarse granular materials, such as waste rocks.
    - Conduct experimental investigations to find a minimum specimen width over maximum particle size ratio to be large enough and eliminate the specimen size effect on direct shear test results.
    - Investigate the reliability of scaling down techniques by conducting experimental tests on specimens with large enough size ratios. By the application of best-fitting technique on the relationship between shear strengths and maximum particle size, reliable shear strengths of field materials are obtained.
    - Identify a method to determine the shear strength of coarse grain materials in direct shear tests: with small specimens without specimen size effect.
2) Validate the minimum required specimen size ratio of ASTM D2434-19 and to identify large enough ratios that can be used to determine reliable saturated hydraulic conductivity of coarse particle materials.

1.3 Contributions

The main contribution of this project is a thesis including three published and two submitted articles in peer-reviewed journals:

1. Deiminiat, A., Li, L., Zeng, F., Pabst, T., Chiasson, P., & Chapuis, R. (2020). Determination of the shear strength of rockfill from small-scale laboratory shear tests: a critical review. *Advances in Civil Engineering*, *2020*. 8890237. This article was published on November 29, 2020 and it is presented in Chapter 4.

2. Deiminiat, A., Li, L & Zeng, F. (2022). Experimental study on the minimum required specimen width to maximum particle size ratio in direct shear tests. *CivilEng*, *3*(1), 66-84. This article was published on January 21, 2022 and it is presented in Chapter 5.

3. Deiminiat, A., & Li, L. (2022). Experimental study on the reliability of scaling down techniques used in direct shear tests to determine the shear strength of rockfill and waste rocks. *CivilEng*, *3*(1), 35-50. This article was published on January 8, 2022 and it is presented in Chapter 6.

4. Deiminiat, A., & Li, L. (2022). A method to determine the friction angle of coarse granular materials in direct shear tests: with small specimens without specimen size effects. *Submitted in the International Journal of Geotechnical Engineering, submission ID: 225192922*). This article was submitted on January 25, 2022 and it is presented in Chapter 7.

5. Deiminiat, A., Li, L. & Pabst, T. (2022). Experimental study on specimen size effect and the minimum required specimen diameter to maximum particle size ratio for constant head permeability tests. *Submitted in Environmental Earth Sciences, submission ID: ENGE-D-22-00329*. This article was submitted on February 09, 2022 and it is presented in Chapter 8.

The realization of this research project leads also to the following two conference papers:

1. Deiminiat, A., Li, L., Zeng, F., Pabst, T., Chapuis, R., & Chiasson, P. (2020). An overview on the determination of the shear strength of coarse grain materials (rockfills) from small scale laboratory tests. *GeoVirtual2020*, Canada.
2. Deiminiat, A., Li, L., & Zeng, F. (2021). How to obtain reliable shear strength by direct shear tests: A revision to the minimum required specimen size to d_{max} ratio of ASTM D3080/D3080M-11. *Canadian Geotechnique Society*, GeoNiagara2021, Niagara, ON, Canada.

Several presentations have been also given during the research as follows:

1. A review on determination of the shear strength of waste rocks from small scale laboratory tests to large scale field tests. *Colloquium UQAT-Poly*, 2019, Rouyn-Noranda, QC, Canada.
2. Variation de la résistance au cisaillement de matériaux granulaires en fonction de tailles d'éprouvettes : quelques résultats d'essais au laboratoire. *Canadian Malartic*, 2019, Valdor, QC, Canada.
3. Variation de la résistance au cisaillement de matériaux granulaires en fonction de tailles d'éprouvettes : quelques résultats d'essais au laboratoire. *Golder Associates Company*, 2019, Montreal, QC, Canada.
4. An overview on the determination of the shear strength of coarse grain materials (rockfills) from small scale laboratory tests. *GeoVirtual*, 2020.
5. How to obtain reliable shear strength by direct shear test: A revision to the minimum required specimen size to d_{max} ratio of ASTM D3080-11. *RIME seminar*, 2021, Virtual.
6. How to obtain reliable shear strength by direct shear tests: A revision to the minimum required specimen size to d_{max} ratio of ASTM D3080/D3080M-11. *GeoNiagara*, 2021, Niagara, ON, Canada.
7. Experimental study on the reliability of scaling down techniques to obtain the shear strength of coarse particle materials from small-scale direct shear tests. *Colloquium Poly-UQAT*, 2021, Montreal, QC, Canada.

The realization of this research project contributes to a better understanding of the existing problems associated with determining reliable hydro-mechanical properties of coarse granular materials such as waste rocks. The reliability of the scalping and parallel scaling down techniques, as well as the validity of the minimum specimen size ratios required by ASTM D3080/D3080M-11 for direct shear tests and ASTM D2434-19 for constant head permeability tests were better understood. It can be expected that the experimental and analytical solutions presented in this document provides the good methods for engineers and researchers of the geotechnique and mining industry to determine reliable shear strength and saturated hydraulic

conductivity of waste rocks by eliminating the specimen size effect and using reliable scaling down technique.

1.4 Organization

The thesis is organized in a paper-based format, which consists of ten chapters. The content of each chapter is summarized as follows:

Chapter 1 (current chapter) provides a short introduction to the research project and briefly describes the content of the thesis.

Chapter 2 presents a comprehensive literature review of relevant previous information, including the application of waste rocks, waste rock properties, shear strength estimation of waste rocks, factors influencing on shear strength of waste rocks, saturated hydraulic conductivity estimation of waste rocks and the factors influencing on saturated hydraulic conductivity.

Chapter 3 provides an overview of the methodologies employed in this thesis to accomplish the set goals via the testing plans.

Chapter 4 (Article 1) presents a critical review on the determination of shear strength of rockfill from small-scale laboratory shear tests. The difficulties of conducting laboratory shear tests to determine the shear strength of coarse granular materials are discussed first. The existing solutions (scaling down techniques) are then discussed, as well as the reliability of their application. Analyses on the existing experimental data of previous studies on specimen size effect (SSE) are presented next. The validity or invalidity of the minimum specimen size ratio required by ASTM D3080/D3080M-11 for direct shear tests is discussed at the end. The literature demonstrates that the methodology used by previous studies to examine the reliability of the scaling down techniques in estimating the shear strength of field materials is not an appropriate method. In addition, the minimum required specimen width to maximum particle size (d_{max}) ratio of 10 stipulated in ASTM D3080/D3080M-11 for direct shear tests is not large enough for coarse granular materials to eliminate SSE. The reliability of conclusions given on the uncertain results can become questionable.

Chapter 5 (Article 2) presents the experimental investigation on the minimum required specimen width to d_{max} ratio in direct shear tests. The minimum required ratio of ASTM D3080/D3080M-

11 is validated for coarse granular materials and revised based on the experimental data from three shear boxes with different sizes. A minimum specimen size ratio to be large enough and eliminate the SSE is proposed by using the existing reliable experimental data and new experimental data obtained in this chapter.

Chapter 6 (Article 3) presents experimental work on the reliability of scaling down techniques used in direct shear tests to determine the shear strength of rockfill and waste rocks. The reliability of scalping and parallel scaling down techniques is investigated by applying scalping and parallel techniques on field samples. The direct shear tests are first performed on the test specimens with large enough specimen size ratio suggested in Chapter 5 to ensure the reliable shear test results are obtained. By applying the best-fit curve technique on the variation of the friction angles of scalping and parallel scaled down samples with d_{max}, the friction angle of the field samples are predicted. Comparisons are made between the friction angles of the field samples predicted by applying scalping and parallel techniques and the measured friction angles of the field samples to find the reliability of the scaling down techniques.

Chapter 7 (Article 4) presents a method to determine the friction angle of coarse granular materials in direct shear tests: with small specimens without SSE. Two sets of experimental tests, including direct shear testing and pile tests, are used to verify the suggested equation. The friction angles obtained by performing direct shear tests on the specimens having not large enough specimen size ratio and suggested equation are used to obtain the friction angles of the specimens that are exempt of SSE. Comparisons are then made between the friction angles exempt of SSE and the friction angles predicted by applying the proposed equation on the friction angles of the specimens having not large enough specimen size ratios to find the reliability of the proposed equation. The results showed the reliability of the proposed method.

Chapter 8 (Article 5) presents experimental investigation on specimen size effect and the minimum required specimen diameter to maximum particle size ratio for constant head permeability tests. The experimental data of four columns with different sizes are used to validate and revise the minimum specimen diameter to d_{max} ratio specified by ASTM D2434-19 for constant head permeability tests. The outcomes demonstrated that the minimum ratio of 12 specified by the ASTM for constant head permeability tests is too small to remove the influence of specimen size. So, the variations of saturated hydraulic conductivity measured at the same

applied hydraulic gradients are evaluated against specimen diameter to d_{max} ratio for all the materials to find a minimum specimen size ratio to be large enough and eliminate the specimen size effect.

Chapter 9 presents discussion of the results presented in the thesis.

Chapter 10 presents the conclusion with key findings and recommendations for further work.

Appendix A presents the additional results related to Chapter 5.

Appendix B presents the additional results related to Chapter 6.

Appendix C presents the additional results related to Chapter 7.

Appendix D presents the additional results related to Chapter 8.

CHAPTER 2 LITERATURE REVIEW

2.1 Infrastructures made of waste rocks

Large volumes of waste rocks are produced annually during mining operations. Their content of valued minerals is nil or below the cut-off values. They are usually transported by trucks and disposed on ground surface as waste rock piles (Wickland & Wilson, 2005; Tachie-Menson, 2006; McLemore et al., 2009). Waste rocks deposited by using conventional methods (i.e., end-dumping, push dumping, free dumping and dragline) can be subjective of compaction, segregation (Nicholas, 1986; Valenzuela et al., 2008), and heterogeneity (Morin et al., 1991; Fala et al., 2013). All these can affect the permeability and strength of waste rocks. For a waste rock pile, its stability can be controlled by the geometry, shear strength, pore pressure and foundation condition (Gomez et al., 2014). These factors need to be properly measured. It is however not a easy task due to the large range of particle size distribution (PSD) from fine particles as small as silt and as large as boulders of a few meters. Nevertheless, waste rocks are considered as a good building materials that have been commonly used in the in and off site constructions such as waste rock inclusions in tailing storage facilities (Aubertin et al., 2002; James et al., 2011; Saleh-Mbemba et al., 2019), rock fills in underground mine stopes (Hassani & Archibald, 1998), and barricades made of waste rocks (Li et al., 2009; Li & Aubertin, 2011; Yang et al., 2017; Zhai et al. 2021a, 2021b).

2.1.1 Waste rock piles

A waste rock pile is a structure formed by surface disposal of waste rocks. These structures are usually very high and large (McCarter, 1990; Aubertin et al., 2002). Several methods are used for the construction of waste rock piles.

2.1.1.1 Construction methods

2.1.1.1.1 End dumping

In this method, waste rocks are transported by trucks and dumped directly over the crest of the pile. Typically, this method results in a heterogeneous internal structure with segregated particles. The fine particles concentrate near the crest of the pile, whereas the coarser particles accumulate

at the toe of the pile. Field simulations have shown that an end-dumped rock pile consists of three zones with different PSDs: an upper zone consisting of fine particles, a toe zone with very coarse particles and an intermediate zone consisting of relatively uniformly graded particles. Such phenomenon with three distinct zones of segregation is observed in all cases, even though the degree of segregation may become less pronounced when waste rocks have finer texture (Morin et al., 1991; Aubertin et al., 2002). The simplicity and low costs associated with this method explains its wide employment. However, the application of this method does not allow quality control. The density and strength of the materials can be low.

2.1.1.1.2 Push dumping

In this method, waste rocks are first transported by trucks and deposited close to pile crest. Waste rocks are then pushed down over the crest by a bulldozer. Field observations have shown that this method typically results in rock piles with an accumulation of coarse particles near the toe and insignificant segregation on top (Pearce et al., 2016).

In comparison to end-dumping method, pushing-dumping usually results in a much less degree of particle segregation with an average of 40% of the coarse particles collected at the toe of the pile, compared to an average of 75% in end-dumping rock piles (Pearce et al., 2016). This difference is mainly due to the greater momentum gained by coarse particles when dumped from trucks in end-dumping method. This momentum causes the particles to roll down farther on the slope. In push-dumping method, this initial momentum is smaller and many coarse particles remain at top of the slope (Morin et al., 1991; Aubertin et al., 2002).

Push dumping method may be employed when the dumping point is not accessible for mining trucks or there is a safety concern for the stability of the rock pile. This method can also result in a better dust suppression. This method is however slower and more expensive than the end-dumping method (Pearce et al., 2016).

2.1.1.1.3 Free dumping

In this method, waste rocks are dumped in separate piles with a height of approximately 2 m. These rock piles are then graded and compacted, resulting in a rock pile that is more compacted with less particle segregation than in the two previous methods (Morin et al., 1991; Aubertin et

al., 2002). The higher degree of compaction results in higher shear strength and better stability. However, this method is more expensive and time consuming than the previous two methods, and it is mainly used at the beginning of the construction of a rock pile at level ground. Once a high platform is constructed, the less expensive end-dumping or push-dumping methods are used (Morin et al., 1991).

2.1.1.1.4 Dragline

This method is usually used in large-scale coal mines. The segregation is low. The rock piles are seldom built in lifts. The compaction is lower than free-dumping method (Morin et al., 1991; Aubertin et al., 2002).

2.1.1.2 Potential problems

With a waste rocks pile, the occurrence of failure associated with mechanical instability is rare, but happened (Pinto et al., 1985; Blijenberg, 1995; McLemore et al., 2009; Blight, 2010). To increase the stability and especially to minimize the consequence associated with the failure of a waste rocks pile, Brown et al., (2014) proposed to construct waster rocks piles in benches by considering the fact that the friction angle of rock fills decreases as the confining stress increases and the vertical stress increases with the depth from the top surface to the base of a waste rocks pile. An economic and safe design of waste rocks pile requires the knowledge of the shear strength of this material.

When waste rocks are chemically reactive, acid mine drainage (AMD) can take place. Water and its flow through a waste rocks pile are critical for the generation of AMD. Determining the hydraulic conductive of waste rocks is important to estimate the potential of AMD or design preventing measures for minimizing the generation of AMD.

2.1.2 Waste rock inclusions

Waste rocks are well-known as a good building material for its high shear strength and high permeability. When they are placed inside a tailing impoundment in the form of closed compartments or isolated columns as shown in Figure 2.1, the linear structures made of waste rocks are called waste rock inclusions (WRI). WRI can help to accelerate the drainage and

consolidation of tailings impoundments. This can in turn improve the geotechnical performance of surface impoundments (Aubertin et al., 2002; James, 2009; Bolduc & Aubertin, 2014).

Figure 2.1 Waste rock inclusions in a tailings impoundment (taken from Bolduc & Aubertin (2014) with the permission of reproduction from Canadian Science Publishing)

There are some advantages with WRI built in tailings impoundment, including for instance:

- Minimize the consequence of tailings impoundment failure because WRI may have effect to retain a part of the tailings that would be totally released to the environment if there is no WRI constructed in the tailings impoundment (Azam & Li, 2010).
- Facilitate the mine closure and reclamation.
- Accelerate the drainage and consolidation of tailings and improve the stability. Waste rocks have a higher permeability than that of tailings. The drainage and consolidation of the tailings can be accelerated, resulting in reduced potential of liquefaction.

2.1.3 Barricades made of waste rocks for underground mine backfilled stopes

Waste rocks are used for building barricades in underground mines to hold backfill slurry in the stopes. This practice helps to reduce the quantity of surface disposal of mine wastes, resulting in a reduction of environmental impacts of mine activities (Li et al., 2009). Compared to traditional methods in which barricades are constructed with porous bricks, concrete blocks, and shotcrete reinforced meshes, the construction of barricades made of waste rocks is simpler and faster. The

required material can be obtained at low or no cost if the waste rocks are obtained directly from the underground mine development (Li et al. 2009; Li & Aubertin, 2011). However, the stability of such barricades is an important concern because their failure may result in huge economic loss and even loss of lives (Sivakugan et al., 2006; Yang et al., 2017). Determining the stability of barricades needs a good knowledge of the hydro-geotechnical properties of the waste rocks.

2.2 Hydro-mechanical properties of waste rocks

2.2.1 Particle size distribution

The particle size of waste rocks widely varies from particles as fine as clay to large particles as large as boulders of a few meters (Maknoon, 2016; Kutzner, 2020). The coefficient of uniformity C_u (= d_{60}/d_{10}; d_{60} is particle size that 60% by weight of particles passes it and d_{60} is particle size that 10% by weight of particles passes it) of waste rocks are typically 15 or more (Eriksson & Destouni, 1997; Barbour et al., 2001; Aubertin et al., 2005; Boakye, 2008; Maknoon, 2016).

Barbour et al., (2001) studied the PSD of waste rocks extracted from several mines. They found that waste rocks typically consist of coarse fractions with particle sizes smaller than 0.08 mm. McLemore et al. (2009) performed an extensive review of the physical properties of mine waste rocks. They found that mine waste rocks typically consist of 5 to 70% of gravel, 20 to 53% of sand and 0 to 42% of fine fractions. These results correspond quite well to those obtained from the waste rocks of mines Lac Tio in Quebec (Pepin, 2009) and Golden Sunlight (Azam et al., 2007).

Figure 2.2 presents the PSD curves of the waste rocks reported in previous publications given in Table 2.1. The C_u obtained from the PSD curves are also presented in the table. One can see that the ranges of grain sizes change from fine sands to large gravels and the C_u of the waste rocks rages from 15 to 593.

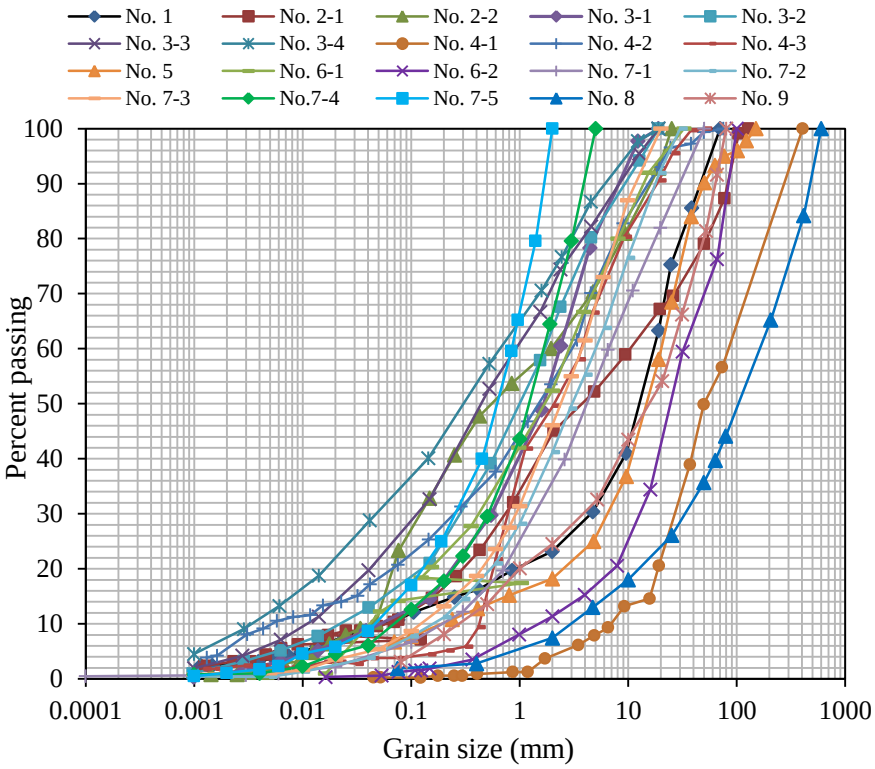

Figure 2.2 PSD curves of waste rocks, taken from the literature (see more details given in Table 2.1)

Table 2.1 Identification of the PSD curves presented in Figure 2.2

Curve number	C_u	**Reference**
No. 1	240	Bonner mine waste rock (Stormont & Farfan, 2005)
No. 2-1, No. 2-2	41–136	B-zone waste rock pile (Ayres et al., 2006)
No. 3-1 to 3-4	37–206	Golden sunlight mine, Montana (Azam et al., 2007)
No. 4-1 to No. 4-3	15–593	Waste rock piles (Boakye, 2008)
No. 5	54	Quarried rocks (Rao et al., 2011)
No. 6-1, No. 6-2	21–335	Libiola Fe-Cu sulfide mine (Marescotti et al., 2008)
No. 7-1 to No. 7-5	17–31	Waste rocks taken form Tino mine (Peregoedova, 2012)
No. 8	54	Waste dump (Dorador et al., 2017)
No. 9	85	Quarried waste rocks (Kouakou et al., 2020)

2.2.2 Water content

Similar to other coarse granular materials, waste rocks have a low capacity of water retention. Its degree of saturation is expected to be low. The natural water content ranges from 3 to 7%, and its

optimum water content for compaction is likely to vary between 10 and 15% (Williams, 2000; Maknoon, 2016).

2.2.3 Density and specific gravity

Density of waste rocks changes upon the degree of compaction. The density of waste rocks typically ranges from 1600 to 2200 kg/m^3 (Williams, 2000).

The specific gravity (G_s) of waste rocks ranges from 2.4 to 4.5 and more (Adams et al., 2007; Azam et al., 2007; Boakye, 2008; Hamidi et al., 2012). Table 2.2 shows the density and specific gravity of waste rocks published in previous studies.

Table 2.2 Summary of density and specific gravity of waste rocks

Material	G_s	**Density (kg/m^3)**	**Reference**
Aberfan mine	2.1	1600-1940	Lucia (1981)
Wharncliffe coal mine	2.16-2.61	1390-1910	Bell (1996)
Yorkshire coal mine	2.04-2.63	1500-1900	
Brancepath coal mine	1.81-2.54	1060-1680	
Lichtenberg pit	2.75	2100	Hockley et al. (2003)
Golden Sunlight	2.63-2.78	1500-2100	Azam et al. (2006)
Tino mine	3.85-4.23	2650-3270	Peregoedova (2012)

2.2.4 Angle of repose (α)

The angle of repose is related to the stability of particulate materials in bulk forms (Terzaghi, 1936; Schulze, 1999). The angle of repose of the waste rocks typically ranges from 37° to 42° (Williams, 2000; Williams & Rohde, 2008).

2.2.5 Saturated hydraulic conductivity (K_{sat})

It has been well known that saturated hydraulic conductivity (K_{sat}) is related to the PSD of granular materials (Freeze & Cherry, 1979). Due to the wide range of particle sizes of waste rocks from very fine to large boulders, these materials are known as permeable materials. Table 2.3 shows some K_{sat} values reported in the literature for various waste rocks. One can see that the K_{sat} of waste rocks ranges from 5×10^{-2} up to 1.7 cm/s.

Table 2.3 K_{sat} values of waste rocks reported in the literature

Source	K_{sat} (cm/s)	Reference
Steel mine, Cu, Zn, Ag	5.2×10^{-4}	Li (2000)
Quirke mine, Uranium	5×10^{-2}	Barbour et al. (2001)
Golden sunlight mine	3.4×10^{-3} to 1×10^{-4}	Herasymuik (1996)
Loose and compacted waste rocks	4.7×10^{-1} to 5.1×10^{-3}	Bussière & Aubertin (1999)
Waste rocks	10^{-3} to 10^{-1}	Hernandez (2007)
Tio mine waste rocks	0.5×10^{-2} - 2×10^{-1}	Gaillot (2007)
Loose waste rocks	Up to 10^{-1}	Peregoedova (2012)
Malartic waste rocks	0.8 to 1.7	Essayad et al. (2018)

Hydraulic conductivity is influenced by many physical and geotechnical factors, most notably porosity, particle shape, fine and gravel content, degree of compaction and etc. (Zięba, 2017).

2.3 Shear strength of waste rocks

Shear strength parameters are important for the design and construction of waste rocks infrastructures. There is a large quantity of few experimental works on rockfill, but very few on waste rcoks, as shown in this section.

2.3.1 Failure criteria for coarse granular materials

2.3.1.1 Mohr-Coulomb

Mohr-Coulomb failure criterion was proposed by Mohr to show the critical combination of normal and shear stresses that causes the failure along a shear plane. On the failure plane, the functional relationship between normal and shear stresses is expressed as (Das, 2008):

$$s = f(\sigma) \tag{2.1}$$

where s is the shear stress at failure and σ is the normal stress on the failure plane.
Coulomb defined function $f(\sigma)$ for soils as follows:

$$s = c + \sigma \tan\phi \tag{2.2}$$

where c is the cohesion and ϕ is the angle of internal friction. For granular materials, the cohesion is usually close to zero, i.e., $c \approx 0$; the Mohr-Coulomb criterion can be written as:

$$s = \sigma \tan\phi \tag{2.3}$$

Based on Equation 2.3, shear strength increases linearly with the normal stress.

When the soil is saturated, the normal stress is effective normal stress and Mohr-Coulomb criterion must be written as:

$$s = c + (\sigma - u)\ \tan\phi = \ c + \sigma'\ \tan\phi \qquad (2.4)$$

where *u* is the pore water pressure and σ' is the effective normal stress on the plane.

2.3.1.2 Charles and Watts (1980)

Charles and Watts (1980) studied the shear strength of compacted rockfill at different confining pressures ranging from 40 to 400 kPa. Figure 2.3 shows the failure envelopes obtained for the range of stresses. The following equation was then proposed to determine the shear strength of the studied rockfill for the given range of confining pressures:

$$s = A(\sigma')^b \qquad (2.5)$$

where s and σ' are the shear stress at failure and effective normal stress, respectively; A and b are constants. The value of b is typically about 0.75. Different values are reported in the literature for different tested materials. Indraratna et al. (1998) obtained b values of 0.65 and 0.69 for two samples of ballast for confining pressures between 1 and 240 kPa. Linero et al. (2007) reported the values of 0.78 and 0.9 for waste rocks. Similarly, Asadzadeh & Soroush (2009) reported the values of 0.821 and 0.824 for two types of rockfill in dry and saturated conditions, respectively. Fakhimi et al. (2012) reported b values ranging between 0.69 and 0.91.

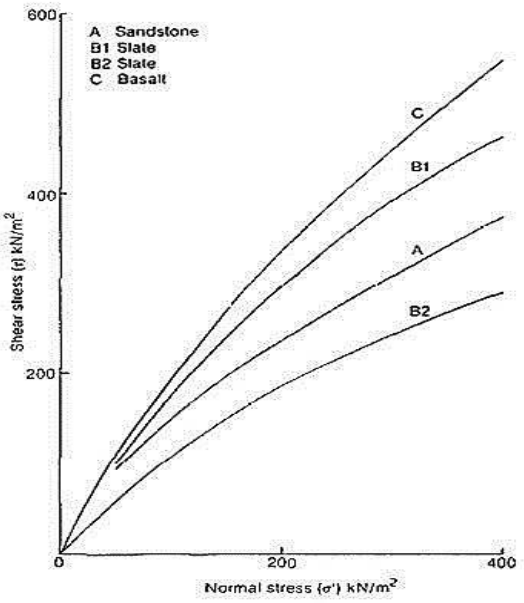

Figure 2.3 Mohr failure envelopes for rockfill at low and medium confining pressures (taken from Charles and Watts (1980) with the permission of reproduction from ICE Publishing)

2.3.1.3 Indraratna (1993)

Indraratna (1993) proposed a modification on the failure criterion given by De Mello (1977). The modified equation is written as follow:

$$\frac{s_n}{\sigma_c} = a \times \left(\frac{\sigma_n}{\sigma_c}\right)^b \tag{2.6}$$

where σ_c is the uniaxial compressive strength; σ_n is confining pressure; a and b are two dimensionless constant parameters. Parameter a can be considered as an intrinsic shear strength index whereas parameter b shows the non-linearity of the failure envelope and presents the deformation responses of rockfill including the influence of particle size and dilation. Figure 2.4 shows the normalized shear strength versus the normalized normal stress on log scales obtained by applying a series of effective normal stresses ranging from 100 kPa to 8 MPa on several types of tested rockfill (Indraratna et al., 1993). Regardless of the particle sizes, initial porosity, angularity of the particles, and moist content, all the experimental data fall within a narrow band shown in Figure 2.4. The lower and upper bounds of parameters a and b are presented on the curves for the normal stresses ranging from 0.1 to 1 MPa and 1 to 7 MPa.

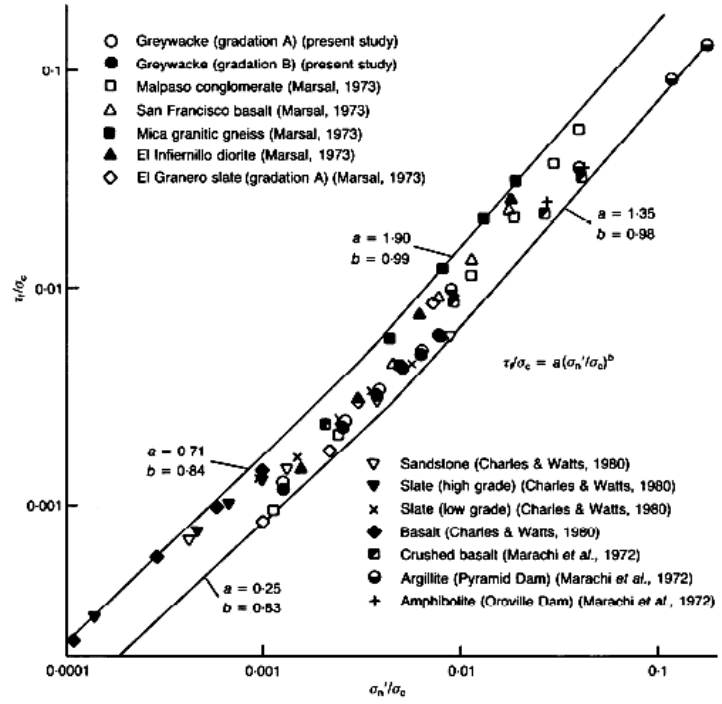

Figure 2.4 Normalized shear strength-normal stress relationship for different rockfill (taken from Indraratna et al. (1993) with the permission of reproduction from ICE Publishing)

Alternatively, Indraratna et al. (1993) presented the failure criterion of rockfill in terms of major and minor principal stresses at failure σ_{1f}' and σ_{3f}' as follows:

$$\frac{\sigma_{1f}'}{\sigma_c} = \alpha \times \left(\frac{\sigma_{3f}'}{\sigma_c}\right)^{\beta} \tag{2.7}$$

The relationship between the major and minor principal stresses at failure of tested rockfill materials normalized by their uniaxial compressive strength (Indraratna et al., 1993) is presented in Figure 2.5.

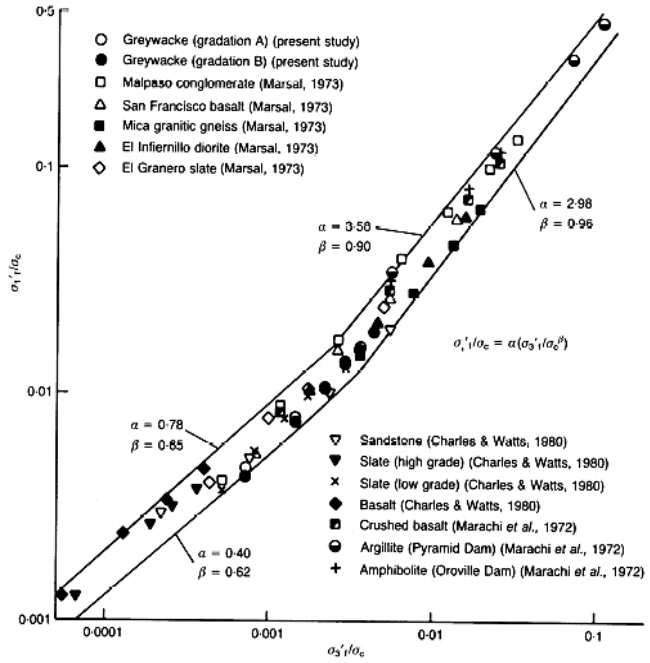

Figure 2.5 Relationship between the normalized major and minor principal stresses at failure for different types of tested rockfill (taken from Indraratna et al. (1993) with the permission of reproduction from ICE Publishing)

2.3.2 Shear strength measurement of coarse granular materials

2.3.2.1 In situ tests

In order to measure shear strength of granular materials such as rockfill and waste rocks containing large size particles, field shear tests have been developed in the last decades. Goodrich (1904) was perhaps the first one to perform in situ direct shear experiments using a 300 mm × 300 mm shear box to measure the friction angles of clay, sand, and gravel materials (Skempton, 1958). The shear tests were conducted by filling the box with the tested materials while normal stresses were applied by adding weights to the scale-pan. The top part of the box was dragged until the occurrence of sliding. To increase normal stress, the tests were repeated by adding additional weights. The applied normal stress could not be very large. Furthermore, the box size is insufficient for testing full-scale field materials. Goodrich (1904) demonstrated that the peak friction angles of tested materials depend on particle size and saturation degree. Yu et al. (2006) obtained similar results in laboratory direct shear testing. Many researchers followed the in situ

testing approach of Goodrich (1904) (Hutchinson & Rolfsen, 1962; Marsland, 1971; Oyanguren et al., 2008). This resulted in the modern direct shear test apparatus (Skempton, 1958).

Due to imposed plane of sliding in direct shear tests, the obtained friction angle may include a dilation angle that depends on the physical properties and testing conditions. As the degree of dilatation decreases with the increased normal stress, one usually observes a reduction of friction angle associated with an increase in the normal stress (Das, 2008). As a result, high friction angle are usually obtained in in situ direct shear tests (Matsuoka et al., 2001; Fakhimi et al., 2007; Boakye, 2008; Zhang et al., 2016).

Matsuoka et al. (2001) performed a modified in situ direct shear test on a rockfill with a maximum particle size (d_{max}) value of 300 mm (Figure 2.6). The specimen sizes were 1200 mm large, 1200 mm long and 170 mm high. The minimum required ratio between specimen size and d_{max} value, specified by ASTM D3080/D3080M (2011), was not respected. The normal stress was provided by dead loads on a rigid loading plate. As a result, the normal stresses used in this equipment are limited and the shear strength of field material a large infrastructure cannot be fully determined.

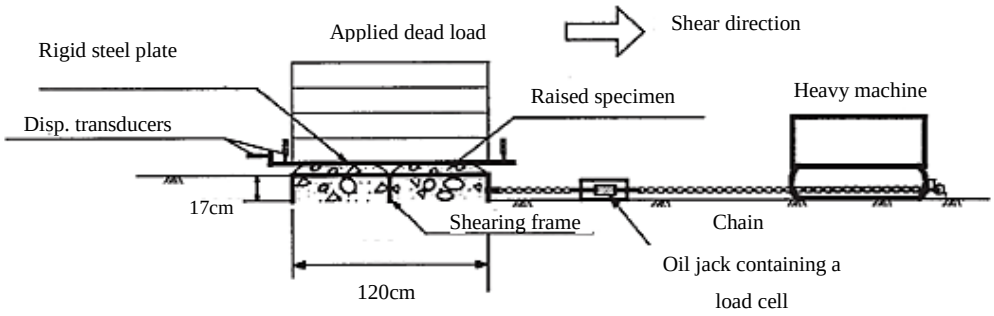

Figure 2.6 Schematic view of the in situ direct shear test instrument (taken from Matsuoka et al. (2001) with the permission of reproduction from ASTM International)

Fakhimi et al. (2007) and Boakye (2008) performed in situ direct shear tests on rock pile materials. As shown in Figure 2.7a, the apparatus consists of a shear box, a metal top plate, a roller plate, normal and shear gages, two hydraulic jacks and cylinders. Two metal shear boxes of 300 mm × 300 mm and 600 mm × 600 mm were used. The normal stresses ranging from 15 to 70 kPa were applied on the specimens. Figure 2.7b shows the results of three in situ shear tests

conducted on the rockfill from Sugar Shack West rock pile using the 600 mm × 600 mm shear box. The obtained peak friction angle was 48°. Cohesion of 9.7 kPa was also observed.

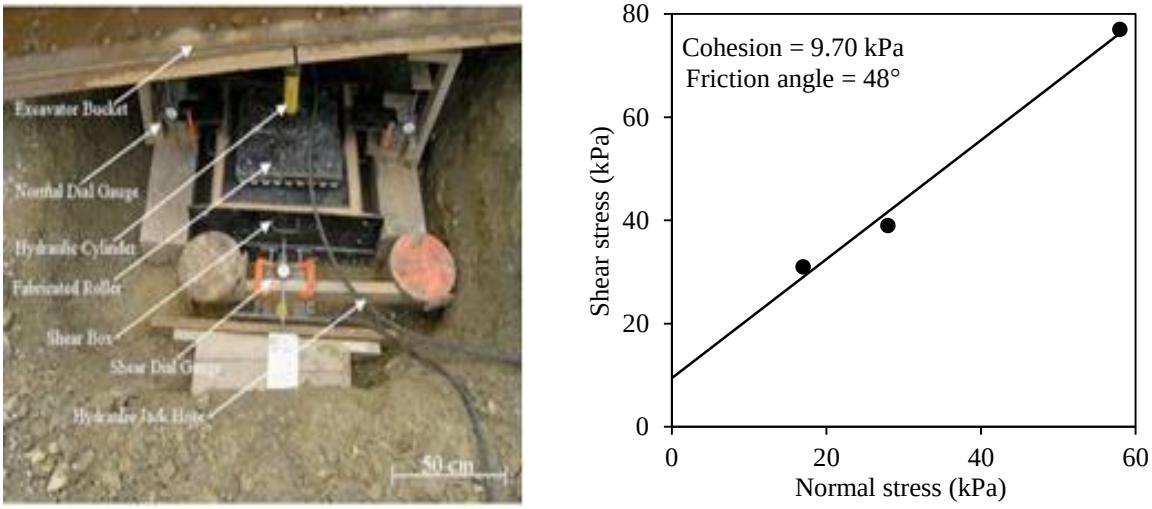

(a) (b)

Figure 2.7 (a) Set up of the in situ direct shear test and (b) Mohr Coulomb failure envelope for the Sugar Shack West rock pile material (taken from Fakhimi et al. (2007) with the permission of reproduction from ASTM International)

Zhang et al. (2016) conducted in situ direct shear tests on a soil-rock sample using a shear box of 600 mm × 600 mm × 300 mm. Figure 2.8 shows the setup of the in-situ shear apparatus. As it is seen in the figure, normal and shear stresses are applied on the sample with jacks. Their experimental results showed that the friction angle of the soil-rock sample decreases as normal stress increases. However, the maximum particle size of the tested samples was not reported.

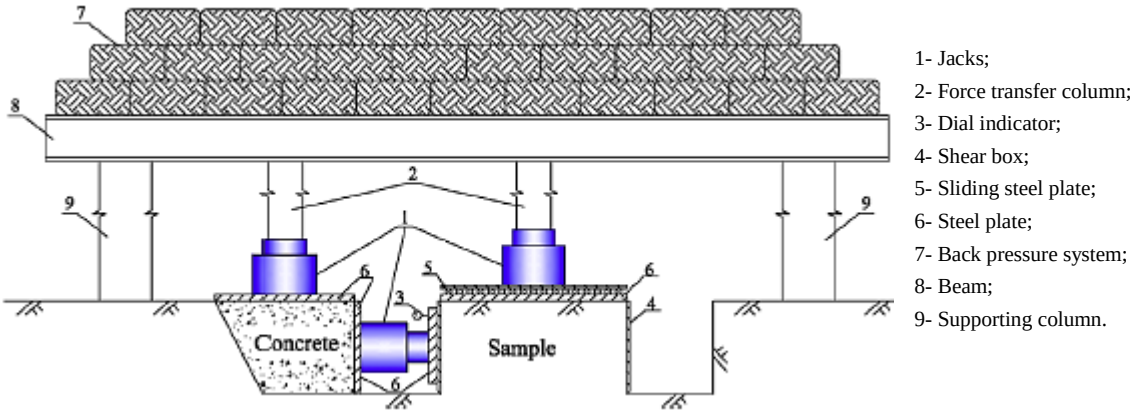

Figure 2.8 Profile of the test equipment of an in situ direct shear test (taken from Zhang et al. (2016) with the permission of reproduction from Elsevier Science & Technology Journals)

Barton and Kjaernsli (1981) conducted in situ tilt tests on rockfill using a rectangular open box composed of three parts (Figure 2.9) to measure the shear strength. To do the tests, the box is first embedded in the rockfill, then filled and compacted. One end of the filled box is lifted after the surrounding fill and the center frame of the box have been removed. The tilt angle at which the upper part of the filled box starts to slide corresponds to the maximum tilt angle α, which is considered as the peak friction angle ϕ at the applied normal stress σ_n. The value of α can be as high as 55° to 65° under a very low normal stress. In comparison to other in situ direct shear test methods, the concept of this technique is simple. Depending on the size of the rockfill, the test box may be as large as required. However, the equipment and test are heavy and costly. When one end of the box is lifted, particles may fall (due to the loss of the confinement originally given by the middle part) before the top part slides. The test results may be not as accurate as expected.

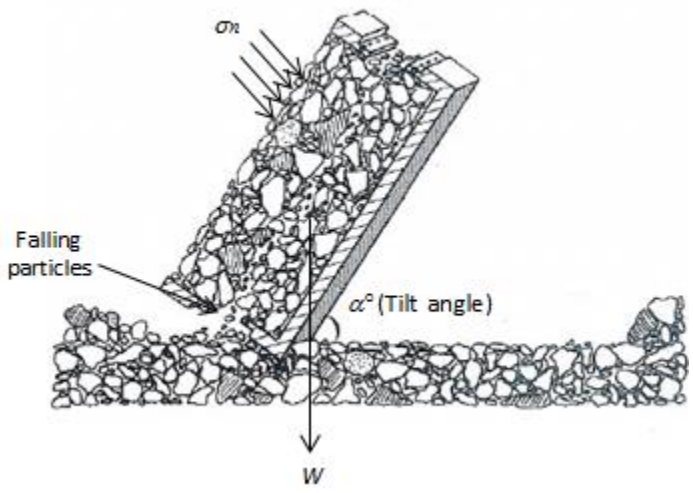

Figure 2.9 A schematic view of the in situ tilt test, when it is lifted for trial rockfill (taken from Barton and Kjaernsli (1981) with the permission of reproduction from ASCE)

With in situ direct shear tests, it is difficult to apply large normal stresses. The peak friction angle can be overestimated for the case of large infrastructures. This problem was partly palliated by Barton and Kjaernsli (1981), who proposed the following equation to estimate friction angle as a function of applied normal stress σ_n:

$$\phi = R.\log(S/\sigma_n) + \phi_b \quad (2.8)$$

where ϕ_b is the base friction angle of the rock (typically ranging from 25° to 35°), and R is equivalent roughness factor, S is the equivalent compression strength of rockfill that can be estimated from the uniaxial compression strength of the rock (σ_c) and d_{50} of the rockfill, as shown in Figure 2.10. σ_c can be estimated from either Schmidt hammer or point load tests. It is seen in the figure that the equivalent strength S decreases with the increased particle size, indicating that the value of this parameter obtained with laboratory samples is probably higher than that of field rockfill.

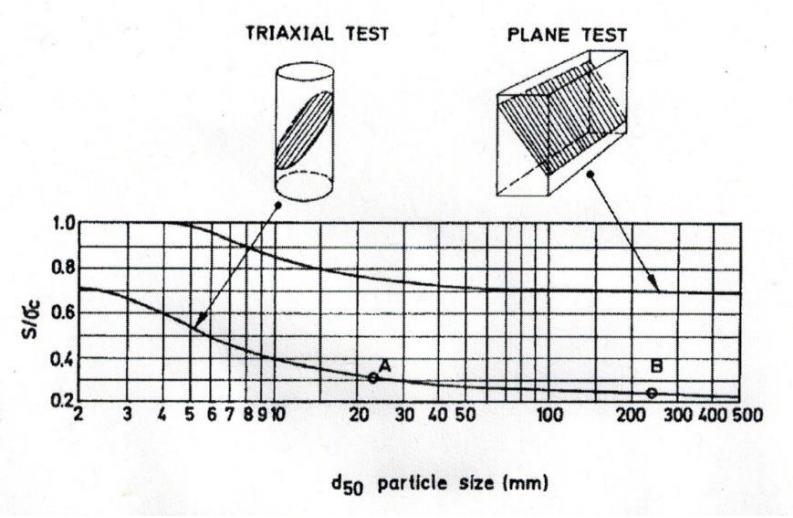

Figure 2.10 Estimation of equivalent strength of rockfill (S) based on σ_c and d_{50} (taken from Barton and Kjaernsli (1981) with the permission of reproduction from ASCE)

The equivalent roughness coefficient (R) can be determined from the porosity of rockfill, roundedness and surface smoothness of particles as shown in Figure 2.11. The degree of roundedness and smoothness of a rockfill depends on its source origin such as quarried rock, talus, moraine, and fluvial deposits. Several classification systems for particle shape and roundedness have also been presented in the past (i.e., Powers, 1953). Based on the previous studies, Barton and Kjaernsli (1981) proposed a graphical method to estimate the parameter R for rockfill by using its origin, roundedness, smoothness and the porosity of materials after compaction (n) (Figure 2.11).

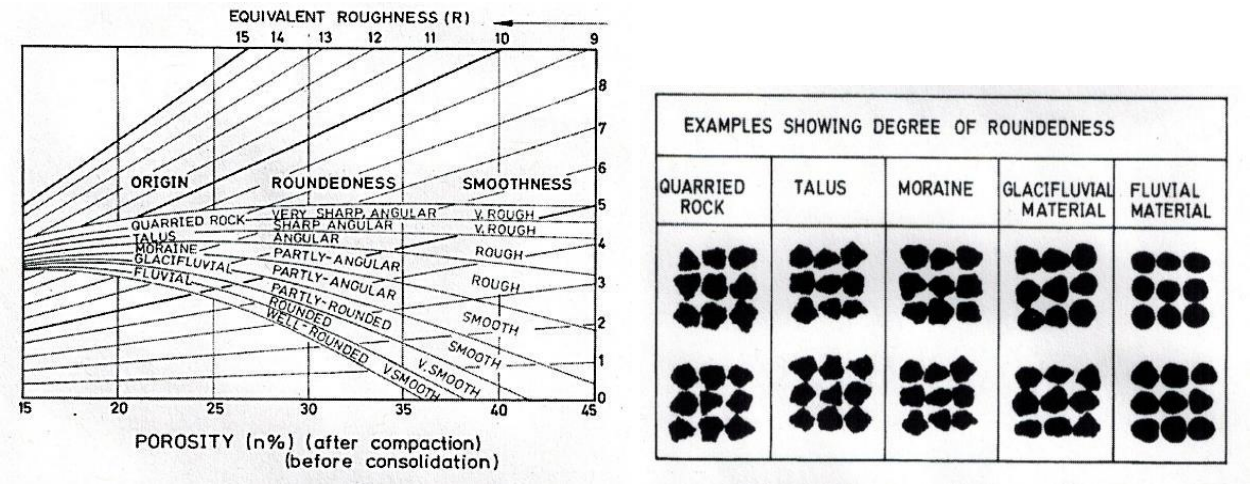

Figure 2.11 Estimation of equivalent roughness of rockfill (*R*) based on the porosity (*n*), origin of materials, roundedness and smoothness (taken from Barton and Kjaernsli (1981) with the permission of reproduction from ASCE)

The equivalent roughness of rockfill (*R*) can also be obtained from large scale tilt tests. Changing the form of Equation (2.8) can lead to the following expression:

$$R = \frac{(\alpha - \phi_b)}{\log(\frac{S}{\sigma_n})} \tag{2.9}$$

In this equation, α is the maximum angle of tilt measured by in situ tilt tests at the applied normal stress σ_n. This equation can be used to back calculate the value of *R*.

Figure 2.12 shows the variation of friction angle as a function of normal stress (σ_n) according to Equations (2.8) and (2.9) with parameters σ_n = 50 kPa, $\phi = \alpha = 50°$, $\phi_b = 28°$ and S = 100 MPa. It indicates that the friction angle decreases as the applied normal stress increases.

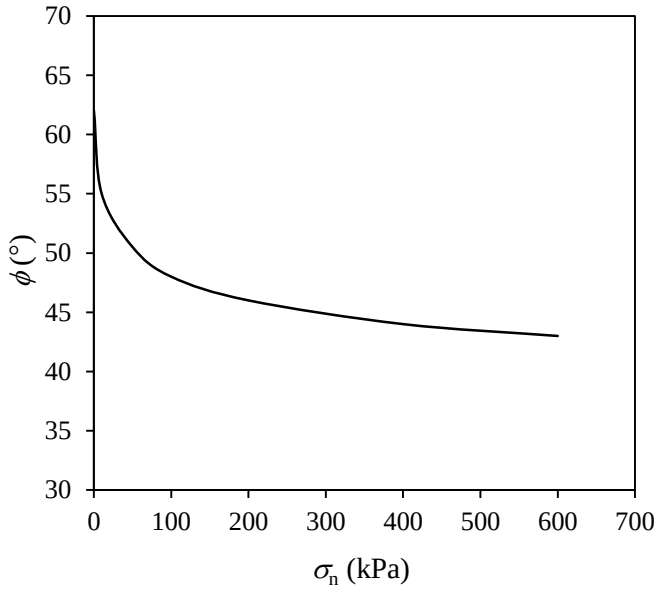

Figure 2.12 Variation of friction angle ϕ (or title angle α) as a function of normal stress (σ_n) according to equations (2.8) and (2.9). (parameters estimated with σ_n = 50 kPa, $\phi = \alpha = 50°$, ϕ_b = 28° and S = 100 MPa)

The short literature review indicates that the normal stresses of in situ tests can be very limited and the test results could be not appropriate for the design of large and high rockfill infrastructures. Other disadvantages of in situ shear tests include the difficulty in supplying equipment and transportation facilities, time-consuming, high costs, and generally intensive labor (Blijenberg, 1995). Finally, finding a suitable and safe location is a non-negligible challenge for in situ shear tests. Consequently, laboratory shear tests are desirable.

2.3.2.2 Laboratory tests

2.3.2.2.1 Large scale shear tests

Large scale shear tests are always preferred to obtain the shear strength of field materials. Large scale direct shear tests and triaxial compression tests can be performed in laboratory. USACE South Pacific Division Laboratory (SPDL; Hall, 1951; Leslie, 1963) and the US Bureau of Reclamation (USBR; Holtz & Gibbs, 1956) are among the earliest ones to have conducted large scale tests in laboratory.

Hall and Gordon (1963) performed large triaxial shear tests to estimate the static and kinetic internal friction angles of a rockfill. A large chamber with 305 mm in diameter and 701 mm in height and a small chamber with 152 mm in diameter and 305 mm in height were used. For the large chamber, applying confining pressure up to 862 kPa and for the small chamber, applying confining pressure up to 6895 kPa was possible. The rockfill with d_{max} values of 38 and 76 mm were used for the small and large apparatuses, respectively. The results showed that the peak friction angle decreases as the confining pressure increases. Their results also showed that the gradation of the materials before and after the triaxial compression tests is different and the difference increases as the confining pressure increases.

Matsuoka and Liu (1998) conducted large scale direct shear tests to determine the shear strength of rockfill. The upper shear box was replaced by two large loading plates. A loading plate of 600 mm × 600 mm × 40 mm was used with a lower shear box (800 mm × 800 mm × 105 mm) to perform direct shear test on an artificial material and rockfill with d_{max} values of 20 and 50 mm, respectively. The specimen width to d_{max} ratios of the tested specimens were 40 and 16, respectively. Another loading plate (600 mm × 600 mm × 100 mm) was used with another lower shear box (800 mm × 800 mm × 210 mm) to conduct direct shear tests on rockfill with d_{max} value of 150 mm. The specimen width to d_{max} ratio of the tested specimen was 5. The minimum specimen width to d_{max} ratio of 12 required by ASTM standard was not respected for the later. Their experimental results showed that the peak friction angle decreases as the normal stress or the initial void ratio increases.

Boakye (2008) determined the shear strength of rock pile materials through laboratory and in situ direct shear tests. In situ shear tests were performed on Sugar Shack West and Spring Gulch Rock Pile materials using large (600 mm × 600 mm) and medium (300 mm × 300 mm) shear boxes. Normal stresses ranging from 15 to 70 kPa were applied to the specimens having a d_{max} value of one 5^{th} the shear box width. Laboratory direct shear tests were conducted on six rock pile materials including Sugar Shack West and Spring Gulch using small (50 mm × 50 mm) shear box. Small (20 to 120 kPa) and large (150 to 650 kPa) normal stresses were applied on the specimens having a d_{max} value of one 5^{th} the shear box width. Their results showed that the peak friction angles obtained by on site direct shear tests are close to those obtained by laboratory direct shear tests when the normal stresses were small. However, the friction angles obtained by

laboratory direct shear tests using large normal stresses were smaller than those obtained by either in situ tests or laboratory shear tests with low normal stresses.

Ovalle et al. (2014) performed triaxial compression tests on quarried calcareous rockfill and quartzite shale rockfill. The test specimen of rockfill with a d_{max} value of 40 mm was prepared having a diameter of 250 mm and a height of 375 mm while the test specimen of rockfill with a d_{max} value of 160 mm had 1000 mm in diameter and 1500 mm in height. The minimum required specimen size ratio of 6 specified by ASTM D4767 (2011) was used. Their test results showed slight decrease in the shear strengths of rockfill materials as d_{max} value increases. Similar results have been reported by Hall and Gordon (1963).

2.3.2.2.2 Scaling down techniques

When large scale equipment is unavailable, small scale shear tests are necessary determine the shear strength of coarse granular materials, including vane shear test, ring shear test, direct simple shear test, unconfined compression test, direct shear test, and triaxial compression test.

Direct shear test and triaxial compression test are the common used methods to determine shear strength of field materials in laboratory. In order to meet the minimum required specimen size to $d_{\max}$ ratios specified in the corresponding test standards (e.g., BS 1377-7 1990; AS 1289.6.2.2 1998; Eurocode 7 2007; ASTM D3080/D3080M 2011), the testing samples have to be prepared by excluding the oversized particles. The obtained samples with smaller $d_{\max}$ values can then be used to perform shear tests (Holtz & Gibbs, 1956; Hamidi et al., 2012; Chang & Phantachang, 2016; Yang et al., 2019; Ovalle et al., 2020). The sample preparation method by excluding oversized particles from the field materials is called scaling down technique (Hennes, 1953; Zeller & Wullimann, 1957; Lowe, 1964; Fumagalli, 1969; Donaghe & Torrey, 1985). There are four scaling down techniques, named scalping, parallel, replacement, and quadratic techniques.

Hennes (1953) proposed the first scaling down technique, known as scalping or truncated method. The oversized particles are eliminated in this method. Lowe (1964) proposed the parallel scaling down technique in order to obtain a gradation curve parallel to that of field material. USACE (1965) developed the replacement scaling down technique to maintain the percentages of fine particles unchanged compared to that of the field material. Quadratic scaling down technique was proposed by Fumagalli (1969) in order to obtain a particular gradation curve.

Scalping technique

Due to the capacity limitations of laboratory equipment, laboratory shear tests are only possible by excluding the particles larger than the targeted d_{max} during field sampling or during sample preparation in the laboratory. The technique was first introduced by Hennes (1953) and named scalping technique. Later, it has been commonly used in sample preparation for laboratory tests (Holtz & Gibbs, 1956; Zeller & Wullimann, 1957; Leslie, 1963; Morgan & Harris, 1967; Hall & Smith, 1971; Williams & Walker, 1983; Donaghe & Torrey, 1985; Seif El Dine et al., 2010; Hamidi et al., 2012; Deiminiat et al., 2020; Dorador & Villalobos, 2020a; MotahariTabari & Shooshpasha, 2021).

Zeller and Wullimann (1957) performed triaxial compression tests to determine shear strength of a rockfill. The scalping technique was applied to obtain scaled down samples with d_{max} values of 100, 30, 10 and 1 mm from a field rockfill having a d_{max} value of 600 mm. Figure 2.13a shows the PSDC of the scalped down samples. The specimen diameter to d_{max} ratio of 5 was used for the all specimens. Figure 2.13b shows the variation of shear strengths of the scalped down samples at a confining pressure of 88 kPa as a function of d_{max} for porosities of 30% and 38%. For each porosity, the shear strength of the scalped samples decreases significantly as the d_{max} increases. By applying the bet-fitting technique, the shear strength of field sample with d_{max} value of 600 mm can be estimated through extrapolation. However, one cannot give any conclusion on the reliability of the predicted shear strength of field rockfill or the reliability of scalping technique since the shear strength of field material with d_{max} value of 600 mm was not measured.

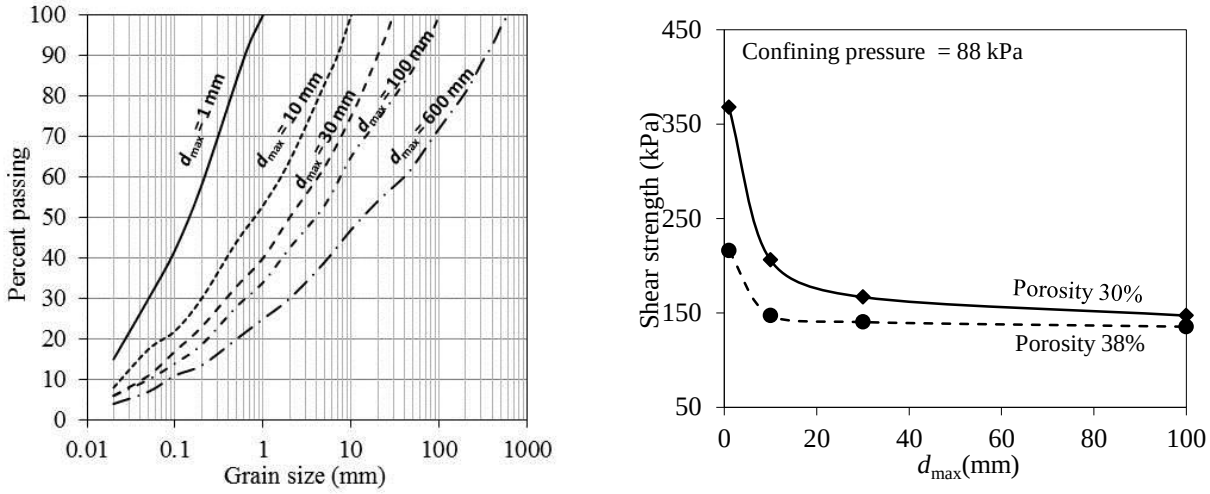

(a) (b)

Figure 2.13 (a) PSD curves of the prototype and scalped samples and (b) variations of shear strength with the d_{max} of the field material and modeled samples for different porosities; data taken from Zeller and Wullimann (1957)

Figure 2.14 shows the PSD curve of a rockfill and those of the scalped down sample reported by Williams and Walker (1983). Scalped down sample with d_{max} of 19 mm was obtained from a field material with d_{max} of 200 mm. As shown in the figure, excluding the oversized particles results in an increase of the percentage of the particle sizes smaller than 19 mm compared to the field material.

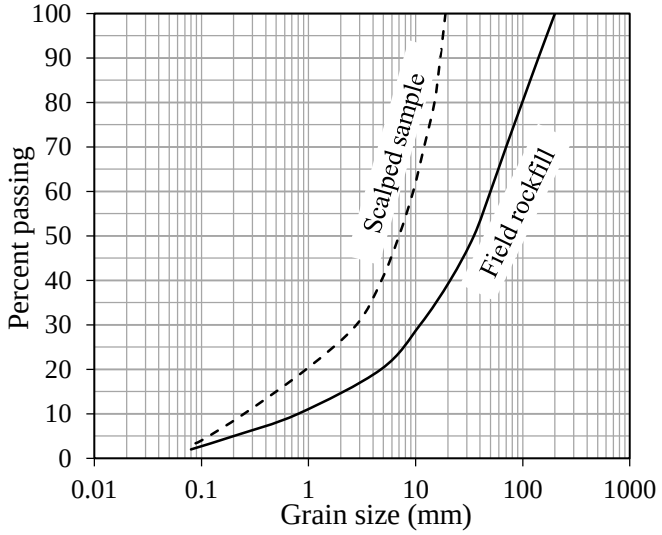

Figure 2.14 PSD curves of the field sample and scalped sample; data taken from Williams and Walker (1983)

The previous studies show that the PSD curve of the scalping samples differs from that of the field material. The percentages of the particle sizes smaller than targeted d_{max} in the scalped sample are higher than those in the field material. The scaled down sample is finer than the field material. The friction angle of scaled down samples is not representative of that of the field material (Fragaszy et al., 1992; Bareither et al., 2008; Dorador & Villalobos, 2020a).

Parallel scaling down technique

Another scaling down technique is to obtain a scaled down sample that has a gradation curve parallel to that of the field material (Lowe, 1964; Tombs, 1969; Charles, 1973). The PSD curve of the scaled down sample looks like a horizontal shift of the field material's PSD curve towards the finer side in the semi-log plane.

To produce a scaled down sample with a d_{max} value of $d_{max.p}$ by applying the parallel technique on a field material with d_{max} value of $d_{max.f}$, the shift distance (N) can be calculated using the following equation:

$$N = \frac{d_{max.f}}{d_{max.m}} \tag{2.10}$$

The particle sizes of the scaled down samples at a given percentage can be obtained by using the following equation:

$$d_{p.m} = \frac{d_{p.f}}{N} \tag{2.11}$$

where $d_{p.m}$ and $d_{p.f}$ are the particle sizes of modeled sample and field material having a percentage passing p, respectively.

When the parallel gradation curve is obtained, the parallel scaled down sample can be prepared by calculating the required masses of different ranges of particle sizes using the portions of the particle sizes and overall mass of the sample.

Although the purpose of using parallel technique is to produce a gradation curve parallel to the field material's gradation curve, its application is difficult in practice. Certain particle sizes

obtained by applying Equations (2.10) and (2.11) may have no matched sizes among the standard sieves. In addition, fine particles smaller than the minimum particle size of the field material are necessary but unavailable. As a result, the scaled down samples may totally differ from the field material.

Figure 2.15 shows the PSD curve of a scaled down sample obtained by applying parallel technique on a field material. The field material has a d_{max} of 305 mm, whereas the d_{max} value of scaled down sample is 38 mm. The scaled down sample is horizontally shifted to the finer (or left) side of the PSD curve using the shift distance of 8 (=305/38).

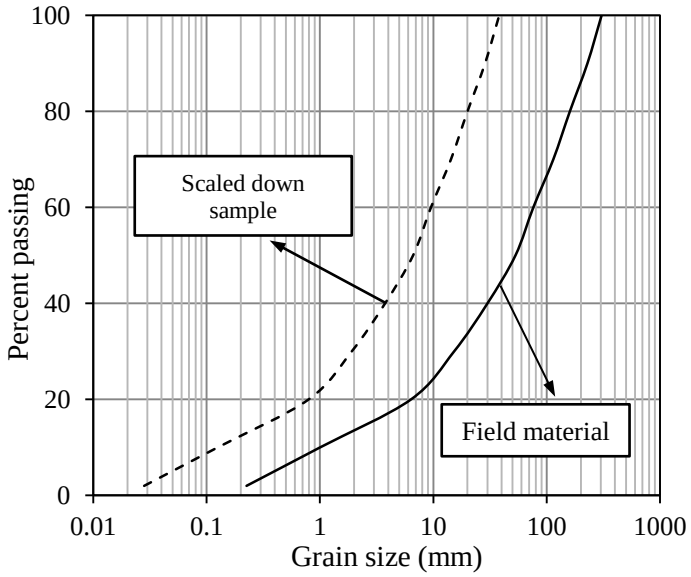

Figure 2.15 PSD curves of the field material and scaled down samples; data taken from Lowe (1964)

Marachi (1969, 1972) performed triaxial shear tests on the scaled down samples obtained by applying parallel technique to PSD of three field materials (Pyramid dam, Crushed basalt and Oroville dam). Two samples contain well-graded and angular particles and the third sample was a mixture of sub-angular and rounded particles. The specimen diameters were 71, 305 and 914 mm for the samples with d_{max} of 12, 51 and 152 mm, respectively. The minimum required specimen size over d_{max} ratio of 6 specified by ASTM D4767 (2011) was used for all the specimens. The same confining pressures of 207, 965, 2896 and 4482 kPa, respectively were also used for all samples. As it is presented in Table 2.4, regardless of the particle shape of the materials, the

internal friction angles of all the samples decrease when the d_{max} increases. Since there are no test results for the field materials, this study cannot help to verify the reliability of the parallel technique.

Table 2.4 Peak friction angles obtained for Pyramid dam, Crushed basalt and Oroville dam materials with different confining pressures; data taken from Marachi et al. (1972)

Material	d_{max} **(mm)**	**Peak friction angle (°)**			
		σ_3 **= 207 kPa**	σ_3 **= 965 kPa**	σ_3 **= 2896 kPa**	σ_3 **= 4482 kPa**
Pyramid dam	12	51.7	43.6	38.8	37.2
	51	47.8	41.0	37.5	36.0
	152	46.2	39.8	36.1	35.0
Crushed basalt	12	51.5	44.0	40.0	39.0
	51	49.0	42.5	39.0	38.0
	152	48.0	40.5	36.5	35.5
Oroville dam	12	51.5	47.0	43.0	41.0
	51	48.5	44.0	41.0	39.0
	152	47.0	43.5	40.0	38.0

Similarly, Charles (1973) applied parallel technique on a rounded rockfill with d_{max} value of 900 mm to conduct triaxial compression tests on the scaled down samples with d_{max} values of 40 mm, 100 mm and 300 mm. The specimen size over d_{max} ratio of all the scaled down samples was 5. Figure 2.16 shows the variation of the peak friction angles of the scaled down samples against d_{max} for different confining pressures. As shown in the figure, the friction angle increases slightly as d_{max} increases. This trend is in opposite with the trend reported by Marachi (1972) for the angular and rounded materials. This inverse trend can be due to the difference in the particle shape of the materials.

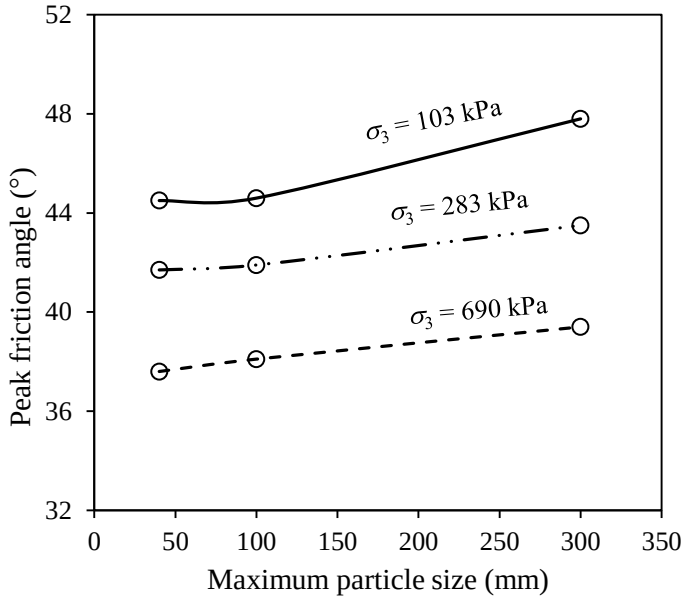

Figure 2.16 Variation of peak friction angle with d_{max} for the scaled down samples with different confining pressures; data taken from Charles (1973)

Table 2.5 shows the variation of peak friction angle (ϕ) with d_{max} for rounded and angular materials collected from the literature. The parallel technique was used in these studies to scale down the field materials to the samples with different d_{max} values. As shown in the table, the friction angle of rounded material increases when the d_{max} increases while the friction angle of angular material decreases when the d_{max} increases.

These results clearly indicate the influence of particle shape on the friction angles of the scaled down samples obtained by applying parallel technique. But it is not clear whether the parallel technique can predict reliable shear strength of field materials.

Table 2.5 Summary of the experimental peak friction angles taken from the literature for rounded and angular materials with different d_{max} (taken from the references given in the table)

Material	**ϕ (°)**	**Variation of ϕ**	**Material**	**ϕ (°)**	**Variation of ϕ**	**Reference**
Rounded, d_{max} = 25 (mm)	31.5	Increase	Angular, d_{max} = 25 (mm)	32.5	Decrease	Varadarajan et al. (2003)
Rounded, d_{max} = 50 (mm)	33.2		Angular, d_{max} = 50 (mm)	31.4		
Rounded,	35.4		Angular,	30.6		

d_{max} = 80 (mm)			d_{max} = 80 (mm)			
Rounded, d_{max} = 25 (mm)	36.0	Increase	Angular, d_{max} = 25 (mm)	40.8	Decrease	Varadarajan et al. (2006)
Rounded, d_{max} = 50 (mm)	39.5		Angular, d_{max} = 50 (mm)	42.0		
Rounded, d_{max} = 80 (mm)	43.0		Angular, d_{max} = 80 (mm)	43.0		
Rounded, d_{max} = 25 (mm)	31.5	Increase	Angular, d_{max} = 25 (mm)	32.5	Decrease	Gupta (2009)
Rounded, d_{max} = 50 (mm)	33.2		Angular, d_{max} = 50 (mm)	31.4		
Rounded, d_{max} = 80 (mm)	35.4		Angular, d_{max} = 80 (mm)	30.6		
Rounded, d_{max} = 4.76 (mm)	44.0	Increase				Bagherzadeh & Mirghasemi (2009)
Rounded, d_{max} = 25.4 (mm)	49.0					
Rounded, d_{max} = 25 (mm)	36.2	Increase	Angular, d_{max} = 25 (mm)	42.9	Decrease	Abbas (2011)
Rounded, d_{max} = 50 (mm)	39.6		Angular, d_{max} = 50 (mm)	42.3		
Rounded, d_{max} = 80 (mm)	42.8		Angular, d_{max} = 80 (mm)	40.8		
			Angular, d_{max} = 25 (mm)	41.5	Decrease	Rao et al. (2011)
			Angular, d_{max} = 50 (mm)	41.0		
			Angular, d_{max} = 80 (mm)	40.1		
Rounded, d_{max} = 25 (mm)	31.0	Increase	Angular, d_{max} = 25 (mm)	33.0	Decrease	Vasistha et al. (2013)
Rounded, d_{max} = 50 (mm)	33.0		Angular, d_{max} = 50 (mm)	31.5		
Rounded, d_{max} = 80 (mm)	36.0		Angular, d_{max} = 80 (mm)	30.0		
Rounded, d_{max} = 20 (mm)	44.9	Increase	Angular, d_{max} = 20 (mm)	45.1	Decrease	Pankaj (2013)
Rounded, d_{max} = 40 (mm)	47.1		Angular, d_{max} = 40 (mm)	44.2		
Rounded, d_{max} = 60 (mm)	48.4		Angular, d_{max} = 60 (mm)	43.7		
Rounded,	49.3		Angular,	43.0		

d_{max} = 80 (mm)			d_{max} = 80 (mm)			
Rounded, d_{max} = 25 (mm)	37.1	Increase	Angular, d_{max} = 25 (mm)	43.4	Decrease	Honcanadavar et al (2014)
Rounded, d_{max} = 50 (mm)	38.4		Angular, d_{max} = 50 (mm)	42.4		
Rounded, d_{max} = 80 (mm)	39.8		Angular, d_{max} = 80 (mm)	40.8		
Rounded, d_{max} = 19 (mm)	39.9	Increase				Honkanadavar et al (2016)
Rounded, d_{max} = 25 (mm)	40.8					
Rounded, d_{max} = 50 (mm)	42.5					
Rounded, d_{max} = 80 (mm)	43.9					

Despite the widespread use of the parallel method in engineering and research projects, it is still unclear whether the friction angle of the field materials can be predicted by applying the extrapolation technique on the friction angles of the scaled down samples prepared by applying parallel technique.

Replacement technique

The replacement technique consists of replacing particles coarser than the targeted d_{max} with particles finer than d_{max} but greater than No. 4 sieve (4.75 mm). The percentage of particles smaller than the No. 4 sieve thus remains constant (USACE, 1965; Frost, 1973; Donaghe & Torrey, 1985). This method was initiated by Frost (1973) to conduct compaction tests on boulder-gravel materials.

Figure 2.17 shows the PSD curves of a field material with a d_{max} value of 80 mm and a scaled sample with a d_{max} value of 20 mm (Donaghe & Townsend, 1976). The PSD curve of the field material was obtained by measuring the mass of the particles retained on different sieves and total mass of the field material. The particles larger than the targeted d_{max} of 20 mm were then weighted and removed. The same masses of the particle sizes larger than 4.75 mm and smaller than 20 mm were added to the sample. The gradation curve of the scaled down sample can then be obtained using the following equation (Donaghe & Townsend, 1976):

$$P_{ij.a} = \frac{P_{ij.f}}{P_{d_{max}} - P_{No.4}} \times P_o \qquad (2.12)$$

where $P_{ij,a}$ is the percentage by mass of added particles passing sieve having size j ($\leq d_{max}$) and retained on the neighbor sieve having size i ($\geq$ 4.75 mm); $P_{ij,f}$ is the percentage by mass of field material particles passing sieve size j ($\leq d_{max}$) and retained on the sieve size i ($\geq$ 4.75 mm); P_{dmax} is the percentage of field material particles passing the targeted d_{max}; $P_{No.4}$ is the percentage of field material particles passing the sieve of 4.75 mm (i.e., sieve No. 4); P_o is the percentage by mass of field material particles retained on the sieve having a size of the targeted d_{max}. All symbols are shown in Figure 2.17 for better understanding on each parameter.

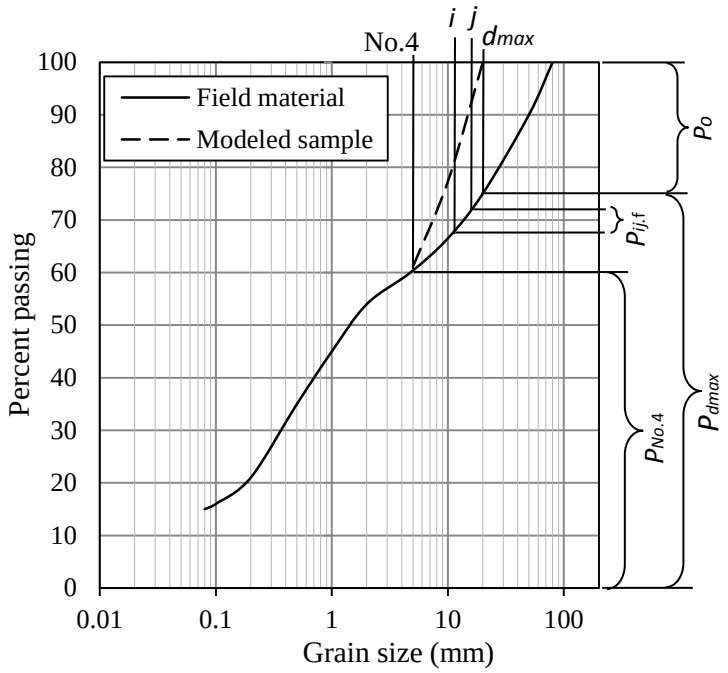

Figure 2.17 PSD curves of field material and scaled down (modeled) sample; data taken from Donaghe and Townsend (1976)

As shown in figure 2.17, the gradation curve of the modeled (i.e. scaled down) sample changes compared to that of the field sample for particles larger than 4.75 mm. As a result, applying the replacement technique significantly modifies the gradation curve of field material (Donaghe & Townsend, 1976; Rathee, 1981; Feng & Vitton, 1997). This observation seems to be highlighted for the field materials having higher percentages of coarse grain particle (Torrey & Donaghe, 1991; Feng & Vitton, 1997).

Quadratic grain-size technique

Fumagalli (1969) proposed to modify the PSD curve of scaled down samples by the following equation:

$$P_Q = \sqrt{d/d_{max}} \times 100\% \quad (2.13)$$

where d is a particle size of the scaled down sample, smaller than the target d_{max}; P_Q is the percentage by mass of the particles smaller than d of the scaled down sample.

Fumagalli (1969) applied quadratic technique on a rockfill with d_{max} value of 260 mm to prepare several scaled down samples with d_{max} values of 10, 20, 30, 60 and 100 mm. The shear strength of the scaled down samples was measured to range from 23° to 25°.

One notes that applying Equation (2.13) results in a PSD curve as long as a target d_{max} value is chosen. The scaled down sample is entirely artificial and independent on the PDS curve shape and d_{max} value of field material. The physical meaning of such scaled down samples is unclear. This may explain why the technique has never been used since its publication in 1969.

Reliability of the scaling down techniques

Over the years, some studies have been accomplished to investigate the reliability of the scaling down techniques. Donaghe and Torrey (1985) studied the validity of scalping and replacement techniques by using mixtures of sub-rounded to sub-angular sand and sub-rounded to sub-angular gravel with d_{max} value of 76 mm. Mixtures were made by using 20% gravel and 80% sand, 40% gravel and 60% sand and 60% gravel and 40% sand. The scalping and replacement techniques were applied to the mixtures to prepare the scaled down samples with d_{max} values of 4.75 mm and 19 mm, respectively. The peak friction angles of the scaled down samples were measured by using triaxial compression tests. The specimen size over d_{max} ratios of the scaled down samples were 32 and 9, respectively and the specimen size over d_{max} ratio of the field material was 5.

Figure 2.18 shows the variations of the peak friction angle as a function of d_{max} for confining pressures of 418 kPa (Figure 2.18a) and 1380 kPa (Figure 2.18b), respectively. In both cases, one can see the direct comparisons between the peak friction angles of the different scaled downs samples and those of the field materials. The friction angles of the scaled down samples using the replacement technique decrease as d_{max} increases, while the friction angles of the scaled down samples using scalping technique increase as d_{max} increases except for the samples with 20%

gravel in which the friction angle remains constant. This methodology used to test the reliability of scaling down techniques is not appropriate because it implicitly assumes that the friction angle of scaled down sample should remain unchanged.

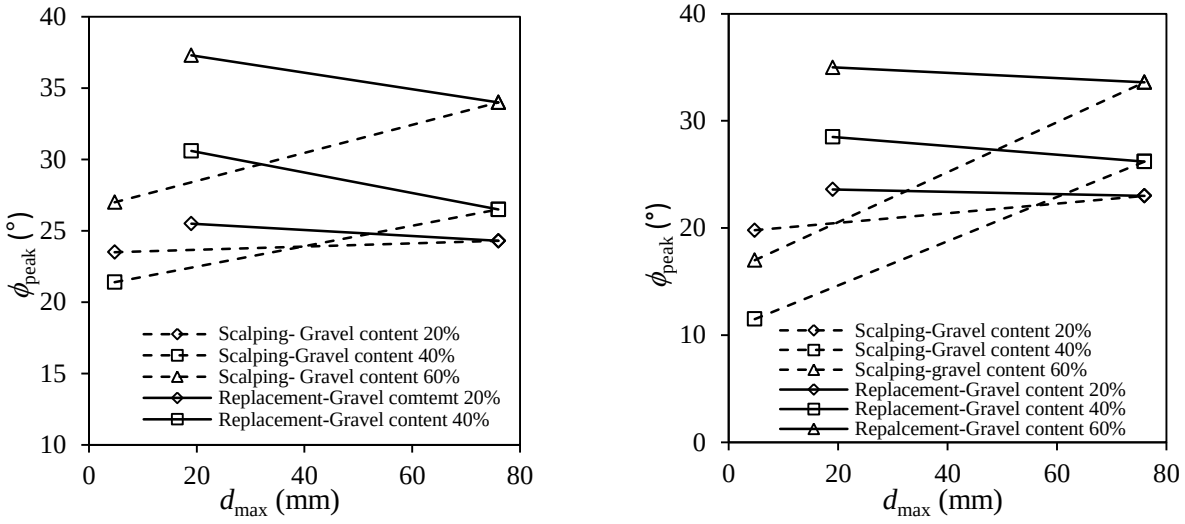

(a) (b)

Figure 2.18 Comparison of the peak friction angles of the scaled down samples with field samples for confining pressure equal to (a) 418 kPa and (b) 1380 kPa; data taken from Donaghe and Torrey (1985)

Hamidi et al. (2012) studied the reliability of scalping and parallel scaling down techniques by conducting direct shear tests using a shear box 300 mm wide, 300 mm long and 170 mm thick. Scalping and parallel techniques were applied to the field material containing a mixture of sand and gravel with d_{max} value of 25.4 mm to prepare the scalping and parallel scaled down samples with $d_{\max}$ value of 12.5 mm. The specimen width over d_{max} ratios of the field material and scaled down samples were 12 and 24, respectively. The specimens were prepared at three states: loose with a relative density of D_r = 35%, intermediate with D_r = 60%, and dense with D_r = 85%. Three normal stresses of 100, 200 and 300 kPa were used. Figure 2.19 shows the variations of peak friction angles obtained at different relative densities with $d_{\max}$ for field samples and scaled down samples. The friction angles of the scalping scaled down samples are closer to those of the field samples than those of the parallel scaled down samples. Again, direct comparison between the friction angles of scaled down samples and those of the field samples is not an appropriate

methodology to test the reliability of a scaling down technique. Rather, more tests on the scaled down samples with different d_{max} values are required to establish a relationship between the friction angle and d_{max} by applying bet-fitting technique. The equation can then be used to predict the friction angle of the field materials through extrapolation. A comparison between the predicted and measured friction angles of the field materials can show the reliability of the scaling down technique.

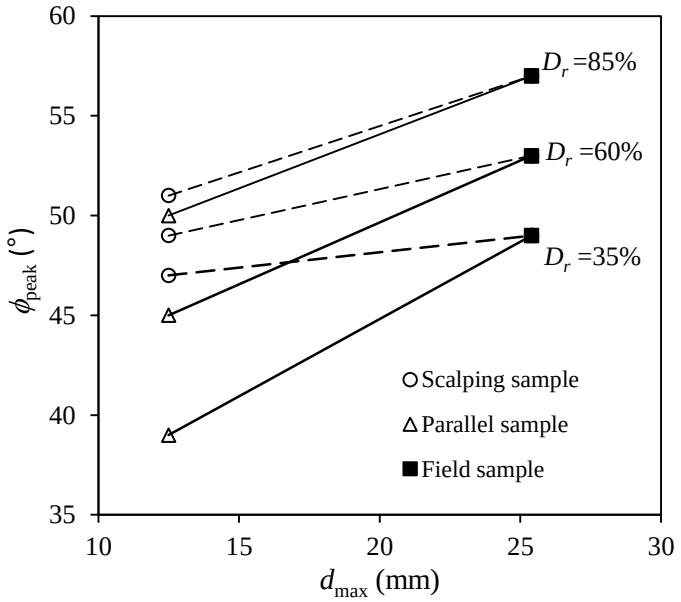

Figure 2.19 Variations of friction angles of field, parallel and scalping samples as a function of maximum particle size for different relative densities; data taken from Hamidi et al. (2012)

Bagherzadeh and Mirghasemi (2009) also investigated the reliability of scalping and parallel techniques. Both techniques were applied to ellipsoidal gravel with d_{max} of 50 mm to prepare the scaled down samples with d_{max} values of 4.76 mm and 25.4 mm. Direct shear tests were conducted on field and scaled down samples using 60 mm × 60 mm and 300 mm × 300 mm shear boxes. Three normal stresses of 95, 196 and 294 kPa were used. The specimens were prepared with the specimen width over d_{max} ratio of 12. The variation of shear strength versus d_{max} at applied normal stresses is plotted in Figure 2.20. As shown in the figure, the shear strength of the field sample can be predicted by scalping and parallel techniques when the normal stress is high, while none of the scaling down techniques predict well the shear strength of the field sample when the normal stress is low or medium.

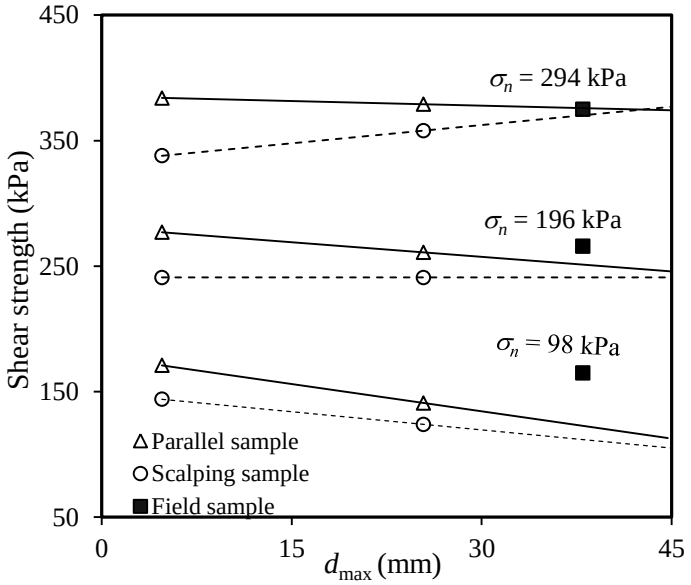

Figure 2.20 Variation of shear strength as a function of d_{max} for parallel, scalping and field samples at different normal stresses; data taken from Bagherzadeh and Mirghasemi (2009)

Xu et al. (2018) studied the variation of the friction angle of scaled down samples prepared by applying scalping technique on a rock fill. The field material has a d_{max} value of 75 mm, while the scaled down samples were prepared to have d_{max} values of 2.36, 4.75, 9.5, 19 and 37.5 mm. Direct shear tests were carried out on the field and scaled down samples using a large square shear box (300 mm × 300 mm × 200 mm) under normal stresses of 250, 500 and 1000 kPa. The specimen width over d_{max} ratios of the specimens were 127, 63, 32, 16, 8 and 4, respectively. The ratios of 4 and 8 are smaller than the minimum required specimen size over d_{max} ratio specified by ASTM D3080/D3080M-11. Figure 2.21 presents the variation of peak friction angle as a function of d_{max} for all the samples. As shown in the figure, the friction angle increases as d_{max} increases. By applying the regression model on the experimental data of scaled down samples, it is clearly seen that the friction angle of the field sample with d_{max} = 75 mm is not well predicted.

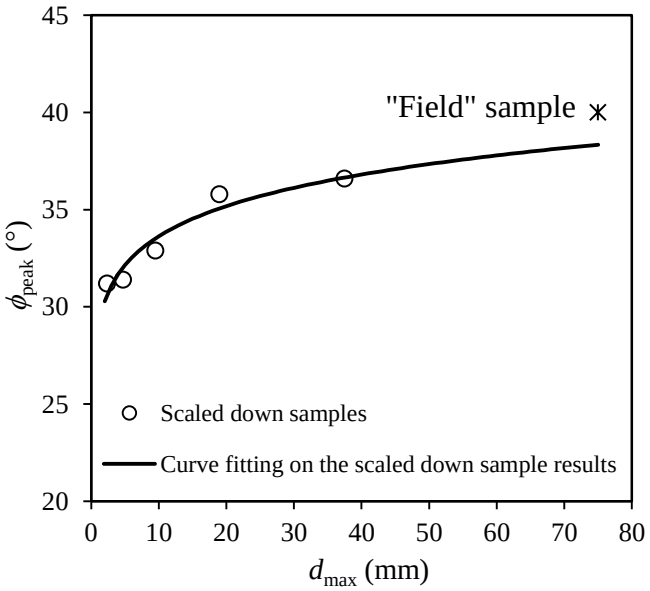

Figure 2.21 Variation of peak friction angle as a function of d_{max}, obtained by direct shear test measurements with samples prepared by applying scalping down technique; data taken from Xu et al. (2018)

Kouakou et al. (2020) investigated the reliability of parallel technique with two types of soils with varying fine contents. The first field material used to prepare the scaled down samples is an angular limestone with a d_{max} value of 80 mm containing a very low percentage of fine particles, while the second one is a sub-round to rounded gravel with a d_{max} value of 120 mm containing a high portion of fine particles. The obtained scaled down samples of gravel have d_{max} values of 5, 15 and 30 mm, while the scaled down samples of limestone have d_{max} values of 5 and 30 mm. The specimen size over d_{max} ratios are 12 and 10, respectively for the direct shear tests. Figure 2.22 shows the variation of peak friction angle with d_{max} for the scaled down samples of gravel and limestone prepared by applying parallel technique. For the limestone, the friction angle of the scaled down sample is very close to that of the field sample. For the gravel samples, the peak friction angle of the field sample cannot be predicted by applying the best-fitting technique on the peak friction angles of the scaled down samples.

These results tend to indicate that the friction angle of scaled down samples prepared by following the parallel technique can be sensitive or insensitive to the variation of d_{max} value. It is

difficult to draw a clear and general conclusion on whether the friction angle of the field sample can be predicted by those of scaled down samples prepared by parallel scaling down technique.

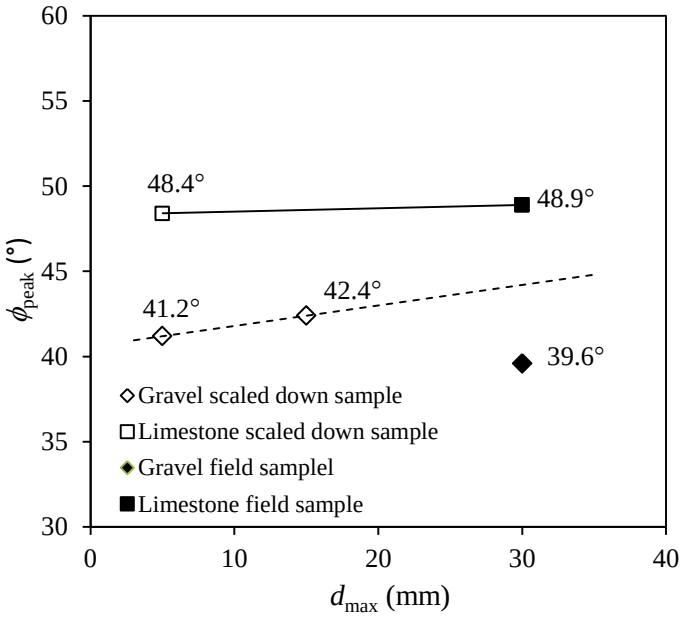

Figure 2.22 Variation of peak friction angle as function of d_{max} obtained by direct shear tests for the field and scaled down samples of gravel and limestone; data taken from Kouakou et al. (2020)

2.3.3 Influencing factors on the shear strength of coarse granular materials

The friction angle of granular materials depends upon several influencing factors such as PSD curve, d_{max}, fine and gravel contents, particle shape, density, water content, etc. Table 2.6 presents some friction angles obtained on different coarse granular materials. The friction angle typically ranges from 35° to 45° (Holtz & Gibbs, 1956; Leslie, 1963; Marachi et al., 1969; Matsuoka & Liu, 1998; Varadarajan et al., 2006; Fakhimi et al., 2007; Boakye, 2008; Abbas, 2011; Vasistah et al., 2013; Honkanadavar et al., 2016).

Table 2.6 Summary of the friction angles (ϕ) of coarse granular materials

Material	**Particle shape**	ϕ (°)	**Reference**
River gravel	Sub-rounded	37.9	Holtz and Gibbs (1956)
Quarry	Sub-angular	40.0	
Pyramid dam rockfill	Angular	33.3 - 51.5	Marachi et al. (1972)
Crushed basalt	Angular	36.5 - 51.5	

Oroville dam rockfill	Rounded	38.0 - 51.5	
Sand and gravel mixture	Sub-rounded and sub-angular	34.0	Donaghe and Torrey (1985)
Coarse discard	Unknown	29.0 – 37.0	Bell (1996)
Mine rock piles	Unknown	35.0 – 40.0	Williams (2000)
Rockfills	Unknown	35.6 – 38.0	Matsuoka et al. (2001)
Porphyry, granite	Unknown	34.1 – 36.9	Earley et al. (2003)
Tehri dam	Angular	36.0 – 42.8	Varadarajan et al. (2006)
Kol dam	Angular	33.0 – 36.0	
Ranjit Sugare dam	Angular	38.0 – 48.0	
Shab Nehar dam	Angular	33.5 – 38.0	
Kol dam	Rounded	41.0 – 43.0	
Pourulia dam	Rounded	39.0 – 42.0	
Parbati dam	Rounded	41.5 – 42.5	
Rock pile materials	Unknown	48.0	Fakhimi et al. (2007)
Sand and gravel mixture D_r = 35%	Rounded	49.0	Hamidi et al. (2012)
Sand and gravel mixture D_r = 60%	Rounded	53.0	
Sand and gravel mixture D_r = 85%	Rounded	57.0	
Quarry rockfill	Angular	43.0 – 45.0	Pankaj et al. (2013)
Riverbed rockfill	Rounded	44.9 – 49.3	
Quarry	Angular	31.2 – 40.0	Xu et al. (2018)
Gravel	Unknown	39.6 – 41.2	Kouakou et al. (2020)

2.3.3.1 Particle size distribution

Many researchers have reported the influence of PSD on the interlocking of coarse granular materials, which in turn affects the shear strength. As the interlocking of particles increases with the increased particle sizes (Hossain et al., 2000; Varadarajan et al., 2006; Valenzuela et al. 2008; Hu et al. 2011; Linero et al., 2007), it can be expected that the friction angle increases with particle size. With a well-graded material having a large coefficient of uniformity ($C_u \geq 20$), the frictional angle can be higher (Marsal, 1967; Leps, 1970; Holtz & Kovacs, 1981; Linero et al., 2007; Bagherzadeh et al., 2011). The friction angle typically decreases as the coefficient of uniformity C_u decreases (Hawley, 2001; Holtz et al., 2011).

Marsal (1967) performed large-scale triaxial compression tests on well-graded and uniform rockfills. The former exhibited larger shear strengths than the latter. The same phenomenon was observed by Leps (1970) and Holtz et al. (2011).

2.3.3.1.1 Fine and gravel contents

In soils with relatively fine particles such as fine sands and gravels, an increase in the coarse grained content results in the increase in friction angle (Leps, 1970; McLemore et al., 2009). With addition of fine particles such as silt and sand, the voids between coarse particles can be filled with such fine particles, resulting in the decrease in the friction angle (Statham, 1974; Douglas, 2002).

Rathee (1981) conducted direct shear tests on a mixture of sand and gravel. The friction angle of the material with a d_{max} value of 25 mm and a relative density of 75 percent increased 8.8%, 14.7% and 22% as the gravel content increased 10%, 20% and 50%, respectively. Similarly, Salimi et al. (2008) performed direct shear tests on rounded and angular materials to investigate the influence of gravel and fine particles on the friction angle of a sand-gravel mixture with a relative density of 60%. Their results show that the peak friction angle increases as the gravel content increases and decreases as the fine content increases, as shown in Figure 2.23, regardless of the particle shape.

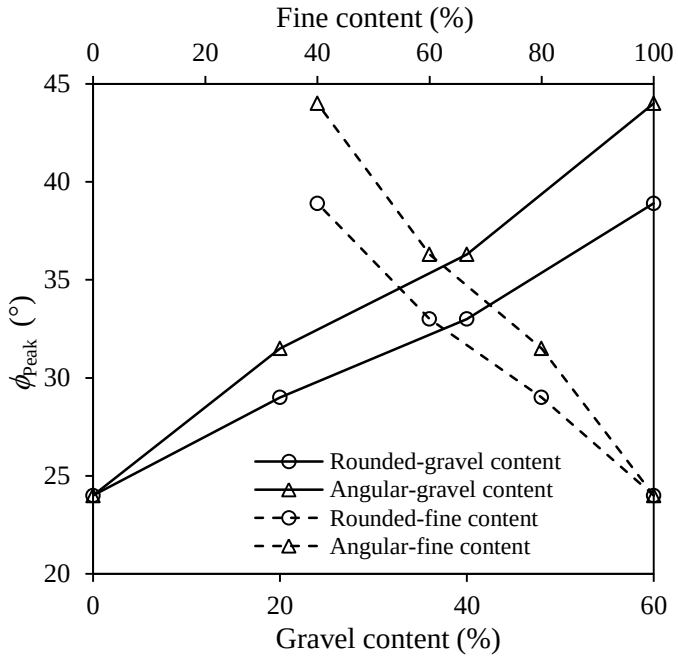

Figure 2.23 Variation of peak friction angle with gravel and fine contents; data taken from Salimi et al. (2008)

2.3.3.1.2 Maximum particle size (d_{max})

Over the decades, many researchers have investigated the influence of d_{max} of granular materials on friction angle (Vallerga et al., 1957; Hall & Gordon, 1963; Ramamurthy & Gupta, 1986; Venkatachalam, 1993; Sharma et al., 1994; Bagherzadeh & Mirghasemi, 2009; Hamidi et al., 2012; Gupta, 2016; Honkanadavar et al., 2016).

Kolbuszewski and Frederick (1963) and Zolkov and Wiseman (1965) showed that friction angle increases when d_{max} increases, while an opposite trend was reported by Kirkpatrick (1965), Marachi et al. (1972), Marsal (1973), Rathee (1981) and Ovalle et al. (2014). Several researchers have also reported that the d_{max} has no effect on the shear strength of granular materials (Vallerga et al., 1957; Charles & Watts, 1980; Selig & Roner, 1987).

Marachi et al. (1972) performed large-scale triaxial tests on rockfills with d_{max} values of 12, 50 and 152 mm. The specimen diameter over d_{max} ratio of all the samples was equal to 6. The results showed that the friction angle of a sample with d_{max} value of 12 mm increases by 4° as the d_{max} increases from 12 to 152 mm.

Varadarajan et al. (2003) performed direct shear tests on the samples with d_{max} values of 25, 50 and 80 mm of two rounded/sub-rounded and angular/sub-angular rockfills. A comparison between the friction angles of the samples showed that for angular/sub-angular rockfill, friction angle increases by 3.9º as the d_{max} increases from 25 to 80 mm, while for rounded/sub-rounded rockfill, the friction angle decreases by 1.9º as the d_{max} increases from 25 mm to 80 mm.

Xu et al. (2018) performed direct shear tests on the samples having d_{max} values of 2.36, 4.75, 9.5, 19, 37.5 and 75 mm. The specimen size over d_{max} ratios were 127, 63, 32, 16, 8 and 4, respectively. The friction angle increases from 31.2° to 36.6° as d_{max} increases from 2.36 to 37.5 mm and then increases by 3.4° as d_{max} further increases to 75 mm.

Table 2.7 summarizes the variation trend of the friction angle of coarse granular soils as d_{max} increases. As one can see, the results are contradictory. These results can be due to the influence of other influencing factors such as scaling down technique, gravel and fine contents, density, normal stress, etc. Nevertheless, the influence of d_{max} on the shear strength of coarse-grained materials such as rockfill and waste rocks has been clearly shown.

Table 2.7 Trend of variation of friction angle of granular materials as d_{max} increases

Variation of ϕ (°)	**Particle shape**	**Reference**
Increase	Angular	Hennes (1952)
Increase	Angular	Lewis (1956)
Increase	Angular	Marachi et al. (1972)
Decrease	Angular with slight rounding	Hribar et al. (1986)
Increase	Angular	Varadarajan et al. (2003)
Increase	Angular	Kouakou et al. (2020)
Decrease	Sub-angular and angular	Ovalle et al. (2014)
Constant	Sub-round, angular	Vallerga et al. (1957)
Decrease	Rounded	Kirkpatrick (1965)
Decrease	Rounded	Marsal (1965)
Decrease	Rounded	Marachi et al. (1972)
Decrease	Rounded	Marsal (1973)
Increase	Rounded	Charles (1973)
Increase	Rounded to sub-rounded	Rathee (1981)
Decrease	Rounded	Varadarajan et al. (2003)
Increase/decrease	Sub-rounded to rounded	Kouakou et al. (2020)
Increase	Unknown	Kolbuszewski and Frederick (1963)
Increase	Unknown	Tombs (1969)
Constant	Unknown	Charles and Wattes (1980)
Constant	Unknown	Selig and Roner (1987)
Increase	Unknown	Fakhimi et al. (2008)
Increase	Unknown	Xu et al. (2018)

2.3.3.2 Shape

Particles of granular material can be angular or rounded. Particle shape along with other influencing parameters controls the geotechnical properties such as void ratio, internal friction angle and hydraulic conductivity of soil material and aggregates (Holtz & Gibbs, 1956; Mora & Kwan, 2000; Santamarina & Cho, 2004).

Powers (1953) defined an index for estimating the roundness and sphericity of particles, as shown in Table 2.8. The roundness varies from very angular to well-rounded and the roundness index ranges from 0.12 for very angular to 1 for well-rounded shape.

Table 2.8 Roundness index of particle shapes (Powers, 1953)

Roundness classes	Very Angular	Angular	Sub-Angular	Sub-Rounded	Rounded	Well Rounded
Roundness Indexes	0.12 - 0.17	0.17 - 0.25	0.25 - 0.35	0.35 - 0.49	0.49 - 0.70	0.70 - 1.00

Holtz and Gibbs (1956) conducted direct shear tests on sub-rounded gravel and sub-angular quarry materials consisting of 65% gravel with the d_{max} of 76.2 mm and 70% relative density. The results showed that the shear strength of the quarry materials was larger than that of the gravel.

Vallerga et al. (1957) performed shear tests on angular and sub-rounded aggregates. The results presented in Figure 2.24 shows that at a given void ratio, the peak friction angle of angular particles is larger than that of the sub-rounded particles. The same results have been reported by Salimi et al. (2008). This observation can be attributed to the increase of interlocking between angular particles.

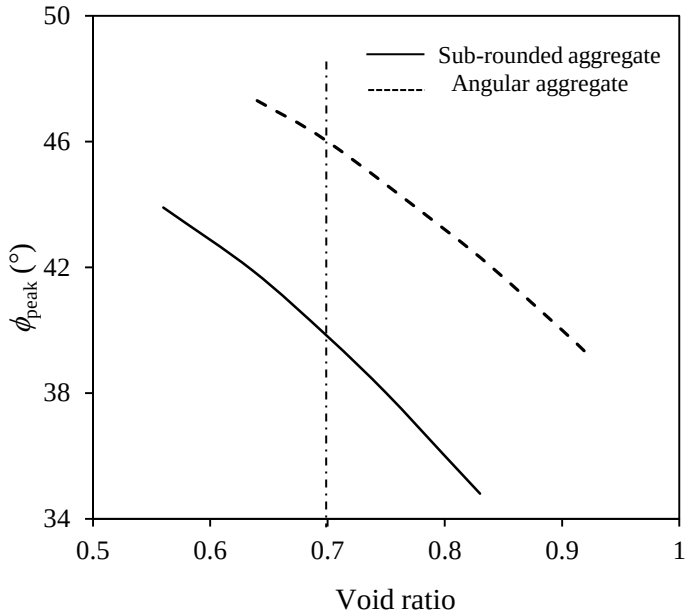

Figure 2.24 The influence of angularity on peak friction angle; data taken from Vallerga et al. (1957)

The influence of particle shape on the peak friction angle of the parallel scaled down samples could also be clearly seen in Table 2.5. The friction angle of scaled down samples increases for rounded particles but decreases for angular particles as the d_{max} value increases.

2.3.3.3 Degree of compaction

A sample may behave like dense, medium or loose sand, as shown in Figure 2.25, depending on its degree of compaction. A dense sand typically shows a high peak in the shear stress-displacement curve (Figure 2.25a) and dilation after the peak in the volume change-shear displacement curve (Figure 2.25b), while these phenomena are absent for a loose sand.

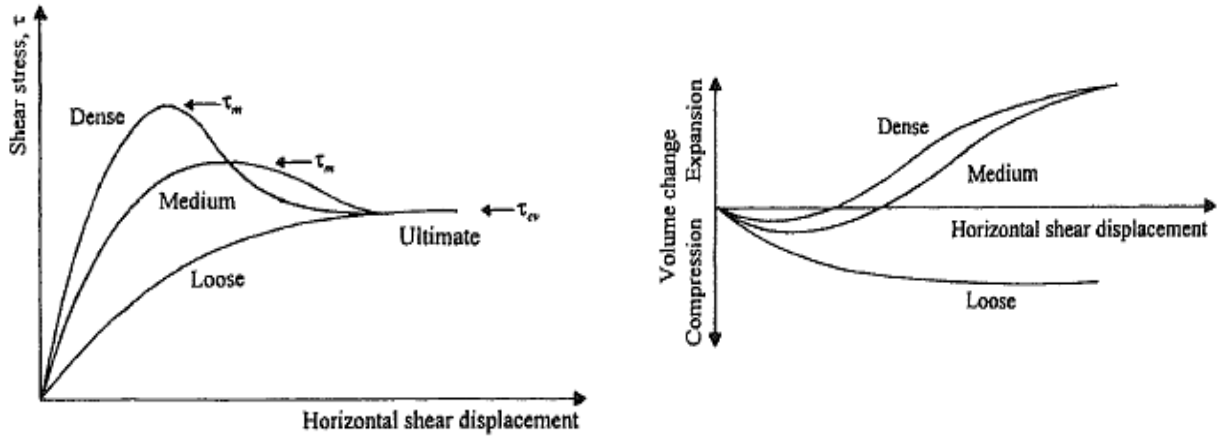

(a) (b)

Figure 2.25 Typical (a) shear stress-shear displacement curve and (b) volume change- shear displacement curve of a loose, medium and dense sands obtained by applying direct shear tests (taken from Das (2008) with the permission of reproduction from Taylor & Francis Informa UK Ltd)

Several researchers studied the variation of shear strength versus density (e.g., Holtz & Gibbs, 1956; Zeller & Wullimann, 1957; Leps, 1970; Rathee, 1981; Al-Hussaini, 1983; Douglas, 2002; Cerato & Lutenegger, 2006). They showed that the shear strength of materials increases as the density increases.

Figure 2.26 shows the variation of friction angle with dry density, void ratio, porosity, relative density and soil classifications (Holtz & Kovacs, 1981; UFC, 2022). One again, the friction angle increases with an increase in density.

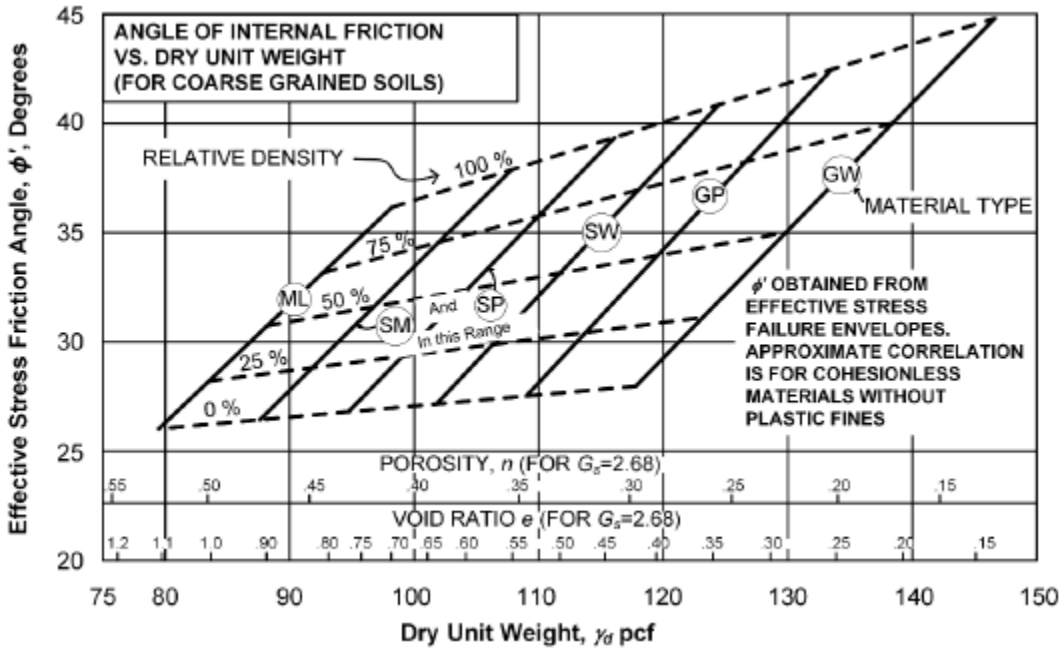

Figure 2.26 Approximate relationship between the effective friction angle and dry unit weight for different relative densities and soil types (taken from UFC (2022) with the permission of reproduction for public access documents)

2.3.3.4 Normal stress or confining pressure

Hall and Gordon (1963) is one of the first researchers who performed large scale tests to study the internal friction angles of rockfill materials. The test results showed that the friction angle decreases as the confining pressure increases, principally because of the high percentage of particle breakage under shearing strains (Hall & Gordon, 1963). The same conclusion has been reported by other researchers such as Matsuoka and Liu (1998), Boakye (2008), Hu et al. (2011) and Ovalle et al. (2014).

Figure 2.27 shows the variation of friction angle of sand as function of void ratio for different normal stresses (Das 1983). For a given void ratio, the friction angle decreases as the normal stress increases.

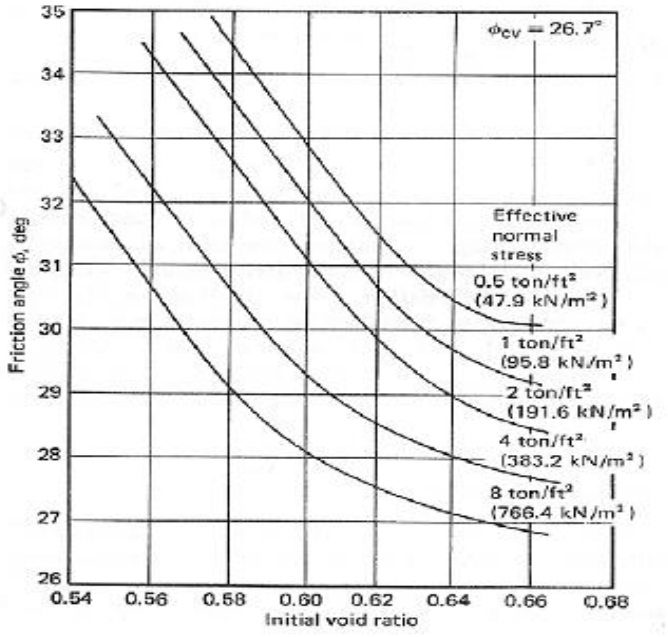

Figure 2.27 Variation of internal friction angle with normal stress for Ottawa sand (taken from Das (1983) with the permission of reproduction from Taylor & Francis Informa UK Ltd)

2.3.4 Specimen size effect (SSE)

To reproduce a test as close as possible to the actual field condition, testing specimens should be as large as possible, while the desired specimen sizes should be as small as possible for the convenience of laboratory test conditions. A compromise has to be taken to obtain an optimal specimen size, by which the specimen size is the smallest, but large enough to ensure the stability and reliability of experimental results. Normally, this should be guaranteed by observing, applying and meeting the minimum requirements specified in the relevant testing standards.

Table 2.9 shows several standards for direct shear tests. In the table, W is specimen width, T is specimen thickness and d_{max} is maximum particle size.

Table 2.9 The requirements of standards for the specimen size of direct shear tests

Standard	***W***	***T***	***W/T***	**Maximum allowed d_{max}**
ASTM D3080/D3080M (2011)	≥ 50 mm	≥ 13 mm	≥ 2	Min{*T*/6, *W*/10}
AS 1289.6.2.2 (1998)	Not specified	≥ 12.5 mm	Not specified	*T*/6
BS 1377-7 (1990)	60 mm	20 mm	3	2 mm

	100 mm	25 mm	4	2.5 mm
	305 mm	150 mm	≈2	15 mm - 20 mm
Eurocode 7 (2007)	Not specified	Not specified	---------	*T*/10

Among the diverse standards presented in Table 2.9, ASTM D3080/D3080M-11 is probably the most popular and the most used one. It requires the specimen width (*W*) and thickness (*T*) to be at least 10 and 6 times d_{max}, respectively. Additionally, the minimum *W* and *T* need to be 50 and 13 mm, respectively. Recently, ASTM D3080/D3080M-11 has been withdrawn for update. One can expect that it remains to be used in practice and research projects because it has been widely accepted and used (Rathee, 1981; Scarpelli & Wood, 1982; Abbas, 2011; Pankaj et al., 2013; Vasistha et al., 2013; Honkanadavar et al., 2014; Amirpour Harehdasht et al., 2018; Xu, 2018; Zhang et al., 2020; Cai et al., 2020; Zahran & Naggar, 2020; Yaghoubi et al., 2020; Nicks et al., 2021; Saberian et al., 2021).

Following the requirement of ASTM D3080/D3080M-11 may not be a problem for fine particle materials, but it is problematic for granular materials with large particle sizes.

To avoid this problem, scaling down technique is largely used by excluding the oversized particles and the minimum required specimen width to d_{max} (W/d_{max}) ratio of 10 is commonly used (Marachi et al., 1972; Varadarajan et al., 2006; Abbas, 2011; Pankaj et al., 2013; Vasistah et al., 2013; Honkanadavar et al., 2016; Xu, 2018; Zhang et al., 2019; Dorador et al., 2017; Motaharitabari & Shooshpasha, 2021). However, the validity of this minimum required ratio of 10 has never been shown.

When very small specimens are used for large particle materials, the effect of individual large particles along the shear sliding plane can be amplified, resulting in a shear strength that differs from that of the material in field conditions. The specimen size should thus be increased until the influence of the individual large particles vanishes. The variation of shear strength with specimen size is a phenomenon, known as specimen size effect (SSE) (Jewell & Wroth, 1987; Palmeira & Milligan, 1989; Cerato & Lutenegger, 2006; Alonso et al., 2012; Mirzaeifar et al., 2013; Amirpour Harehdasht et al., 2018).

Palmeira and Milligan (1989) performed direct shear tests on sand with d_{max} value of 1.2 mm by using small (60 mm × 60 mm × 32 mm), medium (252 mm × 152 mm × 152 mm) and large

(1000 mm × 1000 mm × 1000 mm) size shear boxes. The W/d_{max} ratios corresponding to the three shear boxes were 50, 126.7 and 833, respectively and the T/d_{max} ratios were 27, 127 and 833, respectively. One normal stress of 30 kPa was used for all the tests. All the specimens were prepared in the same relative density using the same method. The direct shear tests resulted in the friction angles of 50.1°, 50.2° and 49.4° for the specimens with W/d_{max} ratios of 50, 127 and 833, respectively. The friction angles of the specimens thus remain almost constant when W/d_{max} ratio increases from 50 to 833. These results tend to indicate that the ratio of 50 is large enough to remove the SSE. But the validity of the minimum required ratio of 10 is not verified because there are no test results for the samples with the ratios between 10 and 50.

Cerato and Lutenegger (2006) studied the influence of specimen size on the friction angles of sand and gravel materials. Direct shear tests were conducted on sand and gravel with different d_{max} and relative densities using small (59.9 mm × 59.9 mm × 26.4 mm), medium (101.6 mm × 101.6 mm × 40.6 mm) and large (304.8 mm × 304.8 mm × 177.8 mm) shear boxes. The results obtained for the specimens of sand with d_{max} values of 0.9, 1.7, 2 and 5 mm cannot be used to evaluate the specimen size effect because the influence of density (or degree of compaction) was also involved in the shear test results. Only the specimens of gravel with d_{max} value of 5 mm were prepared in the same loose state for the shear boxes with different dimensions. Sample with known quantity was placed in the shear boxes with different dimensions to achieve the desired density. The test results of these specimens can be used to evaluate the SSE. The W/d_{max} ratios of the specimens having d_{max} value of 5 mm were 12, 20 and 61 for small, medium and large shear boxes, respectively. Figure 2.28 shows the variation of the peak friction angle of the specimens with d_{max} = 5 mm having different relative densities versus W/d_{max}. The results show that the W/d_{max} ratios of 10 and 12 are not large enough to eliminate the SSE and the ratio of 10 required by ASTM is invalidated. However, it is unclear if the W/d_{max} ratio of 61 is large enough as there is no result for the specimen with a ratio larger than 61.

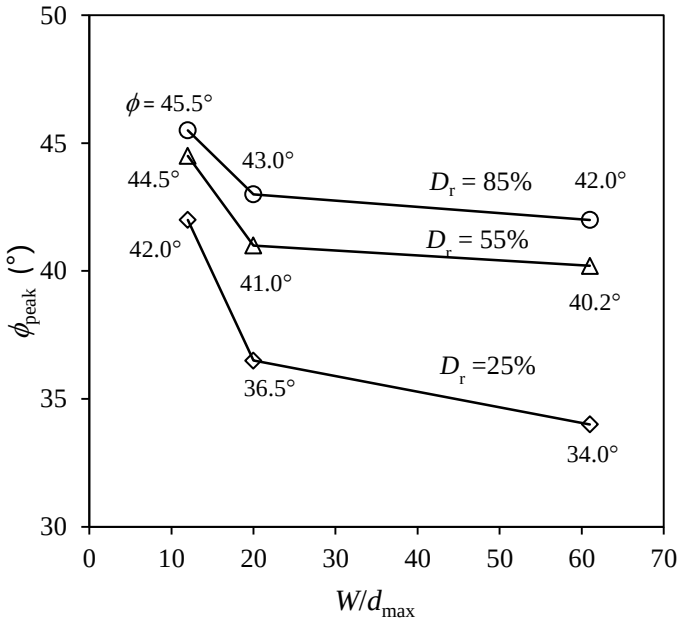

Figure 2.28 Variations of the peak friction angles (ϕ_{peak}) of the specimens with d_{max} value of 5 mm and different relative densities versus W/d_{max}; data taken from Cerato and Lutenegger (2006)

Similarly, Mirzaeifar et al. (2013) studied the SSE of direct shear tests on three samples with a d_{max} value of 1.3 mm and densities of 1.5 g/cm^3, 1.58 g/cm^3 and 1.67 g/cm^3. A small (60 mm × 60 mm × 16 mm), a medium (100 mm × 100 mm × 30 mm) and a large (300 mm × 300 mm × 180 mm) shear box were used. The W/d_{max} ratios of the specimens were 46, 77 and 231. Figure 2.29 shows the variation of obtained friction angles for the samples with different densities versus W/d_{max} ratio. The results clearly indicate that the W/d_{max} ratio of 46 is not large enough. A larger W/d_{max} ratio up to 77 may be large enough to eliminate the SSE. The minimum required W/d_{max} ratio of 10, stipulated by the standard of ASTM is invalidated once again.

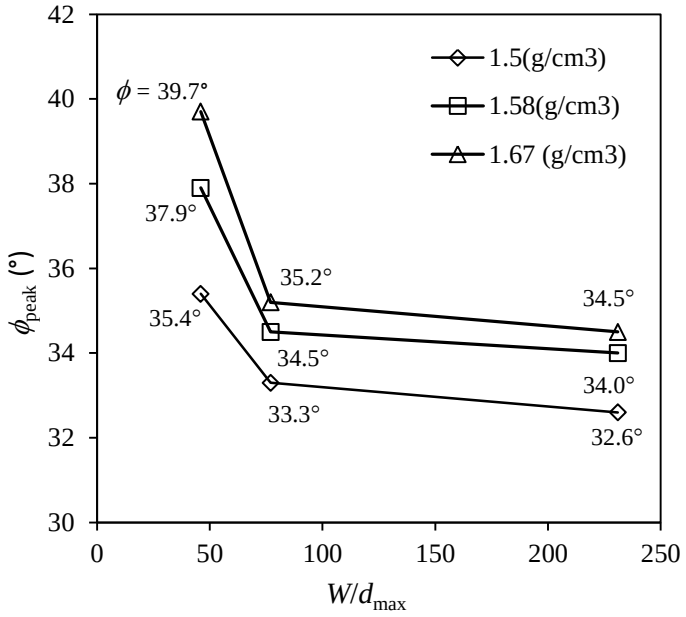

Figure 2.29 Variation of peak friction angle of a sand at three different densities, obtained by direct shear tests with three different size shear boxes versus W/d_{max} ratio; data taken from Mirzaeifar et al. (2013)

Table 2.10 presents a summary of the previous studies on the SSE of direct shear test. Almost all the previous studies show that the minimum specimen width over d_{max} ratio of 10 suggested by ASTM is not large enough to eliminate SSE. The minimum required ratio needs to be updated. Some of the previous studies show that the ratio of 50 can be a large enough ratio to eliminate the SSE, while other studies show that even the ratios of 75 and 95 are not large enough. More experimental work is required to identify the minimum required W/d_{max} ratio that is large enough to eliminate the SSE.

Further analyses show that the minimum specimen size ratio used by the previous studies for fine particle materials with $d_{max} \leq 1$ mm is larger than 50 since using a small shear box of 60 mm for these materials results in $W/d_{max} \geq 50$. So, the minimum ratio of 10 required by ASTM has never been validated by the previous studies. Using a smaller shear box is required for preparing the specimens having $d_{max} \leq 1$ mm with the ratios between 10 and 50 to validate the minimum ratio of 10 required by ASTM.

Table 2.10 Summary of previous studies on SSE of direct shear test

Material	Tested W/d_{max}	Minimum tested W/d_{max} large enough to remove SSE	Validity of the minimum required W/d_{max} of ASTM	Reference
Angular quartz, d_{max} = 0.841 mm	71, 119, 143	Yes at 71	Unknown	Parsons (1936)
Ottawa sand, d_{max} = 0.841 mm				
Rounded to sub-rounded sand and gravel, d_{max} = 6.3 mm	10, 48	Not at 10	Invalidated	Rathee (1981)
Sand, d_{max} = 1.2 mm	50, 127, 833	Yes at 50	Unknown	Palmeira and Milligan (1989)
Angular sand, d_{max} = 0.9 mm	67, 113, 339	Yes at 67	Unknown	Cerato and Lutenegger (2006)
Angular sand, d_{max} = 2.0 mm	30, 51, 152	Not at 50	Invalidated	
Angular gravel, d_{max} = 5.0 mm	12, 20, 61	Not at 20	Invalidated	
Angular to sub-angular sand, d_{max} = 0.42 mm	95, 285	Not at 95	Invalidated	Wu et al. (2008)
Angular sand, d_{max} = 1.3 mm	46, 77, 231	Not at 46	Invalidated	Mirzaeifar et al. (2013)
Angular sand, d_{max} = 0.8 mm	75, 125, 375	Not at 75	Invalidated	Ziaie Moayed et al. (2017)
Silty sand I, d_{max} = 0.8 mm	75, 125, 375	Not at 75	Invalidated	
Silty sand II, d_{max} = 0.8 mm	75, 125, 375	Not at 75	Invalidated	
Silty sand III, d_{max} = 0.8 mm	75, 125, 375	Yes at 75	Unknown	

2.4 Saturated hydraulic conductivity (K_{sat}) of waste rocks

Hydraulic conductivity is a hydraulic property to describe the speed of water movement in soil. When the water flow regime is laminar, Darcy's law applies as follows (Todd & Mays, 2005):

$$Q = KA\frac{dh}{dl} \tag{2.14}$$

Or

$$V = \frac{Q}{A} = K\frac{dh}{dl} \tag{2.15}$$

$$K = V/(\frac{dh}{dl}) \tag{2.16}$$

where Q is flow rate (cm^3/s), V is velocity of flow (cm/s), A is cross section area (cm^2), dh/dl is hydraulic gradient, and K is hydraulic conductivity (cm/s).

It should be noted that the hydraulic conductivity K changes as the degree of saturation of porous material changes. It can considerably decrease with the degree of unsaturation. When the material is fully saturated (i.e. degree of saturation equal to 100%), the value of K reaches its maximum value, called saturated hydraulic conductivity, K_{sat}. In this thesis, only the saturated hydraulic conductivity is addressed.

2.4.1 K_{sat} measurement and estimation

2.4.1.1 Large scale in-situ tests

2.4.1.1.1 Pumping test

In this method, water is pumped from a hole drilled into the soil, with a steady state for at least a day. Meanwhile, observations are made to see how water levels decrease in nearby wells during the pumping process from which the hydraulic conductivity can be calculated (Svensson, 2014). An aquifer model can also be made. By using the Cooper-Jacob method or Theis well equation, some parameters such as transmissivity and specific storage coefficient can be obtained in this method. This method can be used for deep, thick and permeable soils (aquifers) and for the calculations of seepage flow in soil layers (Stibinger, 2014).

2.4.1.1.2 Slug test

Slug test is another in situ method to determine the flow parameters of an aquifer (Fakhry & LaMoreaux, 2004). In this method, a known volume of water is injected or withdrawn quickly from a well and the difference in hydraulic head is measured (Svensson, 2014). The hydraulic conductivity can be estimated by using different slug test solution methods such as Cooper-Bredehoeft-Papadopulous method for confined aquifer and Hvorslev (1951) method for confined and unconfined aquifers as follow:

$$K = r^2 \ln(\frac{L}{R})/2LT_L \quad (2.17)$$

Where K is hydraulic conductivity (cm/s), r is effective radius of piezometer (cm), L is length of borehole (or screen length) (cm), R is borehole radius (cm), T_L is the time lag when h_t/h_0 is equal to 0.37 (s); h_t is the water level at $t > 0$ (cm) and h_0 (cm) is water level at $t = 0$.

The slug tests can be performed quickly at low cost and this test measures the hydraulic conductivity of a small discrete of an aquifer. However, only the hydraulic conductivity of the area surrounding the well can be estimated, which is not representative of the average hydraulic conductivity of the area (Moore, 2012; Svensson, 2014).

2.4.1.1.3 Piezometer tests

In this method, a non-perforated pipe is placed into a hole under the water level. A small cavity should be left at the bottom to allow water flowing through the space. The water table is dropped down in the hole with a bailer and the rate at which the water rises in the pipe is then determined. The hydraulic conductivity can then be determined using the amount of water recharged and the geometry of the cavity. This test may be used to determine the hydraulic conductivity of relatively deep separated soil layers. As the disadvantage of this method, the hydraulic conductivity represents only the area surrounded by the small cavity (Stibinger, 2014).

2.4.1.1.4 Double ring infiltrometer test

In this method, two large steel rings are placed on ground soil surface and struck some centimeters into the soil. The soils around the rings are saturated by infiltration. The rings are also filled with water. Then, the rate of fall in water level is measured for both rings. The rings are refilled with water. The water level in the outer ring is kept constant and the water fall in the inner ring is measured. The outer ring minimizes horizontal flow below the inner ring. So, the measurements are almost vertical flow below the inner ring. This procedure is repeated until the infiltration rate remains stable.

This test method is used to measure the infiltration rate for irrigation and drainage planning purposes, as well as the hydraulic conductivity of rock materials. In this test, results are based on the actual moisture content of tested soil and only the top layers hydraulic conductivity value can be determined (Stibinger, 2014).

2.4.1.1.5 Auger-Hole test (Hooghoudt's test)

In this method, a hole is driven to a certain depth below the groundwater table. The water table in the hole is reduced using a bailer, and the rate at which the water table rises is then measured. The hydraulic conductivity can be measured by the following equation (Todd & Mays, 2005):

$$K = \left(\frac{r.n}{0.19}\right)\left(\frac{2n}{r} - 1\right)^{-1} \times \left(\frac{1}{t_2 - t_1}\right)\ln\left(\frac{y_2}{y_1}\right) \quad (2.18)$$

where r is the radius of hole (cm), n is water level after rise (cm), y_1 and y_2 are measured water levels in the hole (cm) at the corresponding times t_1 and t_2 (s).

This method is used to design underground pipe drainage systems. However, only the horizontal hydraulic conductivity can be measured. This method is not suitable for heavy layered soils or soils with irregular pore space distribution (Stibinger, 2014).

2.4.1.1.6 Inversed Auger-Hole test

In this method, a hole is driven to a certain depth above the groundwater table. Water rises up in the dry hole, and the rate at which the water table drops is then measured. The hydraulic conductivity can be estimated by measuring the rate of decline and the borehole geometry. This method is a common field method for designing surface or subsurface drainage in the absence of a groundwater table. The method has the same disadvantage as the Auger-Hole method.

2.4.1.2 Laboratory tests

Compared to laboratory tests, in situ permeability tests can be performed on a less disturbed soil sample, resulting in more representative results of measurements (Stibinger, 2014). However, in situ tests include also some drawbacks and limitations. For example, the K_{sat} measured by in situ tests represents only the area enclosed by a small cavity, depending on the actual moisture content of the soil. In situ tests become inappropriate in heavily stratified soils or soils with irregular pore space distribution. Measurement errors may occur at the border of the rings during double ring test, resulting in the determination of the K_{sat} of top layers. It is thus impossible for all projects to perform in situ permeability tests due to their limitations, the requirement for special equipment and time consuming.

An alternative for determining the K_{sat} of granular materials is to perform laboratory tests. It important to note that ASTM D2434-19 for constant hydraulic head requires specimen diameter D to be at least 8 or 12 times d_{max}, depending on the percentage of coarse particles. For falling head permeability tests, ASTM D5084-16a requires D/d_{max} ratio to be at least 6 (Svensson, 2014). This is not a problem for fine particle materials such as clay, silts and fine sands. For rockfill or waste rocks, meeting the required specimen size to d_{max} ratios specified by the ASTM standards can become impossible with standard instrumentations of permeability tests and difficult with large and non-standard column tests.

To solve this problem and make the laboratory tests possible, the over-sized particles are usually excluded. In addition, the minimum required specimen diameter over d_{max} ratios stipulated by the ASTM are commonly used even though the validity of these minimum required D/ d_{max} ratios has never been demonstrated. When the specimens have a small D/d_{max} ratio, the preferential flow along the permeameter wall can become pronounced (Franzini, 1968; Dudgeon, 1966, 1967; Somerton & Wood, 1988; Chapuis et al., 2012). The measured hydraulic conductivity may not be representative of that of the field material.

There are a few studies on determining the K_{sat} of granular materials in the literature (Chapuis et al., 1989; Chapuis, 2004; Hernandez, 2007; Gaillot, 2007; Bourrel, 2008; Peregoedova, 2012; Cabalar & Akbulut, 2016; Essayad et al., 2018; Martin et al. 2019). However, all of them used one column to perform tests on the specimens with different d_{max} values or one distinct specimen. The test results could not be used to study the variation of K_{sat} with D/d_{max} ratios and validate the minimum required ratios of the ASTM because the specimen size effect of hydraulic conductivity can only be evaluated by doing permeability with different specimen diameters (D) on a given material (and d_{max}) under the same water content, compactness, hydraulic gradient. This aspect is further addressed in section 2.4.3.

2.4.1.3 Indirect methods (empirical equations)

Many researches have been conducted through the years to find correlations between hydraulic conductivity and particle size descriptors such as the maximum particle size (d_{max}), effective size (d_{10}), median size (d_{50}) and uniformity coefficient (C_u). Almost all the available empirical equations follow a general form as follows (Todd & Mays, 2005):

$$K = cd^2 \tag{2.19}$$

where d is particle size and c is a coefficient and can be described by several parameters as:

$$c = f_s f_a \tag{2.20}$$

where f_s and f_a are grain shape factor and porosity factor, respectively.

Hazen (1892) introduced hydraulic conductivity as a function of temperature (T) and median particle size d_{10}. Slichter (1898) presented an equation relating permeability to the square of d_{50}. Masch and Denny (1966) used d_{50} as the typical size to correlate hydraulic conductivity with grain size. Chapuis (2004) presented an empirical equation based on d_{10}^2 and $e^3/(1+e)$ for non-plastic homogenized materials and fully saturated specimens. However, the application of different predictive methods for the same porous medium material could yield different K_{sat} values, which may differ because of the discrepancies between grain distribution and shape characteristics (Vukovic & Soro, 1992; Odong, 2008).

Table 2.11 presents some predictive equations making use of effective parameters such as d_{10} (particle size at which 10% by weight of particles pass), d_{50} (median particle size), n (porosity) and e (void ratio). It can be seen that each empirical formula has been defined for a specific range of application.

Table 2.11 Predictive equations and their range of application

Reference	**Equation**	**Range of application**
Hazen (1892), taken from Chapuis (2004)	$K_{sat} = 1.5d_{10}^2$	Suitable for sand and gravel; suitable for loose compactness; 0.1 mm < d_{10} < 3 mm; $C_U \leq 5$; K_{sat} at 20° C
Extended Hazen (1892), taken from Chapuis (2004)	$K_{sat} = 1.5d_{10}^2 e^3 \frac{1+e_{max}}{[e_{max}^3(1+e)]}$	
Slichter (1898)	$K_{sat} = 1 \times 10^{-2} \times g/\vartheta \times n^{3.287} \times (d_{10})^2$	0.01 mm < d_{10} < 5.0 mm
Terzaghi (1925)	$K_{sat} = C_0 \frac{\mu_{10}}{\mu_t} (\frac{n-0.13}{\sqrt[3]{1-n}})^2 d_{10}^2$	Suitable for sand; 0.25 mm ≤ d_{10} ≤ 2 mm
Taylor (1948)	$K_{sat} = C_1 \frac{\gamma_w}{\mu_w}\left(\frac{e^3}{1+e}\right) d_{50}^{1.5}$ $C_1 = \frac{K_{sat} \times \mu_w (1+e)}{d_{50}^2 \gamma_w e^3}$	Suitable for loose sand; 0.1 mm < d_{10} < 3 mm
NAVFAC (1974), taken from Chapuis (2004)	$K_{sat} = 10^{1.291e - 0.6425(d_{10})^{10^{0.5504-0.2987e}}}$	Suitable for sand or mix of sand and gravel; 0.1 mm ≤ d_{10} ≤ 2 mm; 2 ≤ C_u ≤ 12; 0.3 ≤ e ≤ 0.7
Shepherd (1989)	$K_{sat} = 3.5 \times 10^{-4}[100 {d_{50}}^{1.5}]$	Suitable for sand and gravel

USBR (Vukovic & Soro 1992)	$K_{sat} = 4.8 \times 10^{-3} \times \frac{g}{\vartheta} \times (d_{20})^{2.32}$	Suitable for sands; $C_u < 5$; 0.06 mm $\leq d_{10} \leq 2$ mm
Breyer (Kresic 1998)	$K_{sat} = 6 \times 10^{-4} \times \frac{g}{\vartheta} \times log\left\lfloor\frac{500}{C_u}\right\rfloor \times (d_{10})^2$	Suitable for heterogeneous porous media 0.06 mm < d_{10} < 0.6 mm; $1 \leq C_u \leq 20$
Modified Kozeny-Carman (KCM) Mbonimpa et al. (2002)	$K_{sat} = C_g \frac{\gamma_w}{\mu_w} C_u^{1/3} d_{10}^2 \frac{e^{3+x}}{1+e}$	Suitable for different types of particulate media from uniform rounded particles to finely ground rock (tailings) with rough edges, to low plasticity silts; 10^{-8} cm/s $\leq K_{sat} \leq 10^{+2}$ cm/s; 0.1 mm $\leq d_{10} \leq 2$ mm
Chapuis (2004)	$K_{sat} = 2.4622 \left(\frac{d_{10}^2 e^3}{1+e}\right)^{0.7825}$	Suitable for natural soil; 0.003 mm $\leq d_{10} \leq 3$ mm; $0.3 \leq e \leq 1$

where:

K_{sat}: Saturated hydraulic conductivity (cm/s)

C_0: Model constant = 8 for smooth, rounded grains and 4.6 for grains of irregular shape

C_1: Form factor

C_u: Uniformity of coefficient

C_g: Model constant = 0.1

d_{10}: Particle size at which 10% by weight of particles pass (mm)

d_{20}: Particle size at which 20% by weight of particles pass (mm)

d_{50}: Particle size at which 50% by weight of particles pass (cm)

e: Void ratio

g: Acceleration of gravity (m/s^2)

n: Porosity

x: Model parameter ≈ 2

ϑ: Kinematic viscosity (m^2/s)

μ_t: Water viscosity at t°C

μ_{10}: Water viscosity at 10°C

μ_w: Dynamic viscosity of water ≈ 10^{-6} kN.s/m^2 at 20°C

γ_w: Unit weight of water = 9.8 (kN/m^3)

2.4.2 Influencing factors on the K_{sat} of coarse granular materials

Hydraulic conductivity of coarse granular material depends on particle shape, particle size, void ratio, distribution of pores, state of compaction, and other influencing factors (Lambe &

Whitman, 1969; Chapuis, 2004; Chapuis, 2012; Stibinger, 2014; Ren et al., 2016; Alakayleh et al., 2018; Xu et al., 2019).

2.4.2.1 Particle size distribution

Particle size distribution of granular materials has been recognized as a useful parameter in calculating hydraulic conductivity by many years (Freeze & Cherry, 1979). Numerous researchers performed many experimental tests and studied the relationship between hydraulic conductivity and grain size descriptors. The particle size distribution curve has been used to define any grain size. The size d_{10} is then called the effective size, the size d_{50} is called as median size, the uniformity coefficient C_u is defined as the ratio d_{60}/d_{10} (d_{60} is particle size at which 60% by weight of particles passes and d_{60} is particle size at which 10% by weight of particles passes) and the size d_{max} is called the maximum particle size.

2.4.2.1.1 Maximum particle size (d_{max})

The d_{max} of materials is an important parameter in the measurement of hydraulic conductivity using laboratory permeability tests. The d_{max} of materials affect the measured K_{sat} through the test specimen. The common standards for laboratory permeability tests, ASTM standards, define the test specimens' dimension and the method of compaction based on the d_{max} of material (ASTM D2434, 2019; ASTM D5084-16a, 2020). According to the requirement of ASTM D2434-19, for the materials with d_{max} values between 2 and 9.5 mm, the specimen diameter should be at least 8 or 12 times d_{max} when less than or more than 35% of total soil retain on sieve opening 2 mm, respectively. While, for the materials with d_{max} values between 9.5 and 19 mm, the specimen diameter should be at least 8 or 12 times d_{max} when less than or more than 35% of total soil retain on sieve opening 9.5 mm, respectively. ASTM D5084-16a also stipulates that the value of D/d_{max} ratio should not be smaller than 6. For the materials having d_{max} of 9.5 mm or greater than that, the method of specimen preparation and compaction also varies.

During the permeability tests, various reasons may cause preferential leakage through the test specimen. One of the important reasons is the usage of too large particles compared to the permeameter size. When the test specimen is too small compared to the d_{max} of tested material, poor compaction with large voids along the permeameter wall may occur, resulting in preferential

leakage (Rose & Rizk, 1949; Franzini, 1968; Chapuis et al., 2012). Another reason is the segregation of the particles within test specimen that also occurs due to the non-uniform compaction of the specimen and it in turns occurs due to the existence of too large particles and large voids within the specimen (Chapuis, 2012).

Despite the significant role of d_{max} in the measurement of hydraulic conductivity, studies on the influence of d_{max} as the only variable parameter on the K_{sat} cannot be found in the literature.

2.4.2.1.2 Gravel and fine contents

Another factor influencing on the K_{sat} value is the percentage of fine and gravel contents. For instance, Alakayleh et al. (2018) performed three sets of constant head permeability tests on samples made of three types of material. For each material, seven samples were prepared with 0, 5, 10, 15, 20, 25 and 30% of fine particles and seven other samples were prepared with 0, 70, 75, 80, 85, 90, and 95% of coarse particles. All experimental tests were conducted by following ASTM D2423-68. All other factors remain constant for the specimens of each distinct material. Figure 2.30 shows the variations of log K_{sat} with the percentage of fine particles (Figure 2.30a) and coarse particles (Figure 2.30b) for different materials. As it is seen in the figure, for all the materials, K_{sat} decreases when fine porous increases and increases as coarse particle content increases.

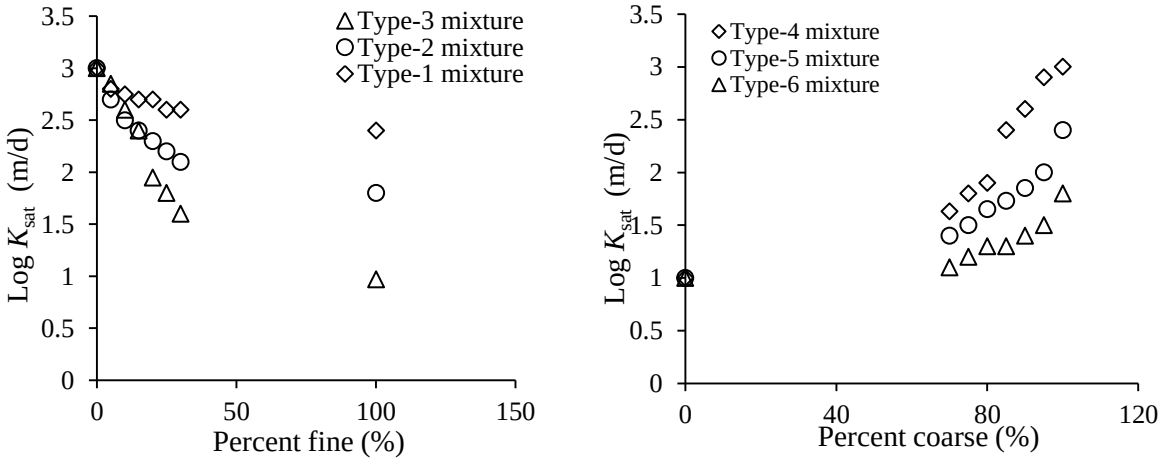

(a) (b)

Figure 2.30 Variations of log K_{sat} with the percentages of (a) fine porous and (b) gravel content for three types of mixtures; data taken from Alakayleh et al. (2018)

2.4.2.2 Void ratio (*e*)

Many researchers have studied the effect of void ratio on the hydraulic conductivity (Taylor, 1948; Lambe & Whitman, 1969; Chapuis, 2012; Ren et al., 2016; Xu et al., 2019; P'kla et al., 2020). Chapuis (1989b) studied the variation of the hydraulic conductivity obtained by constant head permeability tests on saturated clean sand as a function of void ratio. Figure 2.31 shows the variation of the saturated hydraulic conductivity versus void ratio for the tested sand. As shown in the figure, the hydraulic conductivity increases as the void ratio increases.

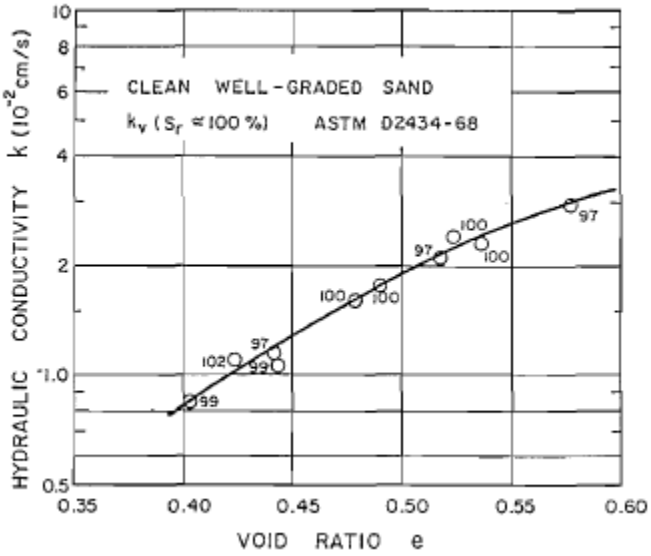

Figure 2.31 Variation of measured hydraulic conductivity versus void ratio for a clean sand (taken from Chapuis et al. (1989b) with the permission of reproduction from Canadian Science Publishing)

Ren et al. (2016) studied the relationship between the hydraulic conductivity obtained by experimental tests and predictive equations and the void ratio of a sand. Figure 2.32 shows the variation of hydraulic conductivity versus void ratio. As shown in the figure, the hydraulic conductivity increases as the void ratio increases for all the methods.

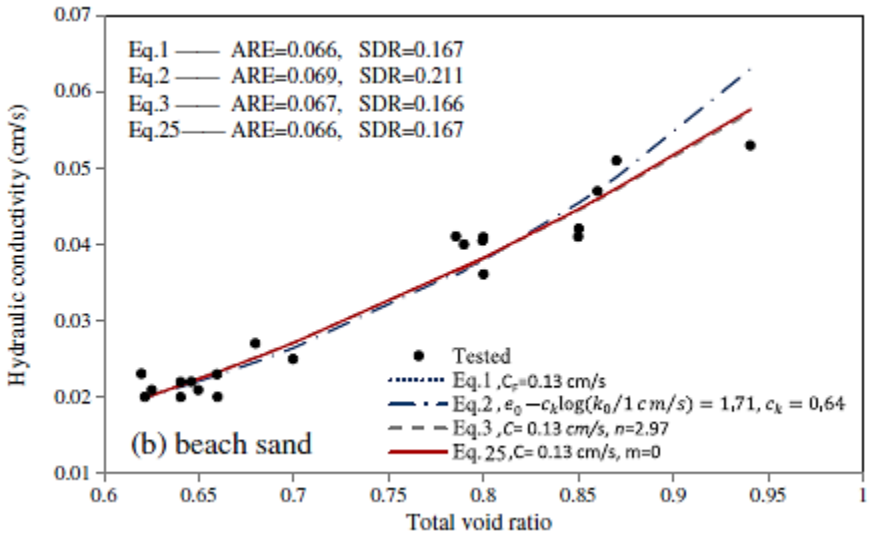

Figure 2.32 Variation of hydraulic conductivity with total void ratio for different methods (taken from Ren et al. (2016) with the permission of reproduction from Elsevier Science & Technology Journals)

P'kla et al. (2020) studied the variation of K_{sat} with void ratio for five clay and clay sand materials with d_{max} value of 0.1 mm using falling head permeability tests and following ASTM D5084-03. The results showed that the K_{sat} value increases when the void ratio increases for all the materials.

2.4.2.3 Particle shape

Particle shape is another factor affecting the hydraulic conductivity of materials (Terzaghi, 1925; Clayton et al., 2009). Several parameters such as roundness, sphericity, angularity and surface roughness are used to define particle shape (Powers, 1953). The surface roughness of the particles has an effect on the pore space, where water flow may occur. Alternatively, it affects the hydraulic conductivity by creating different ways for the water moving through the voids. Thus, particle shape characteristics determine the effective porosity, which is critical for the hydraulic conductivity (Valentin et al., 2016).

Cabalar and Akbulut (2016b) investigated the influence of particle shape on hydraulic conductivity of rounded sand and very angular sand with different gradations. The permeability tests were performed on the materials with different ranges of particle sizes. All samples were

tested by constant head permeability test. Figure 2.33 shows the variation of hydraulic conductivity with particle size ranges for two materials. It is seen in the figure that for the materials containing finer particle sizes, the hydraulic conductivity of sand with rounded particles is close to that of the sand with angular particles. When the particles are coarse, the hydraulic conductivity of the angular material can become significantly higher than that of the rounded material.

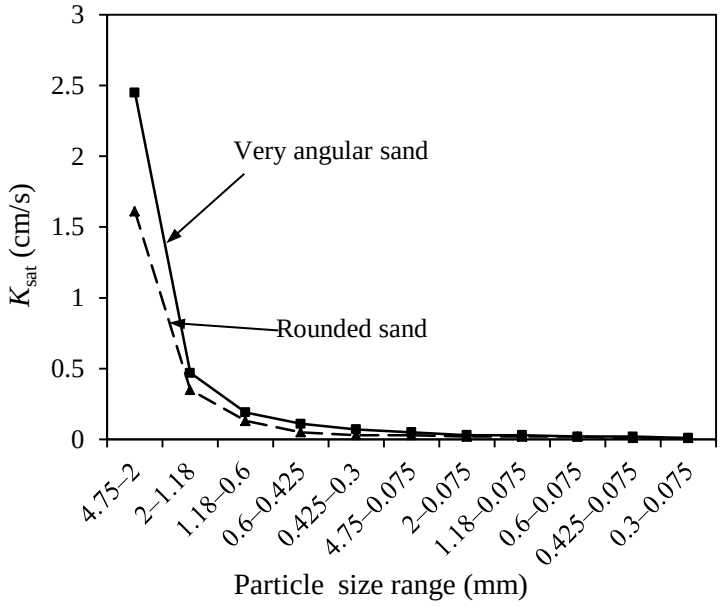

Figure 2.33 Variation of K_{sat} with particle size ranges for rounded and very angular sand; data taken from Cabalar and Akbulut (2016b)

2.4.3 Specimen size effect

Variation of hydraulic conductivity with specimen size is known as specimen size effect. When specimen size is too small for testing granular materials, leakage along the permeameter wall may occur due to the poor compaction in the cross section of specimen (Rose & Rizk, 1949; Franzini, 1968; Chapuis et al., 2012; Chapuis et al., 2015). Therefore, the tested specimen should be large enough to have a representative volume and avoid the specimen size effect. To this purpose, ASTM D2434-19, hereafter denoted as ASTM D2434 for simplification, requires specimen diameter (D) to be at least 8 or 12 times the d_{max} for constant head permeability tests of granular materials. For the materials with d_{max} values between 2 and 9.5 mm, ASTM D2434 requires

D/d_{max} ratio to be at least 8 or 12 when less than or more than 35% of total soil retain on sieve opening 2 mm, respectively. For the test materials with d_{max} values between 9.5 and 19 mm, ASTM D2434 requires D/d_{max} ratio to be at least 8 or 12 when less than or more than 35% of total soil retain on sieve opening 9.5 mm, respectively.

Once again, these minimum required ratios are easier exceeded for fine particles materials. With a coarse granular material, special and large size columns have to be used. The minimum required ratios of 8 or 12 are largely used to prepare specimens of permeability tests (Mavis & Wilsey, 1937; Krumbein & Monk, 1942; Loudon, 1952; Chapuis, 1989b, Hatanaka et al., 1997; Rowe et al., 2000; Mbonimpa et al., 2002; Duhaime et al., 2012; Peregoedova, 2012; Cabalar & Akbulut, 2016a, 2016b; Gan et al., 2019) even though the validity of these ratio has never been shown. For instance, Hernandez (2007) performed permeability tests on 8 samples. Three samples were sand with d_{max} values of 1.25, 5 and 10 mm. Three samples were mixtures of sand and gravel with d_{max} values of 5 and 10 mm. Two samples were made of gravel with d_{max} values of 10 and 50 mm. Table 2.12 shows the K_{sat} of the samples obtained by using different specimen sizes. It is seen that almost all the specimens meet the minimum size ratio required by ASTM D2434. However, these results cannot help to study the specimen size effect on K_{sat} because each sample with a specific $d_{\max}$ represents a distinct material. The variation of K_{sat} against D/d_{max} ratio is thus the result of combined effects of several influencing factors such as d_{max}, density, void ratio, gradation curve, etc.

Table 2.12 The K_{sat} values obtained by Hernandez (2007) for sand, mixtures of sand and gravel and gravel with different $d_{max;}$ D: specimen diameter and H: specimen height

Sample	$d_{\max}$ **(mm)**	**Specimen size** D **(mm)** × H **(mm)**	$D/d_{\max}$	K_{sat} **(cm/s)**
Sand	1.25	100 × 1710	80	0.0155
	5	150 × 1480	30	0.0539
	10	150 × 1350	15	0.0716
80% sand and 20% gravel	5	150 × 1490	30	0.00357
20% sand and 80% gravel	5	150 × 1450	30	0.0725
50% sand and 50% gravel	10	150 × 1290	15	0.00157
Gravel	10	150 × 1440	15	0.0313
	50	300 × 840	6	0.114

Gaillot (2007) studied K_{sat} of a waste rock with d_{max} values of 10, 28, 37.5 and 50 mm by using a permeameter cell with 300 mm diameter and 1000 mm height. The D/d_{max} ratios of the specimens were 30, 11, 8 and 6, respectively. Among the D/d_{max} ratios, the ratio of 6 is smaller than the minimum ratio required by ASTM D2434. Table 2.13 presents the K_{sat} obtained for the specimens with different d_{max} values. Again, the variation of K_{sat} is the test results of combined effects of several factors. The minimum specimen diameter over d_{max} ratio required by ASTM D2434 cannot be validated by using these results.

Table 2.13 The K_{sat} values obtained by Gaillot (2007) for the specimens with different d_{max}

Sample	**d_{max} (mm)**	**Specimen size D (mm) × H (mm)**	**D/d_{max}**	**K_{sat} (cm/s)**
Waste rocks	10	300 × 1000	30	0.06
	28	300 × 1000	11	0.25
	37.5	300 × 1000	8	0.31
	50	300 × 1000	6	0.27

Similar tests to those of Gaillot (2007) have been conducted by Bourrel (2008) on waste rocks with d_{max} values of 19, 25 and 50 mm. The D/d_{max} ratios of the specimens were 16, 12 and 6, respectively. The specimen size ratios met the requirement of ASTM D2434. However, these results could not help to validate the minimum required D/d_{max} ratio of ASTM D2434 due to using same specimen size for the samples with different d_{max}.

Peregoedova (2012) performed permeability tests on the specimens with d_{max} values of 2, 10, 19, 28 and 50 mm by using several permeameter cells. Table 2.14 shows the permeameter sizes (or specimen sizes) and the K_{sat} obtained for the specimens with different d_{max} and different specimen sizes. As it is seen, the D/d_{max} ratio of all specimens meets the minimum requirement of ASTM D2434 except for the ratio of 6. These results are not helpful to evaluate the specimen size effect because one needs to perform permeability tests by using different specimen sizes for each distinct material with a given d_{max} to be able to study the influence of specimen size on the K_{sat}.

Table 2.14 The K_{sat} values obtained by Peregoedova (2012) for the specimens with different d_{max}

Sample	**d_{max} (mm)**	**Specimen size D (mm) × H (mm)**	**D/d_{max}**	**K_{sat} (cm/s)**
Waste rocks	2	290 × 1000	145	0.0036
	5	100 × 2000	20	0.035
	10	290 × 1000	29	0.11

	19	290 × 1000	15	0.12
	28	290 × 1000	10	0.14
	50	290 × 1000	6	0.10

Cabalar and Akbulut (2016b) Performed permeability tests on two sands with different d_{max} by using a permeameter cell with 80 mm diameter. The specimen height is not given by the authors. Table 2.15 presents the specimen diameter over d_{max} ratios of the samples and the obtained K_{sat} values. As it is seen in the table, the specimen diameter to d_{max} ratio of ASTM D2434 is respected for all the specimens. However, a single specimen size was used for all the samples with different d_{max}. Again, these results do not help in validation of the minimum specimen size ratio required by ASTM D2434.

Table 2.15 The K_{sat} values obtained by Cabalar and Akbulut (2016b) for the samples with different d_{max}

Material	**Particle size ranges**	d_{max} **(mm)**	D/d_{max}	K_{sat} **(cm/s)**
Sand 1	0.075 to 0.3 mm	0.3	267	0.01
	0.075 to 0.425 mm	0.425	188	0.01
	0.075 to 0.6 mm	0.6	133	0.02
	0.075 to 1.8 mm	1.8	68	0.02
	0.075 to 2 mm	2.0	40	0.02
	0.075 to 4.75 mm	4.75	17	0.03
Sand 2	0.075 to 0.3 mm	0.3	267	0.01
	0.075 to 0.425 mm	0.425	188	0.015
	0.075 to 0.6 mm	0.6	133	0.02
	0.075 to 1.8 mm	1.8	68	0.03
	0.075 to 2 mm	2.0	40	0.03
	0.075 to 4.75 mm	4.75	17	0.05

2.5 Summary

The scalping technique is the simplest technique. This method, however, results in the increase in the percentage of particles smaller than targeted d_{max} compared to those of field materials (Zeller & Wullimann, 1957; Hamidi et al., 2012; Dorador et al., 2020a; Deiminiat et al., 2020). The parallel technique is widely used due to its advantage in producing a PSDC parallel to that of field material. However, this literature review reveals the fact that the technique need new particle sizes smaller than the minimum particle sizes of field material in order to produce a really parallel PDS curve to that of field material, equally resulting in a modification to the PSDC

of field material. Furthermore, the particle shape of the materials may also change during sample preparation (Charles & Watts, 1980; Varadarajan et al., 2006; Honkanadavar et al., 2016; Ovalle et al., 2020). The validity or invalidity of the parallel and other scaling down techniques has never been demonstrated (Marachi et al., 1972; Wang et al., 2019; Kouakou et al., 2019; Deiminiat et al., 2020). Replacement technique is another few used scaling down technique. This technique results in an increase in the portion of the particles between the target $d_{\max}$ and No. 4 sieve compared to that of field material (Donaghe & Torrey, 1985; Feng & Vitton, 1997; Hu et al., 2010; Deiminiat et al., 2020). Its validity or invalidity has not correctly been shown. Rather, the literature review shows that the reliability of the scaling down techniques was studied by directly comparing the shear strengths of scaled down samples with those of the field material. This methodology is not appropriate. Further analysis of literature review shows that almost all the existing data of direct shear tests performed on coarse granular materials were obtained by using the minimum required specimen size over d_{max} ratios specified by the ASTM D3080/D3080M-11 even though the validity of this minimum required ratio is still unknown. Thus, the results obtained by the previous experimental studies cannot be used to identify reliable scaling down techniques.

In order to investigate the reliability of scaling down techniques, more experimental work is necessary, first to test the validity of the minimum required specimen size over d_{max} ratios specified by ASTM D3080/D3080M-11. Using large enough specimen size over d_{max} ratios is necessary to avoid any specimen size effect and ensure the reliability of direct shear test results. After then, direct shear tests with large enough specimen size over d_{max} ratios can be performed on several scaled down samples with different $d_{\max}$ values. A relationship between the shear strength of scaled down samples and $d_{\max}$ can be established by applying best-fitting technique. The shear strength of the field material can then be predicted by applying the extrapolation technique on the best-fitting curve.

The literature review has also shown that the previous studies made use of the minimum required specimen diameter over $d_{\max}$ ratios stipulated by ASTM D2434-19 to perform permeability tests on coarse granular materials even though the reliability of the minimum required ratios has not been validated. It is noted that the previous experimental studies were realized by using either one column on one material with different d_{max} values or several columns of different dimensions

on several materials with different d_{max} values. In both cases, the variation of measured K_{sat} versus D/d_{max} ratio is the results of combined effects of d_{max}, gradation curve, density or void ratio, etc. The results cannot be used to investigate the specimen size effect on the K_{sat} of granular materials. More experimental work is necessary to obtain the variation of K_{sat} values solely associated with the variation of specimen size. For a material with a given d_{max} under the same conditions of compaction and water content, permeability tests should be performed using several columns with different dimensions. The results can then be used to find the relationship between K_{sat} values and D/d_{max} ratio to test the validity of the minimum required specimen size over d_{max} ratios stipulated by ASTM D2434-19.

CHAPTER 3 METHODOLOGY OF THE RESEARCH PROJECT

The research project started with a comprehensive literature review on the determination of shear strength and hydraulic conductivity of granular materials such as waste rocks considering the scale effect. The in situ and laboratory direct shear tests and permeability tests are presented with the analysis of the advantages and limitations. The existing experimental results and the interpretations on the analyses are then presented. The focus is given to the reliability of experimental results considering the specimen size effect (SSE). The critical literature review indicates that

(i) The minimum required specimen width over d_{max} ratio of ASTM D3080/D3080M-11 used to prepare testing specimens for small scale direct shear tests seem to be not large enough to eliminate the SSE. The results are thus unreliable.

(ii) The reliability of scaling down techniques is still unknown and it is not clear the application of which scaling down technique results in reliable shear strength for field materials.

(iii) The validity of the minimum specimen diameter over d_{max} ratio required by ASTM D2434-19 for constant head permeability tests is still unknown for granular materials. The reliability of the prediction models is thus questionable for these materials.

Therefore, four testing plans are considered to solve the problems as follow:

1) Identify the minimum required specimen width over d_{max} ratio to avoid any specimen size effect on small scale direct shear tests.
2) Identify a scaling down technique that can be used to obtain reliable shear strength of field materials at large scale.
3) Propose and validate a predictive equation to predict the reliable friction angle of the field materials.
4) Identification of the minimum required diameter to d_{max} ratio to avoid any SSE in constant head permeability tests.

3.1 Testing materials

Two types of waste rocks have been provided from two different origins called WR 1 and WR 2. Figure 3.1 shows the pictures of the portions taken from waste rocks origins. Part of waste rocks are first sorted into particle sizes ranging from 0.075 to 25 mm. Different samples with varying grain sizes are prepared from two waste rocks, depending on the testing plans. There was no digital camera available to precisely determine degree of angularity and roundness of the waste rocks. Based on naked-eye observation, particle shapes of the waste rocks are sub-angular to sub-round. However, the same particle shape was observed for different particle sizes.

(a) (b)

Figure 3.1 Photos of two types of waste rocks: (a) WR1 and (b) WR2

3.1.1 Preliminary analyses

Based on the testing conditions described for the research project, the first step is to prepare the samples. Therefore, a portion of the testing materials is taken to prepare the required samples and measure the material characteristics. The methodologies used to prepare the samples are different for different testing plans. However, the preliminary characterization of the samples measured in this research includes particle size distribution curve, relative density and maximum void ratio.

- Particle size analysis: sieve analysis is used to determine the particle size distribution of samples (ASTM D6913/D6913M – 17).
- Specific gravity (G_s): the G_s of the samples with fine particle materials is measured by ASTM C128-15, and the G_s of the samples with coarse grain materials with d_{max} > 4.75 mm is measured using ASTM C127-15.
- Maximum void ratio (e_{max}): the e_{max} value of the samples was calculated using density and Gs of the samples and following ASTM C29/C29M-17a.

3.2 Direct shear tests

Direct shear test is a classic method that has been used widely to determine shear strength of geomaterials (Goodrich, 1904; Casagrande & Albert, 1932; Casagrande, 1936; Terzaghi, 1936; Cooling et al., 1936; Terzaghi & Peck, 1948; Skempton, 1958; Hutchinson, 1962; Marsland, 1971; Zahran & Naggar, 2020; Motaharitabari & Shooshpasha, 2021; Xue et al., 2021).

Some advantages of the direct shear tests toward other methods can be addressed as follow (Takada, 1993):

- There is a prescribed zone for shearing the sample.
- For samples with an appropriate dimension, the shear deformation is approximately plane strain and deformation is simple and applicable for structures design.
- The size of the samples can be varied from small to very large.
- Preparing direct shear test and employing that is simple.
- Partially saturated soil specimens can be tested with the appropriate equipment.

In the direct shear test, a constant normal load applies to the top loading platen. The shear load is then applied to the left or right side of the box (or carriage). During performing test, the shear force, normal and shear displacement are recorded. In order to find the shear strength, several tests with different normal loads should be performed. By plotting the best fit curve for the graph of peak shear stress versus normal stress, the Mohr-Coulomb failure envelope is obtained and the friction angle is determined. The mechanism used in this thesis to conduct direct shear tests is based on ASTM D3080/D3080M (2011).

3.3 Pile tests

Pile test is a simple and old method for determining the repose angle. There are different pile test methods including tilting box, fixed funnel, drum, hollow cylinder and tilting cylinder methods (Rousé, 2014; Montanari et al. 2017; Beakawi & Baghabra, 2018; Santamarina & Cho, 2001). The angle of repose is described as the largest slope angle of a pile made from cohesion-less materials such as gravel and sand. Depending on the amount of pressure (or compaction) required on the pile slopes, pile tests may be performed by lifting a box or using a funnel. The most common method is used in this study to form a pile with the least amount of compaction as follows:

- Fill a funnel, which is supported vertically by hand or by a metal stand, with dry material as slow as possible.
- The funnel must be in contact with the top of the growing cone (a zero distance between the funnel and conical heap), and it must be kept stable without movement during lifting.
- An intermittent sliding can be observed on the surface. The intermittent sliding forms the pile, which looks like a conical heap as shown in Figure 3.2.
- Measure the final vertical height and bottom width of the pile.
- The repose angle can then be obtained using Equation (3.1).

$$\phi_{pt} = \tan^{-1}(\frac{2h_p}{d_p}) \tag{3.1}$$

where ϕ_{pt} is the repose angle measured by the pile test (°), h_p is the vertical height of the pile (mm) and d_p is the bottom diameter of the pile (mm).

The same method is used in this thesis to perform pile tests. More derail information is presented in Chapter 7.

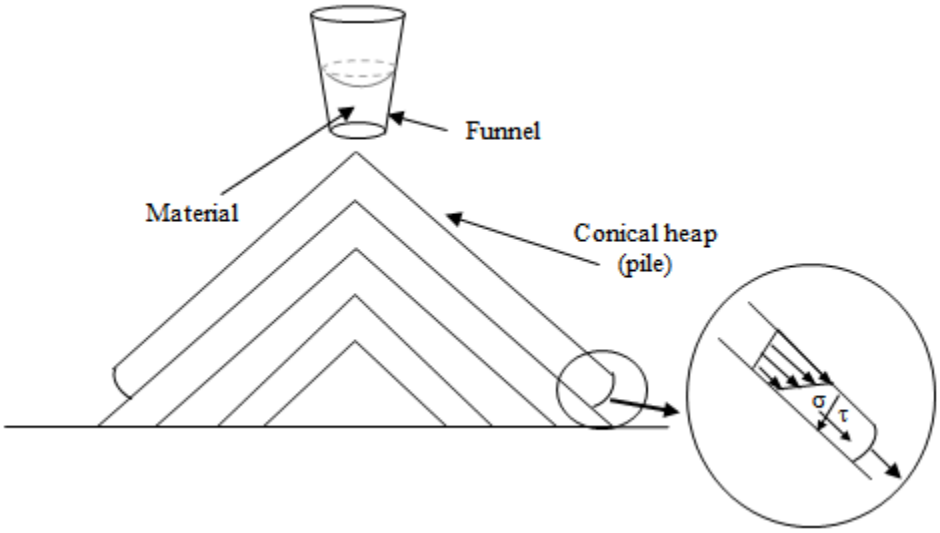

Figure 3.2 Forming a loose conical heap (pile)

3.4 Constant head permeability tests

In this test, water head remains constant over a sample and the amount of water at a certain moment is measured. Using Darcy's law and Equation (3.2) (Todd & Mays, 2005), the hydraulic conductivity can be calculated. A schematic view of a constant head permeameter is shown in Figure 3.3.

$$K = \frac{L}{h}\frac{Q}{tA} \tag{3.2}$$

where L is distance between piezometers (m), h is difference in head on piezometers (m), Q is quantity of water discharged (m^3), t is total time of discharge (s), A is cross section of the specimen (m^2).

The testing procedure employed in this thesis to conduct constant head permeability tests is according to the ASTM D2434-19.

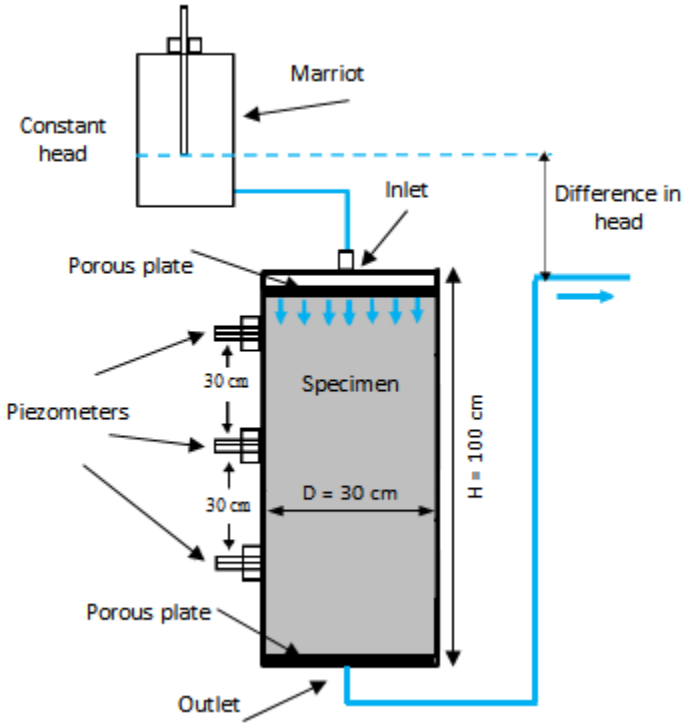

Figure 3.3 Schematic view of constant head permeability test

CHAPTER 4 ARTICLE 1: DETERMINATION OF THE SHEAR STRENGTH OF ROCKFILL FROM SMALL-SCALE LABORATORY SHEAR TESTS: A CRITICAL REVIEW

Akram Deiminiat, Li Li, Feitao Zeng, Thomas Pabst, Paul Chiasson, Robert Chapuis

Article published in Advances in Civil Engineering Journal, 2020, 8890237 on November 29, 2020

Abstract: Determining the shear strength of rockfill is a key task for the design and stability analysis of rockfill structures. When direct shear tests are performed, the well-established ASTM standard requires that specimen width and thickness must be at least 10 and 6 times the maximum particle size (d_{max}), respectively. When the value of $d_{\max}$ is very large, performing such tests in laboratory with field rockfill becomes difficult or impossible. Four scaling down techniques were proposed in the past to obtain a modeled sample excluding oversize particles: scalping, parallel, replacement and quadratic. It remains unclear which of the four scaling down techniques yields reliable shear strength of field rockfill. In this paper, an extensive review is presented on existing experimental results to analyze the capacity of each scaling down technique to determine the field rockfill shear strength. The analyses show that previous researches followed an inappropriate methodology to validate or invalidate a scaling down technique through a direct comparison between the shear strengths of modeled and field samples. None of the four scaling down techniques was shown to be able or unable to predict the field rockfill shear strength by extrapolation. The analyses further show that the minimum ratios of specimen size to d_{max} dictated by well-established standards are largely used, but too small to eliminate specimen size effect. In most cases, this practice results in shear strength overestimation. The validity or invalidity of scaling down techniques based on experimental results obtained by using the minimum ratios is uncertain. Recommendations are given for future studies.

Keywords: Rockfill; Shear strength; Gradation techniques; Specimen size effect; Maximum particle size; ASTM.

4.1 Introduction

Rockfill is usually considered as a good construction material for infrastructures. It is used to build dams for impounding water and reservoirs for hydroelectricity generation and prevent flooding (Marachi et al., 1969; Leps, 1970; Cooke, 1984). Rockfill is also commonly used as ballast bed in the construction of railways to hold railway sleepers and provide high bearing capacity of foundations (Cambio & Ge, 2007; Sevi, 2008; Lam et al., 2017). For steep slope terrains, rockfill permits slope protection from movement or scouring (Blijenberg, 1995; Chang & Phantachang, 2016). In mining industry, large amounts of waste rocks are produced every year (Zahl et al., 1992). In most cases, this material is deposited on surface as rock piles and considered as a waste material. Over recent years, it is increasingly used as a construction material both in and out mine sites (Tardif-Drolet et al., 2020). For instance, waste rocks have been more and more used to construct tailings dams (Azam & Li, 2010; Kossoff et al., 2014; Owen et al., 2020) or waste rock inclusions in tailings storage facilities (Aubertin et al., 2002a, 2002b; James et al., 2011; James & Aubertin, 2012; Saleh-Mbemba, 2016; Boudrias, 2018; Saleh-Mbemba et al., 2019). They are also used as rockfill to fill underground mine stopes (Hassani & Archibald, 1998; Potvin et al., 2005) or to construct barricades to retain backfill slurry in mine stopes (Li et al., 2009; Li & Aubertin, 2011; Yang et al., 2017). All these structures made of waste rocks must be properly designed and constructed to ensure their long-term stability. Failure of such structures may result in serious consequences such as ecological devastations, damage to equipment and infrastructures, personal injury, and even loss of lives (Pinto et al., 1985; Van Steijn, 1991; Blijenberg, 1995; Singh & Varshney, 1995; ICOLD, 2001; McLemore et al., 2009). Good knowledge of rockfill shear strength is fundamental in performing design and stability analyses of these structures.

Rockfill can be of natural origin (riverbed) or produced through rock blasting in a quarry or mine. Physical properties of rockfill can vary significantly in terms of particle size distribution and particle shape (Varadarajan et al., 2006). In general, the particle size of rockfill can vary from material as fine as clay and silt to material as coarse as gravel and boulders (Rao et al., 2011; Chang & Phantachang, 2016) while the particle shape can be qualitatively described as very angular, angular, sub-angular, sub-rounded, rounded and well-rounded (Lambe & Whitman, 1969). For natural rockfill, particles are often rounded with maximum particle sizes (d_{max})

typically varying from 4.75 to 80 mm (Honkanadavar et al., 2016). For rockfills made of blasted rock from quarries or mines, particles are typically angular with d_{max} varying from 4.75 mm to sometimes over 1000 mm (Varadarajan et al., 2006). The content in fine particles may also differ from one rockfill to another (Marsal & Fuentes de la Rosa, 1976; Douglas, 2002; Bazazzadeh et al. 2011). All these factors are well known to influence the shear strength of rockfill.

Previous studies showed that the shear strength of granular materials depends on several influencing factors, including grain-grain contact friction, grain-grain interlock, and compressive strength of solid grains and possibility of dilation (Lee & Farhoomand, 1967; Houston, 1981, Yu et al. 2006). The grain-grain contact friction depends on the base or residual friction and asperity of the grain surfaces (Ladanyi & Archambault, 1969; Brady & Brown, 1993). The grain-grain interlock and dilation depend on the particle angularity, particle gradation (coefficient of uniformity, curvature, $d_{\max}$), degree of compaction, and confining pressure (Holtz & Kovacs, 1981; Yu et al. 2006; Andjelkovic et al. 2018). The mechanisms controlling the shear strength of granular material are important for understanding the role of each influencing factor. However, detailed discussion on this aspect is beyond the scope of the paper because the main purpose of this study is to see if it is possible to determine shear strength of rockfill from small scale laboratory shear tests. Focus will be given on the influence of $d_{\max}$ on the shear strength of rockfill, especially friction angle.

Direct shear tests and triaxial compression tests are commonly used to measure the shear strength of geomaterials. For triaxial compression tests, ASTM D4767 (2011) requires that the specimen diameter must be at least 6 times the maximum particle size, d_{max}. For direct shear tests, the minimum ratios of specimen width and thickness to d_{max}, as required by the commonly used standards, are presented in Table 4.1. For most soils such as clays, silts, and sands having a d_{max} smaller than 2 mm, satisfying the standard requirements is not a problem because the ratio of specimen size to d_{max} can easily exceed 25 even with a small shear box of 50 mm. For rockfill and gravel materials with d_{max} exceeding 75 mm, it is technically very difficult (Marachi et al., 1969) and economically impracticable (Williams et al., 1983) to design testing equipment that can accommodate large size specimens that respect the requirements of testing standards.

To avoid such problems, one may try to perform in situ tests to directly obtain the field rockfill shear strength (Marsland, 1971; Barton & Kjaernsli, 1981; Matsuoka et al., 2001; Oyanguren et

al., 2008; Ghanbari et al., 2008; Liu, 2009; Wang et al., 2016; Haselsteiner et al., 2017; Wei et al., 2018). Goodrich (1904) conducted in situ direct shear tests using a 300 mm × 300 mm shear box on a construction site to determine the friction angles of clay, sand and gravel materials (Skempton, 1958). Tests were carried out by filling the box with the material and adding weights to the scale-pan. The upper half of the box was pulled until sliding. Tests were repeated by adding more weights to increase normal stress. The applied normal stress could not be very large. In addition, the box size is not suitable to test full scale field materials. By performing such tests, Goodrich (1904) showed that the friction angles of studied materials depend on particle size and degree of saturation. Similar results have been shown by Yu et al. (2006) through laboratory direct shear tests.

Table 4.1 Standards of direct shear tests regarding the maximum allowed particle size (d_{max}), specimen width (W), thickness (T) and diameter (D)

Standard	***W***	***T***	***W/T***	**Allowed d_{max}**
ASTM D3080/D3080M (2011)	≥ 50 mm	≥ 13 mm	≥ 2	Min{T/6, W/10}
AS 1289.6.2.2 (1998)	Not specified	≥ 12.5 mm	Not specified	T/6
BS 1377-7 (1990)	60 mm	20 mm	3	2 mm
	100 mm	25 mm	4	2.5 mm
	305 mm	150 mm	≈2	15 mm - 20 mm
Eurocode 7 (2007)	Not specified	Not specified	---------	T/10

The in situ testing approach of Goodrich (1904) was followed by many other researchers (Hutchinson & Rolfsen, 1962; Marsland, 1971; Oyanguren et al. 2008). This resulted in the modern direct shear test apparatus (Skempton, 1958).

As direct shear tests impose a sliding (shear) plane, the measured friction angle usually includes a dilation angle. The dilation degree decreases as normal stress increases and one usually observes a decrease in friction angle with an increase in normal stress (Das, 1983). Subsequently, one generally tends to obtain a high friction angle when large normal stresses cannot be applied in in situ direct shear tests. The experimental results are not representative of those of large and high rockfill infrastructures (Matsuoka et al., 2001; Fakhimi et al., 2007; Boakye, 2008; Zhang et al., 2016).

Barton and Kjaernsli (1981) performed in situ tilt tests to measure the shear strength of rockfill with a rectangular open box composed of three parts. The instrumentation and test procedure are shown in Figure 4.1. The box was first placed on level rockfill, and then filled and compacted. After having removed surrounding rockfill and the middle frame part of the box, one end of the filled box was lifted. The tilt angle at which the upper part of the filled box began to slide was taken as the maximum tilt angle (α), which corresponded to the friction angle ϕ at the applied normal stress σ_n.

Compared to other in situ direct shear tests, the method of Barton and Kjaernsli (1981) is simple. The test box can be as large as necessary, depending on the largest particles of the rockfill. However, the applied normal stress is limited by the upper box thickness and cannot be very large. The instrumentation is heavy and the tests are expensive. Furthermore, when the box is lifted at one end, particles can fall (due to the removal of the confinement initially provided by the middle part) before observing sliding of the upper part. The influence of particle fall on the measurement of shear strength has not yet been investigated.

Apart from the limitations specifically associated with each in situ shear test, other disadvantages associated with in situ shear tests include the difficulty in supplying equipment and transportation facilities, time-consuming, high costs, and generally intensive labor (Blijenberg, 1995). Finding a suitable and safe location is another non-negligible challenge for in situ shear tests.

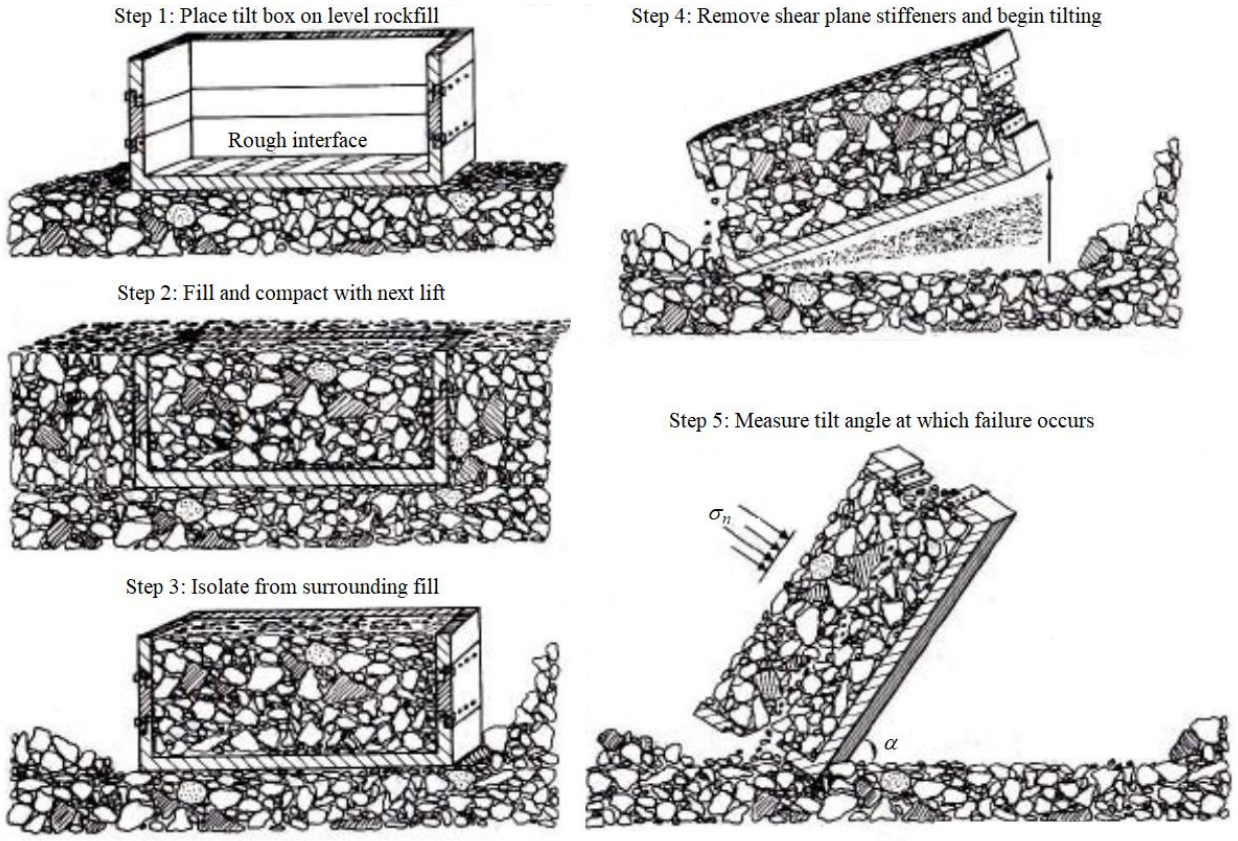

Figure 4.1 Instrumentation and test procedure of in situ tilt tests on rockfill (taken from Barton and Kjaernsli (1981) with the permission of reproduction from ASCE)

A simple and cost-effective alternative for obtaining the shear strength of field rockfill is to perform a series of laboratory shear tests on samples that are made from field rockfill with different $d_{\max}$ values (Holtz & Gibbs, 1956; Hamidi et al., 2012; Chang & Phantachang, 2016; Yang et al., 2019; Ovalle et al., 2020). A relationship between shear strength and d_{max} can then be established and used to predict the shear strength of field rockfill by extrapolation technique, which can be realized with the graphical or regression-based method (Varadarajan et al., 2006; Gupta, 2009; Hu et al., 2010; Abbas, 2011; Frossard et al., 2012; Vasistha et al., 2013; Pnakaj et al. 2013; Honkanadavar et al., 2016; Xu, 2018; Zhang et al., 2019).

Sample preparation by eliminating the oversize particles to fit the capacity of laboratory equipment is known as the scaling down (gradation) method. Several scaling down methods were proposed over the past years and used by researchers. It is unclear which scaling down technique can be used to obtain reliable field rock shear strength by extrapolation. This is the main reason

that motivates this review analysis. The initial and main objective of this paper is to identify a reliable scaling down technique that can be used to predict the shear strength of field rockfill from small scale laboratory tests.

To reach this objective, extensive review and comprehensive analyses on available experimental data are first presented, followed by an examination of the minimum ratios of specimen size to d_{max} suggested by well-established standards. Conclusions and recommendations are given at the end of the paper.

4.2 Laboratory shear tests

4.2.1 Large scale laboratory tests

With a large project having the allowed budget, it is desirable to perform laboratory shear tests with large scale apparatus to obtain the shear strength of in situ materials with less uncertainty. Large scale laboratory tests can be direct shear tests or triaxial compression tests. The earliest research on large scale tests was conducted by the South Pacific Division Laboratory (SPDL) of U.S. Army Corps of Engineers (USACE) (Hall, 1951; Leslie, 1963) and the US Bureau of Reclamation (USBR; Holtz & Gibbs, 1956).

Hall and Gordon (1964) were among the first researchers having performed large scale tests to estimate the static and kinetic internal friction angles of a rockfill containing natural alluvial deposits and coarse dredged tailings. Their test results showed that the friction angle decreases as the confining pressure increases because the particles can be crushed and dilation is diminished at high confining pressures. The same phenomenon was observed by other researchers through large scale direct shear tests on rockfill (Matsuoka & Liu, 1998; Boakye, 2008; Ovalle et al., 2014; Wang et al., 2019).

4.2.2 Scaling down techniques

Although large scale shear tests may provide interesting results as the allowed maximum particles can be quite large, it is impossible for all projects to perform large scale shear tests due to the requirement of special equipment, time-consuming and high costs. With available testing equipment in the laboratory, the maximum allowable specimen size is limited. This in turn limits

the d_{max} value to meet the minimum required ratios of specimen size to d_{max} stipulated by several standards such as the ASTM D3080/D3080M (2011) for direct shear tests and the ASTM D4767 (2011) for triaxial compression tests.

As rockfill can contain boulders equal to 2 m or more (Kutzner, 2020), large scale shear tests are impossible for all cases. Alternatively, one can perform small scale shear tests by excluding the particles larger than the chosen d_{max} of rockfill. This is once again known as scaling down or gradation technique (Marachi et al., 1969, 1972; Varadarajan et al., 2006; Hamidi et al., 2012; Wang et al., 2019; Ovalle et al., 2020). The variation of shear strength as a function of d_{max} can then be used to determine the shear strength of field rockfill through extrapolation.

The earliest scaling down technique, called scalping or truncated method, was proposed by Hennes (1953). In this technique, particles larger than the targeted d_{max} are simply removed, resulting in an increase of the percentages of all the particles smaller than the targeted d_{max} compared to those of the field material. To obtain a gradation curve similar to that of field material, Lowe (1964) proposed a scaling down technique, called parallel technique, in which the scalped sample is further modified in a way that the particle size distribution curve of modeled sample is parallel to that of the field material. Almost in the same time, another scaling down technique, called replacement technique was introduced by USACE (1965) to keep the percentages of fine particles unchanged compared to those of the field material. In 1969, Fumagalli proposed a scaling down technique to obtain a specific gradation curve. Details as well as the advantages and limitations of these scaling down techniques are presented in next subsections.

4.2.2.1 Scalping technique

During field sampling or sample preparation in laboratory, oversize particles (i.e. larger than the desired d_{max}) are simply excluded and removed. This method, called scalping or truncating, is the simplest and earliest scaling down method. First introduced by Hennes (1953), it is commonly used in sample preparation for laboratory tests (Holtz & Gibbs, 1956; Zeller & Wullimann, 1957; Leslie, 1963; Morgan & Harris, 1967; Hall & Smith, 1971; Williams & Walker, 1983; Donaghe & Torrey, 1985; Hamidi et al., 2012).

Figure 4.2 shows the grain size distributions of a field rockfill and a scalped sample reported by Williams and Walker (1983). The field rockfill has a d_{max} of 200 mm while the targeted d_{max} of the scalped sample is 19 mm. To obtain the scalped sample, all the particle sizes larger than 19 mm were removed. After sieving analysis, the grain size distribution curve of the scalped sample is obtained. As seen in the figure, removal of the oversize particles results in different degrees of increase in the percentages of different size particles compared to the field material.

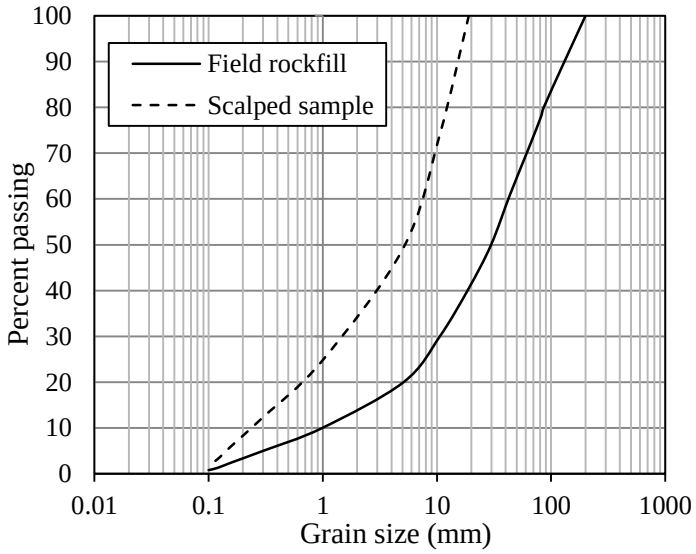

Figure 4.2 Grain size distribution curves of the field rockfill and scalped sample; data taken from Williams and Walker (1983)

Zeller and Wullimann (1957) performed triaxial compression tests to determine the shear strength of a rockfill. The samples were prepared by following scalping down technique. Figure 4.3a shows the particle size distribution curves of scalped samples at four d_{max} values (1, 10, 30 and 100 mm) and field material having d_{max} of 600 mm. The diameters of all tested specimens prepared for the triaxial compression tests were at least 5 times the d_{max} of the scalped sample. Figure 4.3b presents the shear strengths of the scalped samples under a confining pressure of 88 kPa in function of their d_{max} value for porosities of 30% and 38%, respectively. For a given porosity, shear strength significantly decreases as the d_{max} value increases. By extrapolating the experimental data of the scaled down specimens, the shear strength of field rockfill with d_{max} of 600 mm can then be predicted. However, no conclusion can be drawn to evaluate whether the

field rockfill shear strength can be correctly predicted by using the scalping method because the shear strength of field rockfill with d_{max} of 600 mm was not measured.

Through the previous analysis, one sees that sample preparation of scalping technique is very simple. However, the application of the scalping procedure results in a significant change in the gradation curve. The percentages of all particles of the scalped sample increase and become higher than those of the field material.

4.2.2.2 Parallel scaling down technique

Similar to the scalping method, parallel scaling down method also consists of excluding particles larger than the targeted d_{max}. However, the scalped sample is further modified to yield a particle size distribution curve that is parallel to that of the field material (Lowe, 1964; Tombs, 1969; Charles, 1973). The obtained modeled sample thus has a gradation curve looking like a horizontal translation of the field material gradation curve towards the fine particles size side. If N is the ratio of the maximum particle size of field material to that of a modeled sample, the shift distance will be equal to Log(N) along the logarithm axis of particle size (Lowe, 1964).

For example, to produce a modeled sample of parallel scaling down technique having a d_{max} value of $d_{max.m}$ from a field material having a d_{max} value of $d_{max.f}$, the ratio N is calculated as follows:

$$N = \frac{d_{max.f}}{d_{max.m}} \tag{4.1}$$

For a given percentage passing p, the grain size of modeled sample is calculated as:

$$d_{p.m} = d_{p.f}/N \tag{4.2}$$

where $d_{p.m}$ and $d_{p.f}$ are the sizes of modeled sample and field material having a percentage passing p, respectively.

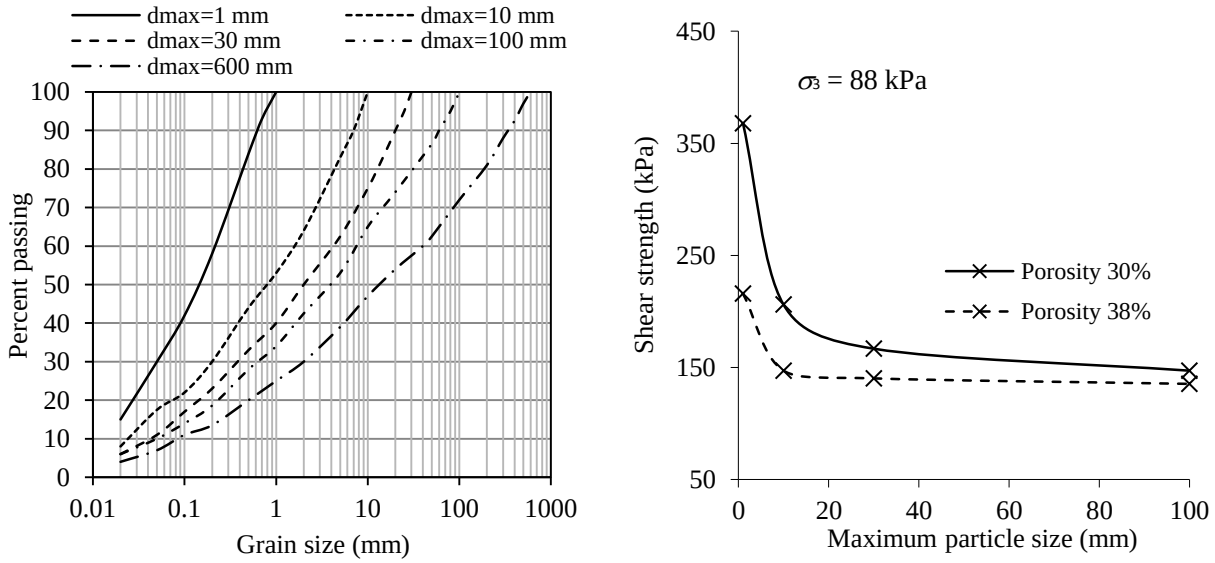

(a) (b)

Figure 4.3 (a) Grain size distribution curves of the field material (rockfill) and the scalped samples; (b) Variation of shear strength with the d_{max} for different porosities; data taken from Zeller and Wullimann (1957)

Once the target parallel gradation curve is determined, the required mass for each range of particle sizes can be obtained by considering the required portion and the total mass of the modeled sample. It is very much possible that some particle size values obtained by Equation (4.2) are missing in the available sizes of standard sieves. In this case, the sieves having the closest sizes to those calculated by Equation (4.2) should be taken as an approximation. In addition, the production of parallel curves requires addition of particles finer than the minimum particle size of field material. Obviously, it is impossible without a grinding operation on the field material or without addition of needed fine particles from another material. In both cases, the origin of the modeled sample is different from that of the field material. In practice, the particle size distribution curves of parallel gradation samples can be nonparallel to that of field material near the fine particle part.

Figure 4.4 shows a particle size distribution curve of modeled sample by applying the parallel gradation method along with that of field material. The d_{max} value of the field material is 305 mm while the target d_{max} of the parallel gradation sample is 38 mm. The ratio between the d_{max} value

of the field material and modeled sample is 8. The shift distance between the gradation curves of the field material and modeled sample is Log(8) along the logarithm axis of particle size.

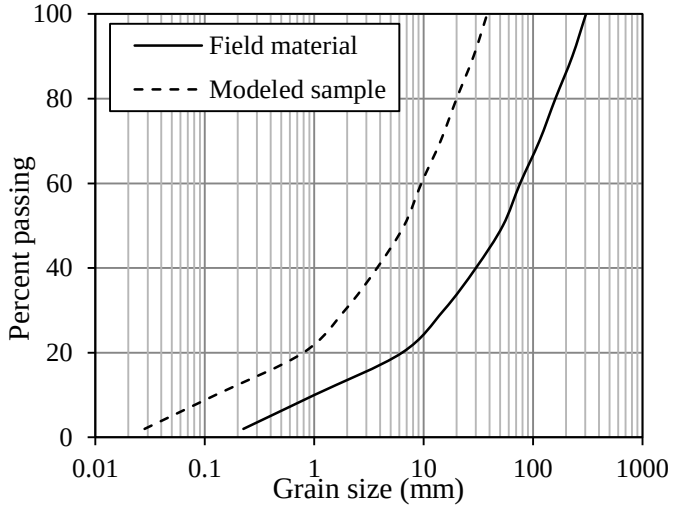

Figure 4.4 Grain size distribution curves of the field material and parallel sample; data taken from Lowe (1964)

The parallel scaling down method was proposed due to the necessity of determining the shear characteristics of several types of gravelly soils for the SPDL of USACE. Leslie (1963) compared the friction angles obtained by triaxial compression tests on specimens prepared by parallel and scalping methods without any conclusive results. No recommendation could be made on the reliability of the two scaling down methods.

Marachi et al. (1972) applied the parallel scaling down method to investigate the influence of d_{max} on the peak friction angle of three samples (Pyramid dam materials, Crushed basalt and Oroville dam materials) through triaxial compression tests. Two samples were made of well-graded and angular particles. The third sample was prepared by a mixture of sub-angular and rounded particles. The content of sub-angular and rounded particles was not specified and the angularity or roundness degree of the mixture was quantitatively unknown. Samples were prepared with diameters of 71, 305 and 914 mm for d_{max} value, respectively, of 12, 50 and 152 mm. The minimum required ratio of 6 (ASTM D4767 2011) of specimen size to d_{max} was thus respected in all the tests. Triaxial compression tests were conducted under confining pressures of 207, 965, 2896 and 4482 kPa, respectively. The experimental results show a decreasing friction angle as d_{max} value increases (Figure 4.5). However, this study does not confirm if the predicted

friction angles through extrapolation correspond to the friction angle of the field materials since no tests were performed on the latter.

Charles (1973) studied the friction angle of a rounded rockfill with d_{max} of 900 mm by triaxial compression tests. The parallel method was used to scale down the field rockfill to three samples with d_{max} of 40 mm, 100 mm and 300 mm, respectively. Samples were prepared at the same porosity as the field sample. A ratio of sample diameter to d_{max} of 5 was used for all the tests. Figure 4.6 shows the variations of peak friction angle with d_{max} for different confining pressures. The test results show that an increase in the confining pressure leads to a reduction in the friction angle for a given d_{max}. Same results were found by previous researchers (i.e., Holts & Kovacs 1981; Marachi et al. 1972). This tends to indicate that confining pressure should be adequately chosen to mimic the stress condition of field material during the application of the scaling down technique. Figure 4.6 also shows that the peak friction angle slightly increases as d_{max} increases. This trend is opposite of that found by Marachi et al. (1972). This may be attributed to the rounded particles of the tested rockfill while those of Marachi et al. (1972) were angular or subangular.

Figure 4.7 further shows a collection of experimental results on the variations of peak friction angle with d_{max} for (alluvial) rounded (Figure 4.7a) and (quarried) angular (Figure 4.7b) materials obtained by applying the parallel scaling down technique. The minimum ratio of specimen size to d_{max} of 10 as required by ASTM D3080/D3080M (2011) was taken in all the tests. One sees that the friction angle of rounded material increases as d_{max} increases while the friction angle of angular material decreases with increasing d_{max} value.

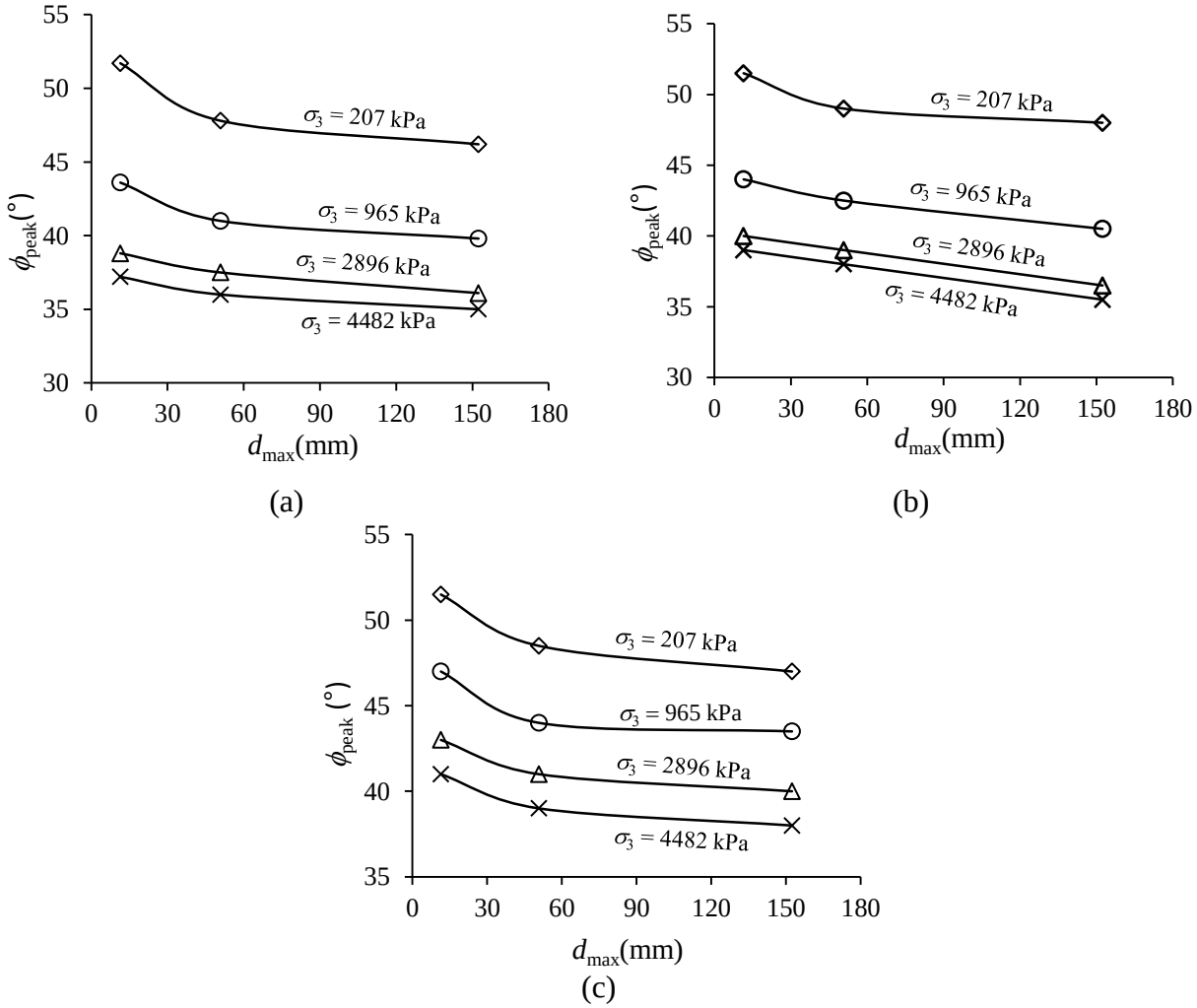

Figure 4.5 Variations of peak friction angle with the maximum particle size for (a) Pyramid dam materials, (b) Crushed basalt and (c) Oroville dam materials with different confining pressures; data taken from Marachi et al. (1972)

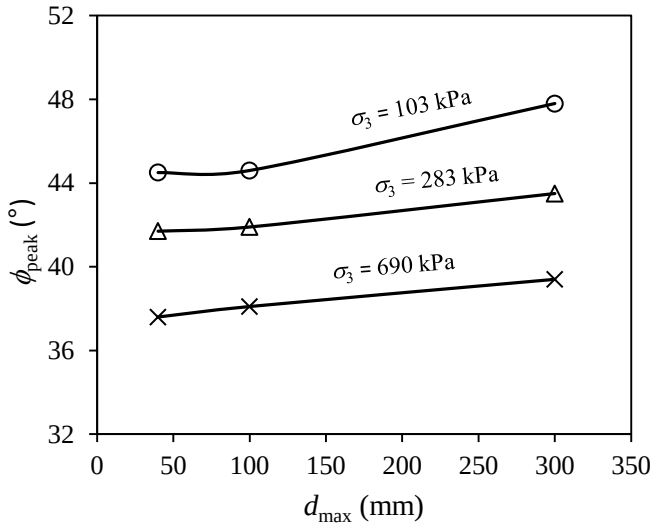

Figure 4.6 Variation of peak friction angle with maximum particle size of parallel modeled samples with different confining pressures; data taken from Charles (1973)

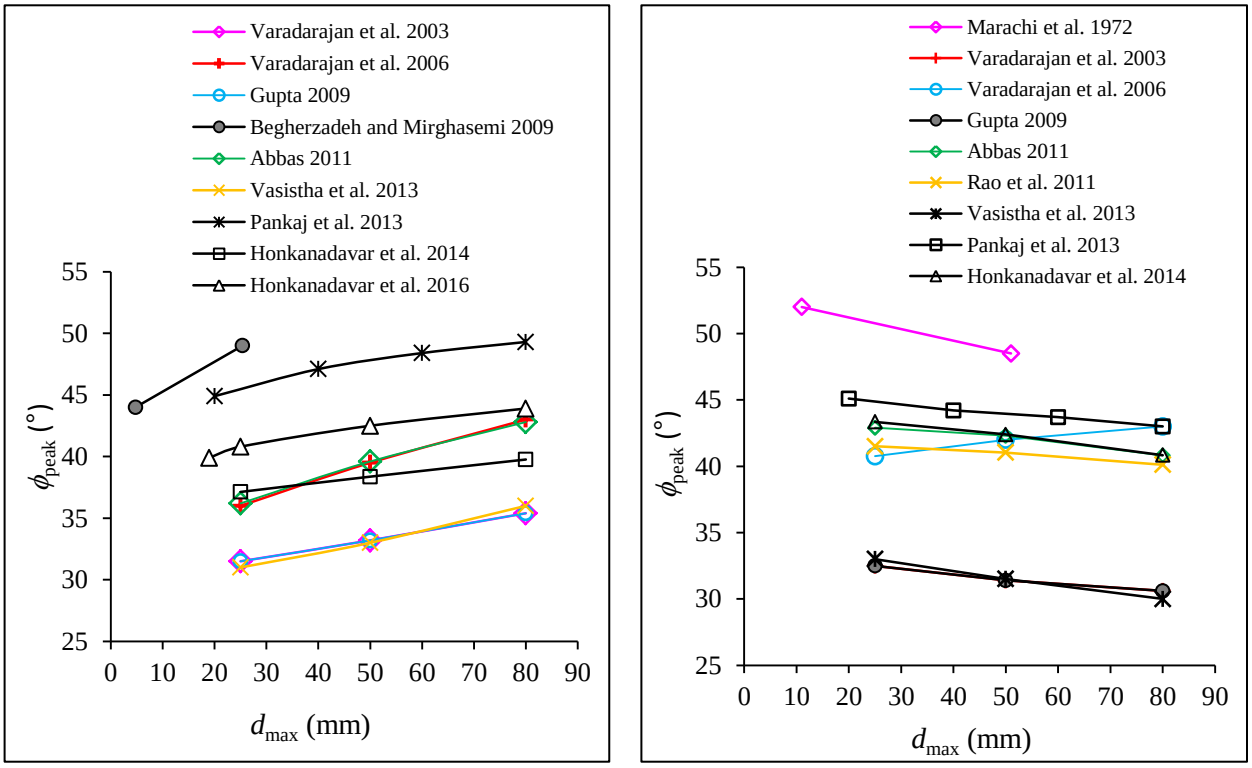

(a) (b)

Figure 4.7 Variations of peak friction angle with d_{max} for (a) rounded materials and (b) angular materials; data taken from Marachi et al. (1972); Rao et al. (2011); Varadarajan et al. (2003); Abbas (2011); Varadarajan et al. (2006); Gupta (2009); Bagherzadeh and Mirghasemi (2009);

Pankaj et al. (2013); Vasistha et al. (2013); Honkanadavar et al. (2014); Honkanadavar et al. (2016)

The parallel scaling down technique was proposed in order to reproduce the shape of the gradation of field materials. In practice, particle shape and fine particle content can change during sample preparation (Lee & Seed, 1967; Charles & Watts, 1980; Sharma et al., 1994; Ramamurthy, 2004; Varadarajan et al. 2006; Verdugo & De la Hoz, 2006; Stober, 2012; Honkanadavar et al., 2016). This can in turn result in a change in the friction angle (Wang et al., 2019; Ovalle & Dano, 2020). Moreover, the reproduction of modeled samples having gradation curves strictly parallel to that of field material requires addition of fine particles smaller than the minimum particle size of the field sample. This in turn requires grinding of field material or the addition of finer particle material of a different source. The modeled samples thus contain a portion of material which has a source different from that of the field material. In practice, the particle size distribution curves of parallel gradation samples can be nonparallel to that of field material, either due to the lack of required (nonstandard) sieve sizes or due to the lack of required fine particles smaller than the minimum particle size of the field material. All these indicate that the parallel scaling down technique has also some drawbacks despite it is widely used in practice. At present, it is still far from being able to conclude whether the friction angle of field rockfill can be predicted by extrapolating test results obtained with the parallel scaling down technique. More investigations are needed on this aspect.

4.2.2.3 Replacement technique

When the portion of removed oversize particles exceeds 10% during the application of the scalping technique, USACE (1965) suggested replacing the removed weight by particles finer than the targeted d_{max} but greater than No. 4 sieve (4.75 mm). The percentage of particles finer than the No. 4 sieve thus remains unchanged (USACE, 1965; Frost, 1973; Donaghe & Torrey, 1985).

The replacement technique was first used by Frost (1973) to conduct compaction tests of boulder-gravel fill for a large dam. Later, a few studies were conducted to verify the reliability of the replacement technique (Donaghe & Townsend, 1973; Donaghe & Torrey, 1985; Houston et al., 1994).

Figure 4.8 shows the grain size distribution curve of a field material having d_{max} of 80 mm and that of modeled sample with d_{max} of 20 mm (Donaghe & Townsend, 1976). The first one was obtained by measuring the masses of particles retained on different sieves and the total mass of the field material. The particles larger than the targeted d_{max} (i.e., 20 mm) were weighed and excluded. The same mass of particles having sizes between 4.75 mm (i.e. sieve No. 4) and d_{max} was added in the sample by applying the following equation to obtain the gradation curve of the modeled sample (Donaghe & Townsend, 1976):

$$P_{ij.a} = \frac{P_{ij.f}}{P_{d_{max}} - P_{No.4}} \times P_o \tag{4.3}$$

where $P_{ij,a}$ is the percentage by mass of added particles passing sieve having size j ($\leq d_{max}$) and retained on the neighbor sieve having size i ($\geq$ 4.75 mm); $P_{ij,f}$ is the percentage by mass of field material particles passing sieve size j ($\leq d_{max}$) and retained on the sieve size i ($\geq$ 4.75 mm); P_{dmax} is the percentage of field material particles passing the targeted d_{max}; $P_{No.4}$ is the percentage of field material particles passing the sieve of 4.75 mm (i.e. sieve No. 4); P_o is the percentage by mass of field material particles retained on the sieve having a size of the targeted d_{max}. The physical meaning of each symbol is shown in Figure 4.8 to ease their understanding.

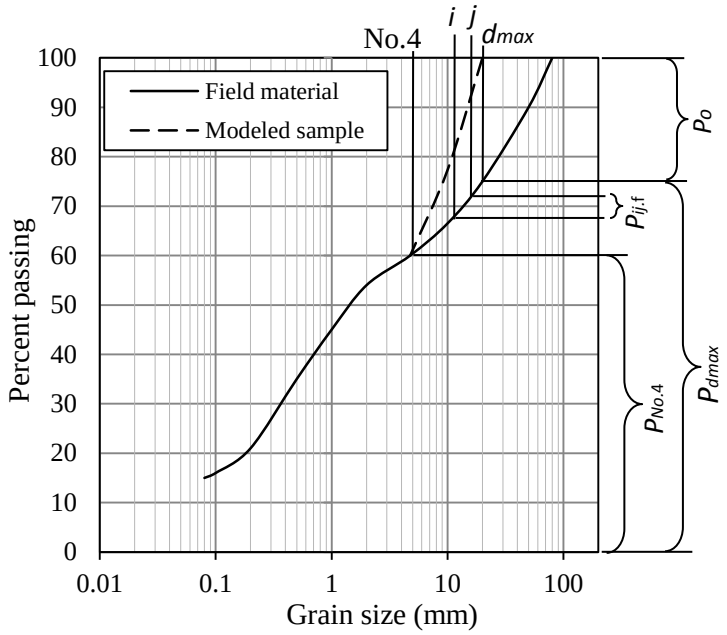

Figure 4.8 Grain size distribution curves of field material and modeled sample; data taken from Donaghe and Townsend (1976)

The application of this procedure results in a change in the gradation curve shape of the modeled sample compared to that of the field material for the particles greater than 4.75 mm. The replacement technique is thus considered as a scaling down method that modifies the gradation of field material (Donaghe & Townsend, 1976; Rathee, 1981; Feng & Vitton, 1997). Only a few researchers have used this technique (Torrey & Donaghe, 1991; Feng & Vitton, 1997). The validity or invalidity of this method for determining shear strength of field materials has not yet been demonstrated.

4.2.2.4 Quadratic grain-size technique

Quadratic grain-size technique was proposed by Fumagalli (1969). In this method, particle size distribution is defined by the following equation (Fumagalli, 1969):

$$P_Q = \sqrt{d/d_{max}} \times 100\% \qquad (4.4)$$

where d is a particle size of the modeled sample, smaller than the target d_{max}; P_Q is the percentage by mass of the particles smaller than d of the modeled sample.

Fumagalli (1969) applied this technique on a rockfill with d_{max} of 260 mm to obtain samples having d_{max} of 10, 20, 30, 60 and 100 mm, respectively. Confined compression tests were performed. A chamber of 100 mm in diameter and 200 mm high was used for the specimens with d_{max} of 10, 20 and 30 mm, respectively and another chamber of 500 mm in diameter and 1000 mm high on the specimens with d_{max} of 10, 60 and 100 mm, respectively. The minimum ratios of chamber diameter to maximum particle size were 3.3 and 5, respectively, for the small and large chamber tests. The confined compression tests were conducted by filling the chosen chamber with a tested specimen. The filled chamber was then submitted to an axial pressure. The axial and hoop strains were monitored. The reliability of the tests is unknown because the obtained friction angles were in the range of 23° to 25°, which are abnormally small for granular materials.

According to Fumagalli (1969), quadratic scaling down technique could be applied to well-graded materials. By applying this method, one can note that a unique particles size distribution curve will be obtained, independently of the field material once the target value of d_{max} is chosen. Table 4.2 shows percentages by mass of different particle sizes normalized by the target d_{max} by applying quadratic scaling down technique.

Table 4.2 Percentage by mass of different particle sizes by applying quadratic scaling down technique (Equation (4.4))

d/d_{max}	1	0.81	0.64	0.49	0.36	0.25	0.16	0.09	0.04	0.01	0.0025	0
P_Q (%)	100	90	80	70	60	50	40	30	20	10	5	0

Figure 4.9 shows the grain size distribution curve of a modeled sample by applying quadratic grain size technique with d_{max} of 20 mm. At P_Q = 20%, the target particle size of the modeled sample is 0.8 mm (= 0.04 × 20 mm).

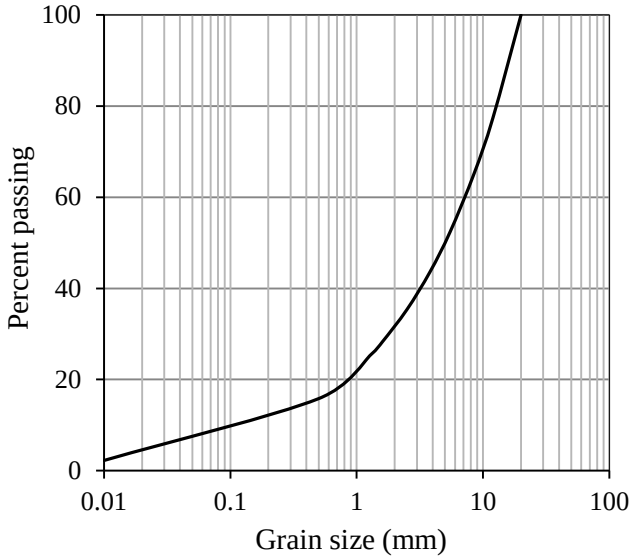

Figure 4.9 Grain size distribution curve of a modeled sample produced by using quadratic technique

Note that the particle size distribution curve of the scaled down sample spreads on a wide range of sizes. This may partly explain why Fumagalli (1969) suggested that quadratic scaling down technique is applicable to well-graded materials. However, as the scaled down sample does not depend on the field material once the allowed d_{max} is chosen, two situations can occur. First, if the particle size distribution curve of the scalped down sample (i.e., after removal of oversize particles) intercepts the target particle size distribution curve on the fine particle side, one or several of the following operations are needed:

1) To add fine particles smaller than the minimum particle size of the field material.

2) To remove a portion of particles larger than the minimum particle size of the field material.

3) To add coarse particle smaller than the allowed d_{max} but larger than the particle size at which the target and scalped particle size distribution curves intercept.

Second, if the particle size distribution curve of a scalped down sample does not intercept the target particle size distribution curve, except at the chosen d_{max}, one has to add a wide range of particles from particles smaller than the minimum particle size of the field material to coarse particles smaller than the allowed d_{max}. In both cases, the resulting gradations highly differ from those of original field sample. This may be why this quadratic scaling down method has not been used by other researchers since 1969.

4.3 Validation of scaling down techniques

The four presented scaling down techniques are not used at the same frequency. Parallel scaling down technique is frequently used in practice. Use of the scalping technique is less frequent than the parallel scaling down method but more than the replacement and quadratic scaling down techniques. The replacement method was used in a few researches while the quadratic scaling down technique is seldom used due to its complex preparation and the non-representativeness of the modeled sample, as shown in Section 2.2.4. None of the four scaling down techniques was shown to be able or unable to predict the shear strength of field rockfill by extrapolation.

To evaluate the validity of scalping and replacement techniques, Donaghe and Torrey (1985) performed triaxial compression tests on a mixture of sub-rounded sand and sub-angular gravel having a d_{max} of 76 mm. The degree of roundness or angularity of the mixture is unknown. The scalping and replacement techniques were used to obtain samples with d_{max} of 4.75 and 19 mm, respectively. All the tested specimens were prepared according to the minimum requirement of the ASTM D4767 (2011) in terms of the ratio between specimen size and d_{max}. Instead of doing more tests with specimens having different d_{max} and applying the extrapolation technique to predict the shear strength of field rockfill, Donaghe and Torrey (1985) directly compared the test results of scalped and replaced samples with that of field sample, as shown in Figure 4.10. They

concluded that the scalping and replacement methods are invalid because they found that the shear strengths of the scaled down samples differed from those of the field rockfill.

The methodology of Donaghe and Torrey (1985) could be adequate in the case where the shear strength of the scalped and replaced materials is insensitive to the variation of the maximum particle size. This is only possible when the angularity or roundness of the sample particles reaches a critical degree. In general, the peak friction angle of rounded or sub-rounded particle samples increases as the d_{max} increases (Figure 4.7a) while the friction angle of angular or sub-angular particle samples decreases as the d_{max} increases (Figure 4.7b). The methodology taken by Donaghe and Torrey (1985) to invalidate the scalping and replacement methods is therefore inappropriate.

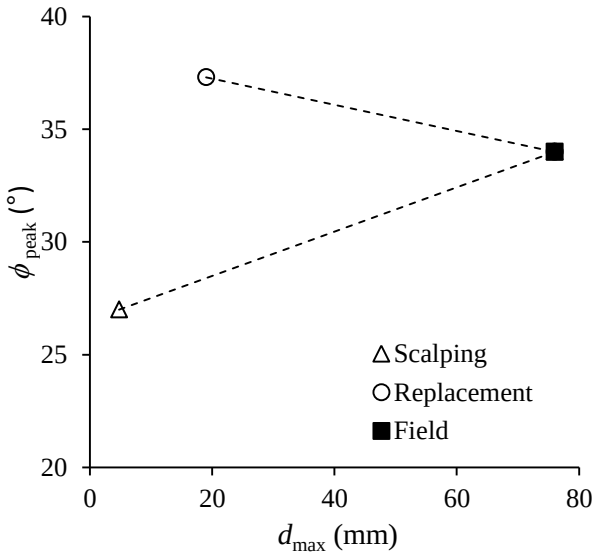

Figure 4.10 Comparison of peak friction angles of scalped and replaced samples relative to the field sample, all having a gravel content of 60%; data taken from Donaghe and Torrey (1985)

The same methodology of Donaghe and Torrey (1985) was followed by several other researchers (Linero et al., 2007; Hamidi et al., 2012). Linero et al. (2007) measured the shear strength of a coarse granular material through triaxial compression tests. The field material with d_{max} of 400 mm was scaled down by applying the parallel and scalping techniques, respectively. The tested specimens had a D/d_{max} ratio of 5, which was smaller than the minimum required ratio of ASTM

D2850 (2015). Again, the methodology is incorrect to evaluate the reliability of the tested scaling down techniques.

Hamidi et al. (2012) performed a series of direct shear tests according to ASTM D3080/D3080M (2011) to investigate the validity of the scalping and parallel techniques. A rounded sand and gravel mixture with a d_{max} of 25.4 mm was scaled down to samples having a d_{max} of 12.5 mm by applying the parallel and scalping techniques. Three normal stresses of 100, 200 and 300 kPa were used in the tests. Figure 4.11 shows the variations of the shear strength in terms of maximum shear stress under a normal stress of 100 kPa (Figure 4.11a) and peak friction angle (Figure 4.11b) as a function of the maximum particle size of the modeled and field samples for different relative densities. One first notes that the peak friction angle increases as the d_{max} increases from 12.5 to 25.4 mm for the rounded alluvium sand-gravel mixtures. This trend agrees with that of rounded materials (Figure 4.7a). Results further show that when the mixture is loose (D_r = 35%), the maximum shear stress (Figure 4.11a) and friction angle (Figure 4.11b) remain constant when the d_{max} of the scalped specimens increases while there is an increasing trend for the intermediate (D_r = 60%) or large (D_r = 85%) relative densities of both scalped and parallel samples. Once again, direct comparison of the shear strengths of modeled and field samples is not a good way to validate or invalidate the tested scaling down techniques. Consequently, one cannot conclude whether the scalping and parallel techniques are reliable to be used in an extrapolation to obtain the shear strength of field materials.

To correctly evaluate the capacity of a scaling down technique, different shear tests on scaled down specimens with different d_{max} values should be done. The shear strength of field materials can then be obtained by extrapolating the shear strengths of specimens with different d_{max} values. Bagherzadeh and Mirghasemi (2009) followed this approach and conducted a series of direct shear tests on coarse-grained material using 60 mm × 60 mm and 300 mm × 300 mm shear boxes to investigate the influence of scalping and parallel techniques on ellipsoidal gravel particles. The tested specimens were prepared to obtain a ratio value of 12 between specimen size and d_{max}. As shown in Figure 4.12a, a field sample with a d_{max} of 50 mm was scaled down to Samples 1 and 2 by applying the parallel scaling down technique and to Samples 3 and 4 by following the scalping technique. The small shear box was used for Samples 2 and 4 and the larger shear box was used for Samples 1 and 3. The maximum particle sizes were 25.4 mm for Samples 1 and 3 and 4.76

mm for Samples 2 and 4, respectively. Figure 4.12b shows the shear stresses at failure versus the d_{max} value under different normal stresses. The results show that the shear strength of the field specimens having a d_{max} of 38 mm (number given in Bagherzadeh and Mirghasemi 2009, but 50 mm according to Figure 4.12) can be predicted by extrapolating the test results of the parallel and scalped samples when the normal stress is high (294 kPa). When the normal stress is low (98 kPa) or intermediate (196 kPa), none of the two scaling down techniques can be used to predict the shear strength of the field material.

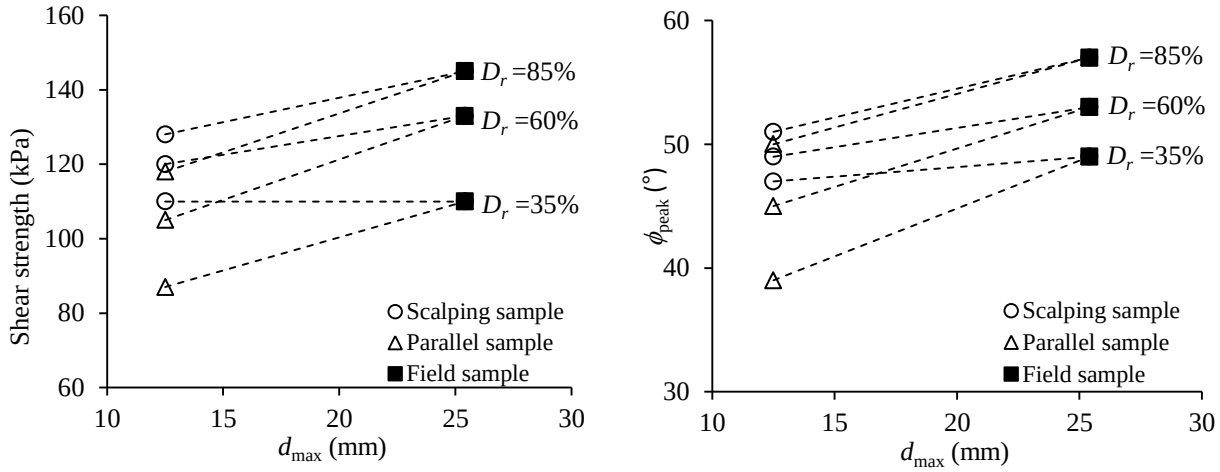

Figure 4.11 Variations of (a) shear strength (normal stress = 100 kPa) and (b) peak friction angle of field, parallel and scalping samples as a function of d_{max}; data taken from Hamidi et al. (2012)

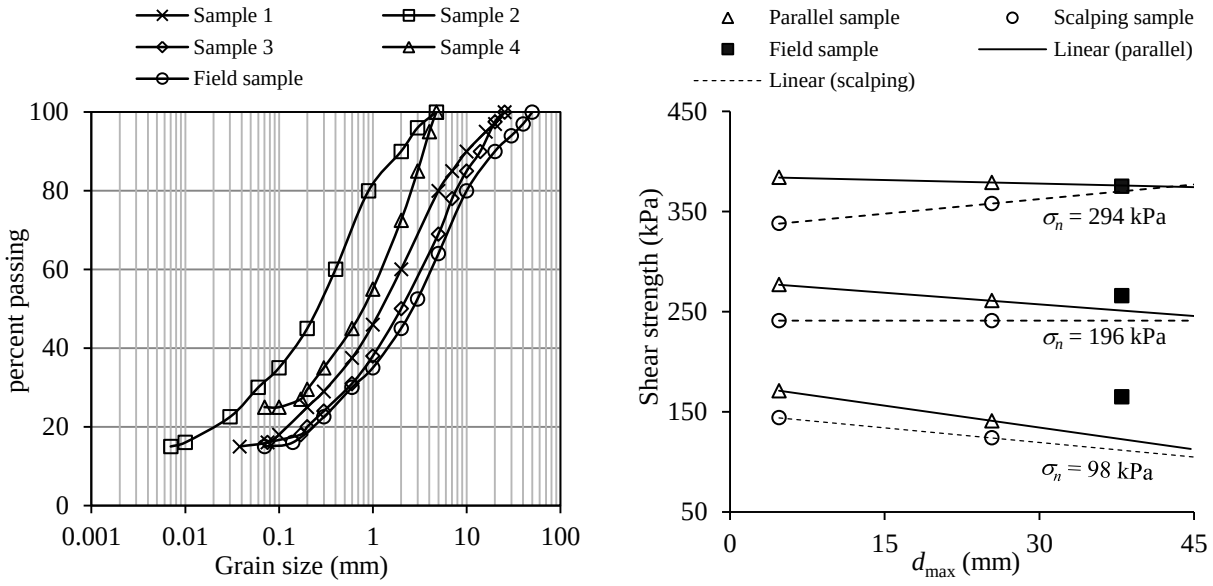

(a) (b)

Figure 4.12 (a) Distribution curves of field and scaled samples; (b) variation of shear strength as a function of d_{max} of parallel, scalping and field samples under different normal stresses; data taken from Bagherzadeh and Mirghasemi (2009)

Direct comparison between the shear strengths of modeled and field samples is not an appropriate methodology to validate or invalidate a scaling down technique. The invalidity of replacement technique is not correctly shown. The previous analyses seem to show that both scalping and parallel techniques can be used to predict the shear strength of field rockfill through extrapolation on laboratory shear test results when normal stress is high. Both the techniques fail when the normal stress is intermediate or low. However, it is noted that most of the previous experimental shear tests have been done by using the minimum (sometimes even smaller) required ratio of specimen size over d_{max} specified in ASTM D3080/D3080M (2011) for direct shear tests or ASTM D4767 (2011) for triaxial compression tests.

4.4 Specimen size effect

The variation of shear strength of granular materials with specimen size is known as a phenomenon of specimen size effect (Alonso et al., 2012; Kermani, 2016; Amirpour Harehdasht et al., 2017, 2018). For the convenience of laboratory tests, one tends to use specimens as small as possible. When the specimen size is too small, the measured shear strength cannot represent

that of the tested material in field conditions where the volume of the tested material can be very large. Therefore, the tested specimen should be large enough to avoid any specimen size effect, also known as a problem of representative volume element size (Drugan & Willis, 1996; Kanit et al., 2003; Wen et al., 2018). That is why the diverse standards specify minimum required ratios between specimen dimensions and d_{max}.

To determine the shear strength of granular materials by direct shear tests, ASTM D3080/D3080M-11 requires specimens to be at least 50 mm wide and 13 mm thick (Table 4.1). In addition, the width and thickness should, respectively, be at least 10 and 6 times the maximum particle size (d_{max}). The standards AS 1289.6.2.2 (1998) and Eurocode 7 (2007) require, respectively, a thickness of at least 6 and 10 times the d_{max} value (Table 4.1). For fine particle soils such as clay, silt and fine sand, the d_{max} values are smaller than 2 mm. The minimum required specimen sizes of 50 mm in width and 13 mm in thickness give a ratio of 25 between specimen width and d_{max} and a ratio of 6.5 between specimen thickness and d_{max}; these satisfy the minimum required ratios. However, these requirements are not yet undoubtedly validated by experimental results.

Rathee (1981) studied the influence of specimen size on the friction angle of mixtures of sand and gravel in four proportions (10, 30, 50 and 100%) by using two shear boxes of 60 mm × 60 mm and 300 mm × 300 mm. The tested specimens with d_{max} of 50, 37.5, 25, 19, 12.5 and 6.3 mm were obtained by the parallel scaling down technique on a field material with d_{max} of 450 mm. The test results, not presented here, involved simultaneously the effects of d_{max} and specimen size. The methodology followed in this study is inappropriate to investigate the specimen size effect.

Palmeira and Milligan (1989) performed direct shear tests on ~~a~~ sand with a d_{max} of 1.2 mm by using small (60 mm × 60 mm × 32 mm), medium (252 mm × 152 mm × 152 mm) and large (1000 mm × 1000 mm × 1000 mm) size shear boxes. The W/d_{max} ratios corresponding to the three shear boxes were 50, 126.7 and 833, respectively, while the T/d_{max} ratios were 26.7, 126.7 and 833, respectively. The results showed that the friction angles remained almost constant when the W/d_{max} ratio increased from 50 to 833. However, these ratios are much larger than the minimum values required in ASTM D3080/D3080M-11. There were no shear test results on

specimens prepared with the W/d_{max} ratios between 10 and 50. Thus, these results cannot be considered as a validity of the minimum required specimen size ratio of ASTM D3080/D3080M-11.

Cerato and Lutenegger (2006) studied the influence of specimen size on the friction angles of five sands with different d_{max} values considering compactness states of loose, medium and dense sands. Three shear boxes were used. Table 4.3 shows the testing program and specimen sizes. All the ratios of specimen width and thickness to d_{max} met the requirements of AS 1289.6.2.2 (1998), ASTM D3080/D3080M-11, Eurocode 7 (2007) except for the GP3 and Winter sands with d_{max} of 5 mm when using the smallest shear box. The ratio of 5 between specimen thickness and maximum particle size is slightly smaller than the minimum required value (Table 4.1).

Table 4.3 Materials and specimen sizes used in direct shear tests by Cerato and Lutenegger (2006)

Materials	d_{max} **(mm)**	**60 mm × 60 mm × 26.4 mm**		**101.6 mm × 101.6 mm × 40.64 mm**		**304.8 mm × 304.8 mm × 177.8 mm**	
		T/d_{max}	W/d_{max}	T/d_{max}	W/d_{max}	T/d_{max}	W/d_{max}
Ottawa	0.9	29	67	45	113	198	339
FHWA	1.7	16	36	24	60	105	179
Morie	2.0	13	30	20	51	89	152
GP3	5.0	5	12	8	20	36	61
Winter	5.0	5	12	8	20	36	61

Figure 4.13 shows the peak friction angle versus the ratios of specimen width and thickness over d_{max} for materials with different densities. For the Ottawa sand with d_{max} of 0.9 mm (Figure 4.13a), the friction angle remains almost constant when the W/d_{max} ratio increases from 67 to 339 and the T/d_{max} ratio increases from 29 to 198. There was no specimen size effect for these ratios. However, there were no test results on specimens with the W/d_{max} ratio from 10 to 67. It is impossible to know whether a specimen size effect is removed for specimens with a W/d_{max} ratio of 10. Thus, the minimum ratio of specimen size to d_{max} as required in ASTM D3080/D3080M-11 is not validated.

For the material with a d_{max} of 1.7 mm (Figure 4.13b), the friction angle increases by more than 3 degrees when the W/d_{max} ratio increases from 36 to 179 and the T/d_{max} ratio from 16 to 105. For the material with a d_{max} of 2 mm (Figure 4.13c), the friction angle decreases by more than 2

degrees when the W/d_{max} ratio increases from 30 to 152 and the T/d_{max} ratio from 13 to 89. These results indicate that the specimen size effect on the friction angle of these materials is not eliminated in these ratio ranges, which invalidated the minimum requirements of ASTM D3080/D3080M-11 for these ratios.

For coarse grain materials with a d_{max} of 5 mm (Figures 4.13d and 4.13e), the friction angle decreases by more than 5 degrees as the W/d_{max} ratio increases from 12 to 20 and the T/d_{max} ratio from 5 to 8. The friction angle further decreases 2 degrees when the W/d_{max} ratio increases from 20 to 61 and the T/d_{max} ratio from 8 to 36. These results further illustrate that the specimen size effect on the friction angle of the coarse grain materials is not eliminated for a W/d_{max} ratio between 12 and 61, which again invalidates the minimum requirements of ASTM D3080/D3080M-11.

Ziaie Moayed et al. (2017) also performed direct shear tests by following ASTM D3080/D3080M-11 on a sand with d_{max} of 0.8 mm mixed with different silt contents (0, 10%, 20% and 30%). Three shear boxes 60 mm × 60 mm × 24.5 mm, 100 mm × 100 mm × 35 mm and 300 mm × 300 mm × 154 mm were used. The W/d_{max} ratios were 75, 125 and 375, respectively and the T/d_{max} ratios were 31, 44 and 192, respectively. For sand mixed with 30% silt, the friction angle only decreased by 1.3 degrees when the W/d_{max} ratio increased from 75 to 125 and remained almost constant when the W/d_{max} ratio further increased from 125 to 375. For these tests, one cannot validate the minimum requirement of ASTM D3080/D3080M-11 because no specimen was tested with a W/d_{max} ratio between 10 and 75. For the pure sand specimens, the friction angle decreased by more than 3 degrees when the W/d_{max} ratio increased from 75 to 125 and then by 2 degrees when the W/d_{max} ratio further increased from 125 to 375. These results tend to indicate that a W/d_{max} ratio of 75 is not large enough to remove the specimen size effect. This invalidates the minimum requirements of ASTM D3080/D3080M-11.

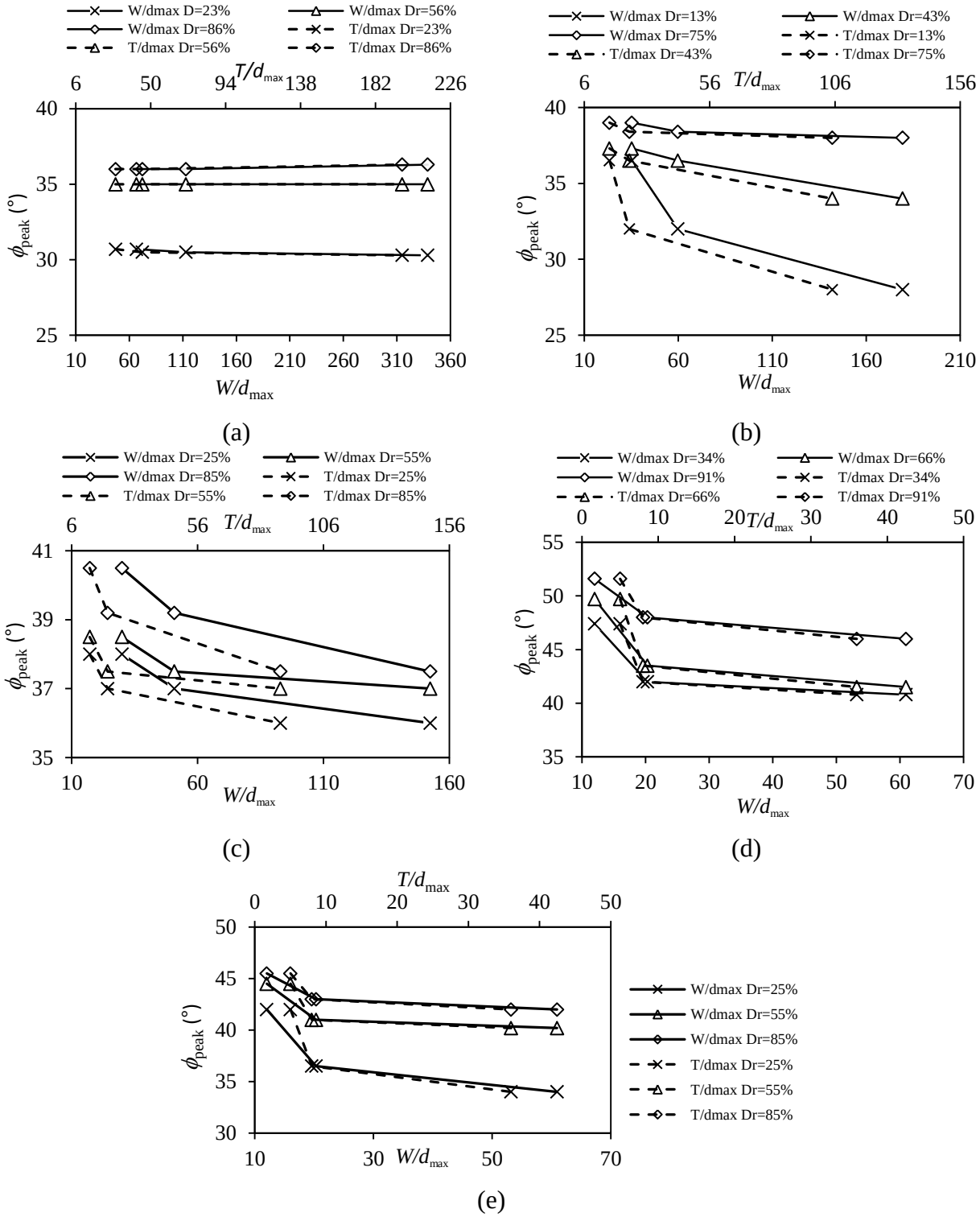

Figure 4.13 Variation of the peak friction angle in terms of specimen width and thickness to d_{max} ratios for specimens with different relative densities; data taken from Cerato and Lutenegger

(2006): (a) Ottawa sand, (b) FHWA (Brown Mortar), (c) Morie, (d) Winter and (e) Gravel Pack #3.

Table 4.4 summarizes the previous studies regarding the specimen size effect on the peak friction angle of granular materials. All specimen sizes met the minimum requirement ratios of the studied standards (AS 1289.6.2.2, 1998; Eurocode 7, 2007; ASTM D3080/D3080M 2011) except those highlighted by an asterisk. For the fine particle materials with d_{max} less than approximately 1.2 mm, the minimum specimen size ratio required by the studied standards is either invalidated or not validated. For the materials with d_{max} equal to or larger than 1.7 mm, the minimum required ratios of specimen sizes (width and/or thickness) to maximum particle size dictated by the studied standards (ASTM, AS, and Eurocode) are invalidated. More experimental works are needed to find the minimum required ratios that remove specimen size effect on friction angle of granular materials. The minimum required ratios in the diverse norms between specimen size and maximum particle size need to be revised upward.

Table 4.4 Summary of the previous studies on how the specimen size affects the peak friction angle of granular materials

Material type	d_{max} **(mm)**	W/d_{max}	T/d_{max}	**Respect the standards**		**Validity of standards**	**Reference**
				W/d_{max} > 6	T/d_{max} > 10		
Silty sand	0.8	75, 125, 375	30.6, 43.7, 192.5	Yes	Yes	Not validated	Ziaie Moayed et al. (2017)
Sand	0.8	75, 125, 375	30.6, 43.7, 192.5	Yes	Yes	Invalidated	
	0.9	72, 119, 352	31, 45.2, 209	Yes	Yes	Not validated	Cerato and Lutenegger (2006)
	1.2	50, 126.7, 833	26.7, 126.7, 833	Yes	Yes		Palmeira and Milligan (1989)
	1.7	36, 60, 179	16, 24, 105	Yes	Yes	Invalidated	Cerato and Lutenegger (2006)
	2	30, 51, 152	13, 20.5, 89	Yes	Yes		
Gravel	5	12, 20, 6	5*, 8*, 36	Yes	Yes for the largest box		

Note: * Specimens not meeting the minimum requirement ratio of ASTM D3080/D3080M (2011). Standard BS 1377-7 (1990) defines specific d_{max} for specified specimen sizes. The BS is not thus examined in this paper.

4.5 Discussion

In this paper, the influence of d_{max} on shear strength of granular materials has been presented by considering scaling down techniques and specimen size. Once the shear strengths of modeled samples with different d_{max} are obtained, graphical or equation relationship can be established between the shear strengths and d_{max}. The shear strength of field rockfill can then be obtained by extrapolation on the shear strength and d_{max} curve or equation.

However, one keeps in mind that the shear strength of granular materials can also be influenced by other influencing factors such as particle shape, fine particle content, gravel content, initial gradation (coefficient of uniformity, and curvature), compactness (relative density), confining stress, strength of solid grain, and breakage of particles. In order to see the influence of d_{max} on shear strengths of granular materials, one has to keep other influencing parameters constant. More works are necessary to analyze the influence of d_{max} on the shear strength of granular material by considering different values of other influencing parameters. More works are also necessary to see the influences of other influencing parameters. Obviously, full and comprehensive analysis of the shear strength of granular materials still requires considerable heavy work both in experimental and analyzing work. It is interesting and promising to see the application of machine learning models and approaches such as artificial neural network (ANN) model, random and cubist forest models and genetic algorithm on this aspect (Armaghani et al. 2014; Kaunda, 2015; Zhou et al. 2019). The influences of different influencing parameters can be simultaneously considered. Of course, the application of these powerful models and approaches requires the input of big and reliable experimental data. This is again closely related to the specimen size effect in the shear strength tests.

Finally, it is noted that a number of empirical equations have been proposed to relate the shear strength of granular materials and d_{max} based on experimental results obtained by applying parallel scaling down technique (Varadarajan et al. 2003, 2006; Abbas 2011; Pankaj et al. 2013; Honkanadavar et al. 2014, 2016). The review analyses presented in this paper indicate that it should be careful to use these models to predict shear strength of in situ field materials because the reliability of the parallel scaling down technique has not yet been shown.

4.6 Conclusions

The review and analysis on experimental data of shear strengths obtained by performing direct shear tests and triaxial compression tests on samples prepared by applying different scaling down techniques lead to the following conclusions:

- Applying any one of the four scaling down techniques results in a modified gradation compared to that of the original field material. Unlike a common belief, the application of parallel scaling down technique also results in a modification of the physical composition. In terms of complexity to obtain a target gradation curve, the scalping technique is the simplest to achieve, followed by the replacement method and the parallel scaling down technique. The quadric scaling down technique is the most complicated to achieve, and the target gradation curve is only a function of the targeted d_{max}, with no consideration to other gradation characteristics of the field material. Its physical justification and applicability are unclear.
- Parallel scaling down is the most used technique in practice, followed in decreasing order by scalping and replacement methods. Quadratic scaling down technique has never been used since its publication.
- In previous studies, the validity or invalidity of a scaling down technique was conducted by directly comparing shear strengths of modeled and field samples. This methodology is inappropriate and unreliable. The invalidity of the replacement technique by this methodology is uncertain.
- The minimum ratios of specimen size to d_{max}, as suggested by well-established standards for direct shear tests, are too small to eliminate specimen size effect. The minimum size ratios given in the studied norms are thus not reliable. Specifically:
  - For fine particle materials, the minimum size ratios of well-established standards (ASTM, AS, Eurocode) for direct shear tests are either invalidated or not validated.
  - For coarse granular materials, the minimum size ratios of well-established standards (ASTM, AS, Eurocode) are invalidated.

- Almost all available shear test results on granular materials were obtained by following minimum required ratios specified in well-established norms. Conclusions based on these experimental results are thus uncertain. Shear strengths of field granular material were overestimated. Structure design based on such results is thus on the non-conservative side.
- The primary analyses seem to show that both scalping and parallel techniques can be used to predict shear strength of field rockfill through extrapolation of laboratory shear test results when normal stress is high, but both techniques failed for low to intermediate normal stress. These conclusions are however uncertain since the experimental results were obtained by using the minimum ratio of specimen size to d_{max} specified by ASTM D3080/D3080M-11.

4.7 Recommendations

The review and analyses presented in this paper indicate that none of the four scaling down techniques can be used in a reliable way to obtain the shear strength of field rockfill despite the parallel scaling down technique is the most used one. In addition, the minimum ratios of specimen size to d_{max} suggested by well-established standards for direct shear tests are too small to eliminate specimen size effect. The shear strengths obtained by following these minimum ratios values are unreliable. More works are necessary, as indicated by the following recommendations:

- More direct shear tests using different shear box sizes are needed to determine the minimum required ratios of specimen size to d_{max} by which specimen size effect can be entirely eliminated or considered as negligible. The minimum specimen size to d_{max} ratios required in the well-established standards (ASTM, AS, Eurocode) can thus be updated.
- More experimental work is necessary to identify a reliable scaling down technique that can be used to predict the shear strength of field materials by extrapolating the laboratory shear test results. Of course, this work can only be performed after the previous task to make sure that all shear tests are realized by using specimens large enough to eliminate any specimen size effect. The shear strength measurement of field rockfill using large enough specimens to avoid any specimen size effect is necessary to verify if the shear

strength of field rockfill can be correctly predicted through extrapolation on the variation of shear strength as a function of d_{max}.

- More experimental works are necessary to analyze the influences of other influencing parameters such as particle shape, fine particle content, gravel content, initial gradation (coefficient of uniformity, curvature, and d_{max}), compact (relative density), confining stress, strength of solid grain and breakage of particles. Once again, this work can only be done when the minimum required ratios of specimen size to d_{max} are known to avoid any specimen size effect.

Data Availability

No data were used to support this study.

Conflicts of Interest

The authors declare that there are no conflicts of interest regarding the publication of this paper.

Acknowledgments

The authors acknowledge the financial support from the Natural Sciences and Engineering Research Council of Canada (NSERC RGPIN-2018-06902), Fonds de recherche du Québec—Nature et Technologies (FRQNT 2017-MI-202860), industrial partners of the Research Institute on Mines and the Environment (RIME UQAT-Polytechnique; http://rime-irme.ca/), and Mitacs Elevate Postdoctoral Fellowship (IT12569). Prof. Michel Aubertin and Mr. Ali Mahdavi are acknowledged for their involvement and discussions at the beginning of the project.

Notation

The following symbols are used in this paper:

d	Particle size of modeled sample
$d_{p.m}$	Particle sizes of modeled sample having a percentage passing p
$d_{p.f}$	Particle size of field material having a percentage passing p
d_{max}	Maximum particle size
$d_{max.f}$	Maximum particle size of field material

$d_{\text{max.m}}$	Maximum particle size of modeled (parallel) sample
D	Diameter of cylinder sample for direct shear tests or triaxial compression tests
D_{r}	Relative density
N	Ratio of $d_{max.f}$ to $d_{max.m}$
P_{dmax}	Percentage of field material particles passing the targeted d_{max}
$P_{ij.f}$	Percentage by mass of field material particles passing sieve size j ($\leq d_{max}$) and retained on the sieve size i ($\geq$ 4.75 mm)
$P_{\text{No.4}}$	Percentage of field material particles passing the sieve of 4.75 mm
P_o	Percentage by mass of field material particles retained on the sieve having a size of the targeted d_{max}
P_Q	Percentage by mass of the modeled particle size
$P_{ij.a}$	Percentage by mass of added particles passing sieve having size j ($\leq d_{max}$) and retained on the neighbor sieve having size i ($\geq$ 4.75 mm)
T	Thickness of specimen for direct shear tests
W	Width of specimen for direct shear tests
α	Tilt angle
σ_3	Confining pressure for triaxial compression tests
σ_n	Normal stress for direct shear tests
ϕ	Friction angle
ϕ_{peak}	Peak friction angle

4.8 References

Abbas, S. M. (2011). *Behaviour of rockfill materials: based on nature of particles*. Saarbrücken, Germany: LAP Lambert Academic Publishing.

Alonso, E. E., Tapias, M., & Gili, J. (2012). Scale effects in rockfill behaviour. *Géotechnique Letters*, *2*(3), 155-160.

Andjelkovic, V., Pavlovic, N., Lazarevic, Z., & Radovanovic, S. (2018). Modelling of shear strength of rockfills used for the construction of rockfill dams. *Soils and Foundations*, *58*(4), 881-893.

Amirpour Harehdasht, S., Karray, M., Hussien, M. N., & Chekired, M. (2017). Influence of particle size and gradation on the stress-dilatancy behavior of granular materials during drained triaxial compression. *International Journal of Geomechanics*, *17*(9), 04017077.

Amirpour Harehdasht, S., Hussien, M. N., Karray, M., Roubtsova, V., & Chekired, M. (2019). Influence of particle size and gradation on shear strength–dilation relation of granular materials. *Canadian Geotechnical Journal*, *56*(2), 208-227.

Armaghani, D. J., Hajihassani, M., Bejarbaneh, B. Y., Marto, A., & Mohamad, E. T. (2014). Indirect measure of shale shear strength parameters by means of rock index tests through an optimized artificial neural network. *Measurement*, *55*, 487-498.

AS 1289.6.2.2. (1998). Soil strength and consolidation tests-determination of the shear strength of a soil-direct shear test using a shear box. *Standards Australia*, Sydney, NSW, Australia.

ASTM D4767. (2011). Standard test method for consolidated undrained triaxial compression test for cohesive soils. *ASTM International*, West Conshohocken, PA, USA.

ASTM D3080/D3080M. (2011). Direct shear test of soils under consolidated drained conditions. *ASTM International*, West Conshohocken, PA, USA.

ASTM D2850. (2015). Standard test method for unconsolidated-undrained triaxial compression test on cohesive soils. *ASTM International*, West Conshohocken, PA, USA.

Aubertin, M., Bussière, B., Bernier, B. (2002). Environnement et gestion des rejets miniers, Manuel sur cédérom, *Presses Internationales Polytechnique*, Montreal, QC, Canada.

Aubertin, M., Mbonimpa, M., Jolette, D., Bussière, B., Chapuis, R. P., James, M., & Riffon, O. (2002). Stabilité géotechnique des ouvrages de retenue pour les résidus miniers: problèmes persistants et méthodes de contrôle. In *Défis & Perspectives: Symposium*.

Azam, S., & Li, Q. (2010). Tailings dam failures: a review of the last one hundred years. *Geotechnical news*, *28*(4), 50-54.

Bagherzadeh, A., & Mirghasemi, A.A., (2009). Numerical and experimental direct shear tests for coarse grained soils. *Particuology*, *7*, 83-91.

Barton, N., & Kjærnsli, B. (1981). Shear strength of rockfill. *Journal of the Geotechnical Engineering Division*, *107*(7), 873-891.

Bazazzadeh, H., Kalantary, F., & Asakereh, A. (2011). An investigation on the effect of particle breakage on rockfill constitutive parameters. *Electronic Journal of Geotechnical Engineering*, *15*(9), 847-864.

Blijenberg, H. M. (1995). In-situ strength tests of coarse, cohesionless debris on scree slopes. *Engineering Geology*, *39*(3-4), 137-146.

Boakye, K. (2008). Large in situ direct shear tests on rock piles at the Questa Min, Taos county, New Mexico. *Doctoral Dissertation*, New Mexico Institute of Mining and Technology.

Boudrias, G. (2018). *Évaluation numérique et expérimentale du drainage et de la consolidation de résidus miniers à proximité d'une inclusion de roches stériles* (Doctoral dissertation, Ecole Polytechnique, Montreal, Canada).

Brady, B. H., & Brown, E. T. (1993). *Rock mechanics: for underground mining*. Dordrecht, The Netherlands: Springer.

BS 1377. (1990). Methods of test for soils for civil engineering purposes. Shear strength tests (total stress). Part 7. *British Standard Institution*, London, UK,

Cambio, D., & Ge, L. (2007). Effects of parallel gradation on strength properties of ballast materials. In *Advances in Measurement and Modeling of Soil Behavior* (pp. 1-7).

Cerato, A. B., & Lutenegger, A. J. (2006). Specimen size and scale effects of direct shear box tests of sands. *Geotechnical Testing Journal*, *29*(6), 507-516.

Chang, W. J., & Phantachang, T. (2016). Effects of gravel content on shear resistance of gravelly soils. *Engineering Geology*, *207*, 78-90.

Charles, J. A. (1973). *Correlation between laboratory behaviour of rockfill and field performance, with particular reference to Scammonden Dam* (*Doctoral Dissertation*, University of London, London, UK).

Charles, J. A., & Watts, K. S. (1980). The influence of confining pressure on the shear strength of compacted rockfill. *Geotechnique*, *30*(4), 353-367.

Cooke, J. B. (1984). Progress in rockfill dams. *Journal of Geotechnical Engineering*, *110*(10), 1381-1414.

Das, B. M. (2008). *Advanced soil mechanics* (Vol. 270). New York, USA: Taylor & Francis.

Donaghe, R., & Townsend, F. (1976). Scalping and replacement effects on the compaction characteristics of earth-rock mixtures. *In Soil Specimen Preparation for Laboratory Testing: ASTM Special Technical Publication, 599, 248-277.*

Donaghe, R. T., & Torrey, V. H. (1985). Strength and deformation properties of earth-rock mixtures. *US Army Corps of Engineers*, AD-A160 701.

Douglas, K. (2002). *The shear strength of rock masses* (Doctoral Dissertation, University of New South Wales. Australia).

Drugan, W. J., & Willis, J. R. (1996). A micromechanics-based nonlocal constitutive equation and estimates of representative volume element size for elastic composites. *Journal of the Mechanics and Physics of Solids*, *44*(4), 497-524.

Eurocode 7. (2007). Geotechnical design - Part 1: General rules: EN 1997-1. *The European Union Per Regulation*, Brussels, Belgium.

Fakhimi, A., Boakye, K., Sperling, D. J., & McLemore, V. T. (2007). Development of a modified in situ direct shear test technique to determine shear strength parameters of mine rock piles. *ASTM Geotechnical Testing Journal*, 31(3), 269-273.

Feng, G., & Vitton, S. J. (1999). Laboratory determination of compaction criteria for rockfill material embankments. *In International Conference on Soil Mechanics and Foundation Engineering* (pp. 485-488).

Frossard, E., Hu, W., Dano, C., & Hicher, P. Y. (2012). Rockfill shear strength evaluation: a rational method based on size effects. *Geotechnique*, *62*(5), 415-427.

Frost, R. J. (1973). Some testing experiences and character. *In Evaluation of Relative Density and Its Role in Geotechnical Projects Involving Cohesionless Soils: A Symposium Presented at the Seventy-Fifth Annual Meeting, American Society for Testing and Materials*, Los Angeles, California., 25-30 June 1972 (Vol. 523, p. 207).

Fumagalli, E. (1969). Tests on cohesion less materials for rockfill dams, *Journal of Soil Mechanics and Foundation Engineering, ASCE, 95*(1), 313-330.

Ghanbari, A., Sadeghpour, A. H., Mohamadzadeh, H., & Mohamadzadeh, M. (2008). An experimental study on the behavior of rockfill material using large scale tests, *Electronic Journal of Geotechnical Engineering, 13*, Bundle G. 1-16.

Goodrich, E. P. (1904). Lateral Earth Pressures and Related Phenomena. *Transactions of the American Society of Civil Engineers*, *53*(2), 272-304.

Gupta, A. K. (2009). Triaxial behaviour of rockfill materials. *Electronic Journal of Geotechnical Engineering*, *14*(Bund. J), 1-18.

Hall, E. B. (1951). A triaxial apparatus for testing large soil specimens. *ASTM, 106*, 152-161.

Hall, E. B., & Gordon, B. B. (1963). Triaxial testing with large-scale high pressure equipment. Laboratory Shear Testing of Soils, 361, 315-328.

Hall, E. B., & Smith, T. (1971). Special Tests for Design of High Earth Embankments on US-101. *Highway Research Record*, (345).

Hamidi, A., Azini, E., & Masoudi, B. (2012). Impact of gradation on the shear strength-dilation behavior of well graded sand-gravel mixtures. *Scientia Iranica*, *19*(3), 393-402.

Haselsteiner, R., Pamuk, R., & Ersoy, B. (2017). Aspects concerning the shear strength of rockfill material in rockfill dam engineering. *Geotechnic, 40*(3), 193-203.

Hazen, A. (1892). Some physical properties of sand and gravel, with special reference to their use in filtration. Massachusetts State Board of Health, *24th annual report*, Boston, USA, (pp. 539-556).

Hawley, P.M. (2001). Site Selection, characterization, and assessment. In: W.A. Hustrulid, M.K. McCarter and D.J.A. van Zyl (Editors), *Slope Stability in Surface Mining: Society for Mining, Metallurgy, and Exploration, Inc (SME)*. Littleton, USA, (pp. 267-274).

Herasymuik, G.M. (1996). *Hydrogeology of a sulphide waste rock dump* (Master Thesis, University of Saskatchewan, Saskatoon, Saskatchewan, Canada).

Hassani, F., & Archibald J. H. (1998). *Mine backfill*. CIM, CD-ROM.

Hennes, R. G. (1952). The strength of gravel in direct shear. Symposium on Direct Shear Testing of Soils, ASTM STP 131, *American Society for Testing and Materials*, 51-62.

Holtz, W., & Gibbs, H. J. (1956). Triaxial shear tests on pervious gravelly soils. *Journal of the Soil Mechanics and Foundations Division, 82*(1), 1-22.

Holtz, R. D., & Kovacs, W. D. (1981). *An Introduction to Geotechnical Engineering*, New York, USA: Prentice Hall.

Honkanadavar, N. P., Dhanote, S., & Bajaj, S. (2016). 161 Prediction of shear strength parameter for prototype alluvial rockfill material. *Indian Geotechnical Conference* IGC2016.

Honkanadavar, N. P., Kumar, N., & Ratnam, M. (2014). Modeling the behavior of alluvial and blasted quarried rockfill materials. *Geotechnical and Geological Engineering, 32*(4), 1001-1015

Houston, W. (1981). Course notes, *Soil mechanics and foundation engineering course*, U.C. Berkeley: Berkeley, California, Department of Civil Engineering.

Houston, W., Houston, S. L., & Walsh, K. D. (1994). Compacted high gravel content subgrade materials. *Journal of Transportation Engineering, 120*, 193-205.

Hutchinson, J. N., & Rolfsen, E. N. (1962). Large scale field shear box test and quick clay, *Geologie and Bauwesen, Vienna, 28*(1), 31 – 42.

International Commission on Large Dams (ICOLD). (2001). Tailings dams – risk of dangerous occurrences – lessons learnt from past experiences. *Bulletin No. 121. Commission Internationale des Grands Barrages*, Paris. France.

James, M., Aubertin, M., Wijewickreme, D., & Wilson, G. W. (2011). A laboratory investigation of the dynamic properties of tailings. *Canadian Geotechnical Journal*, *48*(11), 1587-1600.

James, M., & Aubertin, M. (2012). The use of waste rock inclusions to improve the seismic stability of tailings impoundments. In *GeoCongress 2012: State of the art and practice in geotechnical engineering* (pp. 4166-4175).

Kanit, T., Forest, S., Galliet, I., Mounoury, V., & Jeulin, D. (2003). Determination of the size of the representative volume element for random composites: statistical and numerical approach. *International Journal of solids and structures*, *40*(13-14), 3647-3679.

Kaunda, R. (2015). Predicting shear strengths of mine waste rock dumps and rock fill dams using artificial neural networks. *International Journal of Mining and Mineral Engineering*, *6*(2), 139-171.

Kermani, M. (2016). *Prediction of post-construction settlements of rockfill dams based on construction field data* (Doctoral Dissertation, Laval University. Laval, QC, Canada).

Kossoff, D., Dubbin, W. E., Alfredsson, M., Edwards, S. J., Macklin, M. G., & Hudson-Edwards, K. A. (2014). Mine tailings dams: characteristics, failure, environmental impacts, and remediation. *Applied Geochemistry*, *51*, 229-245.

Kutzner, C. (2020). *Grouting of rock and soil*. London, UK: Taylor & Francis Group.

Ladanyi, B., & Archambault, G. (1969). Simulation of shear behavior of a jointed rock mass. In *The 11th US Symposium on Rock Mechanics (USRMS)*. OnePetro.

Lam, H. F., Alabi, S. A., & Yang, J. H. (2017). Identification of rail-sleeper-ballast system through time-domain Markov chain Monte Carlo-based Bayesian approach. *Engineering Structures*, *140*, 421-436.

Lambe, T., & Whitman, R. (1969). *Soil mechanics*. New York, NY, USA: John Wiley & Sons.

Lee, K. L., & Seed, H. B. (1967). Drained strength characteristics of sands. *Journal of Soil Mechanics & Foundations Division*, *93*(6), 117-141.

Lee, K. L., & Farhoomand, I. (1967). Compressibility and crushing of granular soil in anisotropic triaxial compression. *Canadian Geotechnical Journal*, *4*(1), 68-86.

Leps, T. M. (1970). Review of shearing strength of rockfill. *Journal of Soil Mechanics & Foundations Division*, *96*(4), 1159-1170.

Leslie, D. (1963). Large scale triaxial tests on gravelly soils. *In Proc. of the 2nd Pan-American Conf. on SMFE, Brazil* (Vol. 1, pp. 181-202).

Li, L., Ouellet, S., & Aubertin, M. (2009). A method to evaluate the size of backfilled stope barricades made of waste rock. *GeoHalifax*, Halifax (Vol. 1, p. 1).

Li, L., & Aubertin, M. (2011). Limit equilibrium analysis for the design of backfilled stope barricades made of waste rock. *Canadian Geotechnical Journal*, *48*(11), 1713-1728.

Linero, S., Palma, C., & Apablaza, R. (2007). Geotechnical characterization of waste material in very high dumps with large scale triaxial testing. *Paper presented at the Proceedings of International Symposium on Rock Slope Stability in Open Pit Mining and Civil Engineering*, Perth, Australia, (pp. 59-75).

Liu, S. H. (2009). Application of in situ direct shear device to shear strength measurement of rockfill materials. *Water Science and Engineering*, *2*(3), 48-57.

Lowe, J. (1964). Shear strength of coarse embankment dam materials. *In Proc., 8th Int. Congress on Large Dams*, Paris: International Commission on Large Dams, (Vol. 3, pp. 745-761).

Marachi, N., Seed, H., & Chan, C. (1969). Strength characteristics of rockfill materials. *Seventh International Conference on Soil Mechanics and Foundation Engineering.*

Marachi, N. D., Chan, C. K. & Seed, H. B. (1972). Evaluation of properties of rockfill materials. *Journal of Soil Mechanics & Foundations Division*, *98*(1), 95-114.

Marsal, R., & Fuentes de la Rosa, A. (1976). Mechanical properties of rockfill soil mixtures. *Paper presented at the Transactions of the 12th International Congress on Large Dams*, Mexico City (Vol. 1, pp. 179-209).

Marsland, A. (1971). The use of in-situ tests in a study of the effects of fissures on the properties of stiff clays. In *Proc. First Aust.-NZ Conf. on Geomechanics, Melbourne,* (Vol. 1, pp. 180-189).

Matsuoka, H., & Liu, S. (1998). Simplified direct box shear test on granular materials and its application to rockfill materials. *Soils and Foundations, 38*(4), 275-284

Matsuoka, H., Liu, S. H., Sun, D., & Nishikata, U. (2001). Development of a new in situ direct shear test. *Geotechnical Testing Journal, 24*(1), 92-102.

McLemore, V. T., Sweeney, D., Dunbar, N., Heizler, L., & Writer, E. P. (2009). Determining quantitative mineralogy using a modified MODAN approach on the Questa rock pile materials. *In SME Annual Meeting, New Mexico*, (pp. 9-20).

Morgan, G. C., & Harris, M. C. (1967). Portage mountain dam: II. Materials. *Canadian Geotechnical Journal*, *4*(2), 142-166.

Ovalle, C., Frossard, E., Dano, C., Hu, W., Maiolino, S., & Hicher, P. Y. (2014). The effect of size on the strength of coarse rock aggregates and large rockfill samples through experimental data. *Acta Mechanica*, *225*(8), 2199-2216.

Ovalle, C., & Dano, C. (2020). Effects of particle size–strength and size–shape correlations on parallel grading scaling. *Geotechnique Letters*, *10*(2), 191-197.

Ovalle, C., Linero, S., Dano, C., Bard, E., Hicher, P. Y., & Osses, R. (2020). Data compilation from large drained compression triaxial tests on coarse crushable rockfill materials. *Journal of Geotechnical and Geoenvironmental Engineering*, *146*(9), 06020013.

Owen, J. R., Kemp, D., Lébre, É., Svobodova, K., & Murillo, G. P. (2020). Catastrophic tailings dam failures and disaster risk disclosure. *International Journal of Disaster Risk Reduction*, *42*, 101361.

Oyanguren, P. R., Nicieza, C. G., Fernández, M. Á., & Palacio, C. G. (2008). Stability analysis of Llerin Rockfill Dam: An in situ direct shear test. *Engineering Geology*, *100*(3-4), 120-130.

Palmeira, E. M. & Milligan, G. W. E. (1989). Scale effects in direct shear tests on sand, *Proceedings of the 12th International Conference on Soil Mechanics and Foundation Engineering, Rio de Janeiro* (Vol. 1, pp. 739-742).

Pankaj, S., Mahure, N., Gupta, S., Sandeep, D., & Devender, S. (2013). Estimation of shear strength of prototype rockfill materials. *International Journal of Engineering*, *2*(8), 421-426.

Pinto, N. L. D. S., Filho, P. L. M., & Maurer, E. (1985). Foz do Areia Dam\= Design, Construction, and Behaviour. *Concrete Face Rockfill Dams\= Design, Construction, and Performance*, (pp. 173-191).

Potvin, Y., Thomas, E., & Fourie, A. (2005). *Handbook on mine fill*. Perth, Autaralia: Australian Centre for Geomechanics.

Ramamurthy, T. (2004). A geo-engineering classification for rocks and rock masses. *International Journal of Rock Mechanics and Mining Sciences, 41*(1), 89-101.

Rao, S. V., Bajaj, S., & Dhanote, S. (2011). Evaluations of strength parameters of rockfill material for Pakaldul hydroelectric project, Jammu and Kashmir—a case study. In *Proceedings of the 2011 Indian Geotechnical Conference*, Kochi, India (pp. 991-994).

Rathee, R. K. (1981). Shear strength of granular soils and its prediction by modeling techniques. *Journal of Institution of Engineers, 62*, 64-70.

Saleh-Mbemba, F. (2016). Analyse et optimisation de la performance des inclusions rigides durant la consolidation, le drainage et la dessiccation des résidus miniers. *Polytechnique de Montréal*, Montréal, Canada.

Saleh-Mbemba, F., Aubertin, M., & Boudrias, G. (2019). Drainage and consolidation of mine tailings near waste rock inclusions. *Sustainable and Safe Dams Around the World,* (pp. 3296-3305).

Sevi, A. F. (2008). *Physical odeling of railroad ballast using the parallel gradation scaling technique within the cyclical triaxial framework* (Doctoral Dissertation, Missouri University of Science and Technology, USA).

Sharma, V. M., Venkatachalam, K., & Roy, A. (1994). Strength and deformation characteristics of rockfill materials. *In Proceeding of the International Conference on Soil Mechanics and Foundation Engineering*, (pp. 959-962).

Singh, B., & Varshney, R.S. (1995). *Engineering for embankment dams*. Brookfield, VT, USA: A.A. Balkema.

Skempton, A. W. (1958). Arthur Langtry Bell (1874 – 1956) and his contribution to soil mechanics. *Geotechnique, 8*(4), 143-157.

Stober, J. n. (2012). *Effects of maximum particle size and sample scaling on the mechanical behaviour of mine waste rock; a critical state approach* (Master Thesis, Colorado State University, Colorado, USA).

Tardif-Drolet, M., Li, L., Pabst, T., Zagury, G. J., Mermillod-Blondin, R., & Genty, T. (2020). Revue de la réglementation sur la valorisation des résidus miniers hors site au Québec. *Environmental Reviews*, *28*(1), 32-44.

Tombs, S. G. (1969). *Strength and deformation characteristics of rockfill* (Doctoral Thesis, Imperial College London, London, UK).

Torrey III, V. H., & Donaghe, R. T. (1991). Compaction characteristics of earth-rock mixtures. *Army Engineer Waterways Experiment Station Vicksburg* MS Geotechnical Lab.

US Army Corps Engineers. (1965). *Laboratory soil testing*. Technical Report, EM 1110-2-1906.

Van Steijn, H. (1991). Frequency of hill slope debris flows in part of the French Alps. *Bulletin of Geomorphology*, *19*, 83-90.

Varadarajan, A., Sharma, K. G., Abbas, S. M., & Dhawan, A. K. (2006). The role of nature of particles on the behavior of rockfill material. *Soils and Foundations*, *46*(5), 569-584.

Varadarajan, A., Sharma, K. G., Venkatachalam, K., & Gupta, A. K. (2003). Testing and modeling two rockfill materials. *Journal of Geotechnical and Geoenvironmental Engineering*, *129*(3), 206-218.

Vasistha, Y., Gupta, A. K., & Kanwar, V. (2013). Medium triaxial testing of some rockfill materials. Electron. *Journal of Geotechnical Engineering*, *18*(D), 923-964.

Wang, J. J., Yang, Y., & Chai, H. J. (2016). Strength of a roller compacted rockfill sandstone from in-situ direct shear test. *Soil Mechanics and Foundation Engineering*, *53*(1), 30-34.

Wang, Y., Shao, S., & Wang, Z. (2019). Effect of particle breakage and shape on the mechanical behaviors of granular materials. *Advances in Civil Engineering*, *2019*.

Hu, W., Frossard, E., Hicher, P. Y., & Dano, C. (2010). Method to evaluate the shear strength of granular material with large particles. In *Soil Behavior and Geo-Micromechanics, GeoShanghai, Shanghai* (pp. 247-254).

Wei, H., Xu, W., Wei, C., & Meng, Q. (2018). Influence of water content and shear rate on the mechanical behavior of soil-rock mixtures. *Science China Technological Sciences*, *61*(8), 1127-1136.

Wen, R., Tan, C., Wu, Y., & Wang, C. (2018). Grain size effect on the mechanical behavior of cohesionless coarse-grained soils with the discrete element method. *Advances in Civil Engineering*, *2018*.

Williams, D. J., & Walker, L. K. (1983). Laboratory and field strength of mine waste rock, *Research Report No. CE 48*, University of Queensland, Australia.

Xu, Y. (2018). Shear strength of granular materials based on fractal fragmentation of particles. *Powder Technology*, *333*, 1-8.

Yang, P., Li, L., Aubertin, M., Brochu-Baekelmans, M., & Ouellet, S. (2017). Stability analyses of waste rock barricades designed to retain paste backfill. *International Journal of Geomechanics*, *17*(3), 04016079.

Yang, G., Jiang, Y., Nimbalkar, S., Sun, Y., & Li, N. (2019). Influence of particle size distribution on the critical state of rockfill. *Advances in Civil Engineering*, *2019*.

Yu, X., Ji, S., & Janoyan, K. D. (2006). Direct shear testing of rockfill material. In *Soil and Rock Behavior and Modeling* (pp. 149-155).

Zeller, J., & Wullimann, R. (1957, August). The shear strength of the shell materials for the Go-Schenenalp Dam, Switzerland. In *4th International Conference on Soil Mechanics and Foundation Engineering* (Vol. 2, pp. 399-415).

Zahl, E.G., Biggs, F., Boldt, C.M.K., Connolly, R.E., Gertsch, L., & Lambeth, R.H. (1992), Waste disposal and contaminant control, *in* Hartman, H.L., ed., *SME Mining Engineering Handbook, Littleton, CO, Society for Mining, Metallurgy and Exploration Inc*., (pp.1170-1180).

Zhang, Z. L., Xu, W. J., Xia, W., & Zhang, H. Y. (2016). Large scale in situ test for mechanical characterization of soil rock mixture used in an embankment dam. *International Journal of Rock Mechanics and Mining Sciences*, *86*, 317-322.

Zhou, J., Li, E., Wei, H., Li, C., Qiao, Q., & Armaghani, D. J. (2019). Random forests and cubist algorithms for predicting shear strengths of rockfill materials. *Applied sciences*, *9*(8), 1621.

Ziaie Moayed, R., Alibolandi, M., & Alizadeh, A. (2017). Specimen size effects on direct shear test of silty sands. *International Journal of Geotechnical Engineering*, *11*(2), 198-205.

CHAPTER 5 ARTICLE 2: EXPERIMENTAL STUDY ON THE MINIMUM REQUIRED SPECIMEN WIDTH TO MAXIMUM PARTICLE SIZE RATIO IN DIRECT SHEAR TESTS

Akram Deiminiat, Li Li, Feitao Zeng

Invited article published in CivilEng Journal, 2022, 3, 66-84 on January 21, 2022

Abstract: Conducting laboratory direct shear tests on granular materials is a common practice in geotechnical engineering. This is usually done by following the ASTM D3080/D3080M-11 (hereafter named ASTM), which stipulates a minimum required value of 10 for specimen width (W) to the maximum particle size (d_{max}) ratio. Recently, a literature review performed by the authors showed that the minimum required W/d_{max} ratio given in the ASTM is not large enough to eliminate the specimen size effect (SSE). The minimum required W/d_{max} ratio of ASTM needs to be revised. In this study, a critical analysis is first made on existing data in order to identify the minimum required W/d_{max} ratio. The analysis shows that more experimental data obtained on specimens having W/d_{max} ratios between 10 and 50 are particularly necessary. To complete this need, a series of direct shear tests were performed on specimens having different d_{max} by using three shear boxes of different dimensions. The results show once again that the minimum required W/d_{max} ratio of 10, defined in the ASTM is not large enough to eliminate the SSE. Further analysis on these and existing experimental results indicates that the minimum required W/d_{max} ratio is about 60 to remove the SSE of friction angles. These results along with the limitations of this study are discussed.

Keywords: shear strength; direct shear tests; friction angle; specimen size effect; minimum required specimen sizes; ASTM D3080/D3080M-11

5.1 Introduction

Direct shear test is a very old but still regularly used method to determine the shear strength of geomaterials (Goodrich, 1904; Casagrande & Albert, 1932; Rutledge, 1935; Casagrande, 1936; Terzaghi, 1936; Cooling et al., 1936; Terzaghi & Peck, 1948; Hutchinson, 1962; Marsland 1971; Cerato & Lutenegger, 2006; Afzali-Nejad et al., 2017, 2018; Zhang et al., 2019; Cai et al., 2020; Zahran & Naggar, 2020; Motaharitabari & Shooshpasha, 2021; Xue et al., 2021; Deiminiat & Li,

2022). For a given project, one usually needs to take samples from the project site. Specimens can then be prepared in laboratory with a small portion of the samples. For the convenience of laboratory tests, tested specimens are preferred to be as small as possible. However, the method imposes a shear plane through tested material between the upper and lower half parts of the shear box. When the specimen size is too small, the effect of individual particles along and near the imposed shearing plane can be amplified in terms of rotation, crushing, shearing, and dilation during direct shear tests. The distributions of stresses and strains can be non-uniform along the shearing plane (Jewell & Wroth, 1987; Jewell, 1989; Shibuya et al., 1997; Lings & Dietz, 2004). The measured shear strength may be overestimated and not representative of that of the tested material in field conditions where the volume of the tested material can be very large (Amirpour Harehdasht et al., 2017). Specimen size of tested material should not be too small.

Increasing the specimen size of tested material reduces the effect of individual large particles and boundary effects associated with the stiff shear box walls. The measured shear strength can be closer to that of the tested material in field conditions. When the specimen size is large enough, the measured shear strength can then become constant with any further increase in the specimen size. The variation of shear strength as function of specimen size is known as specimen size effect or specimen scale effect (SSE). The large enough specimen size to avoid any SSE is also known as a problem of representative volume element size (Drugan & Willis, 1996; Kanit et al. 2003; Wen et al., 2018).

Over the years, a number of researches have been published on SSE of direct shear tests. Most of them were realized by performing laboratory tests (e.g., Parsons, 1936; Rathee, 1981; Vucetic & Lacasse, 1982; Palmeira & Milligan, 1989; Stone & Wood, 1992; Cerato & Lutenegger, 2006; Wu et al., 2008; Alonso et al., 2012; Mirzaeifar et al., 2013; Amirpour Harehdasht et al., 2019; Ziaie Moayed et al., 2017; Zahran & Naggar, 2020; Motaharitabari & Shooshpasha, 2021. A few studies have been realized through numerical modeling (Potts et al. 1987; Wang et al. 2007; Zhang & Thornton, 2007; Jacobson et al., 2007; Wang & Gutierrez, 2010). Each method has advantages and limitations. With experimental investigation, the test results are direct, tangible and more convincing as long as the tests are properly realized. Its limitations are also obvious: shear box and specimen sizes are limited. The reliability of test results depends on the representativeness of assumptions, implicitly or explicitly used in the result interpretation. The

accessibility to observe the movements of particles or other mechanism responses of the tested specimen during shear tests is difficult, if not impossible (DeJong & Westgate, 2009, 2010; Lashkari & Jamali, 2021). With numerical modeling, the stress and deformation anywhere through the modeled specimen can be visualized. This allows an insight to the micromechanical behaviour, which can, in turn, lead to a better understanding of the macro mechanical behavior of material under direct shear test condition. However, all the numerical models, whatever continuum or discrete with or without meshes, are established with some debatable assumptions. Model calibrations are always necessary against experimental results to obtain model parameters. The representativeness of constitutive model or particle size distribution of granular material used in the numerical models depends on the reliability of the experimental results used for parameter calibration. In addition, ensuring the stability and reliability of numerical results is another challenging issue, especially at the zones of soil-wall interfaces and high gradient stress or deformation.

In this study, focus is given on the experimental study of SSE in direct shear tests.

5.2 Previous laboratory tests on SSE of direct shear tests

In the past, a large number of experimental studies have been published on the SSE of direct shear tests. As the objective of present study is to identify the minimum required specimen sizes to avoid SSE in direct tests, instead of an exhaustive literature review, analyses are only made on a few published works.

Over the years, several standards have been proposed to specify minimum required ratios between specimen sizes and maximum particle size (d_{max}) of tested material. Table 5.1 shows a few standards commonly used in geotechnical engineering with the specification of specimen sizes. For example, ASTM D3080/D3080M-11 (2011) (hereafter named ASTM), the most used standard for direct shear tests all over the world, requires specimen width (W) to be at least 10 times d_{max}. In addition, specimen width W should not be smaller than 50 mm. For fine particle materials such as clay, silt and sand with d_{max} not larger than 1 mm, the requirement of $W \geq 50$ mm automatically results in $W/d_{max} \geq 50$, a value largely exceeding the minimum required ratio. There is no problem with respecting the standard of ASTM. Problems appear when direct shear tests are needed with coarse particle materials such as rockfill and waste rocks.

Table 5.1 Standards of direct shear tests regarding maximum particle size (d_{max}), specimen width (W) and thickness (T)

Standard	**Required shear box size**			**Maximum allowed d_{max}**
	***W* (mm)**	***T* (mm)**	***W/T***	
ASTM D3080/D3080M-11 (2011)	≥ 50	≥ 13	≥ 2	Min{*T*/6, *W*/10}
Eurocode 7 (2007)	Not specified	Not specified	Not specified	*T*/10
AS 1289.6.2.2 (1998)	Not specified	≥ 12.5	Not specified	*T*/6
BS 1377-7 (1990)	60	20	3	2 mm
	100	25	4	2.5 mm
	305	150	≈ 2	15 mm - 20 mm

Rockfill and chemically inert waste rocks are widely used to construct geotechnical infrastructures such as rockfill dikes of hydraulic reservoirs, waste rock piles (McLemore et al., 2009; Zhai et al., 2021a), tailings dams (Azam & Li, 2010; Owen et al., 2020), waste rock inclusions in tailings storage facilities (Aubertin et al. 2002; Azam et al. 2007; Boudrias 2018; Saleh-Mbemba et al., 2019), and waste rock barricades in underground mines to maintain backfill slurry in mine stopes (Li et al., 2009; Li & Aubertin, 2011; Yang et al., 2017; Zhai et al., 2021b). Design of these infrastructures requires the knowledge of shear strength of rockfill or waste works. Direct shear tests are then needed to be performed on these materials. However, rockfill and waste rocks usually contain fine particles as small as silts and coarse particles as large as boulders. Using standard direct shear test box (6 cm for most cases) with field materials and respecting the minimum required specimen sizes to d_{max} ratio is impossible. Scaling down techniques are thus employed by removing oversized particles during sample preparation to make laboratory tests possible (Hall, 1951; Holtz & Gibbs, 1956; Leslie, 1963; Marachi et al., 1969; 1972; Varadarajan et al., 2003; Hamidi et al., 2012; Chang & Phantachang, 2016; Yang et al., 2019; Ovalle et al., 2020; Deiminiat & Li, 2022). For most cases, the d_{max} of the resulting samples can still be too large compared to any available, standard or nonstandard direct shear test apparatus. The minimum required specimen size to d_{max} ratio of 10 (ASTM D3080 1972; ASTM D3080/D3080M-11 2011) has thus been universally used in direct shear tests (Marachi et al., 1972; Varadarajan et al., 2006; Abbas, 2011; Pankaj et al., 2013; Vasistah et al., 2013; Honkanadavar et al., 2016; Xu, 2018; Zhang et al., 2019) even though the validity of this

minimum required value of 10 has never been verified. In other words, it remains unclear if the SSE of direct shear tests is eliminated with specimens having a width to d_{max} ratio of 10.

Parsons (1936) studied the SSE of a crushed quartz and Ottawa sand with a d_{max} value of approximately 0.841 mm. Direct shear tests were conducted with small square (60 mm × 60 mm), medium rectangular (120 mm × 100 mm) and large rectangular (120 mm × 200 mm) shear boxes. Loose samples were poured in the shear boxes with a spoon at a constant falling height. The surface of the samples was smoothed to a standard thickness. The measured friction angles are presented in Table 5.2 along with the corresponding values of W/d_{max}. For the test results with the crushed quartz, it is difficult to evaluate if the minor diminution of friction angle is an exhibition of SSE or simply due to the precision of measurement, sample variation or shape effect. As the smallest W/d_{max} ratio of 71 is already much higher than 10, these results do not provide valuable information on the validity of the minimum required specimen size over d_{max} ratio of ASTM. For the test results with Ottawa sand, Table 5.2 indicates that the friction angle continues to change significantly as the W/d_{max} ratio increases from 71 to 143. These results tend to indicate that the minimum required ratios of ASTM are not large enough to eliminate the SSE even at W/d_{max} ratio of 71. However, this conclusion may not be strong enough because the test results may contain several uncertainties associated with the precision of measurement, sample variation from small to large box, and shape effect.

Table 5.2 Variation of friction angle (ϕ) obtained by Parson (1936) with different specimen sizes through direct shear tests; L is the length of shear box

L (mm) × W (mm)	W/d_{max}	ϕ (°)	
		Crushed quartz	**Ottawa sand**
60 × 60	71	31.5	31.0
120 × 100	119	31.1	29.6
200 × 120	143	30.7	28.5

Similar tests to those of Parsons (1936) have been conducted by Palmeira and Milligan (1989) with one single normal stress of 30 kPa on a sand with d_{max} = 1.2 mm by using small square (60 mm × 60 mm × 32 mm), medium rectangular (252 mm × 152 mm × 152 mm) and large square (1000 mm × 1000 mm × 1000 mm) shear boxes. All the specimens were prepared by applying pluviation technique with a constant falling height. The test results are shown in Table 5.3. One sees that the friction angles of the specimens remain almost constant when W/d_{max} increases from

50 to 833, values much larger than the minimum required W/d_{max} ratio of ASTM. These results tend to indicate that a W/d_{max} ratio of 50 is large enough to remove the SSE, but cannot help to evaluate if the minimum required ratios of ASTM are large enough to eliminate the SSE. In addition, it is unclear if $W/d_{max} = 50$ is the minimum required ratio or can be smaller to remove the SSE.

Table 5.3 Friction angles of a sand with $d_{max} = 1.2$ mm, obtained by direct shear tests with three shear box sizes; data taken from Palmeira and Milligan (1989)

L (mm) × W (mm) × T (mm)	W/d_{max}	T/d_{max}	ϕ (°)
60 × 60 × 32	50	27	50.1
252 × 152 × 152	127	127	50.2
1000 × 1000 × 1000	833	833	49.4

Rathee (1981) investigated the SSE on the measurement of friction angle by direct shear tests. One tested material was made of pure gravel and another was a mixture of sand and gravel with the same portion. A small (60 mm × 60 mm) and a large (300 mm × 300 mm) shear box were used (the heights of the shear boxes were not provided in Rathee 1981). For the pure gravel material, only the large shear box was used to measure the friction angles of different samples having different d_{max} prepared by applying a scaling down technique. These results cannot be used to evaluate the SSE because each sample having a distinct value of d_{max} represents a distinct material. The variation of friction angle results from combined effects associated with the variation of d_{max}, particle size distribution and specimen size to d_{max} ratio. The employed methodology is inappropriate to investigate the SSE. For the sand-gravel mixture material with $d_{max} = 6.3$ mm, both the small and large shear boxes were used by Rathee (1981) to measure the friction angle by direct shear tests. The experimental results showed that the friction angle decreases by about 1.7° when the W/d_{max} ratio increases from 10 to 48. These results clearly indicate that the SSE is not eliminated with a W/d_{max} ratio of 10. The minimum required specimen size to d_{max} ratio defined by ASTM is invalidated. However, as there are no results with W/d_{max} smaller or larger than 48, it is unclear if the W/d_{max} ratio of 48 is large enough to eliminate SSE.

The influence of specimen size on friction angle was further studied by Cerato and Lutenegger (2006), who conducted direct shear tests with a small (59.9 mm × 59.9 mm × 26.4 mm), a

medium (101.6 mm × 101.6 mm × 40.6 mm) and a large (304.8 mm × 304.8 mm × 177.8 mm) shear box on a sand and a gravel with different d_{max} and relative densities. For the specimen of gravel with d_{max} value of 5 mm, a known quantity of sample was placed in each box and compacted to achieve the desired relative density. Table 5.4 shows the measured friction angles of the gravel compacted to different relative densities. The experimental results clearly indicate that the W/d_{max} ratios of 12 and 20 are not large enough to remove the SSE, invalidating once again the minimum required W/d_{max} ratio of 10 given in ASTM. It is however unclear if the W/d_{max} ratio of 61 is large enough to remove the SSE.

Table 5.4 Friction angles of gravel having a d_{max} value of 5 mm with different relative densities (D_r), obtained by direct shear tests with three shear box sizes; data taken from Cerato and Lutenegger (2006)

***W* (mm) × *W* (mm) × *T* (mm)**	W/d_{max}	T/d_{max}	ϕ (°)		
			D_r=25%	D_r=55%	D_r=85%
59.9 × 59.9 × 26.4	12	5	42.0	44.5	45.5
101.6 × 101.6 × 40.64	20	8	36.5	41.0	43.0
304.8 × 304.8 × 177.8	61	36	34.0	40.2	42.0

Wu et al. (2008) conducted direct shear tests on sand with a d_{max} value of 0.42 mm with a small square (40 × 40 × 20 mm), a medium square (120 × 120 × 120 mm), a large square (300 × 300 × 300 mm) and a very large rectangular (800 × 500 × 600 mm) shear boxes. The minimum W/d_{max} ratio is 95. Among the numerous specimens, only two have close enough compactness and void ratio. The test results presented in Table 5.5 tend to indicate the SSE is not eliminated even at W/d_{max} = 95. The minimum required W/d_{max} = 10, given in ASTM, is invalidated once again.

Table 5.5 Friction angles of the sand samples obtained by Wu et al. (2008)

Void ratio	***W* (mm) × *W* (mm) × *T* (mm)**	W/d_{max}	T/d_{max}	ϕ (°)
0.654	40 × 40 × 20	95	48	45.8
0.659	120 × 120 × 120	285	285	41.8

Mirzaeifar et al. (2013) performed direct shear tests with a mall (60 mm × 60 mm × 16 mm), a medium (100 mm × 100 mm × 30 mm) and a large (300 mm × 300 mm × 180 mm) shear box. The tested material is sand with a d_{max} value of 1.3 mm. Three samples were prepared, the first one at a density of 1.5 g/cm^3, the second at 1.58 g/cm^3 and the third at 1.67 g/cm^3, respectively. Table 5.6 shows the friction angles obtained by the direct shear tests. The results tend to indicate

that the W/d_{max} ratio of 46 is not large enough while a W/d_{max} ratio up to 77 may be necessary to remove the SSE. The minimum required W/d_{max} ratio of 10, stipulated by the standard of ASTM is invalidated once again.

Table 5.6 Friction angles of sand at three different densities, obtained by direct shear tests with three different size shear boxes; data taken from Mirzaeifar et al. (2013)

W (mm) × W (mm) × T (mm)	W/d_{max}	T/d_{max}	ϕ (°)		
			at 1.5 (g/cm^3)	at 1.58 (g/cm^3)	at 1.67 (g/cm^3)
60 × 60 × 16	46	12	35.4	37.9	39.7
100 × 100 × 30	77	23	33.3	34.5	35.2
300 × 300 × 180	231	138	32.6	34.0	34.5

Ziaie Moayed et al. (2017) studied the SSE on the friction angles of silty sand with a d_{max} value of 0.8 mm. The samples were prepared by mixing sand with different silt contents (Sand, 0%; Silty sand I, 10%; Silty sand II, 20%; Silty sand III, 30%). Small (60 mm × 60 mm × 24.5 mm), medium (100 mm × 100 mm × 35 mm) and large (300 mm × 300 mm × 154 mm) shear boxes were used to perform direct shear tests. Table 5.7 shows the friction angles obtained by only considering the direct shear test results of Ziaie Moayed et al. (2017) with the normal stresses of 109, 163 and 218 kPa; the experimental results obtained with the normal stresses of 327 and 436 kPa were ignored due to the lack of tests using the large shear box with these two normal stresses. The friction angles were obtained by applying the linear fitting technique without imposing the straight lines passing through the origin in the shear stress–normal stress plane, resulting in apparent cohesions varying from 11 to 27 kPa with the small shear box tests and apparent cohesion ranging from -0.4 to 5 kPa with the large shear box tests. The results of the sand and Silty sand I tend to show that the W/d_{max} ratio of 75 is not large enough to eliminate SSE, invalidating once again the minimum required W/d_{max} ratio of 10, stipulated by the standard of ASTM. With the test results of Silty sand III, the W/d_{max} ratio of 75 seems to be large enough to avoid SSE. These results do not help to validate or invalidate the minimum required W/d_{max} ratio of 10, stipulated by the standard of ASTM.

Table 5.7 Friction angles of sand and silty sands, obtained by only considering the direct shear test results of Ziaie Moayed et al. (2017) with the normal stresses of 109, 163 and 218 kPa

W (mm) × W (mm) × T (mm)	W/d_{max}	T/d_{max}	ϕ (°)			
			Sand[1]	Silty sand I[2]	Silty sand II[3]	Silty sand III[4]

60 × 60 × 24.5	75	30.6	43.9	39.7	34.4	30.4
100 × 100 × 35	125	43.8	39.0	31.4	31.2	31.0
300 × 300 × 154	375	192.5	34.9	33.7	30.8	31.3

Note: For sand and Silty sand II, the peak shear stresses at the three normal stresses are taken from the stress-displacement curves to obtain the friction angles because the use of the peak shear stresses from Fig. 10 of Ziaie Moayed et al. (2017) may result in negative cohesion. For Silty sand I and III, no stress-displacement curves were given in Ziaie Moayed et al. (2017). [1]Results based on Fig.5 of Ziaie Moayed et al. (2017); [2]Results based on Fig.10b of Ziaie Moayed et al. (2017); [3]Results based on Fig.6 of Ziaie Moayed et al. (2017); [4]Results based on Fig.10d of Ziaie Moayed et al. (2017).

More studies on the SSE of geomaterials can be found in the literature. For instance, Dadkhah et al. (2010) studied the SSE of clayey sand. The SSE was clearly showed and the minimum required W/d_{max} ratio of 10 is invalidated again. The experimental results are however difficult to be exploited because the values of d_{max} were not explicitly given (4.75 mm in a table and 10 mm in a figure of particle size distribution curves). In addition, it is unclear if the tested specimens were made of remoulded or unremoulded samples and how the designated densities of specimens were achieved. These results are thus not addressed further.

More recently, MotahariTabari and Shooshpasha (2021) studied the SSE of a coarse grain material in direct shear tests. Similarly to Rathee (1981), the test results involve the effects of several influencing factors such as d_{max}, fine and gravel contents and density. These results can neither be included in this study.

Table 5.8 shows a summarization of the previous analyses on the existing experimental results obtained to investigate the SSE. None of the existing experimental results shows validation of the minimum required W/d_{max} ratio of 10 by ASTM for direct shear tests. Rather, almost all of them show that SSE cannot be eliminated by using specimens having a W/d_{max} ratio of 10. The minimum required W/d_{max} ratio of 10 stipulated by ASTM is invalidated and needs to be revised.

Table 5.8 also shows that a W/d_{max} ratio of 50 is large enough based on some of the existing data while some other results indicate that even a specimen having W/d_{max} ratio as large as 75 is not large enough to remove SSE. In addition, more experimental results are particularly necessary with specimens having W/d_{max} ratio between 10 and 50. With fine particle materials, this is only possible with shear box smaller than the minimum required specimen size of 50 mm, stipulated by the ASTM. To fill this gap, a series of direct shear tests were performed on specimens with d_{max} in the range of 0.85 to 6 mm by using a mini shear box of 38 mm × 38 mm × 45 mm, a small shear box of 60 mm × 60 mm × 45 mm and a large shear box of 300 mm × 300 mm × 180 mm. The tested specimens then have a W/d_{max} ratio between 10 and 353. In this paper, the

experimental results of these laboratory tests are first presented. Minimum required W/d_{max} ratio is identified and proposed to eliminate SSE.

Table 5.8 Summarization of the analyses on existing test data obtained to investigate the SSE

References		**Tested W/d_{max}**	**Minimum require W/d_{max}**	**Minimum tested W/d_{max} large enough to remove SSE**	**Minimum required W/d_{max} of ASTM**
Parsons (1936)		71, 119, 143	~71	Yes at 71	Unknown
Rathee (1981)		10, 48	Unknown	Not at 10	Invalidated
Cerato and Lutenegger (2006)		12, 20, 61	Unknown	Not at 20	Invalidated
Wu et al. (2008)		95, 285	Unknown	Not at 95	Invalidated
Mirzaeifar et al. (2013)		46, 77, 231	~77	Not at 46	Invalidated
Palmeira and Milligan (1989)		50, 127, 833	≤ 50	Yes at 50	Unknown
Ziaie Moayed et al. (2017)	Sand	75, 125, 375	Unknown	Not at 75	Invalidated
	Silty sand I	75, 125, 375	Unknown	Not at 75	Invalidated
	Silty sand II	75, 125, 375	~125	Not at 75	Invalidated
	Silty sand III	75, 125, 375	≤ 75	Yes at 75	Unknown

5.3 Laboratory tests

5.3.1 Test apparatus

In the Geotechnical Laboratory of Polytechnique Montreal, a standard (Figure 5.1a) and a large (Figure 5.1b) direct shear test system are available. The standard direct shear test apparatus is equipped with a small (standard) shear box of 60 mm × 60 mm × 45 mm while the large direct shear apparatus is equipped with a large shear box of 300 mm × 300 mm × 180 mm. A mini shear box of 38 mm × 38 mm × 45 mm was designed and manufactured by the Geotechnical Laboratory of Polytechnique Montreal in order to conduct direct shear tests on specimens of fine particle materials with a W/d_{max} ratio smaller than 50 (based on the critical review of Deiminiat et al. 2020). Figure 5.2 shows a picture of the three shear boxes used in this study. The mini shear box was made to have the same external dimensions as those of the small (standard) shear box in order for it to be compatible with the standard direct shear test system. The testing procedure is thus mainly the same as the standard one of ASTM with the small (standard) shear box. The only difference is in the normal stress loading system. The lever system is removed and the normal

stress is applied by the self-weight of the loading frame and addition of dead load on the holding plate.

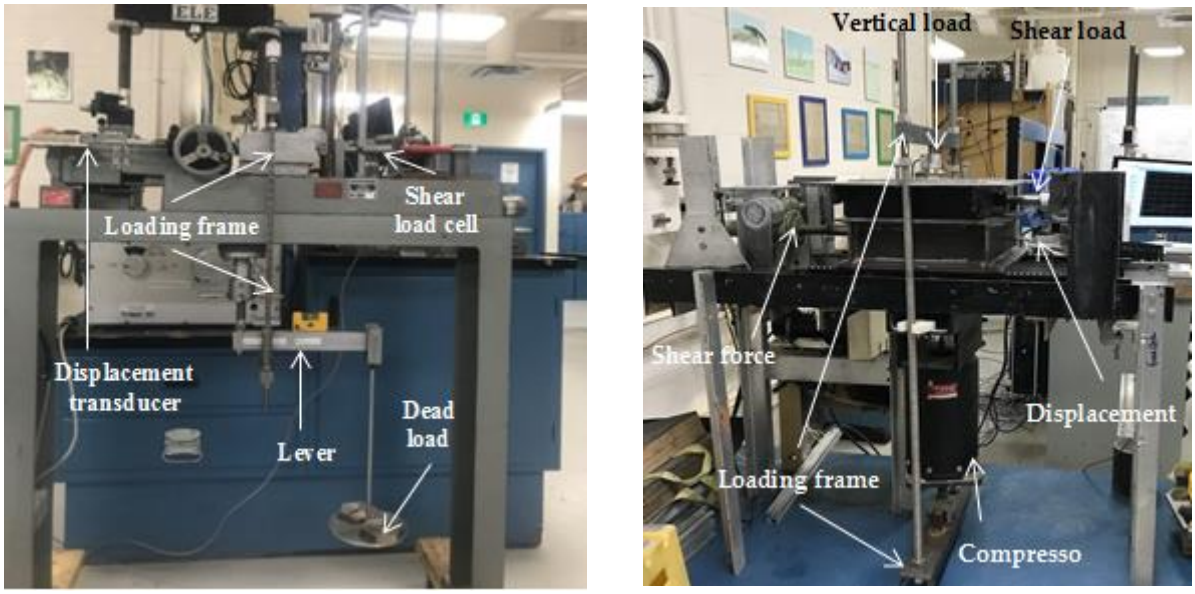

(a) (b)

Figure 5.1 Direct shear apparatuses: (a) standard one for mini and small shear boxes; (b) large one for large shear box.

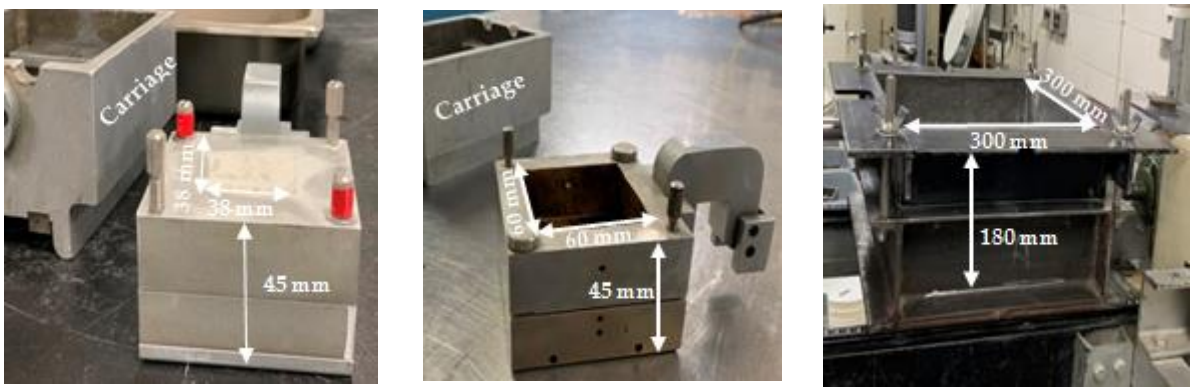

(a) (b) (c)

Figure 5.2 Shear boxes used in this study: (a) house-made mini square shear box (38 mm × 38 mm × 45 mm); (b) small (standard) square shear box (60 mm × 60 mm × 45 mm); (c) large square shear boxes (300 mm × 300 mm × 180 mm)

5.3.2 Materials and testing procedure

Keeping in mind that the scope of this study is to only analyze the SSE on the peak friction angle of granular material, it is very important to make sure that all the specimens prepared with a given material in the mini, small and large shear boxes have the same compactness (density) and water content (dry).

The testing materials in this study are two types of waste rocks, called WR 1 and WR 2, respectively. These waste rocks contain sub-angular and sub-rounded particles. Figure 5.3 shows pictures of the original WR 1 (Figure 5.3a) and WR 2 (Figure 5.3b).

(a) (b)

Figure 5.3 Photos of original (a) WR 1 and (b) WR 2

The two types of waste rocks were first sieved in different portions having particle sizes ranging from 0.08 to 0.85 mm, 0.85 to 1.19 mm, 1.19 to 1.4 mm, 1.4 to 2.36 mm, 2.36 to 3.36 mm, 3.36 to 5 mm, and 5 to 6 mm. Mixtures were made to obtain dry samples having d_{max} of 0.85, 1.19, 1.4, 2.36, 3.36, 5, and 6 mm. Details of different portions used to make the different mixtures are given in Table 5.9.

Table 5.9 Portions of waste rocks used to make the different mixtures

Ranges of particle sizes	**Mass of different portions (g)**						
	d_{max}=6 mm	**5 mm**	**3.36 mm**	**2.36 mm**	**1.4 mm**	**1.19 mm**	**0.85 mm**
5 to 6 mm	3618						

3.36 to 5 mm	5899	6190					
2.36 to 3.36 mm	4314	4432	5062				
1.4 to 2.36 mm	3272	3227	2586	4663			
1.19 to 1.4 mm	524	721	789	1334	2301		
0.85 to 1.19 mm	1326	1379	1603	2202	2220	3283	
0.63 to 0.85 mm	121	125	369	327	1549	2401	6500
0.315 to 0.63 mm	370	385	291	449	710	853	1440
0.16 to 0.315 mm	345	359	408	315	539	568	590
0.08 to 0.16 mm	1063	1105	791	972	771	832	1300
≤ 0.08 mm	2942	3060	2531	2691	2186	2324	3550

Figure 5.4 shows the target and obtained grain size distribution curves of samples having different d_{max}. The grain size distribution curves were also used to produce seven other materials by WR 2. There are thus 14 samples prepared for the direct shear tests with the three different shear boxes. It should also be mentioned that the scope of this paper is to study the SSE, not the scaling down techniques or the effect of d_{max} on the friction angle of granular materials. The different d_{max} values are thus used here as an identification of one material. Each d_{max} along with the type of waste rocks constitute a distinct material.

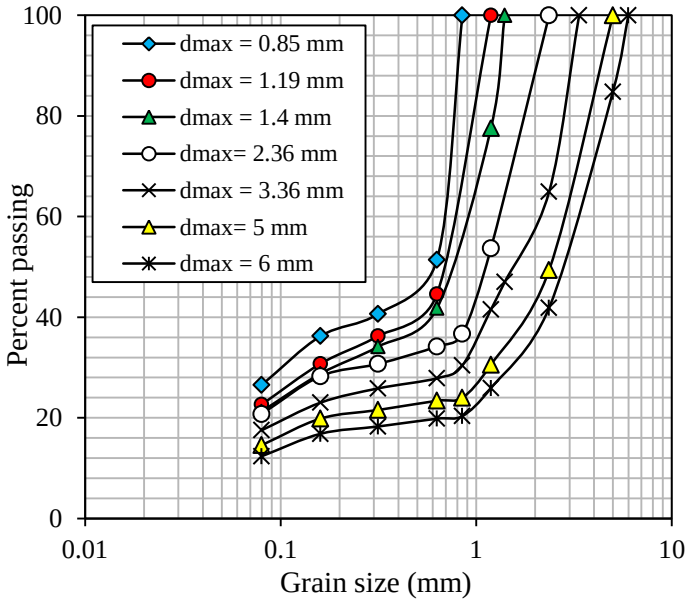

Figure 5.4 Grain size distribution curves of the samples with different d_{max} (same for WR 1 and WR 2)

All the specimens for the mini, small and large shear boxes were prepared with dry waste rocks in the loosest state in order to ensure that the variation of the test results is only associated with

the variation of specimen sizes; the effects of other influencing factors (density, water content, particles shapes, etc.) on the test results are excluded. The specimen was prepared with a spoon by slowly placing waste rocks into each shear box without any compaction. The required mass of material was calculated according to the box volume, specific gravity (Gs) and the maximum void ratio (or desired dry density of 1450 kg/m^3). After filling the box to the top edge of the upper box, the surface of the specimen was smoothed with a brush and the rigid plate was placed slowly to avoid any shock or compact on the material. More details on the preparation of the specimens are presented in Appendix A.

Table 5.10 shows the shear boxes and specimen sizes to d_{max} ratios along with the maximum void ratios (e_{max}) for the two types of waste rocks. The values of e_{max} were estimated by following ASTM C29/C29M-17a. 2007. One notes a decrease of e_{max} with an increased d_{max} value. This is straightforward to understand. As seen in Figure 5.4, the materials with larger d_{max} values have better gradations. With a well graded material, the pore or void spaces can easily be filled with fine particles, resulting in a denser material compared to a poorly graded material. This along with the dense and heavy large particles associated with a large d_{max} value results in a small e_{max}. However, it should be noted that the scope of this study is to evaluate the SSE of direct shear tests. The value of d_{max} is only an identification of the material. Focus should be put on the variation of friction angle as a function of specimen width for one given material (defined by the type of material and a d_{max} value), not on the variation of physical or mechanical properties as a function of d_{max} value.

From Table 5.10, one sees that no tests were planned with the mini box for the specimens with d_{max} of 5 and 6 mm in order to respect the minimum required specimen size to d_{max} ratio of 10 defined by ASTM. All the 19 specimen sizes meet the requirement of ASTM with W/d_{max} ranging from 10 to 353. Since each d_{max} along with the type of waste rocks is only used as an identification of a material, the testing program contains 14 materials (made of WR 1 and WR 2) completely different from each other.

As the shear strength of each specimen is obtained by direct shear tests with three normal stresses (50, 100 and 150 kPa), 57 direct shear tests were carried out for each type of waste rocks. A total number of 114 direct shear tests were realized for the two types of waste rocks. The direct shear

tests were conducted by applying constant rates of 0.015 mm/s (0.9 mm/min) and 0.025 mm/s (1.5 mm/min) for the standard and large shear apparatuses, respectively.

Table 5.10 Shear boxes and specimen size to d_{max} ratios, used in the direct shear tests on the two types of waste rocks

d_{max} (mm)	e_{max}		38 mm × 38 mm × 45 mm		60 mm × 60 mm × 45 mm		300 mm × 300 mm × 180 mm	
	WR 1	WR 2	W/d_{max}	T/d_{max}	W/d_{max}	T/d_{max}	W/d_{max}	T/d_{max}
0.85	0.93	0.91	45	53	71	53	353	212
1.19	0.87	0.86	32	38	50	38	252	151
1.4	0.84	0.83	27	32	43	32	214	129
2.36	0.88	0.85	16	19	25	19	127	76
3.36	0.85	0.86	11	13	18	13	89	54
5.0	0.80	0.87	--	--	12	9	60	36
6.0	0.78	0.87	--	--	10	8	50	30

5.3.3 Test results

Figure 5.5 shows some typical shear stress and shear displacement curves obtained by using the mini (Figure 5.5a), small (Figure 5.5b) and large (Figure 5.5c) shear boxes on WR 1 with a d_{max} value of 0.85 mm. It can be seen that the material tested with different boxes at a given normal stress has the same mechanical behavior. For example, at a normal stress of 50 kPa, the material tested with the mini, small and large boxes has a mechanical behavior of loose sand. At a normal stress of 150 kPa, the material tested with the three boxes starts to have a mechanical behavior of dense sand. These results indirectly indicate that the specimens prepared in the three different boxes do have the same state and density. Subsequently, they do have the same mechanical behavior under a given normal stress: loose sand under a normal stress of 50 kPa and slightly dense sand under a normal stress of 150 kPa.

By taking the peak value of shear stress for each curve, one then obtains three shear stresses at yield, each corresponding to one normal stress. The peak friction angle (hereafter called “friction angle” for simplicity) can then be obtained by applying the linear fitting technique without imposing the straight line passing to the origin in Mohr plane.

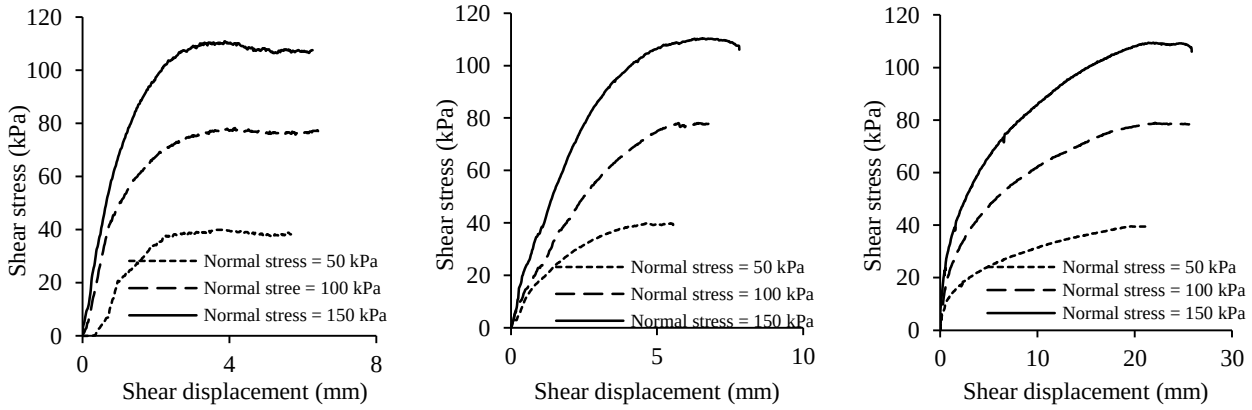

(a) (b) (c)

Figure 5.5 Shear stress vs. shear displacement curves of WR 1 specimens with d_{max} value of 0.85 mm under three normal stresses obtained with the mini (a), small (b) and large (c) shear boxes

Table 5.11 shows the obtained friction angles of all the specimens with different d_{max} for WR 1 and WR 2. Once again, each d_{max} along with the type of waste rocks can only be considered as an identification of a material. The table thus presents the friction angles of 38 samples made of the 14 materials. It is unnecessary to analyze how the friction angles change with the value of d_{max} or with the type of waste rocks.

Table 5.11 Friction angles of the specimens obtained by mini, small and large shear boxes for WR 1 and WR 2

d_{max} (mm)	38 mm × 38 mm × 45 mm				60 mm × 60 mm × 45 mm				300 mm × 300 mm × 180 mm			
	W/d_{max}	T/d_{max}	ϕ (°)		W/d_{max}	T/d_{max}	ϕ (°)		W/d_{max}	T/d_{max}	ϕ (°)	
			WR 1	WR 2			WR 1	WR 2			WR 1	WR 2
0.85	45	53	37.1	35.3	71	53	37.0	35.2	353	212	36.9	35.0
1.19	32	38	38.0	36.2	50	38	37.9	36.1	252	151	37.5	36.0
1.4	27	32	38.7	37.2	43	32	38.0	36.4	214	129	37.7	36.2
2.36	16	19	40.9	38.2	25	19	39.1	37.3	127	76	37.9	37.1
3.36	11	13	42.1	40.5	18	13	40.2	39.3	89	54	38.7	37.4
5.0	--	--	--	--	12	9	41.4	40.1	60	36	39.5	38.4
6.0	--	--	--	--	10	8	43.0	40.9	50	30	39.9	39.2

Figure 5.6 shows the variations of friction angles as a function of W/d_{max} for the specimens made of WR 1 (Figure 5.6a) and WR 2 (Figure 5.6b), respectively. In this figure, the variation of the friction angle is evaluated against W/d_{max} for the specimens of each given material.

From Figure 5.6a, it is seen that the friction angle of the specimens with d_{max} = 0.85 mm remains constant as the W/d_{max} ratio increases from 45 to 353. For the specimens with d_{max} = 1.19 mm, the friction angle decreases by 0.1° as W/d_{max} increases from 32 to 50 and remains almost constant as W/d_{max} further increases to 252. For the specimens with d_{max} = 1.4 mm, the friction angle decreases by 0.7° when W/d_{max} increases from 27 to 43 and it remains almost constant when W/d_{max} further increases from 43 to 214. These results tend to indicate that a W/d_{max} ratio of 43 to 50 is large enough to remove the SSE while the minimum required W/d_{max} ratio of 10 suggested by the ASTM is too small for eliminating the SSE.

For the specimens with d_{max} = 2.36 mm, the friction angle decreases by 1.8° as W/d_{max} increases from 16 to 25 and then decreases by 1.2° when W/d_{max} further increases from 25 to 127. Similarly for the specimens with d_{max} = 3.36 mm, the friction angle decreases by at least 1.9° as W/d_{max} increases from 11 to 18 and decreases by 1.5° as W/d_{max} further increases from 18 to 89. These test results indicate that a W/d_{max} ratio of 18 or 25 is not large enough to eliminate the SSE. The minimum required W/d_{max} ratio of 10 defined by ASTM is invalidated again.

For the specimens with d_{max} = 5 mm, the friction angle decreases by 2.2° as W/d_{max} increases from 12 to 60. For the specimens with d_{max} = 6 mm, the friction angle decreases by 3.1° as W/d_{max} increases from 10 to 50. These results show once again that the minimum required W/d_{max} ratio of 10 defined by ASTM is not large enough to remove SSE.

All the above test results confirm what has been illustrated by Deiminiat et al. (2020). The minimum required W/d_{max} ratio of 10 defined in the ASTM is not validated for the fine particle material with a d_{max} value of 0.85 mm due to the lack of test results with W/d_{max} ratio in the range of 10 to 45, but clearly invalidated for the coarse particle materials with d_{max} ranging from 3.36 to 6 mm. A W/d_{max} ratio of 10 is not large enough to eliminate the SSE on the friction angles of granular materials. The minimum required W/d_{max} ratio of ASTM should be revised.

Similar observations can be made on the experimental results shown in Figure 5.6b for WR 2. The friction angle of the specimens with d_{max} = 0.85 mm remains constant as W/d_{max} increases from 45 to 353. For the specimens with d_{max} = 1.19 mm, the friction angle decreases by 0.2° as W/d_{max} increases from 32 to 50 and remains almost constant as W/d_{max} further increases to 252. The friction angle of the specimens with d_{max} = 1.4 mm decreases by 0.8° when W/d_{max} increases

from 27 to 43 and remains almost constant when W/d_{max} further increases from 43 to 214. For the specimens with d_{max} = 2.36 mm, the friction angle decreases by 0.9° as W/d_{max} increases from 16 to 25 and then decreases by 0.2° when W/d_{max} further increases from 25 to 127. The friction angle of the specimens with d_{max} = 3.36 mm decreases by at least 1.2° as W/d_{max} increases from 11 to 18 and decreases by 1.9° as W/d_{max} further increases from 18 to 89. For the specimens with d_{max} = 5 mm, the friction angle decreases by 1.7° as W/d_{max} increases from 12 to 60. The friction angle of the specimens with d_{max} = 6 mm decreases by 1.7° as W/d_{max} increases from 10 to 50. These results show once again that a W/d_{max} ratio of 43 to 50 is large enough to eliminate the SSE while a W/d_{max} ratio of 10 to 32 is too small to eliminate the SSE on the friction angles of granular materials. The minimum required W/d_{max} ratio of 10 defined in the ASTM needs to be revised (Deiminiat et al., 2020).

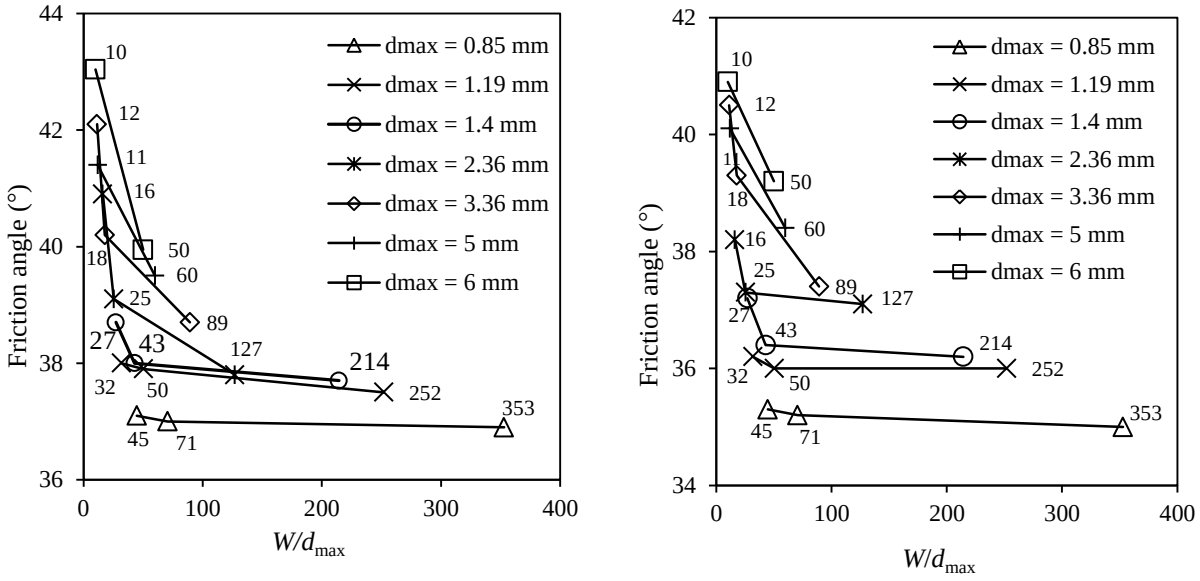

Figure 5.6 Variations of the friction angles of the specimens as a function of W/d_{max} for the materials made of (a) WR 1 and (b) WR 2

5.4 Identification of the minimum required W/d_{max} ratio to eliminate SSE

With the experimental results of fine particle materials with d_{max} values ranging from 0.83 to 1.4 mm shown in Figure 5.6, a W/d_{max} ratio of 43 to 50 seems to be large enough to eliminate the

SSE on the friction angles of granular materials. It still remains unclear if these ratios can be applied to the specimens with d_{max} values ranging from 2.36 to 6 mm to remove the SSE.

One recalls that each d_{max} along with the type of waste rocks must be considered as the identification of one material. It is thus normal to see the test result points as a cloud, as shown in Figure 5.6. It is however very difficult, with such presentation, to identify a unique value respectively for the minimum required W/d_{max} ratio that can be considered as large enough to eliminate the SSE on the friction angle of granular materials.

Table 5.12 shows the friction angles of experimental results obtained in this study and those of existing data, normalized by the measured friction angle of sample having a large enough W/d_{max} ratio. Only a selected part of the existing data presented in Table 5.8 is included and presented in the table because the normalization can only be made on the experimental results with at least one specimen having W/d_{max} ratio large enough to eliminate the SSE. The experimental results of Rathee (1981) and Wu et al. (2008) are thus excluded.

Regarding the direct shear tests of Palmeira and Milligan (1989), the results obtained with the rectangular shear box should be excluded in order to avoid any specimen shape effect. The remaining results should be included because it is difficult to justify that a specimen of 1 m by 1 m is still not large enough to eliminate the SSE with a tested material having a d_{max} = 1.2 mm and a W/d_{max} ratio of 833.

In this study, the experimental results of Ziaie Moayed (2017) have also been excluded because their experimental results involve too many uncertainties pertaining to the SSE of friction angles. For example, their tested materials were prepared at optimum water contents. The very high apparent cohesions obtained with the small shear box can be well explained by the suction associated with the unsaturated state of the sample. However, the very small and even negative apparent cohesion obtained by the medium and large shear boxes cannot be explained by the unsaturated state of the samples. In addition, the shear stress–shear displacement curves clearly showed that the specimens in the small box received more compactness, having a mechanical behaviour of dense sand while the specimens in the large box did not receive enough compactness, showing a mechanical behaviour of loose sand. The problem of compactness can further be confirmed by the number of layers during their specimen preparation: three layers both

in the small and medium sizes of shear box, five layers in the large shear box (Ziaie Moayed 2017).

Regarding the experimental results of Mirzaeifar et al. (2013), it is noted that the desired densities of 1.5, 1.58 and 1.67 g/cm^3 were obtained by compacting the sand in 4, 6 and 8 layers, respectively. With the same number of layers in small, medium and large shear boxes, the resulting densities could be expected very different. Their test results thus not only involve the SSE, but also the effects of compactness or density. The experimental results of Mirzaeifar et al. (2013) should thus also be excluded in the identification of the minimum required $W/d_{\max}$ ratio.

Figure 5.7 presents the variation of the normalized friction angles as a function of $W/d_{\max}$ of the experimental results obtained in this study and taken from the literature. It can be seen that the normalized friction angle varies from 1.12 to 1 depending on the W/d_{max} ratio. The normalized friction angle decreases as $W/d_{\max}$ increases from 10 to a certain value before it becomes constant when the $W/d_{\max}$ ratio further increases from this critical value to a value as high as 353. The critical value of $W/d_{\max}$ ratio beyond which the normalized friction remains constant is the searched minimum required $W/d_{\max}$ ratio to eliminate the SSE on friction angle of granular materials.

To identify these critical values, one first draws a horizontal line at normalized friction angles equal to 1. Eye-based best-fitted curves are then plotted to the experimental results having the $W/d_{\max}$ ratio between 10 and 50. One sees that the critical $W/d_{\max}$ ratio should be in the range of 50 to 70. One recommends a value of 60 for the minimum required $W/d_{\max}$ ratio, identified as large enough to eliminate the SSE. This value is chosen as a compromise between accuracy and practical convenience.

Table 5.12 Normalized friction angles of the experimental results obtained in this study and taken from the literature

Id. of material	$W/d_{\max}$	$T/d_{\max}$	ϕ (°)	**Normalized** ϕ	**Id. of material**	$W/d_{\max}$	$T/d_{\max}$	ϕ (°)	**Normalized** ϕ	**References**
WR 1, $d_{\max}$=0.85 mm	45	53	37.1	1.005	WR 2, $d_{\max}$=0.85 mm	45	53	35.3	1.009	This study
	71	53	37.0	1.003		71	53	35.2	1.006	
	353	212	36.9	1		353	212	35.0	1	
WR 1, $d_{\max}$=1.19 mm	32	38	38.0	1.013	WR 2, $d_{\max}$=1.19 mm	32	38	36.2	1.006	
	50	38	37.9	1.011		50	38	36.1	1.002	
	252	151	37.5	1		252	151	36.0	1	

WR 1, d_{max}=1.4 mm	27	32	38.7	1.027	WR 2, d_{max}=1.4 mm	27	32	37.2	1.028	
	43	32	38.0	1.008		43	32	36.4	1.006	
	214	129	37.7	1		214	129	36.2	1	
WR 1, d_{max}=2.36 mm	16	19	40.9	1.082	WR 2, d_{max}=2.36 mm	16	19	38.2	1.030	
	25	19	39.1	1.034		25	19	37.3	1.005	
	127	76	37.8	1		127	76	37.1	1	
WR 1, d_{max}=3.36 mm	11	13	42.1	1.088	WR 2, d_{max}=3.36 mm	11	13	40.5	1.083	
	18	13	40.2	1.039		18	13	39.3	1.051	
	89	54	38.7	1		89	54	37.4	1	
WR 1, d_{max}=5 mm	12	9	41.4	1.048	WR 2, d_{max}=5 mm	12	9	40.1	1.044	
	60	36	39.5	1		60	36	38.4	1	
Gravel, d_{max}=5 mm, D_r=25%	12	5	42.0	1.235	Gravel, d_{max}=5 mm, D_r=55%	12	5	44.5	1.107	Cerato and Lutenegger (2006)
	20	8	36.5	1.074		20	8	41.0	1.020	
	61	36	34.0	1		61	36	40.2	1	
Gravel, d_{max}=5 mm, D_r=85%	12	5	45.5	1.083						
	20	8	43.0	1.024						
	61	36	42.0	1						
Sand, d_{max}=1.2 mm	50	27	50.1	1.014						Palmeira and Milligan (1989)
	833	833	49.4	1						

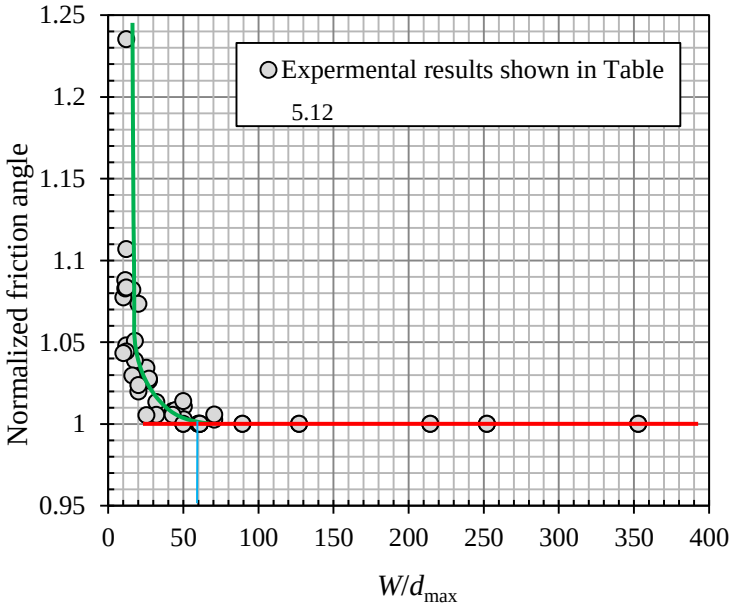

Figure 5.7 Variations of the normalized friction angles as a function of W/d_{max} of the experimental results obtained in this study and taken from the literature. The minimum required specimen size is identified as W/d_{max} = 60

5.5 Discussion

Direct shear test is a very old but still regularly used method to determine shear strength of geomaterials (Goodrich, 1904; Casagrande & Albert, 1932; Rutledge, 1935; Casagrande, 1936; Terzaghi, 1936; Cooling et al., 1936; Terzaghi & Peck, 1948; Hutchinson, 1962). Not like triaxial compression tests, direct shear test imposes a sliding plane determined by the upper and lower half boxes. Several shortages can be attributed to this imposed sliding plane. By following the standard of ASTM D3080 published in 1972 can doubtlessly ensure higher quality of experimental results. Nevertheless, people are aware of the limitations. ASTM D3080 has to be regularly revised and updated every eight years. Recently, ASTM D3080/D3080M-11 2011 it was temporarily withdrawn by the ASTM technical committees due to an excess of eight years from the last update. It seems that main concern of this update is related to the gap thickness to be left. One can expect that the updated version remains unchanged with respect to the minimum required specimen sizes. The current study is thus useful to feed its future updates.

This experimental study leads to a recommendation of a minimum required W/d_{max} ratio of 60. It is interesting to note that the same value was recommended by Wang and Gutierrez (2010), who studied the SSE of direct shear tests through a 2D discrete element modeling and made such recommendation based on their experience[§]. They also studied the influence of specimen thickness on the stress ratio (ratio of shear stress to normal stress) in order to validate the minimum ratio of 6 required by ASTM. The stress ratio increases due to the increase in the specimen thickness and its influence on the stress distribution of the specimen shear plane during shearing.

A minimum ratio of 40 between specimen thickness and $d_{\max}$ was then suggested by Wang and Gutierrez (2010) as a consequence of their finding and experience. However, this hypothesis has never been verified by previous experimental investigations, perhaps because at least three nonstandard shear boxes with varied heights and the same width are required.

[§] Personal communication by email between the first author and Prof. Jianfeng Jerry Wang on October 25, 2021

Despite the important and interesting discovery of this study, one has to point out that there are also several limitations.

In this study, the effect of specimen width was evaluated by trying to keep other influencing parameters constant. For one given material, all the shear tests with different shear boxes were performed with the same compact state and moist content. However, due to lack of shear boxes, the thickness of tested specimens meets the minimum required T/d_{max} ratio of ASTM, but is not constant. The influence of this parameter, the gap thickness between upper and lower half boxes as well as the specimen aspect ratio W/T were not taken into account (Hight & Leroueil, 2003; Wang & Gutierrez, 2010). More experimental work is thus necessary not only to verify the validity of the recommended value of the minimum required W/d_{max} ratio, but also to verify if the minimum required T/d_{max} ratio of ASTM is large enough to eliminate the SSE in direct shear tests. The finding might be also used to verify the hypothesis given by Wang and Gutierrez (2010) for the minimum required T/d_{max} ratio.

Another limitation of this work is associated with the unique consideration of specimen size to d_{max} ratios. It is however well-known that the mechanical properties of geomaterials are not only controlled by the size of d_{max}, but also by the content of d_{max}. Two materials having the same d_{max} with different contents can behave differently. It is thus interesting and important to take into account other influencing factors, such as the portion of the coarsest particles, median size d_{50}, coefficient of uniformity, particle shapes, contents of fine and coarse particles, and crushability of particles. It is also well-known that the friction angle of geomaterials depends on the compactness, water content and confining pressure. More experimental work is necessary with more types of materials of different sources by taking into account these different influencing factors.

Finally, more experimental work can be necessary to evaluate if the minimum required specimen diameter over d_{max} ratio of 6 specified by ASTM D4767 (2011) is large enough to eliminate SSE of triaxial compression tests by following the methodology presented in this study (Deiminiat et al., 2022).

5.6 Conclusions

The minimum required specimen width to d_{max} ratio of ASTM has been revised based on an analysis on existing data and new experimental results. The following conclusions can be drawn:

- The experimental results confirm what has been reported in Deiminiat et al. (2020), who showed that the minimum requirement of ASTM was not validated for fine particle materials due to the lack of experimental data with W/d_{max} ranging from 10 to 50, but invalidated for coarse particle materials. An update is necessary for the minimum required ratio between specimen sizes and d_{max}, stipulated by the ASTM D3080/D3080M-11 for direct shear tests.
- The minimum required W/d_{max} ratio is identified as equal to 60 to eliminate the SSE on the shear strengths of granular materials.
- For fine particle materials having a d_{max} not larger than 1 mm, using the standard shear boxes having W = 60 mm automatically results in $W/d_{max} \geq 60$. The obtained friction angles can be considered as fully representative to that of the tested material in field conditions. The ASTM D3080/D3080M-11 can thus be continued to be applied without any problem of SSE.
- For granular materials having d_{max} larger than 1 mm, applying the minimum requirements of ASTM D3080/D3080M-11 may result in a W/d_{max} ratio much smaller than the identified minimum required W/d_{max} ratio. The obtained friction angles can be erroneous.
- More experimental works are necessary, not only with shear boxes of different sizes, but also with more materials by considering different testing conditions, including different densities, water contents, particle shapes, normal stresses, etc.

Acknowledgments

The authors acknowledge the financial support from the Natural Sciences and Engineering Research Council of Canada (NSERC RGPIN-2018-06902), Fonds de recherche du Québec—Nature et Technologies (FRQNT 2017-MI-202860), industrial partners of the Research Institute on Mines and the Environment (RIME UQAT-Polytechnique; http://rime-irme.ca/), and Mitacs

Elevate Postdoctoral Fellowship (IT12569). Samuel Chenier, Eric Turgeon and Noura El-Harrak are gratefully acknowledged for their assistance in the laboratory work.

5.7 References

Abbas, S. M. (2011). *Behaviour of rockfill materials: based on nature of particles*. Saarbrücken, Germany: LAP Lambert Academic Publishing.

Afzali-Nejad, A., Lashkari, A., & Shourijeh, P. T. (2017). Influence of particle shape on the shear strength and dilation of sand-woven geotextile interfaces. *Geotextiles and Geomembranes*, *45*(1), 54-66.

Afzali-Nejad, A., Lashkari, A., & Farhadi, B. (2018). Role of soil inherent anisotropy in peak friction and maximum dilation angles of four sand-geosynthetic interfaces. *Geotextiles and Geomembranes*, *46*(6), 869-881

Alonso, E. E., Tapias, M., & Gili, J. (2012). Scale effects in rockfill behaviour. *Géotechnique Letters*, *2*(3), 155-160.

Amirpour Harehdasht, S., Karray, M., Hussien, M. N., & Chekired, M. (2017). Influence of particle size and gradation on the stress-dilatancy behavior of granular materials during drained triaxial compression. *International Journal of Geomechanics*, *17*(9), 04017077.

Amirpour Harehdasht, S., Hussien, M. N., Karray, M., Roubtsova, V., & Chekired, M. (2019). Influence of particle size and gradation on shear strength–dilation relation of granular materials. *Canadian Geotechnical Journal*, *56*(2), 208-227.

AS 1289.6.2.2. (1998). Soil strength and consolidation tests-determination of the shear strength of a soil-direct shear test using a shear box. *Standards Australia*, Sydney, NSW, Australia.

ASTM C29/C29M-17a. (2007). Standard test method for bulk density (unit weight) and voids in aggregate, *ASTM International*, West Conshohocken, PA, USA.

ASTM D3080. (1972). Direct shear test of soils under consolidated drained conditions. *ASTM International*, West Conshohocken, PA, USA.

ASTM D3080/D3080M. (2011). Direct shear test of soils under consolidated drained conditions. *ASTM International*, West Conshohocken, PA, USA.

Aubertin, M., Bussière, B., Bernier, B., (2002). *Environnement et gestion des rejets miniers, Manuel sur cédérom*, Presses Internationales Polytechnique, Polytechnique Montreal, Canada.

Azam, S., Wilson, G. W., Herasymuik, G., Nichol, C. & Barbour, L. S. (2007). Hydrogeological behavior of an unsaturated waste rock pile: a case study at the Golden Sunlight Mine, Montana, USA. *Bulletin of Engineering Geology and the Environment*, *66*(3), 259-268.

Azam, S., & Li, Q. (2010). Tailings dam failures: a review of the last one hundred years. *Geotechnical News*, *28*(4), 50-54.

Boudrias, G. (2018*). Évaluation numérique et expérimentale du drainage et de la consolidation de résidus miniers à proximité d'une inclusion de roches stériles* (Doctoral dissertation, Ecole Polytechnique, Montreal, Canada).

BS 1377. (1990). Methods of test for soils for civil engineering purposes. Shear strength tests (total stress). Part 7. *British Standard Institution*, London, UK,

Cai, H., Wei, R., Xiao, J. Z., Wang, Z. W., Yan, J., Wu, S. F., & Sun, L. M. (2020). Direct shear test on coarse gap-graded fill: plate opening size and its effect on measured shear strength. *Advances in Civil Engineering*, *2020*.

Casagrande, A. (1936). Characteristics of cohesionless soils affecting the stability of slopes and earth fills. *Journal of Boston Society of Civil Engineers*, *23*(1), 13-32.

Casagrande, A., & Albert, S. G. (1932). *Research on the shearing resistance of soils*, International Society for Soil Mechanics and Geotechnical Engineering, (pp. 85-97).

Cerato, A. B., & Lutenegger, A. J. (2006). Specimen size and scale effects of direct shear box tests of sands. *Geotechnical Testing Journal*, *29*(6), 507-516.

Chang, W. J., & Phantachang, T. (2016). Effects of gravel content on shear resistance of gravelly soils. *Engineering Geology*, *207*, 78-90.

Cooling, L. F., Smith, D. B., & Subcomerpre. (1936). Egineering research. Institution reseahc committee on earth-pressures. The shearing resistance of soils. *Journal of the Institution of Civil Engineers*, *3*(7), 333-343.

Dadkhah, R., Ghafoori, M., Ajalloeian, R., & Lashkaripour, G. R. (2010). The effect of Scale Direct Shear Tests on The Strength parameters of Clayey Sand in Isfahan city, Iran. *Journal of Applied Sciences*, *10*(18), 2027-2033.

Deiminiat, A., Li, L., Zeng, F., Pabst, T., Chiasson, P., & Chapuis, R. (2020). Determination of the shear strength of rockfill from small-scale laboratory shear tests: a critical review. *Advances in Civil Engineering*, *2020*.

Drugan, W. J., & Willis, J. R. (1996). A micromechanics-based nonlocal constitutive equation and estimates of representative volume element size for elastic composites. *Journal of the Mechanics and Physics of Solids*, *44*(4), 497-524.

Eurocode 7. (2007). Geotechnical design - Part 1: General rules: EN 1997-1. *The European Union Per Regulation*, Brussels, Belgium.

Goodrich, E. P. (1904). Lateral Earth Pressures and Related Phenomena. *Transactions of the American Society of Civil Engineers*, *53*(2), 272-304.

Gupta, A. K. (2009). Triaxial behaviour of rockfill materials. *Electronic Journal of Geotechnical Engineering*, *14*(Bund. J), 1-18.

Hall, E. B. (1951). A triaxial apparatus for testing large soil specimens. *ASTM*, *106*, 152-161.

Hamidi, A., Azini, E., & Masoudi, B. (2012). Impact of gradation on the shear strength-dilation behavior of well graded sand-gravel mixtures. *Scientia Iranica*, *19*(3), 393-402.

Hight, D. W., & Leroueil, S. (2003). Characterisation of soils for engineering purposes. *Characterisation and Engineering Properties of Natural Soils*, *1*, 255-360.

Holtz, W., & Gibbs, H. J. (1956). Triaxial shear tests on pervious gravelly soils. *Journal of the Soil Mechanics and Foundations Division*, 82(1), 1-22.

Honkanadavar, N. P., Dhanote, S., & Bajaj, S. (2016). 161 Prediction of shear strength parameter for prototype alluvial rockfill material. *Indian Geotechnical Conference* IGC2016, Chennai, India.

Honkanadavar, N. P., Kumar, N., & Ratnam, M. (2014). Modeling the behavior of alluvial and blasted quarried rockfill materials. *Geotechnical and Geological Engineering*, *32*(4), 1001-1015

Hutchinson, J. N., & Rolfsen, E. N. (1962). Large scale field shear box test and quick clay, *Geologie and Bauwesen*, Vienna, *28*(1), 31 – 42.

Jacobson, D. E., Valdes, J. R., & Evans, T. M. (2007). A numerical view into direct shear specimen size effects. *Geotechnical Testing Journal*, *30*(6), 512-516.

Jewell, R.A., & Wroth, C.P. (1987). Direct shear tests on reinforced sand. *Geotechnique*, 37(1), 53–68.

Kanit, T., Forest, S., Galliet, I., Mounoury, V., & Jeulin, D. (2003). Determination of the size of the representative volume element for random composites: statistical and numerical approach. *International Journal of solids and structures*, *40*(13-14), 3647-3679.

Kermani, M. (2016). *Prediction of post-construction settlements of rockfill dams based on construction field data* (Doctoral Dissertation, Laval University. Laval, QC, Canada).

Leslie, D. (1963). Large scale triaxial tests on gravelly soils. *In Proc. of the 2nd Pan-American Conf. on SMFE, Brazil* (Vol. 1, PP. 181-202).

Li, L., Ouellet, S., & Aubertin, M. (2009). A method to evaluate the size of backfilled stope barricades made of waste rock. *GeoHalifax, Halifax, Canada*, (Vol. 1, p. 1).

Li, L., & Aubertin, M. (2011). Limit equilibrium analysis for the design of backfilled stope barricades made of waste rock. *Canadian Geotechnical Journal*, *48*(11), 1713-1728.

Lings, M. L., & Dietz, M. S. (2004). An improved direct shear apparatus for sand. *Geotechnique*, *54*(4), 245-256.

Marachi, N., Seed, H., & Chan, C. (1969). Strength characteristics of rockfill materials. *Seventh International Conference on Soil Mechanics and Foundation Engineering.*

Marachi, N. D., Chan, C. K., & Seed, H. B. (1972). Evaluation of properties of rockfill materials. *Journal of the Soil Mechanics and Foundations Division*, *98*(1), 95-114.

Marsland, A. (1971). The use of in-situ tests in a study of the effects of fissures on the properties of stiff clays. In *Proc. First Aust.-NZ Conference on Geomechanics, Melbourne* (Vol. 1, pp. 180-189).

McLemore, V. T., Sweeney, D., Dunbar, N., Heizler, L., & Writer, E. P. (2009). Determining quantitative mineralogy using a modified MODAN approach on the Questa rock pile materials. *In Society of Mining, Metallurgy and Exploration Annula Convention, Denver* (pp. 9-20).

Mirzaeifar, H., Abouzar, A., & Abdi, M. R. (2013). Effects of direct shear box dimensions on shear strength parameters of geogrid-reinforced sand. In *66th Canadian geotechnical conference and the 11th joint CGS/IAH-CNC groundwater conference, Montreal* (pp. 1-6).

Ovalle, C., Linero, S., Dano, C., Bard, E., Hicher, P. Y., & Osses, R. (2020). Data compilation from large drained compression triaxial tests on coarse crushable rockfill materials. *Journal of Geotechnical and Geoenvironmental Engineering*, *146*(9), 06020013.

Owen, J. R., Kemp, D., Lébre, É., Svobodova, K., & Murillo, G. P. (2020). Catastrophic tailings dam failures and disaster risk disclosure. *International Journal of Disaster Risk Reduction*, *42*, 101361.

Palmeira, E. M. & Milligan, G. W. E. (1989). Scale effects in direct shear tests on sand, *Proceedings of the 12th International Conference on Soil Mechanics and Foundation Engineering, Rio de Janeiro* (Vol. 1, pp. 739-742).

Pankaj, S., Mahure, N., Gupta, S., Sandeep, D., & Devender, S. (2013). Estimation of shear strength of prototype rockfill materials. *International Journal of Engineering*, *2*(8), 421-426.

Parsons, J. D. (1936). Progress report on an investigation of the shearing resistance of cohesionless soils. *Proceedings of the 1st International Conference on Soil Mechanics and Foundation Engineering* (Vol. 2, pp. 133-138).

Potts, D. M., Dounias, G. T., & Vaughan, P. R. (1987). Finite element analysis of the direct shear box test. *Geotechnique, 37*(1), 11-23.

Rasti, A., Adarmanabadi, H., Pineda, M., & Reinikainen, J. (2021). Evaluating the Effect of Soil Particle Characterization on Internal Friction Angle. *American Journal of Engineering and Applied Sciences*.

Rathee, R. K. (1981). Shear strength of granular soils and its prediction by modeling techniques. *Journal of Institution of Engineers*, 62, 64-70.

Rutledge, P. C. (1935). *Report developments in soil testing apparatus*. Journal of the Boston Society of Civil Engineers, Boston, USA.

Saleh-Mbemba, F., Aubertin, M., & Boudrias, G. (2019). Drainage and consolidation of mine tailings near waste rock inclusions. In *Sustainable and Safe Dams Around the World* (pp. 3296-3305).

Shibuya, S., Mitachi, T., & Tamate, S. (1997). Interpretation of direct shear box testing of sands as quasi-simple shear. *Geotechnique*, *47*(4), 769-790.

Stone, K. J., & Wood, D. M. (1992). Effects of dilatancy and particle size observed in model tests on sand. *Soils and Foundations*, *32*(4), 43-57.

Terzaghi, K. V. (1936). The shearing resistance of saturated soils and the angle between the planes of shear. In *First International Conference on Soil Mechanics* (Vol. 1, pp. 54-59).

Terzaghi, K., & Peck, R.B. (1948). *Soil mechanics in engineering practice*. New York, USA: John Wiley and Sons, Inc.

Varadarajan, A., Sharma, K. G., Abbas, S. M., & Dhawan, A. K. (2006). The role of nature of particles on the behavior of rockfill material. *Soils and Foundations*, *46*(5), 569-584.

Varadarajan, A., Sharma, K. G., Venkatachalam, K., & Gupta, A. K. (2003). Testing and modeling two rockfill materials. *Journal of Geotechnical and Geoenvironmental Engineering*, 129(3), 206-218.

Vucetic, M., & Lacasse, S. (1982). Specimen size effect in simple shear test. *Journal of the Geotechnical Engineering Division*, *108*(12), 1567-1585.

Wang, J., & Gutierrez, M. (2010). Discrete element simulations of direct shear specimen scale effects. *Géotechnique*, *60*(5), 395-409.

Wang, J., Dove, J. E., & Gutierrez, M. S. (2007). Discrete-continuum analysis of shear banding in the direct shear test. *Géotechnique*, *57*(6), 513-526.

Wen, R., Tan, C., Wu, Y., & Wang, C. (2018). Grain size effect on the mechanical behavior of cohesionless coarse-grained soils with the discrete element method. *Advances in Civil Engineering*, *2018*.

Wu, P. K., Matsushima, K., & Tatsuoka, F. (2008). Effects of specimen size and some other factors on the strength and deformation of granular soil in direct shear tests. *Geotechnical Testing Journal*, *31*(1), 45-64.

Xu, Y. (2018). Shear strength of granular materials based on fractal fragmentation of particles. *Powder Technology*, *333*, 1-8.

Xue, Z. F., Cheng, W. C., Wang, L., & Song, G. (2021). Improvement of the shearing behaviour of loess using recycled straw fiber reinforcement. *KSCE Journal of Civil Engineering*, 1-17.

Yang, P., Li, L., Aubertin, M., Brochu-Baekelmans, M., & Ouellet, S. (2017). Stability analyses of waste rock barricades designed to retain paste backfill. *International Journal of Geomechanics*, *17*(3), 04016079.

Yang, G., Jiang, Y., Nimbalkar, S., Sun, Y., & Li, N. (2019). Influence of particle size distribution on the critical state of rockfill. *Advances in Civil Engineering*, *2019*.

Zahran, K., & Naggar, H. E. (2020). Effect of sample size on TDA shear strength parameters in direct shear tests. *Transportation Research Record*, *2674*(9), 1110-1119.

Zhai, Y., Li, L., & Chapuis, R. P. (2021a). Analytical, Numerical and Experimental Studies on Steady-State Seepage Through 3D Rockfill Trapezoidal Dikes. *Mine Water and the Environment*, *40*(4), 931-942.

Zhai, Y., Yang, P., & Li, L. (2021b). Analytical solutions for the design of shotcreted waste rock barricades to retain slurried paste backfill. *Construction and Building Materials*, *307*, 124626.

Zhang, Z., Sheng, Q., Fu, X., Zhou, Y., Huang, J., & Du, Y. (2020). An approach to predicting the shear strength of soil-rock mixture based on rock block proportion. *Bulletin of engineering Geology and the Environment*, *79*(5), 2423-2437.

Ziaie Moayed, R., Alibolandi, M., & Alizadeh, A. (2017). Specimen size effects on direct shear test of silty sands. *International Journal of Geotechnical Engineering*, *11*(2), 198-205.

CHAPTER 6 ARTICLE 3: EXPERIMENTAL STUDY ON THE RELIABILITY OF SCALING DOWN TECHNIQUES USED IN DIRECT SHEAR TESTS TO DETERMINE THE SHEAR STRENGTH OF ROCKFILL AND WASTE ROCKS

Akram Deiminiat, Li Li

Invited article published in CivilEng, 2022, 3, 35-50 on January 8, 2022

Abstract: The determination of shear strength parameters for coarse granular materials such as rockfill and waste rocks is challenging due to their oversized particles and the minimum required ratio of 10 between the specimen width (W) and the maximum particle size (d_{max}) of tested samples for direct shear tests. To overcome this problem, a common practice is to prepare test samples by excluding the oversized particles. This method is called the scalping scaling down technique. Making further modifications on scalped samples to achieve a specific particle size distribution curve (PSDC) leads to other scaling down techniques. Until now, the parallel scaling down technique has been the most popular and most commonly applied, generally because it produces a PSDC parallel and similar to that of field material. Recently, a critical literature review performed by the authors revealed that the methodology used by previous researchers to validate or invalidate the scaling down techniques in estimating the shear strength of field materials is inappropriate. The validity of scaling down techniques remains unknown. In addition, the minimum required W/d_{max} ratio of 10, stipulated in ASTM D3080/D3080M-11 for direct shear tests, is not large enough to eliminate the specimen size effect (SSE). The authors' recent experimental study showed that a minimum W/d_{max} ratio of 60 is necessary to avoid any SSE in direct shear tests. In this study, a series of direct shear tests were performed on samples with different d_{max} values, prepared by applying scalping and parallel scaling down techniques. All tested specimens had a W/d_{max} ratio equal to or larger than 60. The test results of the scaled down samples with d_{max} values smaller than those of field samples were used to establish a predictive equation between the effective internal friction angle (hereafter named "friction angle") and d_{max}, which was then used to predict the friction angles of the field samples. Comparisons between the measured and predicted friction angles of field samples demonstrated that the equations based on scalping scaling down technique correctly predicted the friction

angles of field samples, whereas the equations based on parallel scaling down technique failed to correctly predict the friction angles of field samples. The scalping down technique has been validated, whereas the parallel scaling down technique has been invalidated by the experimental results presented in this study.

Keywords: direct shear tests; scaling down technique; shear strength; maximum particle size; scalping technique; parallel technique

6.1 Introduction

The determination of shear strength parameters is challenging for coarse granular materials such as rockfill and waste rocks due to their oversized particles and the minimum required ratio of 10 between specimen width (W) and the maximum particle size (d_{max}) of tested samples for direct shear tests (ASTM D3080/D3080M-11 2021). For the convenience of laboratory tests, it is always preferable to use specimens as small as possible. However, when the specimens are too small, the measured shear strength can be significantly different from that of the tested material in field conditions. Thus, the tested specimens must be large enough to eliminate any specimen size effect (SSE) (Rathee, 1981; Palmeira & Milligan, 1989; Cerato & Lutenegger, 2006; Wu et al., 2008; Mirzaeifar et al., 2013; Omar & Sadrekarimi, 2015; Ziaie Moayed et al., 2017; Zahran & Naggar, 2020; Deiminiat et al., 2020, 2021). The minimum required specimen volume to avoid any SSE is called the representative element volume (Drugan & Willis, 1996; Kanit et al., 2003; Wen et al., 2018).

For direct shear tests, several standards have been proposed and used in practice. Among them, the ASTM D3080/D3080M-11, hereafter called ASTM, is the most popular and the most used worldwide (e.g., Rathee, 1981; Gupta, 2009; Pankaj et al., 2013; Honkanadavar et al., 2014; Amirpour Harehdasht et al., 2019; Zhang et al., 2019; Cai et al., 2020; Zahran & Naggar, 2020; Nicks et al., 2021; Rasti et al., 2021; Saberian et al., 2021). It was published as ASTM D3080 in 1972 and updated every eight years by the ASTM technical committees. Recently, it was temporarily withdrawn due to over eight years passing since the last update (ASTM D3080/D3080M-11 2021). The withdrawn rationale has nothing to do with d_{max}; therefore, it can be expected that the updated ASTM standard for direct shear tests will remain unchanged with respect to the minimum required specimen sizes. The width (W) and thickness (T) of the tested

square specimen should be: $W \geq 50$ mm; $T \geq 13$ mm; $W/d_{max} \geq 10$; $T/d_{max} \geq 6$; $W/T \geq 2$. Similar requirements can be found in other standards (e.g., AS 1289.6.2.2, Eurocode 7 and Bs 1377).

For fine particle materials such as clay, silt and sand with a d_{max} smaller than or equal to 1 mm, applying ASTM in specimen preparation is not a problem because the standard direct shear test system is usually equipped with a square shear box 60 mm wide (i.e., W = 60 mm). The specimens prepared with this standard shear box automatically have a W/d_{max} ratio up to 60, a value largely exceeding the ASTM's minimum required ratio of 10. For coarse materials such as gravel, rockfill and waste rocks, applying ASTM in specimen preparation can become problematic. The problem is particularly prominent with rockfill and waste rocks, which usually contain fine particles as small as silts and coarse particles as large as boulders. Conducting laboratory tests with original field material and respecting the ASTM's requirements are economically impossible if technically not impossible.

To overcome this problem, a common practice is to prepare test samples by excluding the oversized particles (Hall, 1951; Holtz & Gibbs, 1956; Leslie, 1963; Marachi et al., 1969; 1972; Varadarajan et al., 2003; Hamidi et al., 2012; Ovalle et al., 2014; Chang & Phantachang, 2016; Yang et al., 2019; Dorador & Villalobos, 2020b; Ovalle et al., 2020; Deiminiat et al., 2020; Kouakou et al., 2020; MotahariTabari & Shooshpasha, 2021). The method is called the scalping scaling down technique.

Scalping technique is probably the simplest and earliest method to obtain laboratory samples having an admissible d_{max} from field materials (Hennes, 1953; Zeller & Wullimann, 1957; Leslie, 1963; Morgan & Harris, 1967; Hall & Smith, 1971; Williams & Walker, 1983; Donaghe & Torrey, 1985; Seif El Dine et al., 2010; Hamidi et al., 2012; Deiminiat et al., 2020; Dorador & Villalobos, 2020; MotahariTabari & Shooshpasha, 2021). By applying this technique, the particle size distribution curve (PSDC) of the obtained samples can differ from that of the field material due to the reduction in coarse particles. Some researchers made use of this method when the excluded oversized particles represented 10% to 30% (Zeller & Wullimann, 1957; Fragaszy et al., 1992; Bareither et al., 2008; Dorador & Villalobos, 2020b).

Further modifications on scalped samples to achieve a specific PSDC have led to other scaling down techniques. When the PSDC of the scaled down sample is modified to be parallel to that of

field material, the method is called the parallel scaling down technique (Lowe, 1964; Tombs, 1969; Charles, 1973). The PSDC of the obtained sample thus looks like a horizontal shift of the PSDC of the field material towards the finer side in the semi-log plane of the PSDC.

The third scaling down technique, called the replacement method, consists of replacing the oversized particles by the same mass of particles having size between 4.75 mm (No. 4 sieve) and the admissible d_{max} (Frost, 1973; Donaghe & Townsend, 1973; Donaghe & Torrey, 1985; Houston et al., 1994). The obtained samples can have a PSDC very different from that of the field material (Donaghe & Townsend, 1976; Rathee, 1981; Feng & Vitton, 1997).

The fourth scaling down method, called the quadratic grain-size technique, produces a PSDC by following an equation that has nothing to do with the PSDC of field materials (Deiminiat et al., 2000). The physical meaning of the proposed modification is unclear, and it will not be discussed further in this study.

Until now, the parallel scaling down technique has been the most popular and the most widely used (Marachi et al., 1969, 1972; Feng & Vitton, 1997; Varadarajan et al., 2003, 2006; Gupta, 2009; Abbas, 2011; Rao et al., 2011; Stober, 2012; Vasistha et al., 2013; Honkanadavar et al., 2014, 2016; Sukkarak et al., 2018; Deiminiat et al., 2020; Ovalle and Dano, 2020; Kouakou et al., 2020; Ovalle et al., 2020). This is mainly because the parallel scaled down samples are considered to be the most faithful to the field material, due to the similarity between the PSDC of scaled down samples and that of the field material (Lowe, 1964; Charles, 1973; Varadarajan et al., 2003, 2006; Abbas, 2011; Stober, 2012; Ovalle & Dano, 2020; Deiminiat et al., 2020; Dorador & Villalobos, 2020a; Kouakou et al., 2020; MotahariTabari & Shooshpasha, 2021). This is, however, a not valid justification. Recently, a critical review given by Deiminiat et al. (2020) has shown that it is impossible to reproduce a PSDC strictly parallel to that of field material without adding fine particles smaller than the minimum particle size of the field material, as shown by Sukkarak et al. (2018). Adding finer particle material, either by grinding material or from a different source, results in an entirely different material from the field material. Changes in particle size and shape associated with particle breaking during sample preparation are other aspects that do not guarantee a faithful scaled down sample to the field material (Lee & Seed, 1967; Charles & Watts, 1980; Ramamurthy, 2004; Varadarajan et al., 2006; Stober, 2012; Honkanadavar et al., 2016; Wang et al., 2019; Deiminiat et al., 2020; Dorador & Villalobos,

2020a; Ovalle & Dano, 2020). Therefore, none of the four scaling down techniques can be used to produce a scaled down sample faithful to the field material. In addition, the critical analysis of Deiminiat et al. (2000) revealed that the methodology used in previous studies (Donaghe & Torrey, 1985; Hamidi et al., 2012; Kouakou et al., 2020) to validate or invalidate scaling down techniques through direct comparisons between the effective internal friction angles (hereafter named "friction angle" for the sake of simplicity) of field materials and those of scaled down samples is inappropriate. The subsequent conclusion is invalid.

To correctly evaluate the reliability of a scaling down technique, a series of shear tests should be performed on several scaled down specimens having different d_{max} values. A relationship between the shear strength and d_{max} can then be established and used to predict the shear strength of the field material by applying the extrapolation technique (Varadarajan et al., 2006; Gupta, 2009; Hu et al., 2010; Abbas, 2011; Frossard et al., 2012; Vasistha et al., 2013; Pankaj et al., 2013; Honkanadavar et al., 2016; Xu, 2018; Zhang et al., 2019; Yang et al., 2019). This methodology was followed by several researchers (Bagherzadeh & Mirghasemi, 2009; Xu et al., 2018). However, their direct shear tests were performed by using a W/d_{max} ratio equal to or even smaller than the minimum required value of 10 stipulated by the ASTM standard, exactly the procedure carried out by other researchers (Marachi et al., 1972; Varadarajan et al., 2006; Abbas, 2011; Pankaj et al., 2013; Vasistha et al., 2013; Honkanadavar et al., 2016; Xu, 2018; Zhang et al., 2019; Cai et al., 2020; Zahran & Naggar, 2020; Yaghoubi et al., 2020; Nicks et al., 2021; Rasti et al., 2021; Saberian et al., 2021). Recently, Deiminiat et al. (2020) have shown that the minimum required W/d_{max} ratio of 10, stipulated by the ASTM standard, is too small to eliminate SSEs. Deiminiat et al. (2021) further showed that the minimum required W/d_{max} ratio should be around 60 to avoid any SSE. The published experimental results obtained by using the minimum required W/d_{max} ratio of 10 and the subsequent conclusions are not reliable. The validation or invalidation of scaling down techniques shown in previous studies is questionable. Further validation or invalidation of the scaling down techniques is necessary against reliable experimental results. To this end, a series of direct shear tests were performed by using specimens having W/d_{max} ratios equal to or larger than 60, prepared by applying the scalping and parallel scaling down techniques; the replacement scaling down technique could not be applied because the d_{max} value of the "field" material is too close to the critical value of 4.75 mm. It is

important to note that the shear strength of coarse granular materials is not only controlled by d_{max}, but also by particle shapes, content of fine or gravel particles, compact or relative density, water content, normal stress, specimen shape, etc. One methodology is to simultaneously consider all the influencing parameters together. This is good for a specific project of design and construction, but it is not suitable in research because the test results would be a consequence of the combined effects of several influencing factors. The results do not allow a good and accurate understanding of the effect of each individual influencing parameter. The unique scope of this paper is to verify the validity/invalidity of scaling down techniques associated with variation in the d_{max} value; thus, the only allowed changing parameter is the d_{max} value. For one given material, all other influencing parameters must be kept constant.

In this paper, some of the experimental results are presented. The test results are then used to test the validity of the scalping and parallel scaling down techniques through the processes of curve-fitting and prediction by extrapolation.

6.2 Laboratory tests

6.2.1 Testing materials

In this study, two types of waste rocks, called WR 1 and WR 2, were tested. Figure 6.1 shows a photograph of WR 1 (Figure 6.1a) and a photograph of WR 2 (Figure 6.1b). The two waste rocks contained a wide range of sub-angular and sub-rounded particles. Based on the visual observation, different particle size ranges of the waste rocks have almost same particle shape. They were used to prepare three testing materials, called M1, M2 and M3. M1 and M2 were made of WR 1 and WR 2, whereas M3 was made of WR 2 based on the PSDC of WR 1.

(a) (b)

Figure 6.1 Photos of (a) WR 1 and (b) WR 2

The largest shear box had a square section of 300 mm by 300 mm; therefore, the largest admissible d_{max} was 5 mm in order to have W/d_{max} ratios not smaller than 60 (Deiminiat et al., 2021).

To prepare the testing samples with different d_{max} values, a portion of waste rocks was first sorted with sieves of opening sizes of 5, 3.36, 2.36, 1.4, 1.19, 0.85, 0.63, 0.315, 0.16 and 0.08 mm. Thus, all the particles larger than 5 mm were excluded. The obtained samples with d_{max} = 5 mm were considered as "field" materials. To avoid any confusion with the in situ field materials, the laboratory "field" materials are hereafter called field samples. Figure 6.2 shows the PSDCs of field samples of M1, M2 and M3.

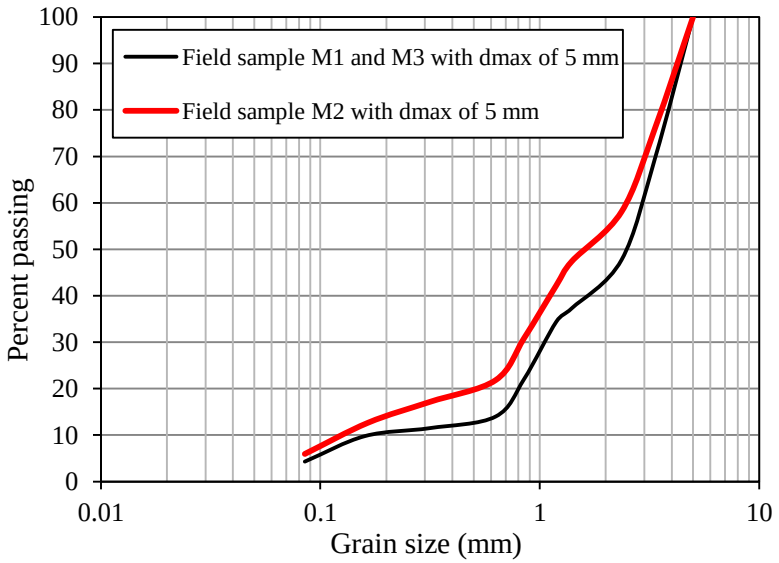

Figure 6.2 PSDCs of field samples M1, M2 and M3

Table 6.1 shows the different portions of field samples M1, M2 and M3. They were used as the base materials for making scaled-down samples with d_{max} values of 1.19, 1.4, 2.36, and 3.36 mm by applying the scalping and parallel scaling down techniques.

Table 6.1 Portion distributions of field samples M1, M2 and M3

Range of particle size	**Portion (%)**		**Sieve opening size (mm)**	**Passing (%)**	
	M1 and M3	**M2**		**M1 and M3**	**M2**
3.36–5 mm	30.3	23.8	5	100.0	100.0
2.36–3.36 mm	22.0	18.1	3.36	69.7	76.2
1.40–2.36 mm	10.4	10.7	2.36	47.7	58.1
1.19–1.40 mm	2.9	5.2	1.4	37.3	47.4
0.85–1.19 mm	12.3	11.3	1.19	34.4	42.2
0.63–0.85 mm	8.0	9.1	0.85	22.1	30.9
0.315–0.63 mm	2.5	4.7	0.63	14.0	21.8
0.16–0.315 mm	1.8	4.5	0.315	11.5	17.1
0.08–0.16 mm	5.4	6.7	0.16	9.8	12.7
<0.08 mm	4.3	5.9	0.08	4.3	5.9

To apply the scalping scaling down technique, one can either calculate the required mass of each range of particle size based on Table 6.1 to obtain a sample by controlled mixture (hereafter called the controlled scalped sample), or directly pour field sample through a sieve with the target d_{max} to obtain a sample without any control (hereafter called the uncontrolled scalped sample). For a given admissible d_{max}, the scalped samples obtained by applying the two methods should be

identical. In reality, difference can appear as the source materials are not entirely homogeneous. In this study, controlled scalped samples were obtained from field sample M1, whereas uncontrolled scalped samples of field sample M2 were obtained directly from WR 2. Controlled scalped samples made of field sample M3 were obtained by again considering the PSDC of field sample M1. Figure 6.3 shows the PSDC of scalped samples of M1 and M3 (Figure 6.3a) and those of M2 (Figure 6.3b); the PSDCs of field samples M1 to M3 are also plotted on the figure.

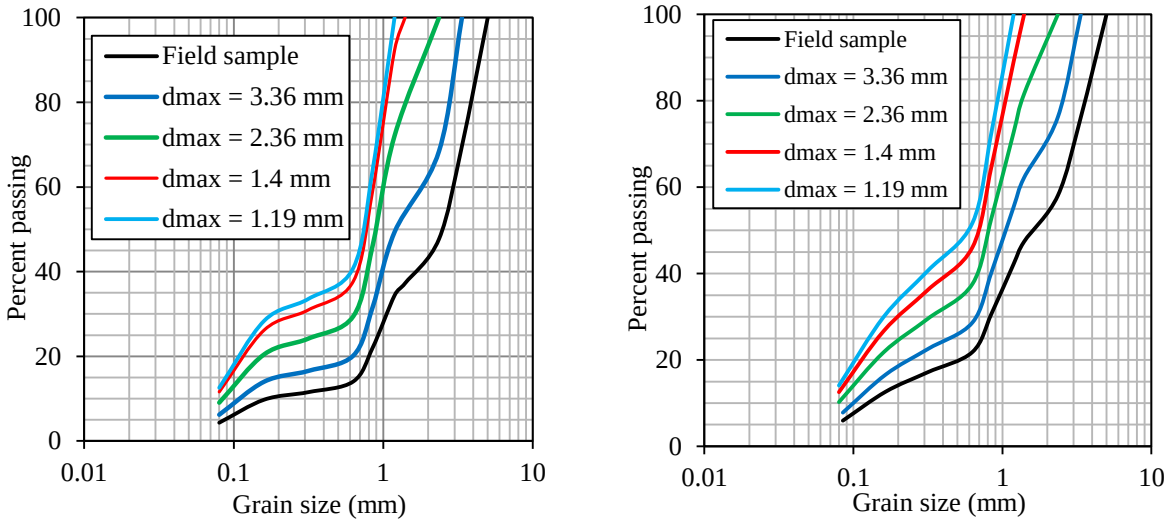

Figure 6.3 PSDCs of scalped samples of field samples (a) M1 and M3 and (b) M2

To apply the parallel scaling down technique, one has to determine the required mass of each portion by considering the PSDC of the field sample and applying the following equation (Lowe 1964):

$$d_{p.s} = d_{p.f}/N \tag{6.1}$$

where $d_{p.s}$ and $d_{p.f}$ are the particle sizes of the scaled down sample and field sample having a percentage passing p, respectively; N is the scaled down ratio between the d_{max} values of field and scaled down samples. The scaled down sample is thus a material obtained from the controlled mixture, not a fully natural material.

As an example, one explains how to prepare the parallel scaled down sample having d_{max} = 3.36 mm from the field sample with d_{max} = 5 mm. One first obtains the scaled down ratio N = 1.488

(=5 mm/3.36 mm). Afterwards, applying this scaled down ratio to all the ranges of particle sizes of the field sample results in new ranges of particle sizes for the scaled down sample, as shown in Table 6.2. For the calculated range of particle sizes, which do not have matched sieves, approximation has to be made, as shown in Table 6.2. In addition, fine particles in the range from 0.053 to 0.1 mm and fine particles smaller than 0.053 mm have to be added. The parallelism between the PSDCs of scaled down samples and field samples is impossible for these fine particle parts. The same method has been followed by several researchers (Lowe 1964; Bagherzadeh & Mirghasemi 2009; Hamidi et al. 2012; Dorador & Villalobos 2020a; Ovalle & Dano 2020; Motahari Tabari & Shooshpasha 2021). An alternative method is addressed in the Discussion section.

Figure 6.4 shows the PSDC of parallel scaled down samples made of field samples M1 and M3 (Figure 6.4a) and M2 (Figure 6.4b); the PSDCs of the field samples are also plotted on the figure.

Table 6.2 Calculation and selection of particle sizes for making parallel scaled samples with d_{max} = 3.36 mm for field samples M1, M2 and M3

Range of particle size of field material	**Range of particle sizes of parallel scaled down samples**		**Portion (%)**	
	Calculated	**Chosen**	**M1 and M3**	**M2**
3.36–5 mm	2.26–3.36 mm	2.36–3.36 mm	30.3	23.8
2.36–3.36 mm	1.60–2.26 mm	1.60–2.36 mm	22.0	18.1
1.40–2.36 mm	0.95–1.60 mm	1.0–1.60 mm	10.4	10.7
1.19–1.40 mm	0.80–0.95 mm	0.80–1.0 mm	2.9	5.2
0.85–1.19 mm	0.56–0.80 mm	0.56–0.80 mm	12.3	11.3
0.63–0.85 mm	0.42–0.56 mm	0.42–0.56 mm	8.0	9.1
0.315–0.63 mm	0.21–0.42 mm	0.21–0.42 mm	2.5	4.7
0.16–0.315 mm	0.10–0.21 mm	0.10–0.21 mm	1.8	4.5
0.08–0.16 mm	0.053–0.10 mm	0.053–0.10 mm	5.4	6.7
<0.08 mm	<0.053 mm	<0.053 mm	4.3	5.9

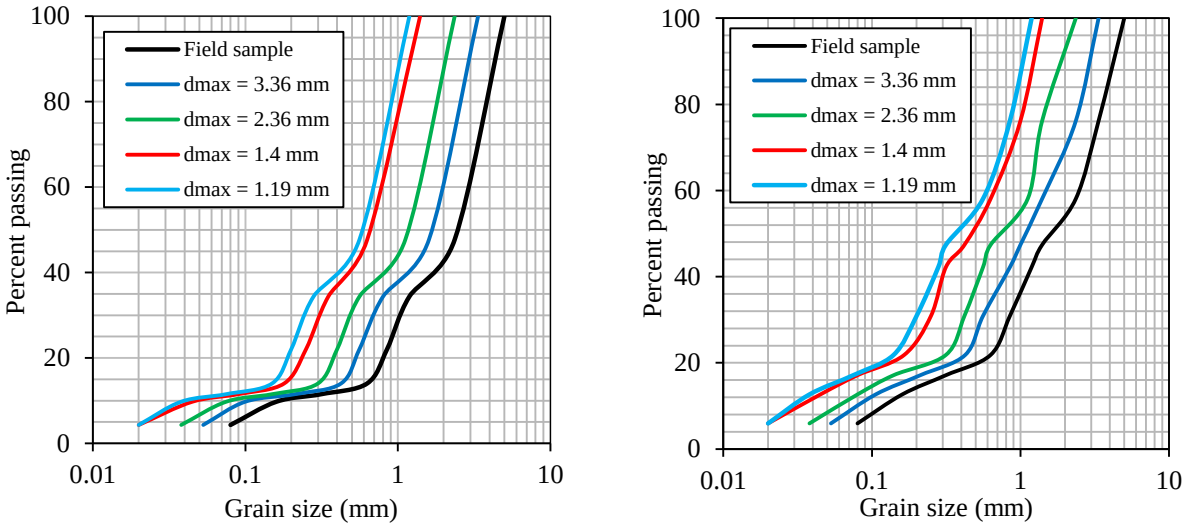

Figure 6.4 PSDCs of the field sample and parallel samples with different d_{max} values for: (a) M1 and M3; (b) M2

6.2.2 Direct shear tests

In the geotechnical laboratory of Polytechnique Montreal, several square shear boxes are available. Only two (the large one, with dimensions of 300 mm × 300 mm × 180 mm, and the small one, 100 mm × 100 mm × 45 mm) have been used to have W/d_{max} ratios not smaller than 60.

As previously outlined, the scope of this study is to analyze the reliability of scaling down techniques. It is thus very important to ensure that variations in the measured friction angle of one given material prepared by following one scaling down technique are only due to the variations in d_{max}, instead of a result due to the combined effects of several influencing factors. The scaled down samples and the field samples should have the same compactness (void ratio) and the same moisture content, under the same normal stresses. All the samples were thus prepared with dry waste rocks. Another advantage associated with dry materials is the removal of any possible influence of loading rate on the shear test results (Lambe & Whitman 1979; Hamidi et al., 2012). The tested specimens were prepared by slowly placing the materials in the shear boxes to determine the loosest state. The density of the loosest field sample was first obtained by

considering the volume of the large shear box of 300 mm × 300 mm × 180 mm and the mass of the filled material at the loosest state. The specific gravity (G_s) of the sample was measured to be equal to 2.65 by following ASTM C128-15. The maximum void ratio (e_{max}) of the loosest field sample can then be obtained. To obtain the same void ratio and density for scaling down specimens, the required masses were calculated by using the volume of the large shear box, the values of G_s and the e_{max} of the field sample. Details on the preparation of field and scaled down specimens are given in Appendix B.

Table 6.3 shows the tested specimens along with their specimen sizes to d_{max} ratios and e_{max}. For each sample, direct shear tests were repeated three times to obtain three values of friction angle; each value was obtained by performing three direct shear tests with normal stresses of 50, 100 and 150 kPa, respectively. These values are relatively small, due to the limited capacity of air compressor on the large size specimens of 300 mm × 300 mm. The void ratios of the tested specimens after the application of the normal stresses before applying shear strains were estimated and are presented in Table 6.4. It can be seen that the void ratios of the tested specimens decrease slightly as the applied normal stress increases from 0 to 50 kPa. The decrease degree becomes smaller when the normal stress is further increased from 50 to 150 kPa. When the system became stable, shear loads were applied by using a strain rate of 0.025 mm/s (1.5 mm/min). A total number of 243 direct shear tests were performed to complete the test program in this study.

Table 6.3 Tested specimens along with sizes to d_{max} ratios and e_{max} for M1, M2 and M3

Samples	d_{max} **(mm)**	e_{max}			**Large shear box**		**Small shear box**	
		M1	**M2**	**M3**	W/d_{max}	T/d_{max}	W/d_{max}	T/d_{max}
Field sample	5.0	0.59	0.70	0.68	60	36	--	--
Scalping down technique samples	3.36	0.58	0.69	0.66	89	54	--	--
	2.36	0.57	0.68	0.68	127	76	--	--
	1.4	0.60	0.67	0.65	214	129	71	32
	1.19	0.60	0.66	0.67	252	151	84	38
Parallel scaling down technique samples	3.36	0.58	0.68	0.66	89	54	--	--
	2.36	0.61	0.67	0.65	127	76	--	--
	1.4	0.60	0.68	0.68	214	129	71	32
	1.19	0.62	0.67	0.66	252	151	84	38

Table 6.4 Void ratio (e) of the tested specimens after the application of normal stresses (σ_n) before applying shear strains

Samples	d_{max} (mm)	*e* of M1 under σ_n of			*e* of M2 under σ_n of			*e* of M3 under σ_n of		
		50 kPa	100 kPa	150 kPa	50 kPa	100 kPa	150 kPa	50 kPa	100 kPa	150 kPa
Field sample	5	0.52	0.51	0.49	0.64	0.63	0.63	0.62	0.62	0.61
Scalping down technique samples	3.36	0.50	0.49	0.48	0.65	0.62	0.62	0.60	0.60	0.60
	2.36	0.49	0.48	0.48	0.64	0.61	0.61	0.63	0.63	0.62
	1.4	0.52	0.51	0.50	0.63	0.60	0.61	0.60	0.60	0.59
	1.19	0.52	0.50	0.50	0.63	0.60	0.60	0.62	0.61	0.61
Parallel down technique samples	3.36	0.51	0.50	0.49	0.62	0.61	0.60	0.60	0.60	0.59
	2.36	0.52	0.51	0.50	0.63	0.61	0.61	0.61	0.60	0.59
	1.4	0.53	0.52	0.50	0.64	0.62	0.61	0.62	0.62	0.61
	1.19	0.53	0.52	0.51	0.63	0.61	0.61	0.60	0.60	0.60

Figure 6.5 shows typical shear stress–shear displacement curves obtained with the large shear box on the field and scaled down samples of M1 (graphs on left column), M2 (graphs in the center column) and M3 (graphs on right column). One sees that the shear stress and displacement curves of different specimens of the same material under a given normal stress (σ_n) have the same variation trend. For example, for M1 under a normal stress of 50 kPa, all the shear stress and displacement curves of field, scalped and parallel scaled down samples exhibit a loose sand-like mechanical behavior. This indicates that the tested samples are all very loose and their compactness states are close to each other.

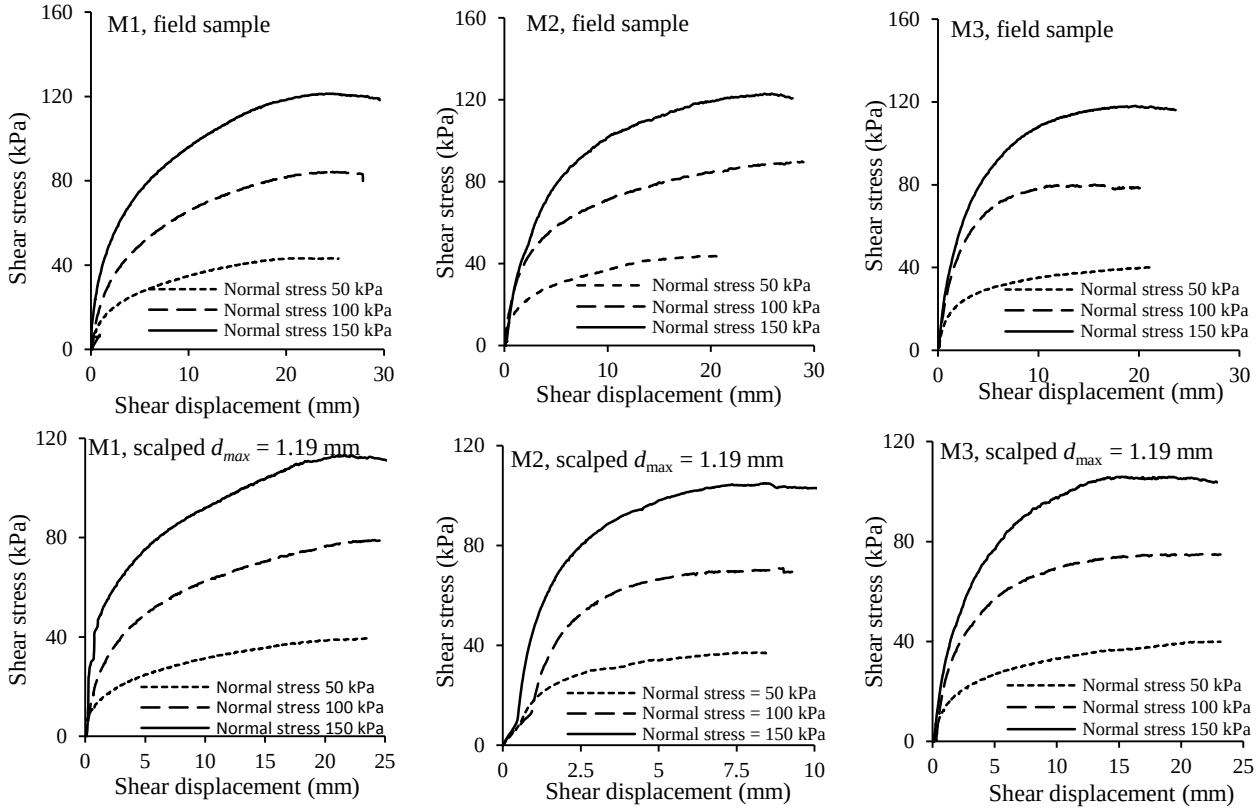

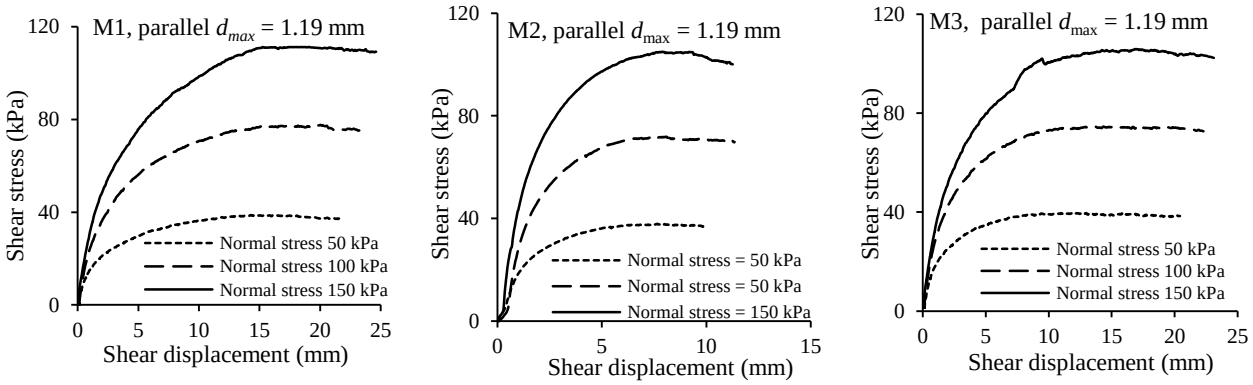

Figure 6.5 Shear stress vs. shear displacement curves obtained with the large shear box on field samples and scaled down samples with d_{max} value of 1.19 mm for M1 (graphs on left column), M2 (graphs in the center column) and M3 (graphs on right column)

6.2.3 Experimental results

For each sample with three shear stress– displacement curves obtained by direct shear tests under three normal stresses, three peak shear stress values (or steady shear stress due to the loose state of the specimens) can be obtained. A friction angle can then be determined by linear fitting on the three points.

Table 6.5 presents the friction angles of the field, scalping and parallel scaled down samples with different d_{max} values for the three materials. The average friction angles were then calculated for each sample. Notably, all the friction angles increased as d_{max} increased, even though the tested waste rocks had sub-angular and sub-rounded shapes (see Figure 6.1). This trend shows a typical behavior of rounded particle materials, not angular or sub-angular materials. This aspect is further addressed in the Discussion section.

Table 6.5 Measured friction angles (ϕ) of the field and scaled down samples made of M1, M2 and M3

Samples	**d_{max} (mm)**	**M1**		**M2**		**M3**	
		ϕ (°)	**Avg. ϕ (°)**	**ϕ (°)**	**Avg. ϕ (°)**	**ϕ (°)**	**Avg. ϕ (°)**
Field sample	5	39.5	39.8	38.7	38.7	38.4	38.5
		40.1		38.6		38.3	
		39.8		38.9		38.7	
Scalping down technique	3.36	38.7	39.0	37.6	37.5	37.4	37.8
		39.1		37.5		38.1	

samples		39.2		37.3		37.8	
		37.9		37.3		37.1	
	2.36	38.4	38.2	37.2	37.0	37.5	37.2
		38.2		36.6		36.9	
		37.6		35.4		36.2	
	1.40	37.2	37.3	35.8	35.6	35.9	35.9
		37.1		35.6		35.6	
		37.2		35.2		35.9	
	1.19	37.0	37.1	35.5	35.5	35.7	35.6
		37.0		35.7		35.3	
Parallel down technique samples		39.0		37.1		37.5	
	3.36	38.7	38.6	37.9	37.8	36.8	37.2
		38.0		38.5		37.2	
		38.7		36.2		37.3	
	2.36	38.1	38.0	36.6	36.6	36.8	36.7
		37.2		37.2		36.1	
		37.4		35.5		36.4	
	1.4	36.9	37.1	35.8	36.0	35.7	36.0
		37.1		36.8		36.0	
		37.0		35.4		35.9	
	1.19	36.1	36.3	35.9	35.9	35.1	35.5
		35.7		36.5		35.6	

6.3 Validation of scaling down techniques

The friction angles obtained by direct shear tests on scaled down samples prepared by applying scalping and parallel scaling down techniques are first used to establish relationships between friction angle ϕ and d_{max} values.

Figure 6.6 shows the variation of the average friction angle as function of d_{max} for samples M1 (Figure 6.6a), M2 (Figure 6.6b) and M3 (Figure 6.6c). The relationships established by applying curve-fitting technique on the test results of scaled down samples are presented in Table 6.6. The measured friction angles of field samples are also plotted on Figure 6.6, whereas the friction angles of the field samples predicted by applying the curve-fitting equations are presented in Table 6.6. From the figure, one sees that the friction angles of the field samples can be correctly predicted by the curve-fitting equations of scalped samples, but fail to be predicted by the curve-fitting equations of parallel scaled down samples. These results thus tend to indicate that the scalping scaling down technique can be used for sample preparation in direct shear tests, whereas the parallel scaling down technique is not appropriate for sample preparation in direct shear tests.

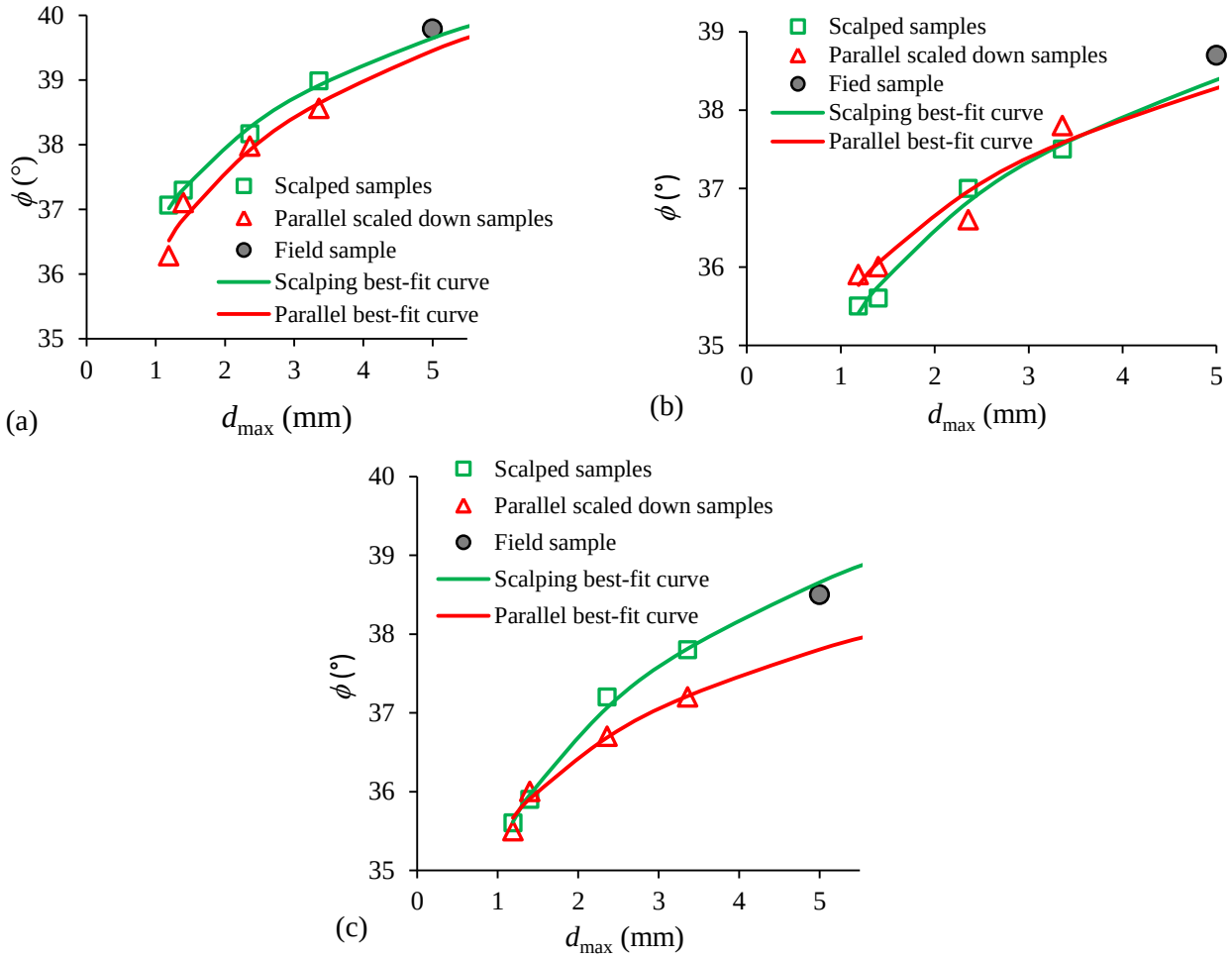

Figure 6.6 Variations of average ϕ values as a function of d_{max}, obtained by direct shear tests on scaled down and field samples (a) M1, (b) M2 and (c) M3.

Table 6.6 The ϕ values of field samples measured and predicted by applying the scalping and parallel prediction equations for field samples of M1, M2 and M3

Material	**Scaling down technique**	**Curve fitting equations based on the test results of scaled down samples**	R^2	**Friction angle ϕ (°) of field samples (d_{max} = 5 mm)**	
				Predicted	**Measured**
M1	Scalping	$\phi = 1.834718\ \mathrm{Ln}(d_{max}) + 36.6953$	0.97	39.6	39.8
	Parallel	$\phi = 2.045707\ \mathrm{Ln}(d_{max}) + 36.16165$	0.86	39.4	
M2	Scalping	$\phi = 2.070025\ \mathrm{Ln}(d_{max}) + 35.05567$	0.96	38.4	38.7
	Parallel	$\phi = 1.749663\ \mathrm{Ln}(d_{max}) + 35.46517$	0.80	38.3	
M3	Scalping	$\phi = 2.118069\ \mathrm{Ln}(d_{max}) + 35.24663$	0.96	38.7	38.5
	Parallel	$\phi = 1.488585\ \mathrm{Ln}(d_{max}) + 35.4078$	0.86	37.8	

6.4 Discussion

In this paper, the reliability of scalping and parallel scaling down techniques used to prepare samples for direct shear tests has been evaluated through experimental studies. All the direct tests have been performed by using W/d_{max} ratios not smaller than 60, a value recently established by Deiminiat et al. (2021) to avoid any SSE. Equations were established by applying a curve-fitting technique on the test results of the scaled down sample. They were then used to predict the friction angles for field samples. The comparisons between the measured and predicted friction angles of field samples tended to show that the scalping technique can be used to predict the friction angle of field samples, whereas the application of a parallel scaling down technique cannot guarantee a reliable prediction of the friction angle of field materials. Despite these interesting results, however, the test program was realized with several limitations. For instance, the three samples (M1, M2 and M3) were made of two types of dry waste rocks. The direct shear tests were realized by delicately placing the materials in shear boxes to reach the loosest state. This was to ensure that the variations in the test results are only due to the variation in d_{max} value for one given material with one chosen scaling down technique. More tests are needed where tested samples are prepared with more materials of different source origins having different particle shapes, initial fine and gravel contents, compactness, and moisture contents under different ranges of normal stresses to determine whether the conclusions are generally valid or only specifically valid for the tested (specific) materials under the tested (specific) conditions. In addition, the differences between the d_{max} values of scaled down and field samples are not very large. More experimental work is thus necessary, using larger shear boxes with field samples having larger d_{max} values. The reliability of the replacement scaling down technique can also be studied. In all cases, it is important to note that any new tests should be performed by following the methodology presented in this paper.

In this study, the parallel scaled down samples were prepared by considering a given percentage and reducing the ranges of particle sizes. Approximations had to be made for the calculated sizes, which did not have any match with available sieves (Lowe, 1964; Bagherzadeh & Mirghasemi, 2009; Hamidi et al., 2012; Dorador & Villalobos, 2020a; Ovalle & Dano, 2020; Motahari Tabari & Shooshpasha, 2021). In future, the following process of preparation can be considered:

- Calculate the scaled down ratio N;
- Draw the PSDC of the scaled down sample, which is parallel to the PSDC of the field sample in the semi-log plane;
- Determine the percentage of each available sieve.

Most previous studies showed a decreasing trend in the friction angle of sub-angular and angular materials as d_{max} increased (Marachi et al., 1972; Varadarajan et al., 2003, 2006; Gupta, 2009; Bagherzadeh & Mirghasemi, 2009; Abbas, 2011; Vasistha et al., 2013; Honkanadavar et al., 2016; Dorador et al., 2017; Deiminiat et al., 2020; MotahariTabari & Shooshpasha, 2021); however, the experimental results obtained with sub-angular and sub-rounded materials presented in Table 6.5 and Figure 6.6 show an increase in the friction angles as d_{max} increases. This difference is probably due to the fact that most previous experimental studies were realized by using large confining pressures. Large shear stresses were thus necessary to shear the tested samples. Particle crushing during the application of confining and/or shear stresses could be an associated and pronounced phenomenon (Matsuoka & Liu, 1998; Boakye, 2008; Ovalle et al., 2014, 2020; Wang et al., 2019). The decrease in friction angle with increasing d_{max} was explained by the breakage of rock particles. The strength of rock decreases with specimen size, known as the size effect of rock strength (Li et al., 1999, 2001, 2007); therefore, the friction angle of coarse particle materials decreases with increasing d_{max} values (Ovalle et al., 2014). In this study, however, the maximum value of the normal stresses was 150 kPa. The PSDCs of tested samples before and after shear tests shown in Figure 6.7 clearly indicate that there was no particle crushing or breakage during and after the application of normal and shear stresses. Size effects of rock strength or the influence of particle shape changes were not involved. The trend in friction angle obtained in this study corresponded to what is usually observed in practice: at the same compact state, sand usually has a smaller friction angle than rockfill because the former usually has smaller d_{max} values than the latter.

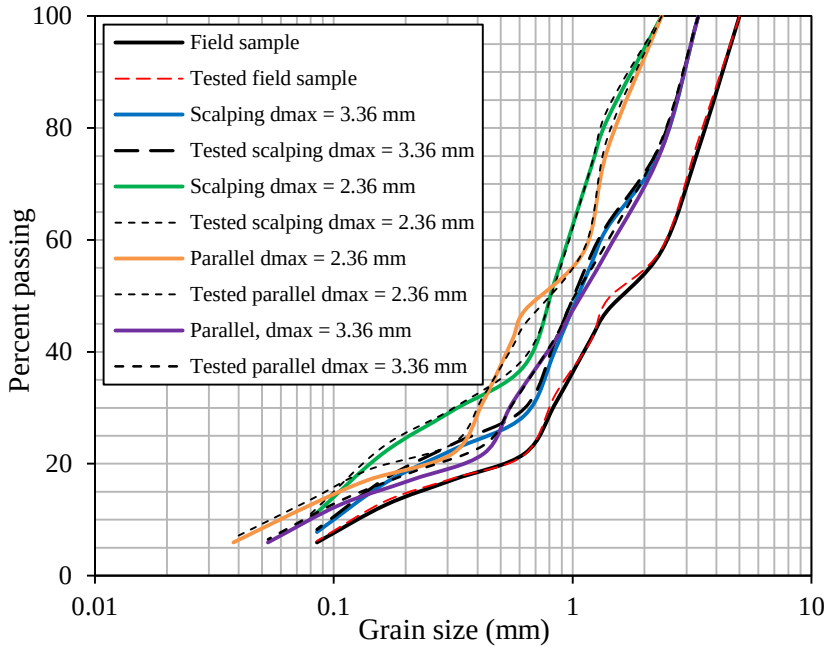

Figure 6.7 PSDCs of scaled down and field samples of M2 before (solid lines) and after (dashed lines) direct shear tests

Finally, because scaling down techniques are not only used in direct shear tests, but also used in triaxial compression tests, more experimental investigation is necessary, performing triaxial compression tests with scaled down samples to test the validity of the scaling down technique. Of course, the tested specimens used in triaxial compression tests must be large enough to avoid any SSE (Deiminiat et al., 2021).

6.5 Conclusions

In this study, the validity of scalping and parallel scaling down techniques used to prepare samples for direct shear tests has been for the first time evaluated through experimental work by using W/d_{max} ratios not smaller than 60. The test results are thus exempt from SSE. The experimental results show that the friction angles with scaled down samples prepared by both scalping and parallel scaling down techniques decrease as the d_{max} values increase even though the particle shapes are not rounded. This variation trend is quite different from that presented in the literature, probably due to the low normal stresses applied in this study. In addition, the comparisons between the friction angles obtained by measurements and those predicted by applying curve-fitting equations established on the friction angles of scaled down samples

indicate that the scalping technique can be used to predict the friction angle of field samples, whereas the application of parallel scaling down technique cannot guarantee a reliable prediction on the friction angle of field materials.

Acknowledgments

The authors acknowledge the financial support from the Natural Sciences and Engineering Research Council of Canada (NSERC RGPIN-2018-06902), Fonds de recherche du Québec—Nature et Technologies (FRQNT 2017-MI-202860), and industrial partners of the Research Institute on Mines and the Environment (RIME UQAT-Polytechnique; http://rime-irme.ca/). Samuel Chenier, Eric Turgeon and Noura El-Harrak are gratefully acknowledged for their assistance in the laboratory work.

6.6 References

Abbas, S. M. (2011). *Behaviour of rockfill materials: based on nature of particles*. Saarbrücken, Germany: LAP Lambert Academic Publishing.

Amirpour Harehdasht, S., Hussien, M. N., Karray, M., Roubtsova, V., & Chekired, M. (2019). Influence of particle size and gradation on shear strength–dilation relation of granular materials. *Canadian Geotechnical Journal*, *56*(2), 208-227.

ASTM C29/C29M-17a. (2007). Standard test method for bulk density (unit weight) and voids in aggregate, *ASTM International*, West Conshohocken, PA, USA.

ASTM D4767. (2011). Standard Test Method for Consolidated Undrained Triaxial Compression Test for Cohesive Soils. *ASTM International*, West Conshohocken, PA, USA.

ASTM D3080/D3080M. (2011). Direct shear test of soils under consolidated drained conditions. *ASTM International*, West Conshohocken, PA, USA.

Aubertin, M., Li, L., & Simon, R. (2000). A multiaxial stress criterion for short-and long-term strength of isotropic rock media. *International Journal of Rock Mechanics and Mining Sciences*, *37*(8), 1169-1193.

Bagherzadeh, A., Mirghasemi, A.A., (2009). Numerical and experimental direct shear tests for coarse grained soils. *Particuology*. 7, 83-91.

Bareither, C. A., Benson, C. H., & Edil, T. B. (2008). Comparison of shear strength of sand backfills measured in small-scale and large-scale direct shear tests. *Canadian Geotechnical Journal*, *45*(9), 1224-1236.

Barton, N., & Kjærnsli, B. (1981). Shear strength of rockfill. *Journal of the geotechnical engineering division*, *107*(7), 873-891.

Blijenberg, H. M. (1995). In-situ strength tests of coarse, cohesionless debris on scree slopes. *Engineering Geology*, *39*(3-4), 137-146.

BS 1377. (1990). Methods of test for soils for civil engineering purposes. Shear strength tests (total stress). Part 7. *British Standard Institution*, London, UK,

Boakye, K. (2008). *Large in situ direct shear tests on rock piles at the Questa Min, Taos county, New Mexico* (Doctoral dissertation, New Mexico Institute of Mining and Technology).

Cai, H., Wei, R., Xiao, J. Z., Wang, Z. W., Yan, J., Wu, S. F., & Sun, L. M. (2020). Direct shear test on coarse gap-graded fill: plate opening size and its effect on measured shear strength. *Advances in Civil Engineering*, *2020*.

Cerato, A. B., & Lutenegger, A. J. (2006). Specimen size and scale effects of direct shear box tests of sands. *Geotechnical Testing Journal*, *29*(6), 507-516.

Chaney, R. C., Demars, K. R., Matsuoka, H., Liu, S., Sun, D., & Nishikata, U. (2001). Development of a New In-Situ Direct Shear Test. *Geotechnical Testing Journal*.

Chang, W. J., & Phantachang, T. (2016). Effects of gravel content on shear resistance of gravelly soils. *Engineering Geology*, *207*, 78-90.

Charles, J. A. (1973). *Correlation between laboratory behaviour of rockfill and field performance, with particular reference to Scammonden Dam* (*Doctoral Dissertation*, University of London, London, UK).

Charles, J. A., & Watts, K. S. (1980). The influence of confining pressure on the shear strength of compacted rockfill. *Geotechnique*, *30*(4), 353-367.

Deiminiat, A., Li, L., Zeng, F., Pabst, T., Chiasson, P., & Chapuis, R. (2020). Determination of the shear strength of rockfill from small-Scale laboratory shear tests: A Critical Review. *Advances in Civil Engineering*, *2020*, 8890237.

Deiminiat, A., & Li, L. (2022). Experimental study on the reliability of scaling down techniques used in direct shear tests to determine the shear strength of rockfill and waste Rocks. *CivilEng*, *3*(1), 35-50.

Donaghe, R. T., & Townsend, F. C. (1973). *Compaction characteristics of earth-rock mixtures*. US Army Corps of Engineers.

Donaghe, R., & Townsend, F. (1976). Scalping and replacement effects on the compaction characteristics of earth-rock mixtures. *Soil Specimen Preparation for Laboratory Testing: ASTM Special Technical Publication, 599, 248-277.*

Donaghe, R. T., & Torrey, V. H. (1985). Strength and deformation properties of earth-rock mixtures. *US Army Corps of Engineers*, AD-A160 701.

Dorador, L., Anstey, D., & Urrutia, J. (2017). Estimation of geotechnical properties on leached coarse material. In *70 th Canadian Geotechnical Conference, GeoOttawa*, Ottawa, Canada.

Dorador, L., & Villalobos, F. A. (2020). Analysis of the geomechanical characterization of coarse granular materials using the parallel gradation method. *Obras y Proyectos*, *27*, 50-63.

Dorador, L., & Villalobos, F. A. (2020). Scalping techniques in geomechanical characterization of coarse granular materials. *Obras y Proyectos*, (28).

Drugan, W. J., & Willis, J. R. (1996). A micromechanics-based nonlocal constitutive equation and estimates of representative volume element size for elastic composites. *Journal of the Mechanics and Physics of Solids*, *44*(4), 497-524.

Fakhimi, A., Boakye, K., Sperling, D. J., & McLemore, V. T. (2007). Development of a modified in situ direct shear test technique to determine shear strength parameters of mine rock piles. *ASTM Geotechnical Testing Journal*, 31(3), 269-273.

Fakhimi, A., Nunoo, S., Van Zyl, D., & McLemore, V. T. (2012). The effect of material scalping and water content on the shear strength of Questa mine materials. *In 46th US Rock*

Mechanics/Geomechanics Symposium. American Rock Mechanics Association, Chicago, Illinois, USA.

Feng, G., & Vitton, S. J. (1999). Laboratory determination of compaction criteria for rockfill material embankments. In *International Conference on Soil Mechanics and Foundation Engineering* (pp. 485-488).

Fragaszy, R. J., Su, J., Siddiqi, F. H., & Ho, C. L. (1992). Modeling strength of sandy gravel. *Journal of Geotechnical Engineering*, *118*(6), 920-935.

Frossard, E., Hu, W., Dano, C., & Hicher, P. Y. (2012). Rockfill shear strength evaluation: a rational method based on size effects. *Geotechnique*, 62(5), 415-427.

Frost, R. J. (1973). Some testing experiences and character. *In Evaluation of Relative Density and Its Role in Geotechnical Projects Involving Cohesionless Soils: A Symposium Presented at the Seventy-Fifth Annual Meeting, American Society for Testing and Materials*, Los Angeles, California (Vol. 523, p. 207).

Gupta, A. K. (2009). Triaxial behaviour of rockfill materials. *Electronic Journal of Geotechnical Engineering*, *14*(Bund. J), 1-18.

Hall, E. B. (1951). A triaxial apparatus for testing large soil specimens. *ASTM*, 106, 152-161.

Hall, E. B., & Smith, T. (1971). Special tests for design of high earth embankments on US-101. *Highway Research Record*, (345).

Hamidi, A., Azini, E., & Masoudi, B. (2012). Impact of gradation on the shear strength-dilation behavior of well graded sand-gravel mixtures. *Scientia Iranica*, *19*(3), 393-402.

Houston, W., Houston, S. L., & Walsh, K. D. (1994). Compacted high gravel content subgrade materials. *Journal of Transportation Engineering*, *120*(2), 193-205.

Hennes, R. G. (1952). The strength of gravel in direct shear. Symposium on Direct Shear Testing of Soils, ASTM STP 131, *American Society for Testing and Materials*, 51-62.

Holtz, W., & Gibbs, H. J. (1956). Triaxial shear tests on pervious gravelly soils. *Journal of the Soil Mechanics and Foundations Division*, *82*(1), 1-22.

Honkanadavar, N. P., Dhanote, S., & Bajaj, S. (2016). 161 Prediction of shear strength parameter for prototype alluvial rockfill material. *Indian Geotechnical Conference* IGC2016, Chennai, India.

Honkanadavar, N. P., Kumar, N., & Ratnam, M. (2014). Modeling the behavior of alluvial and blasted quarried rockfill materials. *Geotechnical and Geological Engineering*, *32*(4), 1001-1015

Kanit, T., Forest, S., Galliet, I., Mounoury, V., & Jeulin, D. (2003). Determination of the size of the representative volume element for random composites: statistical and numerical approach. *International Journal of solids and structures*, *40*(13-14), 3647-3679.

Kouakou, N. M., Cuisinier, O., & Masrouri, F. (2020). Estimation of the shear strength of coarse-grained soils with fine particles. *Transportation Geotechnics*, *25*, 100407.

Lambe, T., & Whitman, R. (1969). *Soil mechanics*. New York, NY, USA: John Wiley & Sons.

Lee, K. L., & Seed, H. B. (1967). Drained strength characteristics of sands. *Journal of Soil Mechanics & Foundations Division*, *93*(6), 117-141.

Leslie, D. (1963). Large scale triaxial tests on gravelly soils. *In Proc. of the 2nd Pan-American Conf. on SMFE, Brazil* (Vol. 1, pp. 181-202).

Li, L., Aubertin, M., & Simon, R. (1999). Multiaxial failure criterion with time and size effects for intact rock. In *Vail Rocks 1999, The 37th US Symposium on Rock Mechanics (USRMS), Colorado* (PP. ARMA-99-0653).

Li, L., Aubertin, M., & Simon, R. (2001). Stability analyses of underground openings using a multiaxial failure criterion with. *Frontiers of Rock Mechanics and Sustainable Development in the 21st Century*, (PP. 251-256).

Li, L., Aubertin, M., Simon, R., Deng, D., & Labrie, D. (2007). Influence of scale on the uniaxial compressive strength of brittle rock. In *1st Canada-US Rock Mechanics Symposium, Vancouver* (pp. ARMA-07-097).

Liu, S. H. (2009). Application of in situ direct shear device to shear strength measurement of rockfill materials. *Water Science and Engineering*, *2*(3), 48-57.

Lowe, J. (1964). Shear strength of coarse embankment dam materials. *In Proc., 8th Int. Congress on Large Dams*, Paris: International Commission on Large Dams, (Vol. 3, pp. 745-761).

Marachi, N., Seed, H., & Chan, C. (1969). Strength characteristics of rockfill materials. *Seventh International Conference on Soil Mechanics and Foundation Engineering.*

Marachi, N. D., Chan, C. K. & Seed, H. B. (1972). Evaluation of properties of rockfill materials. *Journal of Soil Mechanics & Foundations Division*, *98*(1), 95-114.

Marsland, A. (1971). The use of in-situ tests in a study of the effects of fissures on the properties of stiff clays. In *Proc. First Aust.-NZ Conference. on Geomechanics, Melbourne* (Vol. 1, pp. 180-189).

Matsuoka, H., & Liu, S. (1998). Simplified direct box shear test on granular materials and its application to rockfill materials. *Soils and Foundations*, *38*(4), 275-284.

Mirzaeifar, H., Abouzar, A., & Abdi, M. R. (2013). Effects of direct shear box dimensions on shear strength parameters of geogrid-reinforced sand. In *66th Canadian geotechnical conference and the 11th joint CGS/IAH-CNC groundwater conference, Montreal* (pp. 1-6).

Morgan, G. C., & Harris, M. C. (1967). Portage mountain dam: II. Materials. *Canadian Geotechnical Journal*, *4*(2), 142-166.

MotahariTabari, S., & Shooshpasha, I. (2021). Evaluation of coarse-grained mechanical properties using small direct shear test. *International Journal of Geotechnical Engineering*, *15*(6), 667-679.

Nicks, J. E., Gebrenegus, T., & Adams, M. T. (2021). Interlaboratory Large-Scale Direct Shear Testing of Open-Graded Aggregates: Round One. In *IFCEE* (pp. 361-370).

Omar, T., & Sadrekarimi, A. (2015). Effect of triaxial specimen size on engineering design and analysis. *International Journal of Geo-Engineering*, *6*(1), 1-17.

Ovalle, C., Frossard, E., Dano, C., Hu, W., Maiolino, S., & Hicher, P. Y. (2014). The effect of size on the strength of coarse rock aggregates and large rockfill samples through experimental data. *Acta Mechanica*, *225*(8), 2199-2216.

Ovalle, C., & Dano, C. (2020). Effects of particle size–strength and size–shape correlations on parallel grading scaling. *Geotechnique Letters*, *10*(2), 191-197.

Ovalle, C., Linero, S., Dano, C., Bard, E., Hicher, P. Y., & Osses, R. (2020). Data compilation from large drained compression triaxial tests on coarse crushable rockfill materials. *Journal of Geotechnical and Geoenvironmental Engineering*, *146*(9), 06020013.

Palmeira, E. M. & Milligan, G. W. E. (1989). Scale effects in direct shear tests on sand, *Proceedings of the 12th International Conference on Soil Mechanics and Foundation Engineering, Rio de Janeiro* (Vol. 1, pp. 739-742).

Pankaj, S., Mahure, N., Gupta, S., Sandeep, D., & Devender, S. (2013). Estimation of shear strength of prototype rockfill materials. *International Journal of Engineering*, *2*(8), 421-426.

Ramamurthy, T. (2004). A geo-engineering classification for rocks and rock masses. *International Journal of Rock Mechanics and Mining Sciences*, *41*(1), 89-101.

Rao, S. V., Bajaj, S., & Dhanote, S. (2011). Evaluations of strength parameters of rockfill material for Pakaldul hydroelectric project, Jammu and Kashmir—a case study. In *Proceedings of the 2011 Indian Geotechnical Conference, Kochi, India* (pp. 991-994).

Rasti, A., Adarmanabadi, H., Pineda, M., & Reinikainen, J. (2021). Evaluating the Effect of Soil Particle Characterization on Internal Friction Angle. *American Journal of Engineering and Applied Sciences*.

Rathee, R. K. (1981). Shear strength of granular soils and its prediction by modeling techniques. *Journal of Institution of Engineers*, *62*, 64-70.

Saberian, M., Li, J., Perera, S. T. A. M., Zhou, A., Roychand, R., & Ren, G. (2021). Large-scale direct shear testing of waste crushed rock reinforced with waste rubber as pavement base/subbase materials. *Transportation Geotechnics*, *28*, 100546.

Seif El Dine, B., Dupla, J. C., Frank, R., Canou, J., & Kazan, Y. (2010). Mechanical characterization of matrix coarse-grained soils with a large-sized triaxial device. *Canadian Geotechnical Journal*, *47*(4), 425-438.

Stober, J. n. (2012). *Effects of maximum particle size and sample scaling on the mechanical behaviour of mine waste rock; a critical state approach* (Master Thesis, Colorado State University, Colorado, USA).

Sukkarak, R., Pramthawee, P., Jongpradist, P., Kongkitkul, W., & Jamsawang, P. (2018). Deformation analysis of high CFRD considering the scaling effects. *Geomechanics & engineering*, *14*(3), 211-224.

Tombs, S. G. (1969). *Strength and deformation characteristics of rockfill* (Doctoral Thesis, Imperial College London, London, UK).

US Army Corps Engineers, (1965). *Laboratory soil testing*. Technical Report, EM 1110-2-1906.

Varadarajan, A., Sharma, K. G., Abbas, S. M., & Dhawan, A. K. (2006). The role of nature of particles on the behavior of rockfill material. *Soils and Foundations*, *46*(5), 569-584.

Varadarajan, A., Sharma, K. G., Venkatachalam, K., & Gupta, A. K. (2003). Testing and modeling two rockfill materials. *Journal of Geotechnical and Geoenvironmental Engineering*, *129*(3), 206-218.

Vasistha, Y., Gupta, A. K., & Kanwar, V. (2013). Medium triaxial testing of some rockfill materials. *Electronical Journal of Geotechnical Engineering*, *18*(D), 923-964

Wang, J. J., Yang, Y., & Chai, H. J. (2016). Strength of a roller compacted rockfill sandstone from in-situ direct shear test. *Soil Mechanics and Foundation Engineering*, *53*(1), 30-34.

Wang, Y., Shao, S., & Wang, Z. (2019). Effect of particle breakage and shape on the mechanical behaviors of granular materials. *Advances in Civil Engineering*, *2019*.

Hu, W., Frossard, E., Hicher, P. Y., & Dano, C. (2010). Method to evaluate the shear strength of granular material with large particles. In *Soil Behavior and Geo-Micromechanics, GeoShanghai, Shanghai* (pp. 247-254).

Wei, H., Xu, W., Wei, C., & Meng, Q. (2018). Influence of water content and shear rate on the mechanical behavior of soil-rock mixtures. *Science China Technological Sciences*, *61*(8), 1127-1136.

Wen, R., Tan, C., Wu, Y., & Wang, C. (2018). Grain size effect on the mechanical behavior of cohesionless coarse-grained soils with the discrete element method. *Advances in Civil Engineering*, *2018*.

Williams, D. J., & Walker, L. K. (1983). *Laboratory and field strength of mine waste rock*, Research Report No. CE 48, University of Queensland, Australia.

Wu, P. K., Matsushima, K., & Tatsuoka, F. (2008). Effects of specimen size and some other factors on the strength and deformation of granular soil in direct shear tests. *Geotechnical Testing Journal*, *31*(1), 45-64.

Xu, Y. (2018). Shear strength of granular materials based on fractal fragmentation of particles. *Powder Technology*, *333*, 1-8.

Xu, Y., Williams, D. J., Serati, M., & Vangsness, T. (2018). Effects of scalping on direct shear strength of crusher run and crusher run/geogrid interface. *Journal of Materials in Civil Engineering*, *30*(9), 04018206.

Yaghoubi, E., Arulrajah, A., Yaghoubi, M., & Horpibulsuk, S. (2020). Shear strength properties and stress–strain behavior of waste foundry sand. *Construction and Building Materials*, *249*, 118761.

Yang, G., Jiang, Y., Nimbalkar, S., Sun, Y., & Li, N. (2019). Influence of particle size distribution on the critical state of rockfill. *Advances in Civil Engineering*, *2019*.

Zahran, K., & Naggar, H. E. (2020). Effect of sample size on TDA shear strength parameters in direct shear tests. *Transportation Research Record*, *2674*(9), 1110-1119.

Zeller, J., & Wullimann, R. (1957, August). The shear strength of the shell materials for the Go-Schenenalp Dam, Switzerland. In *4th International Conference on Soil Mechanics and Foundation Engineering* (Vol. 2, pp. 399-415).

Zhang, Z. L., Xu, W. J., Xia, W., & Zhang, H. Y. (2016). Large scale in situ test for mechanical characterization of soil rock mixture used in an embankment dam. *International Journal of Rock Mechanics and Mining Sciences*, *86*, 317-322.

Zhang, Z., Sheng, Q., Fu, X., Zhou, Y., Huang, J., & Du, Y. (2020). An approach to predicting the shear strength of soil-rock mixture based on rock block proportion. *Bulletin of Engineering Geology and the Environment*, *79*(5), 2423-2437.

Ziaie Moayed, R., Alibolandi, M., & Alizadeh, A. (2017). Specimen size effects on direct shear test of silty sands. *International Journal of Geotechnical Engineering*, *11*(2), 198-205.

CHAPTER 7 ARTICLE 4: A METHOD TO DETERMINE THE FRICTION ANGLE OF COARSE GRANULAR MATERIALS IN DIRECT SHEAR TESTS: WITH SMALL SPECIMENS WITHOUT SPECIMEN SIZE EFFECTS

Akram Deiminiat, Li Li

Article submitted in International Journal of Geotechnical Engineering with submission ID 225192922 on January 25, 2022

Abstract: Direct shear test is a popular and commonly used method to determine the shear strength of geomaterials. Recently, Deiminiat and coworkers showed that the minimum required specimen width (W) to maximum particle size (d_{max}) ratio of 10, stipulated by ASTM D3080/D3080M-11, is not large enough to eliminate specimen size effect (SSE). Rather, a minimum W/d_{max} ratio of 60 is necessary to eliminate the SSE. For fine materials with d_{max} smaller than 1 mm, this is not a problem with standard direct shear test apparatus having a shear box of 6 cm large. For coarse materials like gravel, rock fill and waste rocks, meeting this criterion is impossible as long as the value of d_{max} exceeds 5 mm even with special large direct shear box of 30 cm large. Clearly, this d_{max} value of 5 mm is too limitedly small compared to typical d_{max} values of rockfill and waste rocks varying from tens centimeters to meters. In this study, a method is proposed to determine the friction angle without SSE for coarse granular materials having d_{max} value larger than 5 mm using shear box up to 30 cm large. An equation was proposed based on available experimental results to describe normalized friction angles of small specimens by that of large enough specimen as a function of W/d_{max} ratio. This equation along with the experimental results of not large enough specimens can then be used to predict the friction angle of large enough specimens. The validity of the proposed method is tested with experimental results obtained by direct shear tests and pile tests for coarse granular materials at the loosest state.

Keywords: direct shear tests; pile tests, specimen size effect; coarse granular materials.

7.1 Introduction

Direct shear tests are commonly used to obtain the shear strength parameters of geomaterials. Despite numerous criticisms and several drawbacks of the method, it still remains one of the most popular and the most used methods due to its simplicity and cost effectiveness. In addition, it is the only way to test the shear strength parameters of rock joint (Saiang et al., 2005; Saw et al. 2016; Bahaaddini, 2017; Zhang et al., 2019; Morad et al., 2020) or interfaces between two different materials (Choudhary & Krishna, 2016; Koupouli et al., 2016; Punetha et al., 2017; Afzali-Nejad et al., 2017, 2018; Xu et al., 2019).

One of the most important limitations of direct shear test method is its imposition of a sliding plane between the upper and lower parts of shear box. For the convenience of laboratory tests, one tends to use specimen size as small as possible. When the specimen is too small, the effect of individual particles on the sliding plane can become significant and the test results can become non representative of the field material. The change of tests results with the change in specimen size is a phenomenon well-known as specimen size effect (SSE; Parsons 1936; Dadkhah et al. 2010; Mirzaeifar et al. 2013; Ziaie Moayed et al. 2017; Deiminiat et al. 2020; Zahran & Naggar 2020; MotahariTabari & Shooshpasha, 2021; Deiminiat et al. 2022). To avoid any SSE and make sure that the test results are representative of field condition, test specimens must be large enough. Several standards were proposed, specifying the minimum required specimen size as long as the maximum particle size (d_{max}) of the tested material is known. For instance, ASTM D3080/D3080M (2011) stipulates that the specimen width (W) must be equal to or larger than 50 mm. In addition, it should not be smaller than 10 times the value of d_{max}. However, it is unknown why and from where comes this minimum required W/d_{max} ratio of 10.

Over the years, many studies have been reported on the influence of specimen size on direct shear test results (i.e., Parsons, 1936; Rathee, 1981; Jewell & Wroth, 1987; DeJong et al. 2003; Hight & Leroueil, 2003; Cerato & Lutenegger, 2006; Wang et al., 2007; Wu et al., 2008; Wang & Gutierrez, 2010; Dadkhah et al. 2010; Mirzaeifar et al., 2013; Ziaie Moayed et al., 2017; Deiminiat et al., 2020; Zahran & Naggar, 2020; Deiminiat et al., 2022). Among them, only a few have adopted a proper methodology by seeing the variation of friction angle with the change of W/d_{max} ratio and in the mean time keeping other influencing factors (e.g., material, water content, compactness, range of normal stresses, etc.) unchanged (Palmeira & Milligan, 1989; Cerato & Lutenegger, 2006). These along with the recent studies of Deminiat and coworkers (Deiminiat et

al. 2020, 2022) clearly showed that the ASTM minimum required W/d_{max} ratio of 10 is not large enough to avoid SSE. Rather, Deiminiat et al. (2022) have shown that the minimum required W/d_{max} ratio should be 60 to avoid SSE on shear test results. For fine particle materials with $d_{max} \leq 1$ mm, this minimum requirement is automatically satisfied by using standard shear box 60 mm large. For coarse grain materials such as gravel, rockfill and waste rocks, it is impossible to respect this minimum requirement even with the largest shear box of 30 cm large commonly available in geotechnical laboratory as long as the d_{max} value exceeds 5 mm. This explains why the validation study on scaling down techniques given by Deiminiat and Li, (2022) was limited to a d_{max} value of 5 mm. The question is if one has to make use of shear boxes larger than 30 cm large to obtain the friction angle of coarse granular materials having d_{max} value larger than 5 mm.

In this paper, a method is proposed to determine the friction angle of coarse granular materials having d_{max} value larger than 5 mm by using shear box up to 30 cm large. An equation is proposed based on available experimental results to describe the normalized friction angles by that of large enough specimen as a function of W/d_{max} ratio. This equation along with the experimental results of not large enough specimens can then be used to predict the friction angle of large enough specimens. The validity of the proposed method is tested with experimental results obtained by direct shear tests and pile tests for coarse granular materials at the loosest state.

7.2 Relationship between normalized friction angle and W/d_{max} ratio

In order to determine the minimum required W/d_{max} ratio to avoid SSE, Deiminiat et al. (2022) have first made an analysis on experimental results available in the literature. Direct shear tests were performed by Deiminiat et al. (2022) using 14 materials made of two types of waste rocks under the loosest state and the same normal stress range with the same water content (0%). The identified experimental results along with new test results were then used to plot the variation of normalized friction angle as a function of W/d_{max} ratio.

Table 7.1 is a reproduction of Table 12 of Deiminiat et al. (2022). One recalls that the table only contains a selected part of the existing data obtained by following a proper methodology with at least one tested specimen having W/d_{max} ratio large enough to eliminate the SSE. In the table, $\phi_{W/d_{max}}$ means the friction angle of sample obtained by direct tests on specimens having a value of

W/d_{max}, while ϕ_{60} means the friction angle of sample obtained by direct shear tests on specimens having at least a W/d_{max} ratio of 60. The normalized friction angles mean $\phi_{W/d_{max}}/\phi_{60}$.

Table 7.1 Normalized friction angles of experimental results available in the literature (a reproduction of Table 12 of Deiminiat et al. 2022)

Material	W/d_{max}	$\phi_{W/d_{max}}$ (°)	$\frac{\phi_{W/d_{max}}}{\phi_{60}}$	**Material**	W/d_{max}	$\phi_{W/d_{max}}$ (°)	$\frac{\phi_{W/d_{max}}}{\phi_{60}}$	**Reference**
Sand	50	50.1	1.014					Palmeira and Milligan (1989)
	833	49.4	1					
Gravel, D_r = 25%	20	36.5	1.074	Gravel, D_r = 55%	20	41.0	1.020	Cerato and Lutenegger (2006)
	61	34.0	1		61	40.2	1	
Gravel, D_r = 85%	20	43.0	1.024					
	61	42.0	1					
WR1, d_{max} = 0.85 mm	45	37.1	1.005	WR2, d_{max} = 0.85 mm	45	35.3	1.009	Deiminiat et al. (2022)
	71	37.0	1.003		71	35.2	1.006	
	353	36.9	1		353	35.0	1	
WR1, d_{max} = 1.19 mm	32	38.0	1.013	WR2, d_{max} = 1.19 mm	32	36.2	1.006	
	50	37.9	1.011		50	36.1	1.002	
	252	37.5	1		252	36.0	1	
WR1, d_{max} = 1.4 mm	27	38.7	1.027	WR2, d_{max} = 1.4 mm	27	37.2	1.028	
	43	38.0	1.008		43	36.4	1.006	
	214	37.7	1		214	36.2	1	
WR1, d_{max} = 2.36 mm	16	40.9	1.082	WR2, d_{max} = 2.36 mm	16	38.2	1.030	
	25	39.1	1.034		25	37.3	1.005	
	127	37.8	1		127	37.1	1	
WR1, d_{max} = 3.36 mm	11	42.1	1.088	WR2, d_{max} = 3.36 mm	11	40.5	1.083	
	18	40.2	1.039		18	39.3	1.051	
	89	38.7	1		89	37.4	1	
WR1, d_{max} = 5 mm	12	41.4	1.048	WR2, d_{max} = 5 mm	12	40.1	1.044	
	60	39.5	1		60	38.4	1	

Figure 7.1 is a plot of Table 7.1, showing the variations of normalized friction angle ($\phi_{W/d_{max}}/\phi_{60}$) as a function of W/d_{max}. The curve is a plot of the best-fit equation that was found to have an

exponential connection between $\phi_{W/d_{max}}/\phi_{60}$ and W/d_{max}, obtained by applying the curve-fitting technique on the experimental results with a W/d_{max} ratio ≤ 60. The equation can be written as follow for two boundaries:

$$\frac{\phi_{W/d_{max}}}{\phi_{60}} = 0.98 \times exp\left(\frac{1}{W/d_{max}}\right)^{0.92}, \qquad \text{for } 60 \geq \frac{W}{d_{max}} \geq 10 \tag{7.1a}$$

Or

$$\phi_{60} = \frac{\phi_{W/d_{max}}}{0.98 \times exp\left(\frac{1}{W/d_{max}}\right)^{0.92}}$$

$$\frac{\phi_{W/d_{max}}}{\phi_{60}} = 1, \qquad \text{for } \frac{W}{d_{max}} \geq 60 \tag{7.1b}$$

where ϕ_{60} is the predicted friction angle excempt of SSE (°), $\phi_{W/d_{max}}$ is the friction angle obtained by direct shear test on the specimens having W/d_{max} ratio (°), W is the specimen width (mm) and d_{max} is the maximum particle size of tested material (mm).

Even though Equation (7.1) was obtained by applying the curve-fitting technique on a limited number of experimental results, it can be considered as a general solution to describe the variation of normalized friction angle as a function of W/d_{max} ratio because the experimental data used in the curve-fitting process are of different sources obtained on different materials. To obtain the friction angle of one specimen having W/d_{max} ratio to be exempt of SSE (ϕ_{60}), one need first to perform direct shear test on the specimen and then use the obtained friction angle ($\phi_{W/d_{max}}$) in Equation (7.1).

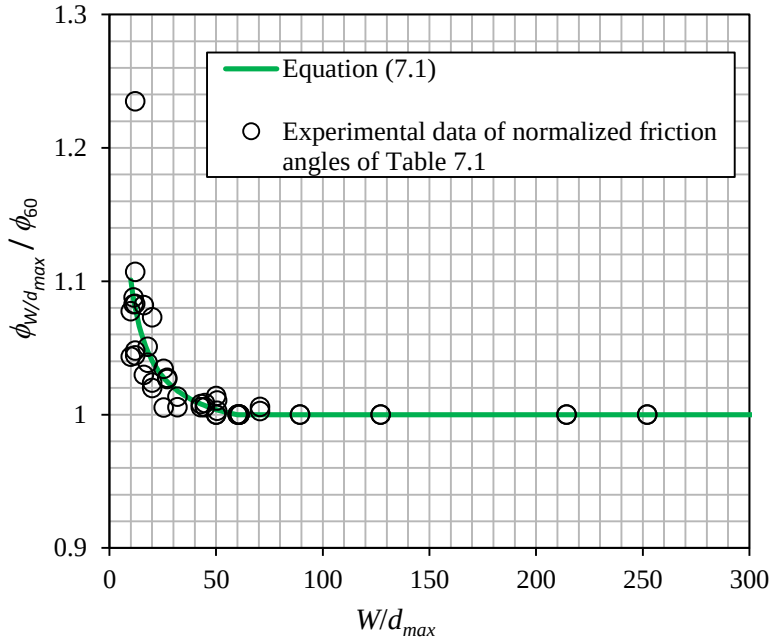

Figure 7.1 The normalized friction angles of all the materials plotted versus $W/d_{\max}$

7.3 Laboratory tests

To investigate the reliability of the proposed method, two series of tests were performed in this study. The first series are direct shear tests with a large shear box of 30 cm × 30 cm × 18 cm on granular materials having $d_{\max}$ value equal to or larger than 5 mm at the loosest state. The $W/d_{\max}$ ratios are thus equal to or smaller than the minimum required value of 60. Normally, the friction angle of large enough specimen can only be measured by doing more direct shear tests with larger shear boxes and specimen size to satisfy the minimum required $W/d_{\max}$ ratio of 60. As this is impossible due to the unavailability of larger shear boxes, the test results obtained on the not large enough specimens and Equation (7.1) are used to obtain a prediction of the friction angles of large enough specimens. To test the validity of these predicted friction angles of large enough specimens, another series of tests performed are pile tests. It is well known that the repose angle of a granular material corresponds to the internal friction angle of the material obtained by direct shear tests at its loosest state (Lambe & Whitman, 1979; Miura et al., 1997; Ghazavi et al., 2008; Fu et al., 2020). This has been illustrated recently by the experiment results of Zheng et al. (2021) through pile tests and direct shear tests on sand having $d_{\max}$ value of 1.2 mm at the loosest state. The repose angles obtained by pile tests on the sample having $d_{\max}$ value equal to or larger than 5

mm will be considered as equivalent to the friction angle of the coarse granular material obtained by direct shear tests on large enough specimens.

7.3.1 Tested materials

A waste rock (WR) taken from a mine site, Quebec, Canada is used in this study to produce eight different materials. Figure 7.2 shows the picture of a portion of WR taken from the mine site. Based on naked-eye observation, one sees that the waste rocks contain particles with sub-angular to sub-rounded shapes. Particle sizes of the waste rocks vary from very fine (~ 0.075 mm) to 40 mm.

Figure 7.2 Picture of a portion of WR before sieving

The portion was sieved in grain sizes ranging from 0.08 to 25 mm. All the particles larger than 25 mm were excluded. Different portions of the grain sizes were mixed to produce four materials, named M1, M3, M5 and M7 with d_{max} values of 5, 9.5, 19 and 25 mm, respectively. Based on this method, controlled particle size distributions are obtained for the materials. Next time, a portion of WR was passed through sieves with openings 5 mm, 9.5, 19 and 25 mm to obtain uncontrolled grain size distributions for another four materials, named M2, M4, M6 and M8 with d_{max} values of 5, 9.5, 19 and 25 mm. These two methods were only used to produce more materials using a type of waste rocks.

Table 7.2 shows the different portions of the grain sizes used to produce the eight materials. Their grain size distribution curves are shown in Figure 7.3. As the case of Deiminiat et al. (2022), the d_{max} value should be considered as one identification of the material because the scope of this paper is on the SSE, not on the effect of d_{max} on the shear strength as the case of Deiminiat and Li (2022). Focus should be given on the variation of friction angle as a function of W/d_{max} ratio, not on the variation of friction angle as a function of d_{max}.

Table 7.2 Different portions of the grain sizes used to produce the eight materials

Range of particle sizes	**Different portions (%)**							
	M1	**M2**	**M3**	**M4**	**M5**	**M6**	**M7**	**M8**
19 – 25 mm							15.9	7.3
14 – 19 mm					5.0	7.2	4.2	14.0
9.5 – 14 mm					12.6	15.5	10.6	5.0
8 – 9.5 mm			13.2	7.0	10.8	1.4	9.1	9.5
5 – 8 mm			15.8	13.3	13.0	16.6	11.0	13.1
3.36 – 5 mm	30.3	14.9	21.5	6.7	17.8	7.9	14.9	5.6
2.36 – 3.36 mm	22.0	10.1	15.6	17.2	12.9	9.9	10.8	14.0
1.40 – 2.36 mm	10.4	10.8	7.4	10.3	6.1	17.5	5.1	12.8
1.19 – 1.40 mm	2.9	9.9	2.1	5.9	1.7	2.5	1.4	0.8
0.85 – 1.19 mm	12.3	5.8	8.7	11.9	7.2	2.8	6.1	2.3
0.63 – 0.85 mm	8.0	7.2	5.7	5.9	4.7	3.1	3.9	5.3
0.315 – 0.63 mm	2.5	20.4	1.8	6.1	1.5	7.6	1.2	4.7
0.16 – 0.315 mm	1.8	6.1	1.3	9.4	1.1	0.8	0.9	0.8
0.08 – 0.16 mm	5.4	9.0	3.8	1.2	3.2	1.5	2.7	2.0
< 0.08 mm	4.3	5.8	3.1	5.2	2.5	4.0	2.1	2.8

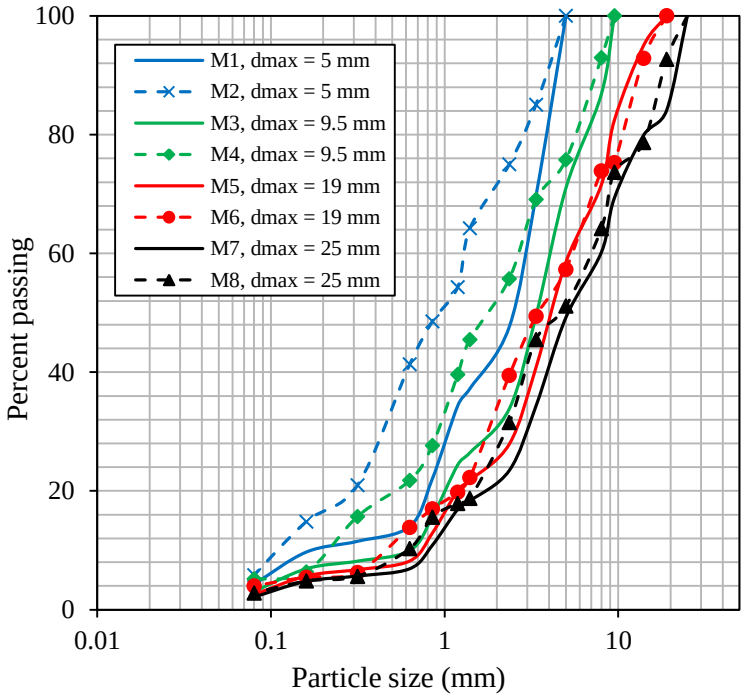

Figure 7.3 Grain size distribution curves of the eight materials

7.3.2 Direct shear tests with not large enough specimens

Direct shear tests on the eight dry materials with d_{max} values of 5, 9.5, 19 and 25 mm were performed using the large shear box (300 mm × 300 mm) available at the Geotechnique laboratory of Polytechnique Montreal. The W/d_{max} ratios of the specimens thus vary from 12 to 60. The specimens were obtained by slowly filling the shear box with a spoon to ensure that the specimens are prepared at the loosest state. The density of the loosest specimen was calculated by taking into account the volume of the shear box and the mass of the filled material in its loosest condition. Following ASTM C127-15, the sample's specific gravity (Gs) was measured. The maximum void ratio (e_{max}) of the specimen was then determined. To ensure all the specimens are obtained in the loose state, the required masses of the specimens were calculated using the volume of the shear box, G_s value and e_{max}. Table 7.3 shows the properties and specimen size ratios obtained for the tested materials.

Table 7.3 The specimen size to d_{max} ratios and some properties of the tested materials

Material	G_s	e_{max}	d_{50} (mm)	**Large shear box**	
				W/d_{max}	T/d_{max}

M1, d_{max} = 5 mm	2.62	0.80	2.5	60	36
M2, d_{max} = 5 mm	2.65	0.82	1.0	60	36
M3, d_{max} = 9.5 mm	2.57	0.77	3.4	32	19
M4, d_{max} = 9.5 mm	2.60	0.79	1.8	32	19
M5, d_{max} = 19 mm	2.55	0.75	4.2	16	9
M6, d_{max} = 19 mm	2.53	0.74	3.5	16	9
M7, d_{max} = 25 mm	2.58	0.71	5.0	12	7
M8, d_{max} = 25 mm	2.56	0.69	4.7	12	7

For each material, the friction angle was obtained by using three normal stresses (50, 100, and 150 kPa) at a loading rate of 0.025 mm/s (1.5 mm/min). The direct shear test for each normal stress was repeated three times. A total of 72 (8 materials × 3 normal stresses/material × 3/normal stress) direct shear tests were conducted to determine the friction angles of the eight materials.

Figure 7.4 shows typical shear stress versus shear displacement curves obtained by direct shear tests for M1, M3, M5, and M7. One sees that the materials do not show any peak values under the normal stresses of 50 and 100 kPa. This is a typical mechanical behavior of loose sand. At a normal stress of 150 kPa however, all the four materials start to show more or less peak values, indicating their gradual change toward the mechanical behaviour of dense sand. The typical shear stress –displacement curves of all materials are presented in Appendix C.

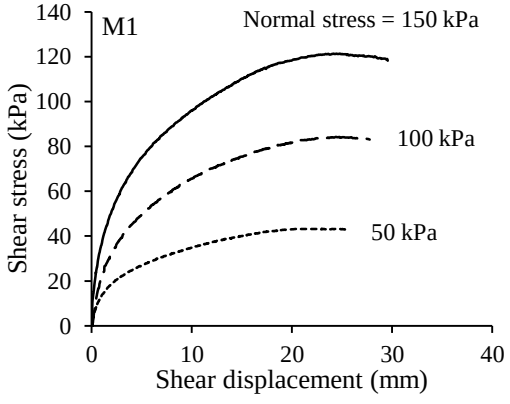

(a)

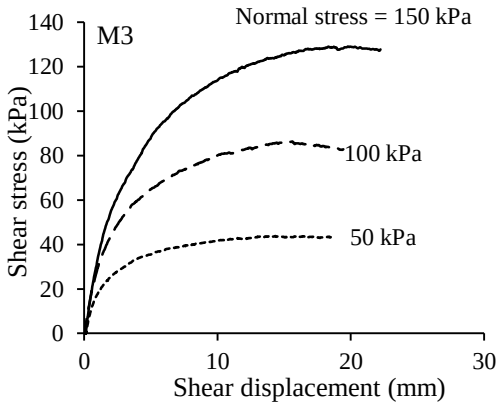

(b)

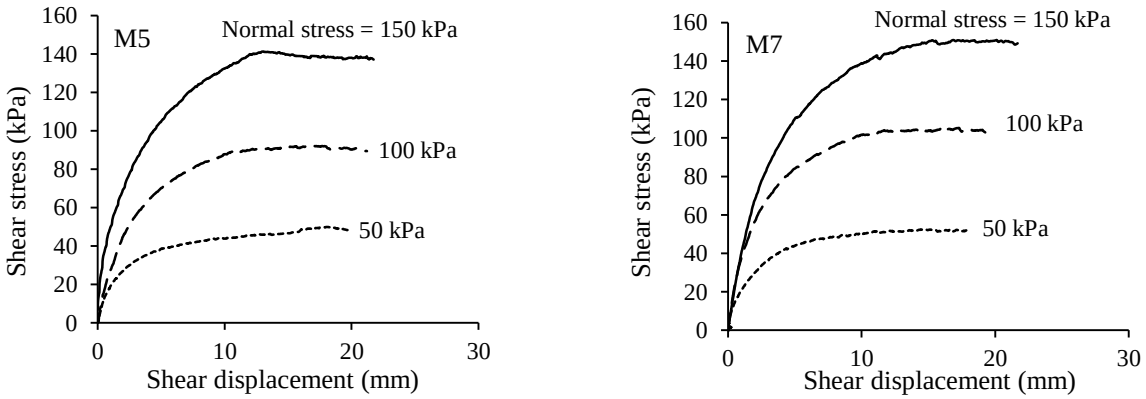

Figure 7.4 Shear stress - displacement curves of (a) M1, (b) M3, (c) M5 and (d) M7 under three normal stresses

Table 7.4 presents the measured $\phi_{W/d_{\max}}$ values and the average value for each sample. One sees a general tendency of increases in the friction angle as $d_{\max}$ increases. This trend is different from that reported in the literature for angular or sub-angular particle materials (Varadarajan et al., 2003, 2006; Abbas, 2011; Vasistha et al., 2013; Honkanadavar et al., 2014; Dorador et al., 2017; Deiminiat et al., 2020). As reported in Deiminiat and Li (2022), the different trends between this study and the published works are probably due to the difference in the normal stresses. In this study, the normal stresses are relatively small with little breakage of particles during the application of normal stress and sample shearing, as what has been shown in Deiminiat and Li (2022), while the normal stresses used in the reported works are much larger than those used in this study and particle breakage is a significant phenomenon. The decrease in friction angle with increased d_{max} was then explained by the size effect of rock strength (Baecher & Einstein, 1981; Li et al., 1999, 2001; Aubertin et al., 2000; Sheng-Qi et al., 2005; Li et al., 2007; Ovalle et al., 2014). After all, one reminds once again that the scope of this study is on the SSE. The value of $d_{\max}$ is only part of the identifying information for a given material. It is irrelevant to further discuss the variation of friction angle with the change of $d_{\max}$ value.

Table 7.4 The $\phi_{W/d_{\max}}$ values measured with large shear box

Material	$W/d_{\max}$	$T/d_{\max}$	$\phi_{W/d_{\max}}$ (°)	Avg. $\phi_{W/d_{\max}}$ (°)
M1, $d_{\max}$ = 5 mm	60	36	39.5	39.8
			40.1	

			39.8	
M2, d_{max} = 5 mm	60	36	39.3 39.6 39.5	39.5
M3, d_{max} = 9.5 mm	32	19	41.3 41.6 41.5	41.5
M4, d_{max} = 9.5 mm	32	19	40.8 41.2 41.5	41.2
M5, d_{max} = 19 mm	16	9	43.9 43.5 44.1	43.8
M6, d_{max} = 19 mm	16	9	43.4 43.7 44.5	43.9
M7, d_{max} = 25 mm	12	7	45.2 45.8 45.5	45.5
M8, d_{max} = 25 mm	12	7	44.9 45.1 45.5	45.2

7.3.3 Pile tests

Pile test is easy to do with few requirements in instrumentation. It can be used to determine the repose angle of a cohesionless material. Different pile test methods have been proposed and used over the years by many researchers (i.e., Rousé, 2014; Montanari et al. 2017; Beakawi & Baghabra, 2018; Santamarina & Cho, 2001). Each method has some advantages and limitations. Figure 7.5a shows a schematic view of pile test setup in the laboratory. On the figure, h_p is the vertical height of the pile (mm) and d_p is the bottom diameter of the pile (mm). Figure 7.5b presents a photo of the test on a portion of material M3. The tests were performed with a funnel having a large enough opening, a spoon used to fill the funnel with the tested materials, a reference ruler to read the vertical height of the pile and a meter to read the bottom diameter of the pile. When the tested dry materials are progressively poured on the table, the conical heap is formed. The angle formed between the pile slope and the horizontal is known as the repose angle, calculated as follows:

$$\phi_p = \text{tang}^{-1}(2h_p / d_p) \quad (7.2)$$

where ϕ_p (°) is the repose angle.

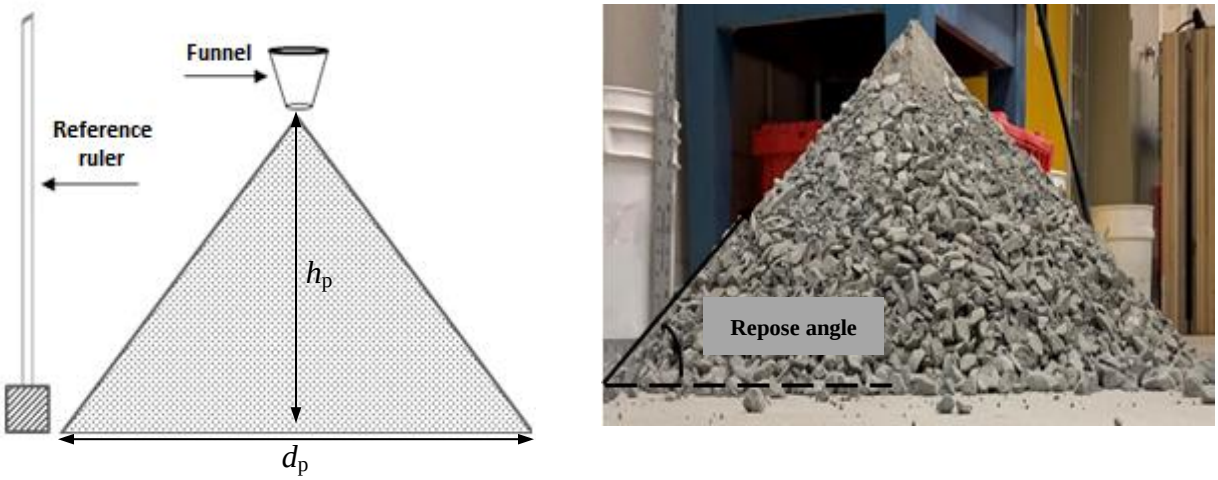

(a) (b)

Figure 7.5 (a) schematic view of pile test setup in the laboratory and (b) photo of the test on a portion of material M3

Before conducting pile tests on the eight materials, it is unclear if size effect is present in pile tests. In other words, it is unknown if the repose angle for a given material changes as the pile size changes. To clarify this question, the repose angles of materials M1, M3, M5 and M7 were measured by making pile tests with different sizes. The falling height, pouring rate and base roughness were kept constant. For each material, pile tests were repeated three times. Table 7.5 shows the average repose angles obtained for each material with different pile sizes. Details of the measurements are given in Appendix C.

The results seem to show that the repose angles do not significantly change with the significant change in pile size. This is further confirmed by the graphical presentation of the results shown in Figure 7.6, indicating that there is no size effect in the measurement of repose angles through pile tests. These results can become particularly interesting for waste rock management engineers because they tend to indicate that the repose angle of large waste rock piles can be obtained by small pile tests.

Table 7.5 The average repose angles obtained by the pile tests for M1, M3, M5 and M7

Material	**d_{max} (mm)**	**h_p (mm)**	**h_p/d_{max}**	**Avg. ϕ_p (°)**	**Material**	**d_{max} (mm)**	**h_p (mm)**	**h_p/d_{max}**	**Avg. ϕ_p (°)**
M1	5	38.1	8	39.4	M3	9.5	47.6	5	40.0
		54.0	11	39.3			69.9	7	40.0
		73.0	15	39.5			82.6	9	40.2
		101.6	20	39.4			98.4	10	40.3
		117.0	23	39.5			114.3	12	40.2
		127.0	25	39.4			130.2	14	39.9
		152.4	30	39.7			142.9	15	39.9
		165.1	33	39.4			158.8	17	40.1
		177.8	36	39.6			184.2	19	39.9
		185.0	37	39.7			209.6	22	40.1
		203.2	41	39.6			235.0	25	40.1
		228.6	46	39.7			260.4	27	39.9
		254.0	51	39.5			285.8	30	40.1
		279.4	56	39.7			311.2	33	40.2
		295.3	59	39.5			336.6	35	40.2
M5	19	41.3	2	41.3	M7	25	38.1	1.5	41.5
		60.3	3	41.2			60.3	2	41.6
		85.7	5	41.3			85.7	3	41.5
		114.3	6	41.3			104.8	4	41.6
		142.9	8	41.4			120.7	5	41.5
		168.3	9	41.3			155.6	6	41.6
		193.7	10	41.3			190.5	8	41.7
		219.1	12	41.3			254.0	10	41.7
		244.5	13	41.3			263.5	11	41.7
		257.2	14	41.4			298.5	12	41.6
		269.9	14	41.3			320.7	13	41.7
		298.5	16	41.2			346.1	14	41.7
		320.7	17	41.2			368.3	15	41.6
		346.1	18	41.2			400.1	16	41.6
		368.3	19	41.3			428.6	17	41.7
		381.0	20	41.3			444.5	18	41.7
		400.1	21	41.4			498.5	20	41.6

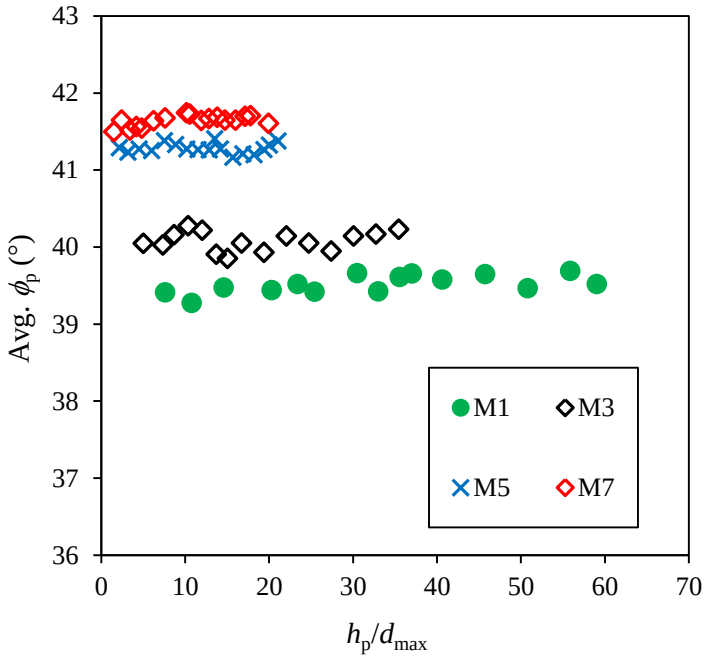

Figure 7.6 Variation of the avg. ϕ_p with h_p/d_{max} for M1, M3, M5 and M7

Table 7.6 shows the repose angles of the eight tested materials obtained by pile tests. Once again, one observes a general tendency of increases in the repose angle as d_{max} increases. This trend corresponds well to what one commonly observed in practice. A structure of rockfill or waste rocks having larger d_{max} values usually exhibits a larger repose angle than a structure of sand having a much smaller d_{max} value. But further discussion on the variation of repose friction angle with d_{max} value is beyond the scope of this paper.

Table 7.6 The ϕ_p and their average values obtained by the pile tests for the eight materials

Material	**h_p (mm)**	**$d_p/2$ (mm)**	**ϕ_p (°)**	**Avg. ϕ_p (°)**
M1, d_{max} = 5 mm	180	220	39.3	39.5
	183	222	39.5	
	184	222	39.7	
M2, d_{max} = 5 mm	170	209	39.1	39.2
	173	208	39.5	
	170	209	39.1	
M3, d_{max} = 9.5 mm	206	246	39.9	40.2
	208	245	40.3	
	209	245	40.5	
M4, d_{max} = 9.5 mm	176	209	40.1	40.0

	175	210	39.8	
	172	205	40.0	
M5, d_{max} = 19 mm	216	247	41.2	41.4
	215	244	41.4	
	220	248	41.6	
M6, d_{max} = 19 mm	172	200	41.0	41.3
	177	201	41.4	
	180	203	41.6	
M7, d_{max} = 25 mm	225	256	41.7	41.9
	232	258	42.0	
	237	262	42.1	
M8, d_{max} = 25 mm	180	201	41.8	41.7
	177	199	41.7	
	176	198	41.6	

7.4 Comparisons between predicted and measured friction angle of large enough specimens

For one given material, the friction angle at its loosest state can either be obtained through the application of Equation (7.1) on direct shear test results or directly measured by pile tests with the repose angle. As an example of calculation for M8 with a d_{max} value of 25 mm, the W/d_{max} ratio is 12 and the measured $\phi_{W/d_{max}}$ is 45.2°. Applying Equation (7.1) leads to the friction angle without SSE as follows:

$$\phi_{60} = \frac{45.2°}{0.98exp\left[\left(\frac{1}{12}\right)^{0.92}\right]} = 41.8°$$

By applying the same procedure, one obtains predicted friction angles without SSE for all the eight tested materials, as shown in Table 7.7 along with the measured repose angle ϕ_p.

Table 7.8 presents the measured $\phi_{W/d_{max}}$ of large enough specimens taken from Deiminiat et al. (2022) and the ϕ_{60} values obtained by applying Equation (7.1) to the $\phi_{W/d_{max}}$ of not large enough specimens taken from Deiminiat et al. (2022).

Figure 7.7 shows comparisons between the measured friction angles of large enough specimens and the friction angles obtained by Equation (7.1) for two series of experimental data. One series, which are given in Table 7.7, are the experimental data obtained in this study, comparing the

measured ϕ_p and the ϕ_{60} values obtained by applying the proposed method to the measured $\phi_{W/d_{max}}$ of the specimens with $\phi_{W/d_{max}} \leq 60$. The second series, which are given in Table 7.8, are the experimental data taken from Deiminiat et al. (2022), comparing the measured $\phi_{W/d_{max}}$ of large enough specimens and the ϕ_{60} values obtained by applying Equation (7.1) to the measured $\phi_{W/d_{max}}$ of the specimens with $\phi_{W/d_{max}} \leq 60$.

The good agreements between the directly or indirectly measured friction angle of large enough specimens and those obtained by applying the proposed method indicate that Equation (7.1) can be used along with direct shear tests on not large enough specimen to obtain the friction angle exempt of SSE. The proposed method can thus be considered as validated by the experimental results.

Table 7.7 The ϕ_{60} values obtained by applying Equation (7.1) to the measured $\phi_{W/d_{max}}$ of not large enough specimens and the measured ϕ_p values

Material	**Measured ϕ_p (°)**	**ϕ_{60} (°)**	**Material**	**Measured ϕ_p (°)**	**ϕ_{60} (°)**
M1, d_{max} = 5 mm	39.5	39.8	M5, d_{max} = 19 mm	41.4	41.5
M2, d_{max} = 5 mm	39.2	39.5	M6, d_{max} = 19 mm	41.3	41.6
M3, d_{max} = 9.5 mm	40.2	40.8	M7, d_{max} = 25 mm	41.9	42.1
M4, d_{max} = 9.5 mm	40.0	40.5	M8, d_{max} = 25 mm	41.7	41.8

Table 7.8 The ϕ_{60} obtained by applying Equation (7.1) to the measured $\phi_{w/d_{max}}$ of not large enough specimens and the measured $\phi_{W/d_{max}}$ of large enough specimens (data taken from Deiminiat et al. 2022)

Material	**Measured $\phi_{W/d_{max}}$ of large enough specimens (°)**	**ϕ_{60} (°)**	**Material**	**Measured $\phi_{W/d_{max}}$ of large enough specimens (°)**	**ϕ_{60} (°)**
WR 1,	37.0	36.9	WR 2,	35.2	35.1
d_{max} = 0.85 mm	36.9	36.9	d_{max} = 0.85 mm	35.0	35.1
WR 1,	37.5	37.3	WR 2,	36.0	35.6
d_{max} = 1.19 mm	37.5	37.8	d_{max} = 1.19 mm	36.0	36.0
WR 1,	37.7	37.8	WR 2,	36.2	36.3
d_{max} = 1.4 mm	37.7	37.7	d_{max} = 1.4 mm	36.2	36.1
WR 1,	37.8	38.7	WR 2,	37.1	36.2
d_{max} = 2.36 mm	37.8	38.0	d_{max} = 2.36 mm	37.1	36.3

WR 1, d_{max} = 3.36 mm	38.7	38.6	WR 2, d_{max} = 3.36 mm	37.4	37.2
	38.7	38.4		37.4	37.5

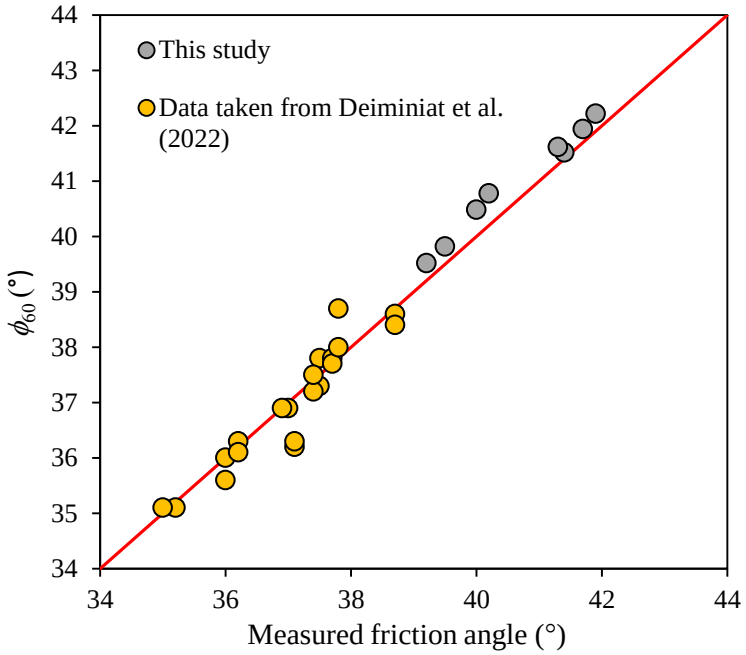

Figure 7.7 Comparisons between the ϕ_{60} values obtained by Equation (7.1) and the measured friction angles exempt of SSE for the experimental data obtained in this study and those obtained in Deiminiat et al. (2022)

7.5 Discussion

In this study, an equation was proposed to describe the friction angle as a function of W/d_{max} ratio. This equation along with measuring friction angle of not large enough specimen can be used to obtain a prediction of the friction angle exempt of SSE. The validity of this proposed method has been tested by direct shear test and pile test results and some taken from Deiminiat et al. (2022). The proposed method can thus be used to determine the friction angle of coarse granular material exempt of SSE. However, it should be noted that the available experimental data used to obtain the predictive equation correspond to the specific tested materials and specific tested conditions. More experimental studies on different materials with different characteristics under different test conditions can be necessary. In addition, the d_{max} was limited to 25 mm due to the available largest shear box of 30 cm large. Performing direct shear tests using larger shear boxes is desirable to further validate or calibrate the proposed solution.

In this study, pile tests were performed in order to test the validity of the predicted friction angles of large enough specimens at the loosest state. It is interesting to note that the repose angle is insensitive to pile size. It thus provides a good alternative for waste rocks managers to obtain an estimate of the possible repose angle of large scale waste rocks pile from small pile tests. However, the pile tests were performed by keeping a constant falling height of zero. More experimental work is necessary by using other pile test methods or pouring the material in a more natural way to see if the repose angle of pile tests is always insensitive of pile size.

Dry waste rocks were used in this study to perform direct shear tests and pile tests. This was to remove any possible influence of loading rate on the shear test results and to ensure both direct shear tests and pile tests are performed in the loosest state without being affected by other influencing factors such as moisture content, density, loading rate (for the case of direct shear test).

Relatively small normal stresses (50, 100 and 150 kPa) were used in this study due to the limited capacity of the air compressor. No particle breakage was observed after performing direct shear tests. More experimental work may be necessary with larger normal stresses to evaluate whether the proposed equation remains valid for the new results.

The measured friction angles of only M1 and M2 with a W/d_{max} ratio of 60 confirm what has been reported by previous studies (i.e., Ghazavi et al., 2008; Fu et al., 2020) and recent study of Zheng et al. (2021). The friction angles obtained by direct shear tests at the loosest state of M1 and M2 are 39.8° and 39.5°, respectively that are almost equal to the obtained repose angles of these materials 39.5° and 39.2°, respectively.

Even though the main scope of this study is on SSE and it is not very relevant to discuss the variation of friction angle with the change in d_{max} value, the results of this study did show a trend different from that reported in the literature for angular or sub-angular particle materials (Marachi et al., 1972; Gupta, 2009; Varadarajan et al., 2003, 2006; Abbas, 2011; Vasistha et al., 2013; Pankaj et al., 2013; Ovalle et al., 2014; Dorador et al., 2017; Deiminiat et al., 2020; Ovalle & Dano, 2020), as shown in Figure 7.8. As reported in Deiminiat and Li (2022), the different trends between this study and the published works are probably due to the difference in the normal stresses. In this study, the normal stresses are relatively small with little breakage of particles

during the application of normal stress and sample shearing, as what has been shown in Deiminiat and Li (2022), while the normal stresses used in the reported works are much larger than those used in this study and particle breakage is a significant phenomenon. The decrease in friction angle with increased specimen size was then explained by the size effect of rock strength (Li et al., 1999, 2001, Sheng-Qi et al., 2005; Li et al., 2007; Ovalle et al., 2014). In addition, it is unclear if the previously reported results are exempt from any SSE. But clearly, the general trend of increases in the repose angle with increased d_{max} trend corresponds well to what one commonly observed in practice because a structure of rockfill or waste rocks having larger d_{max} values usually exhibits a larger repose angle than a structure of sand having a much smaller d_{max} value.

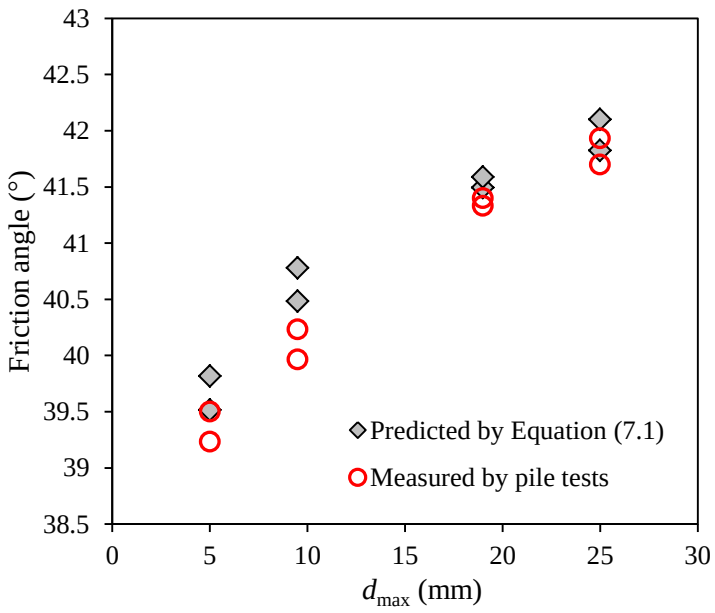

Figure 7.8 Variations of friction angles obtained by Equation (7.1) and measured by pile tests versus d_{max}

7.6 Conclusions

In this paper, an equation was proposed to describe the variation of friction angle of any specimen size as a function of W/d_{max} ratio. The proposed solution has been validated by experimental results. Following conclusions can be drawn:

- The experimental results confirm once again that the repose angle of a granular material corresponds to the internal friction angle of the material obtained by direct shear tests at its loosest state. However, this statement is valid for coarse granular materials when the internal friction angle is exempt of any SSE.
- The proposed solution can be used to obtain friction angle of coarse granular materials exempt of SSE by using the measured friction angle of not large enough specimens.
- The repose angle of pile tests is insensitive of pile size. The repose angle of large waste rocks piles can be estimated by performing small pile tests with the same materials.
- This study shows that the repose angle or the internal friction angle at the loosest state increases with d_{max}. This trend corresponds to what we observe in the practice with commonly observed slopes of dams, waste rock pile, sand dune, etc. But this is different from that shown in previous studies, which showed increasing friction angle for angular or sub-angular particle materials with increased d_{max}.

Acknowledgments

The authors acknowledge the financial support from the Natural Sciences and Engineering Research Council of Canada (NSERC RGPIN-2018-06902), Fonds de recherche du Québec—Nature et Technologies (FRQNT 2017-MI-202860), industrial partners of the Research Institute on Mines and the Environment (RIME UQAT-Polytechnique; http://rime-irme.ca/).

7.7 References

Abbas, S. M. (2011). *Behaviour of rockfill materials: based on nature of particles*. Saarbrücken, Germany: LAP Lambert Academic Publishing.

Afzali-Nejad, A., Lashkari, A., & Shourijeh, P. T. (2017). Influence of particle shape on the shear strength and dilation of sand-woven geotextile interfaces. *Geotextiles and Geomembranes*, *45*(1), 54-66.

Afzali-Nejad, A., Lashkari, A., & Farhadi, B. (2018). Role of soil inherent anisotropy in peak friction and maximum dilation angles of four sand-geosynthetic interfaces. *Geotextiles and Geomembranes*, *46*(6), 869-881.

ASTM C127-15. (2015). Standard test method for relative density (specific gravity) and absorption of coarse aggregate, *ASTM International*, West Conshohocken, PA. US.

ASTM D3080/D3080M, (2011). Direct shear test of soils under consolidated drained conditions, *ASTM International*, West Conshohocken, PA. US.

Aubertin, M., Li, L., & Simon, R. (2000). A multiaxial stress criterion for short-and long-term strength of isotropic rock media. *International Journal of Rock Mechanics and Mining Sciences*, *37*(8), 1169-1193.

Bahaaddini, M. (2017). Effect of boundary condition on the shear behaviour of rock joints in the direct shear test. *Rock Mechanics and Rock Engineering*, *50*(5), 1141-1155.

Baecher, G. B., & Einstein, H. H. (1981). Size effect in rock testing. *Geophysical Research Letters*, 8(7), 671-674.

Beakawi Al-Hashemi, H. M., & Baghabra Al-Amoudi, O. S. (2018). A review on the angle of repose of granular materials, *Powder Technology*, *330*, 397–417.

Cerato, A. B., & Lutenegger, A. J. (2006). Specimen size and scale effects of direct shear box tests of sands. *Geotechnical Testing Journal*, *29*(6), 507-516.

Choudhary, A. K., & Krishna, A. M. (2016). Experimental investigation of interface behaviour of different types of granular soil/geosynthetics. *International Journal of Geosynthetics and Ground Engineering*, *2*(1), 4.

Dadkhah, R., Ghafoori, M., Ajalloeian, R., & Lashkaripour, G. R. (2010). The effect of Scale Direct Shear Tests on The Strength parameters of Clayey Sand in Isfahan city, Iran. *Journal of Applied Sciences*, *10*(18), 2027-2033.

Deiminiat, A., Li, L., Zeng, F., Pabst, T., Chiasson, P., & Chapuis, R. (2020). Determination of the shear strength of rockfill from small-Scale laboratory shear tests: A Critical Review. *Advances in Civil Engineering*, *2020*, 8890237.

Deiminiat, A., & Li, L. (2022). Experimental study on the reliability of scaling down techniques used in direct shear tests to determine the shear strength of rockfill and waste Rocks. *CivilEng*, *3*(1), 35-50.

Deiminiat, A., Li, L. & Zeng, F. (2022). Experimental study on the minimum required specimen width to maximum particle size ratio in direct shear tests. *CivilEng*, 3, 66-84.

DeJong, J. T., Randolph, M. F., & White, D. J. (2003). Interface load transfer degradation during cyclic loading: a microscale investigation. *Soils and Foundations*, *43*(4), 81-93.

Dorador, L., Anstey, D., & Urrutia, J. (2017). Estimation of geotechnical properties on leached coarse material. In *70 th Canadian Geotechnical Conference, GeoOttawa*, Ottawa, Canada.

Dorador, L., & Villalobos, F. A. (2020). Analysis of the geomechanical characterization of coarse granular materials using the parallel gradation method. *Obras y Proyectos*, *27*, 50-63.

Fu, J. J., Chen, C., Ferellec, J. F., & Yang, J. (2020). Effect of particle shape on repose angle based on hopper flow test and discrete element method. *Advances in Civil Engineering*, *2020*.

Ghazavi, M., Hosseini, M., & Mollanouri, M. (2008). A comparison between angle of repose and friction angle of sand. In *The 12th International Conference for International Association for Computer Methods and Advances in Geomechanics (IACMAG)* (pp. 1-6).

Gupta, A. K. (2009). Triaxial behaviour of rockfill materials. *Electronic Journal of Geotechnical Engineering*, *14*(Bund. J), 1-18.

Hight, D. W., & Leroueil, S. (2003). Characterisation of soils for engineering purposes. *Characterisation and engineering properties of natural soils*, *1*, 255-360.

Honkanadavar, N. P., Kumar, N., & Ratnam, M. (2014). Modeling the behavior of alluvial and blasted quarried rockfill materials. *Geotechnical and Geological Engineering*, *32*(4), 1001-1015

Jewell, R.A., & Wroth, C.P. (1987). Direct shear tests on reinforced sand. *Geotechnique*, *37*(1), 53–68.

Koupouli, N. J., Belem, T., Rivard, P., & Effenguet, H. (2016). Direct shear tests on cemented paste backfill–rock wall and cemented paste backfill–backfill interfaces. *Journal of Rock Mechanics and Geotechnical Engineering*, *8*(4), 472-479.

Lambe, T., & Whitman, R. (1969). *Soil mechanics*. New York, NY, USA: John Wiley & Sons.

Li, L., Aubertin, M., & Simon, R. (1999). Multiaxial failure criterion with time and size effects for intact rock. In *Vail Rocks 1999, The 37th US Symposium on Rock Mechanics (USRMS), Colorado* (PP. ARMA-99-0653).

Li, L., Aubertin, M., & Simon, R. (2001). Stability analyses of underground openings using a multiaxial failure criterion with. *Frontiers of Rock Mechanics and Sustainable Development in the 21st Century*, (PP. 251-256).

Li, L., Aubertin, M., Simon, R., Deng, D., & Labrie, D. (2007). Influence of scale on the uniaxial compressive strength of brittle rock. In *1st Canada-US Rock Mechanics Symposium, Vancouver* (pp. ARMA-07-097).

Lings, M. L., & Dietz, M. S. (2004). An improved direct shear apparatus for sand. *Geotechnique*, *54*(4), 245-256.

Marchi, N. D., Chan, C. K., & Seed, H. B. (1972). Evaluation of properties of rockfill materials. *Journal of the Soil Mechanics and Foundations Division*, *98*(1), 95-114.

Mirzaeifar, H., Abouzar, A., & Abdi, M. R. (2013). Effects of direct shear box dimensions on shear strength parameters of geogrid-reinforced sand. In *66th Canadian geotechnical conference and the 11th joint CGS/IAH-CNC groundwater conference, Montreal* (pp. 1-6).

Miura, K., Maeda, K., & Toki, S. (1997). Method of measurement for the angle of repose of sands. *Soils and Foundations*, *37*(2), 89-96.

Montanari, D., Agostini, A., Bonini, M., Corti, G., & Del Ventisette, C. (2017). The use of empirical methods for testing granular materials in analogue modelling. *Materials*, *10*, 635.

Morad, D., Sagy, A., & Hatzor, Y. H. (2020). The significance of displacement control mode in direct shear tests of rock joints. *International Journal of Rock Mechanics and Mining Sciences*, *134*, 104444.

Ovalle, C., Frossard, E., Dano, C., Hu, W., Maiolino, S., & Hicher, P. Y. (2014). The effect of size on the strength of coarse rock aggregates and large rockfill samples through experimental data. *Acta Mechanica*, *225*(8), 2199-2216.

Ovalle, C., & Dano, C. (2020). Effects of particle size–strength and size–shape correlations on parallel grading scaling. *Geotechnique Letters*, *10*(2), 191-197.

Palmeira, E. M. & Milligan, G. W. E. (1989). Scale effects in direct shear tests on sand, *Proceedings of the 12th International Conference on Soil Mechanics and Foundation Engineering, Rio de Janeiro* (Vol. 1, pp. 739-742).

Pankaj, S., Mahure, N., Gupta, S., Sandeep, D., & Devender, S. (2013). Estimation of shear strength of prototype rockfill materials. *International Journal of Engineering*, *2*(8), 421-426.

Parsons, J. D. (1936). Progress report on an investigation of the shearing resistance of cohesionless soils. *Proceedings of the 1st International Conference on Soil Mechanics and Foundation Engineering* (Vol. 2, pp. 133-138).

Punetha, P., Mohanty, P., & Samanta, M. (2017). Microstructural investigation on mechanical behavior of soil-geosynthetic interface in direct shear test. *Geotextiles and Geomembranes*, *45*(3), 197-210.

Rathee, R. K. (1981). Shear strength of granular soils and its prediction by modeling techniques. *Journal of Institution of Engineers*, 62, 64-70.

Rousé, P. (2014). Comparison of methods for the measurement of the angle of repose of granular materials. *Geotechnical Testing Journal*, *37*(1), 164-168.

Saiang, D., Malmgren, L., & Nordlund, E. (2005). Laboratory tests on shotcrete-rock joints in direct shear, tension and compression. *Rock Mechanics and Rock Engineering*, *38*(4), 275-297.

Santamarina, J. C., & Cho, G. C. (2001). Determination of critical state parameters in sandy soils—simple procedure, *Geotechnical Testing Journal*, *24*(2), 185–192.

Scarpelli, G., & Wood, D. M. (1982). Experimental observations of shear patterns in direct shear tests. In *IUTAM Deformation and Failure of Granular Materials Conference* (pp. 473-483).

Sheng-Qi, Y., Cheng-Dong, S., & Wei-Ya, X. (2005). Experimental and theoretical study of size effect of rock material. *工程力学 (Applied Mechanics)*, *22*(4), 112-118.

Sow, D., Rivard, P., Peyras, L., Breul, P., Moradian, Z. A., Bacconnet, C., & Ballivy, G. (2016). Comparison of joint shearing resistance obtained with the Barton and Choubey criterion and with direct shear tests. *Rock Mechanics and Rock Engineering*, *49*(8), 3357-3361.

Varadarajan, A., Sharma, K. G., Venkatachalam, K., & Gupta, A. K. (2003). Testing and modeling two rockfill materials. *Journal of Geotechnical and Geoenvironmental Engineering*, *129*(3), 206-218.

Varadarajan, A., Sharma, K. G., Abbas, S. M., & Dhawan, A. K. (2006). The role of nature of particles on the behaviour of rockfill materials. *Soils and foundations*, *46*(5), 569-584.

Vasistha, Y., Gupta, A. K., & Kanwar, V. (2013). Medium triaxial testing of some rockfill materials. *Electronic Journal of Geotechnical Engineering*, 18, 923–964.

Wang, J., Dove, J. E., & Gutierrez, M. S. (2007). Discrete-continuum analysis of shear banding in the direct shear test. *Géotechnique*, *57*(6), 513-526.

Wang, J., & Gutierrez, M. (2010). Discrete element simulations of direct shear specimen scale effects. *Géotechnique*, *60*(5), 395-409.

Wu, P. K., Matsushima, K., & Tatsuoka, F. (2008). Effects of specimen size and some other factors on the strength and deformation of granular soil in direct shear tests. *Geotechnical Testing Journal*, *31*(1), 45-64.

Xu, X., Fall, M., Alainachi, I., & Fang, K. (2019). Characterisation of fibre-reinforced backfill/rock interface through direct shear tests. *Geotechnical Research*, *7*(1), 11-25.

Zahran, K., & Naggar, H. E. (2020). Effect of sample size on TDA shear strength parameters in direct shear tests. *Transportation Research Record*, *2674*(9), 1110-1119.

Ziaie Moayed, R., Alibolandi, M., & Alizadeh, A. (2017). Specimen size effects on direct shear test of silty sands. *International Journal of Geotechnical Engineering*, *11*(2), 198-205.

Zhang, X., Jiang, Q., Kulatilake, P. H. S. W., Xiong, F., Yao, C., & Tang, Z. (2019). Influence of asperity morphology on failure characteristics and shear strength properties of rock joints under direct shear tests. *International Journal of Geomechanics*, *19*(2), 04018196.

Zheng, J., Li, L., & Daviault, M. (2021). Experimental Study on the Effectiveness of Lubricants in Reducing Sidewall Friction. *International Journal of Geomechanics*, *21*(5), 06021010.

CHAPTER 8 ARTICLE 5: EXPERIMENTAL STUDY ON SPECIMEN SIZE EFFECT AND THE MINIMUM REQUIRED SPECIMEN DIAMETER TO MAXIMUM PARTICLE SIZE RATIO FOR CONSTANT HEAD PERMEABILITY TESTS

Akram Deiminiat, Li Li, Thomas Pabst

Article submitted in Environmental Earth Sciences with submission ID ENGE-D-22-00329 on February 9, 2022

Abstract: Saturated hydraulic conductivity (K_{sat}) is an important property of geomaterials. Its measurement requires tested specimens be large enough to avoid any specimen size effect (SSE). This is challenging for coarse granular materials. Accordingly, the minimum required specimen diameter (D) over maximum particle size (d_{max}) ratio of 8 or 12 specified by ASTM D2434-19 (hereafter named ASTM) is commonly adopted for constant head permeability tests even though its validity has never been illustrated. In order to test the validity of this minimum required D/d_{max} ratio, a series of constant head permeability were performed on four materials using four columns of different sizes. The results show that the minimum D/d_{max} ratio of 8 or 12 specified by ASTM is too small to eliminate SSE. The experimental results further show that a value of D/d_{max} between 170 and 252 seems to be large enough to avoid SSE. As a compromise and by considering the accuracy and the convenience of laboratory tests, a value of 200 is recommended as the minimum required D/d_{max} ratio to eliminate SSE in constant head permeability tests.

Keywords: saturated hydraulic conductivity, constant head permeability tests, specimen size effect, ASTM D2434-19

8.1 Introduction

Knowledge of saturated hydraulic conductivity (K_{sat}) is important to evaluate water flow or migration through geo-materials. It is also an important hydraulic property to consider in regard to the management of infrastructures made from coarse granular materials like rockfill and waste rocks (Aubertin et al., 2002; Fala et al., 2005, 2006; Dawood et al., 2011; Peregoedova, 2012; Chapuis et al., 1989a; Chapuis, 2004; Hernandez, 2007; Gaillot, 2007; Bourrel, 2008; Peregoedova,, 2012; Cabalar & Akbulut, 2016; Essayad et al., 2018). It can either be measured

through permeability tests with constant head by following the standard of ASTM D2434-19 or permeability tests with falling head by following ASTM D5084-16a. Depending on the percentage of coarse particles, the former requires the specimen diameter (D) to be at least 8 or 12 times the maximum particle size (d_{max}) of the tested material, while the latter stipulates that the value of D/d_{max} ratio should not be smaller than 6. For fine particle materials such as silt, clay and fine sands, this is not a problem for specimen preparation. For coarse granular materials like rockfill or waste rocks with particles as large as boulders, meeting the minimum required D/d_{max} ratios is difficult, if not impossible, given the field materials.

A common method to prepare the specimen of granular materials for laboratory permeability tests is to exclude the oversized particles by following one of the four scaling down techniques: scalping, parallel, replacement and quadratic (Zeller & Wullimann, 1957; Lowe, 1964; Hamidi et al., 2012; Sukkarak et al., 2018; Deiminiat et al., 2020; Ovalle & Dano, 2020; Dorador and Villalobos, 2020; MotahariTabari & Shooshpasha, 2021; Deimimiat & Li, 2022a). If the hydraulic conductivity changes with the value of d_{max}, it is necessary to do a series of permeability tests to establish a relationship between the hydraulic conductivity and d_{max}, by which the hydraulic conductivity of field material can be obtained via extrapolation. This problem is known as a scale effect (Deiminiat et al., 2020, 2022). Until now, the most used scaling down technique to prepare the specimens of permeability tests is the scalping down technique (e.g., Hernandez, 2007; Gaillot, 2007; Peregoedova, 2012). However, no studies exist to study the reliability of scalping or the other three scaling down techniques. Further studies on this issue are necessary, but beyond the scope of this paper.

Apart from the scale effect, another problem related to the reliability of experimental results is specimen size effect (SSE). Once a material with a given d_{max} value is identified, one needs to prepare specimens for permeability tests. For fine particle materials having d_{max} smaller than 5 mm, the minimum requirements of the two ASTM standards can be readily satisfied with a standard laboratory test apparatus. For coarse granular materials like rockfill and waste rockfill, it is challenging to meet the minimum required D/d_{max} ratios even with scalped samples (i.e. sample obtained by applying scalping down technique). Subsequently, the minimum required D/d_{max} ratios are commonly used to prepare testing specimens (Mavis & Wilsey, 1937; Krumbein & Monk, 1942; Loudon, 1952; Chapuis et al., 1989a, Hatanaka et al., 1997; Rowe et al., 2000;

Mbonimpa et al., 2002; Duhaime et al., 2012; Peregoedova, 2012; Cabalar & Akbulut, 2016; Gan et al., 2019), even though the validity of the minimum required D/d_{max} ratio specified by the ASTM standards has never been demonstrated in the past.

Table 8.1 shows a summary of existing studies on the measurement of K_{sat} obtained by constant head permeability tests. The minimum D/d_{max} ratio of 8 or 12 stipulated by ASTM D2434-19 (hereafter named ASTM for simplifying) was respected for most cases in their permeability tests, with a few exceptions in Gaillot (2007), Hernandez (2007) and Peregoedova (2012). These results clearly showed that K_{sat} changes as d_{max} changes. However, none of the scaling down techniques and SSE were questioned or evaluated. The validity of the minimum required D/d_{max} ratios of ASTM remains unknown. This requires experimental result obtained by permeability tests on one given material with a d_{max} value prepared with the same density and different diameters. All the specimens must be tested under the same temperature and hydraulic gradient conditions to ensure the variation of measured K_{sat} is only due to the variation of specimen diameter D or the D/d_{max} ratio. The results shown in Table 8.1 cannot be used in this study because the variations of K_{sat} were the results of combined effects associated with the variation of d_{max}, gradation (or scaling down technique) and compact state (density or void ratio). To fill this gap, a series of constant head permeability tests have been performed on several materials by using the smallest, small, medium and large columns. The different test materials were made of the same source materials but with different d_{max} values. As in the case of Deiminiat et al. (2022), the d_{max} values in this study should only be considered as one identificater of the material because the purpose of SSE study is to evaluate the variation of K_{sat} uniquely affected by the variation of D or D/d_{max} ratio, not by the variation of d_{max} value.

Table 8.1 Variation of K_{sat} values as function of d_{max} prepared by following the scalping down technique

Material	d_{max} **(mm)**	D/d_{max}	K_{sat} **(cm/s)**	**Reference**
Sand	1.25	80	0.0155	Hernandez (2007)
	5	30	0.0539	

	10[¶]	15	0.0716	
80% Sand -20% Gravel	5	30	0.0036	
20% Sand -80% Gravel	5	30	0.0725	
50% Sand - 50% Gravel	10	15	0.0016	
Gravel	10	15	0.0313	
	50	6	0.1140	
Waste rock	10	30	0.055	Gaillot (2007)
	28	11	0.250	
	37.5	8	0.310	
	50	6	0.270	
Waste rock	2	145	0.004	Peregoedova (2012)
	5	20	0.035	
	10	29	0.110	
	19	15	0.120	
	28	10	0.140	
	50	6	0.100	
Sand 1	0.3	267	0.01	Cabalar and Akbulut (2016)
	0.425	188	0.01	
	0.6	133	0.02	
	1.8	68	0.02	
	2	40	0.02	
	4.75	17	0.03	
Sand 2	0.3	267	0.01	
	0.425	188	0.015	
	0.6	133	0.02	
	1.8	68	0.03	
	2	40	0.03	
	4.75	17	0.05	

In this paper, the experimental results are presented. It will be seen that the minimum D/d_{max} ratio of 12 required by ASTM for constant head permeability tests is not large enough to eliminate SSE.

[¶] Reported in Hernandez (2007) even though the maximum size of sand particles should not exceed 4.75 mm based on the USCS or AASHTO classification system.

8.2 Laboratory tests

8.2.1 Test apparatus

Figure 8.1 shows the instruments used in this study to measure the hydraulic conductivity of a waste rocks through constant head permeability tests with the smallest, small and medium size columns (Figure 8.1a) and large column (Figure 8.1b). All columns used were transparent to facilitate a naked-eye observation of the sample state and water flow condition during the permeability tests. The dimensions of the columns are shown in Table 8.2. The waterproofing of the permeameters was tested with gas or water to ensure zero leakage.

Table 8.2 Dimensions of columns used in the permeability tests; *D*: diameter and *H*: height

Column	***D* (mm)**	***H* (mm)**
Smallest	102	157
Small	151	250
Medium	202	350
Large	300	1000

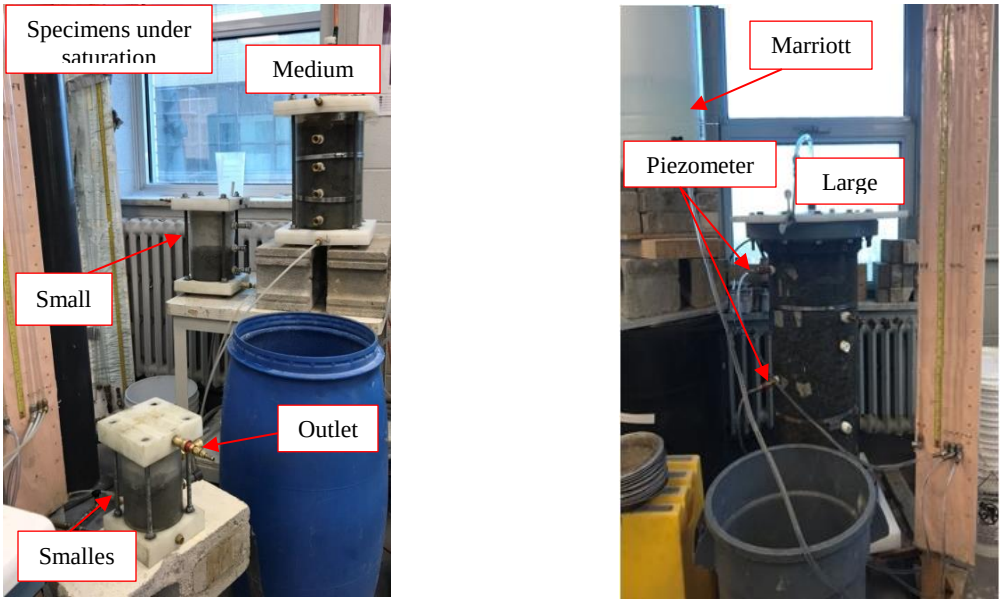

(a) (b)

Figure 8.1 Permeability test instrumentation with: (a) the smallest, small and medium columns; (b) the large column

8.2.2 Materials and testing procedure

The different test materials used consist of waste rocks with sub-angular and sub-rounded particles. The waste rocks were sieved and separated into fractions ranging from 0.08 – 0.16 mm, 0.16 – 0.315 mm, 0.315 – 0.63 mm, 0.63 – 1.19 mm, 1.19 – 2.36 mm, 2.36 – 3.36 mm, 3.36 – 5 mm, and 5 – 8 mm. Four materials, named M1, M2, M3, and M4, having different d_{max} values, were obtained by mixing different portions of different ranges, as shown in Table 8.3. Figure 8.2 shows pictures of the four materials. Obviously, the first difference between them is their difference in their d_{max} values. Figure 8.3 shows their particle size distribution curves (PSDC). The character particle sizes along with the specific gravity G_s of the four materials are presented in Table 8.4 (G_s is obtained by ASTM C128 – 15 for fine particle materials with $d_{max} \leq 4.75$ mm and ASTM C127 − 15 for coarse granular materials with $d_{max} > 4.75$ mm). Once again, it should be noted that d_{max} values are used here as an identification of one material because the focus of this study is to see the variation of hydraulic conductivity as a function of D/d_{max} ratio for a given material (with a given d_{max} value), not on its variation as a function of d_{max} value.

Table 8.3 Four different materials prepared from the same source material by using different particle size ranges

Particle size ranges (mm to mm)	**Portions by mass (%) of the particle size ranges**			
	M1	**M2**	**M3**	**M4**
5 - 8				37.9
3.36 - 5			29.2	24.7
2.36 - 3.36			25.6	13.7
1.19 - 2.36		38.8	17.1	8.2
0.63 - 1.19	41.7	22.3	9.1	3.7
0.315 - 0.63	22.2	16.0	7.9	4.1
0.16 - 0.315	16.7	10.4	2.5	2.6
0.08 - 0.16	11.1	7.0	3.7	2.0
≤ 0.08	8.3	5.5	4.9	3.0

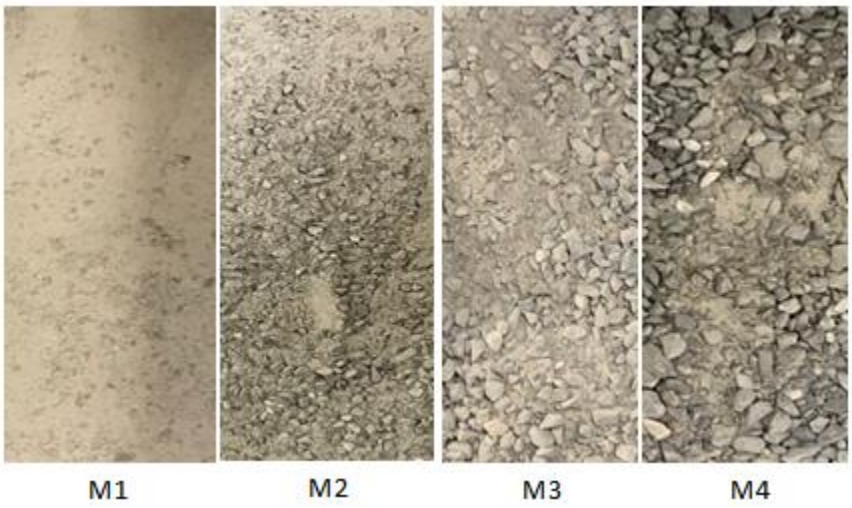

Figure 8.2 Picture of materials M1 to M4 with clear view of difference in their d_{max} values

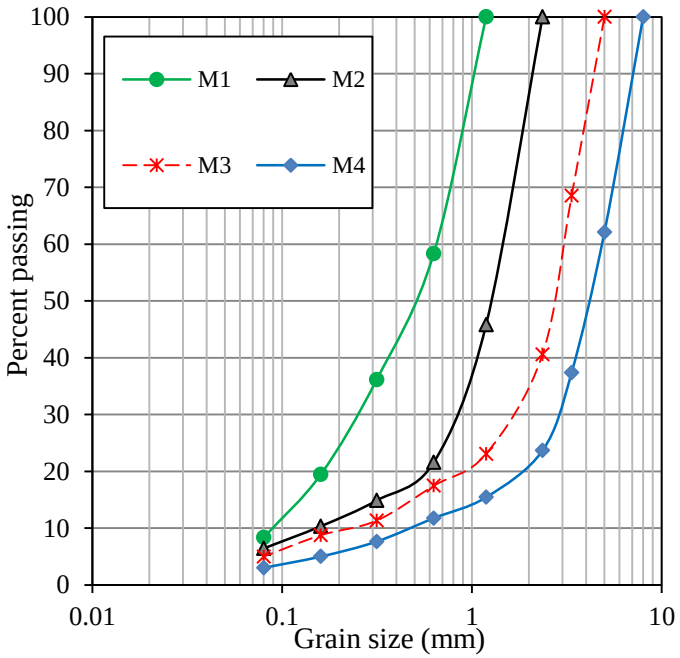

Figure 8.3 PSDC of the materials M1, M2, M3, and M4

Table 8.4 Character particle sizes of the four materials (M1 to M4) used in the permeability tests

Material	**d_{max} (mm)**	**G_s**	**Density (kg/m^3)**
M1	1.19	2.81	1931.6
M2	2.36	2.61	1815.0
M3	5	2.76	1899.2
M4	8	2.78	1800.2

To ensure the same density (or void ratio) across the four different columns, all the specimens were prepared using dry materials of a known mass of to fill the smallest permeameter having known weight. The material was placed into the column in 3 layers using a funnel. Each layer was compacted uniformly by using a sliding tamper with a tamping foot of 51 mm in diameter and a rod for sliding weights of 100 grams with a falling height of 10 cm (ASTM D2434-19). Each layer was compacted by 10 blows. After filling the column to a height of about 2 cm above the upper piezometer outlet, the specimen's surface was leveled with the upper porous plate. The mass of the filled column was then measured. The density and void ratio (e) of the specimen were thus calculated with the measured mass, volume and specific gravity (G_s) of the material.

By using the value of e (or density), G_s as well as the target volumes for the small, medium and large columns, the required masses of materials were calculated. The number of layers and number of blows for each layer required to reach the target void ratio were obtained through trial and error. This resulted in 5, 8 and 15 layers with blows numbers of 10, 12 and 25 on each layer for the small, medium and large columns, respectively.

Table 8.5 shows the specimen size ratios and void ratios. All the D/d_{max} ratios are larger than the minimum required D/d_{max} ratio of 12 stipulated by the ASTM standard.

Table 8.5 Void ratios and D/d_{max} ratios used for the four samples

Material	d_{max} **(mm)**	D/d_{max}				e
		Smallest	**Small**	**Medium**	**Large**	
M1	1.19	86	127	170	252	0.45
M2	2.36	43	64	86	127	0.43
M3	5	20	30	40	60	0.45
M4	8	13	19	25	38	0.50

All the specimens were vacuumed for 15 minutes (ASTM D2434-19) to avoid any air trapped in the pores and bubble production in the void space between the upper porous plate and the top wall of the column. The evacuation was followed by a very slow saturation of the specimens with de-aired water from the bottom upward in order to remove any air remaining in the pore of material or void space between the upper porous plate and upper cover.

Figure 8.4 shows the saturation of the specimens in the smallest, small and medium columns. The saturation levels are horizontal in the three columns, indicating uniform compaction (or uniform distribution of voids) in the cross-section of the columns (Chapuis et al., 1989b; Chapuis, 2012).

(a) (b) (c)

Figure 8.4 Saturation levels of the (a) smallest, (b) small and (c) medium columns during saturating

The saturation degree of the tested specimens was measured during saturation by following the weight method proposed by Chapuis et al. (1989b). Several measurements were made before starting the saturation process, during the saturation process, and before beginning the test as follows:

1) Mass of the dry column with accessories.
2) Mass of the column filled with de-aired water and accessories.
3) Mass of the dry column filled with dry soil and accessories.
4) Total mass of the system including column and accessories, soil and water.
5) Mass of the dry soil.
6) Mass of the moist soil.
7) Mass of water in the specimen.

These measurements were then used along with the equations given by Chapuis et al. (1989b) to calculate the total volume of the pore space, the pore volume filled by water during the saturation process and the degree of saturation. Measurements and calculations of the saturation degree of all specimens are provided in Appendix D.

Once the degree of saturation reached 97% (±2%), the inlet tube and the piezometer tubes were filled with water to ensure there is no air in the system. Then, the piezometers tubes were connected to the piezometer outlets along the column wall. Before starting the test, it was important that water flows into the piezometers and that the water within the piezometers reach stability (Chapuis et al., 2019). Figure 8.5 shows the piezometer connections to the piezometer outlets on the column wall for small and large columns.

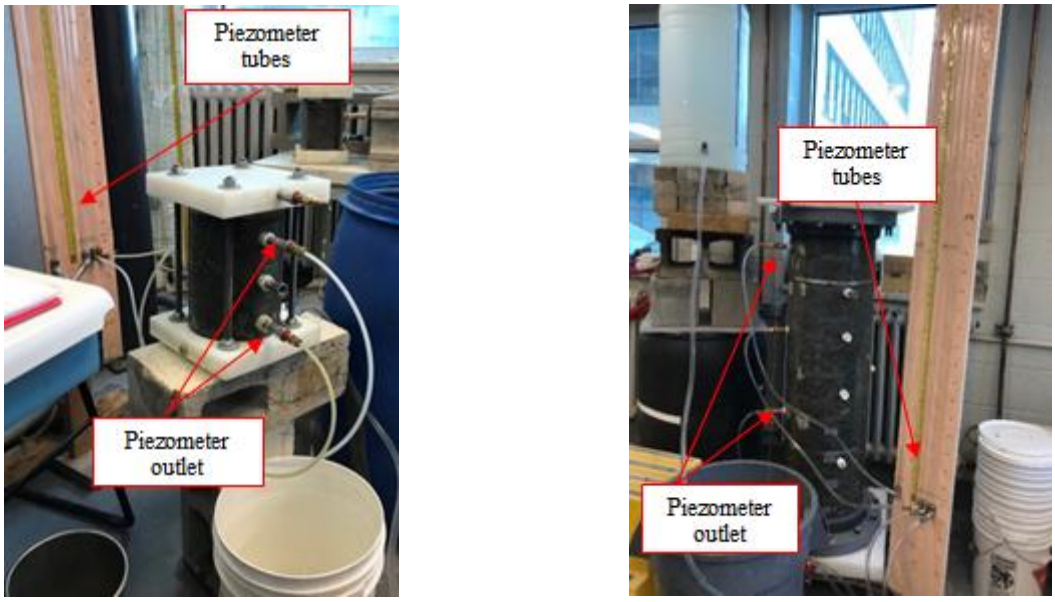

(a) (b)

Figure 8.5 Piezometer connections for (a) small and (b) large columns

Based on ASTM D2434-19, the hydraulic gradient must be small enough to ensure laminar flow condition. Therefore, a constant hydraulic head was applied with a downward flow under low hydraulic gradients (i) (from about 0.2 to 0.4). Precision with permeability tests can be achieved when the K_{sat} values obtained for the three specimens are within the limits ±20% (Chapuis, 2004). To achieve that, two conditions should be respected:

1) The samples should be well saturated with water according to the method of Chapuis et al. (1989b).
2) The tested specimens should not be prone to internal erosion due to the non-uniform compaction or having very large particles (Chapuis, 1992).

In this study, the proper degree of saturation for all specimens was achieved. Details of the measurements are provided in Appendix D. In addition, well-graded materials are used and compacted uniformly and light enough to avoid any possible internal erosion, as shown in Figure 8.4.

For each hydraulic gradient, the K_{sat} value was obtained through the measurement of collected water volume passing through the specimens at a given period of time t (s) based on Darcy law, as follows:

$$K_{sat} = \frac{L}{h}\frac{Q}{t\,A} \tag{8.1}$$

where L is the distance between piezometers (cm), h is the difference in heads (cm), Q is the water discharge (cm^3), A is the cross-sectional area of the specimen (cm^2). The obtained K_{sat} values were corrected to those at 20°C (Freez & Cherry, 1979; ASTM D2434-19, 2019).

The flow condition during the constant head permeability tests can be seen through the relationship between Darcy velocity (V_{Darcy}) and hydraulic gradient as below (Freez & Cherry, 1979):

$$V = kh/L = ki \tag{8.2}$$

where V is Darcy velocity (cm/s).

The Darcy velocity can also be determined by using the following eequation:

$$V = \frac{Q}{t\,A} \tag{8.3}$$

A laminar flow is reflected by a linear relationship between Darcy velocity and hydraulic gradient, as the cases of M1, M2, M3 and M4 show in Figure 8.6 (Freez & Cherry, 1979; Fetter, 2001).

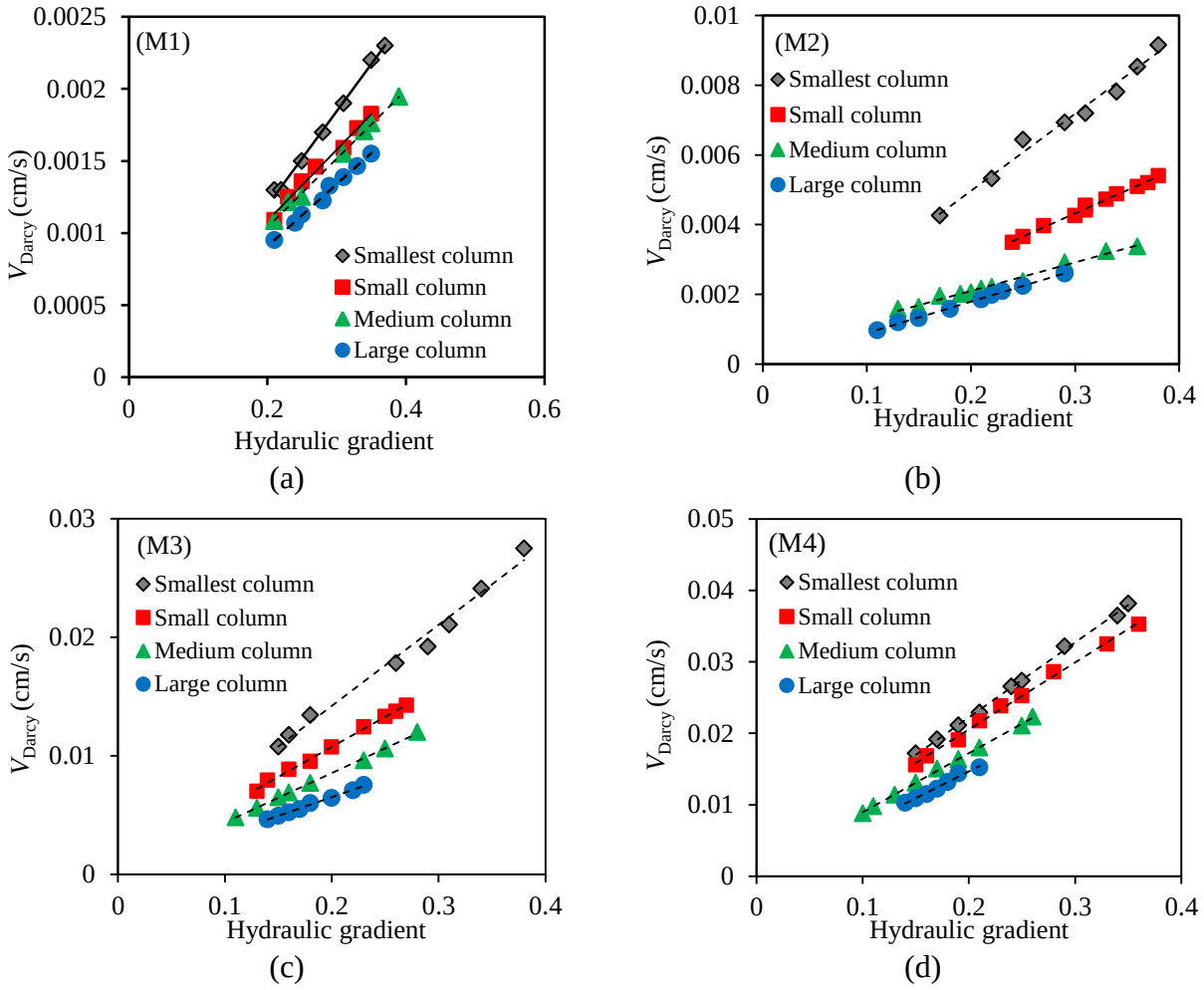

Figure 8.6 Darcy velocity versus hydraulic gradient during constant head permeability tests for (a) M1, (b) M2, (c) M3, and (d) M4, obtained with the four different columns

It is also necessary to keep the hydraulic gradient smaller than the critical value to avoid displacement of fine particles (ASTM 2434-19; Chapuis, 2004). The hydraulic gradients of this study were less than the critical hydraulic gradient obtained by (Terzaghi, 1922):

$$i_{cr} = \frac{\gamma_s - \gamma_w}{\gamma_w}(1 - n) \tag{8.4}$$

where γ_s is the unit weight of soil (kN/m^3), γ_w is the unit weight of water (kN/m^3) and n is the porosity.

8.2.3 Test results

Figure 8.7 shows the measured K_{sat} as a function of the hydraulic gradients of M1 (Figure 8.7a), M2 (Figure 8.7b), M3 (Figure 8.7c), and M4 (Figure 8.7d), obtained by the smallest, small, medium, and large columns.

For the tests with M1, one can see that the K_{sat} values measured by different columns are nearly consistent when the hydraulic gradient increases. For the tests with M2, the measured K_{sat} values by small and large columns are consistent when the hydraulic gradient increases. Slight decreases in the K_{sat} values measured by medium smallest and medium columns can be seen when the hydraulic gradient increases.

For the tests with M3, one can see slight variations in the K_{sat} values corresponding to the smallest column when the hydraulic gradient increases, while it remains consistent for other columns. For the tests with M4, the measured K_{sat} values for different columns remain nearly consistent as the hydraulic gradient increases.

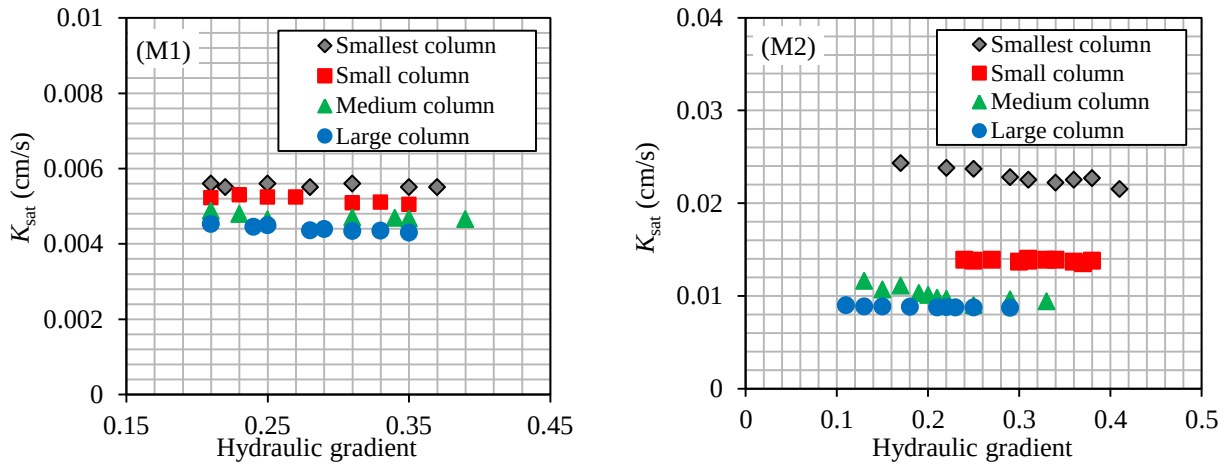

(a) (b)

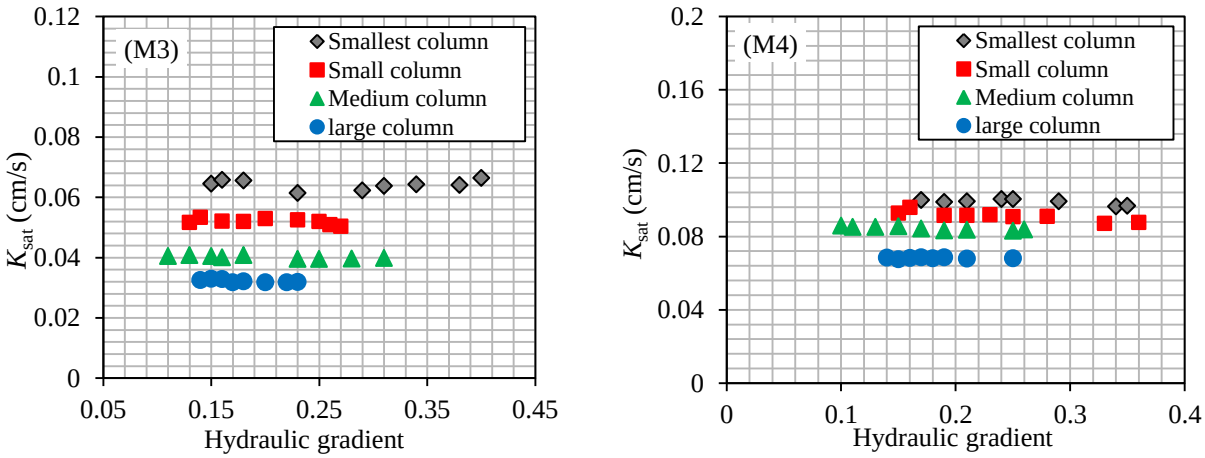

(c) (d)

Figure 8.7 Variations of K_{sat} values as function of hydraulic gradient (i), obtained with the smallest, small, medium and large column: (a) M1, (b) M2, (c) M3, and (d) M4.

In order to evaluate the variation of the K_{sat} uniquely associated with the variation of D/d_{max} ratio, all other influencing factors should be kept constant. As the results presented in Figure 8.7 clearly show that the measured K_{sat} values may change with the applied hydraulic gradient. The comparison can thus only be made by considering the measured K_{sat} values obtained with a small range of hydraulic gradients, applied to the four specimens. The results are given in Tables 8.6 to 8.9 for M1 to M4.

Table 8.6 The measured K_{sat} values of M1 at different hydraulic gradient i obtained with the different columns

i	**Smallest (D/d_{max}=86)**	**Small (D/d_{max}=127)**	**Medium (D/d_{max}=170)**	**Large (D/d_{max}=252)**
0.21	0.0056	0.00524	0.00489	0.00458
0.21-0.25	0.0055	0.00530	0.00479	0.00445
0.25	0.0056	0.00523	0.00488	0.00455
0.25-0.31	0.0055	0.00524	0.00469	0.00437
0.31	0.0056	0.00509	0.00469	0.00434
0.31-0.35	0.0055	0.00510	0.00469	0.00430
0.35	0.0055	0.00510	0.00467	0.00439

Table 8.7 The measured K_{sat} values of M2 at different hydraulic gradient i obtained with the different columns

i	**Smallest (D/d_{max}=43)**	**Small (D/d_{max}=64)**	**Medium (D/d_{max}=86)**	**Large (D/d_{max}=127)**

0.22-0.25	0.0238	0.0139	0.0097	0.0076
0.25	0.0237	0.0138	0.009	0.0074
0.25-0.31	0.0228	0.0138	0.0096	0.0064
0.31-0.34	0.0222	0.0139	0.0094	0.0059

Table 8.8 The measured K_{sat} values of M3 at different hydraulic gradient *i* obtained with the different columns

i	**Smallest (D/d_{max} = 20)**	**Small (D/d_{max} = 30)**	**Medium (D/d_{max} = 40)**	**Large (D/d_{max} = 60)**
0.14-0.15	0.0646	0.0534	0.0406	0.0328
0.15-0.16	0.0658	0.0521	0.0401	0.0329
0.16-0.18	0.0656	0.0520	0.0409	0.032
0.18-0.23	0.0615	0.0530	0.0396	0.0318
0.23	0.0615	0.0526	0.0396	0.0319

Table 8.9 The measured K_{sat} values of M4 at different hydraulic gradient *i* obtained with the different columns

i	**Smallest (D/d_{max} = 13)**	**Small (D/d_{max} = 19)**	**Medium (D/d_{max} = 25)**	**Large (D/d_{max} = 38)**
0.14-0.15	0.1004	0.0928	0.0856	0.0681
0.15-0.19	0.100	0.0959	0.0844	0.0684
0.19	0.0988	0.0915	0.0834	0.0686
0.21	0.0993	0.0916	0.0837	0.0680
0.21-0.25	0.1005	0.0919	0.0832	0.0682
0.25	0.1004	0.0909	0.0832	0.0682

Figure 8.8 shows the variation of K_{sat} as a function of D/d_{max} ratio of M1 to M4 at different hydraulic gradient values. The results obtained on materials M3 and M4 clearly show that the K_{sat} values significantly decrease when the D/d_{max} ratio increases from 13 to 38 for M4 (Figure 8.8a) and from 20 to 60 for M3 (Figure 8.8b), respectively. These results indicate that the minimum required D/d_{max} ratio of 12, as stipulated by the ASTM standard, is not large enough to eliminate the SSE of hydraulic conductivity tests. With these results, we can further conclude that even a D/d_{max} ratio of 40 is not large enough to eliminate the SSE. However, these results cannot determine the minimum required D/d_{max} ratio to eliminate the SSE of hydraulic conductivity tests. Similar observation and conclusion can be drawn on the test results of M2, which tend to indicate a D/d_{max} ratio of 86 is not large enough to eliminate the SSE.

With the measured K_{sat} of M1, it seems that a value between 170 and 252 is the large enough D/d_{max} ratio for this material to ensure a stable K_{sat} and eliminate the SSE. A value of 200 is recommended as the minimum required D/d_{max} ratio to eliminate SSE of constant head permeability tests.

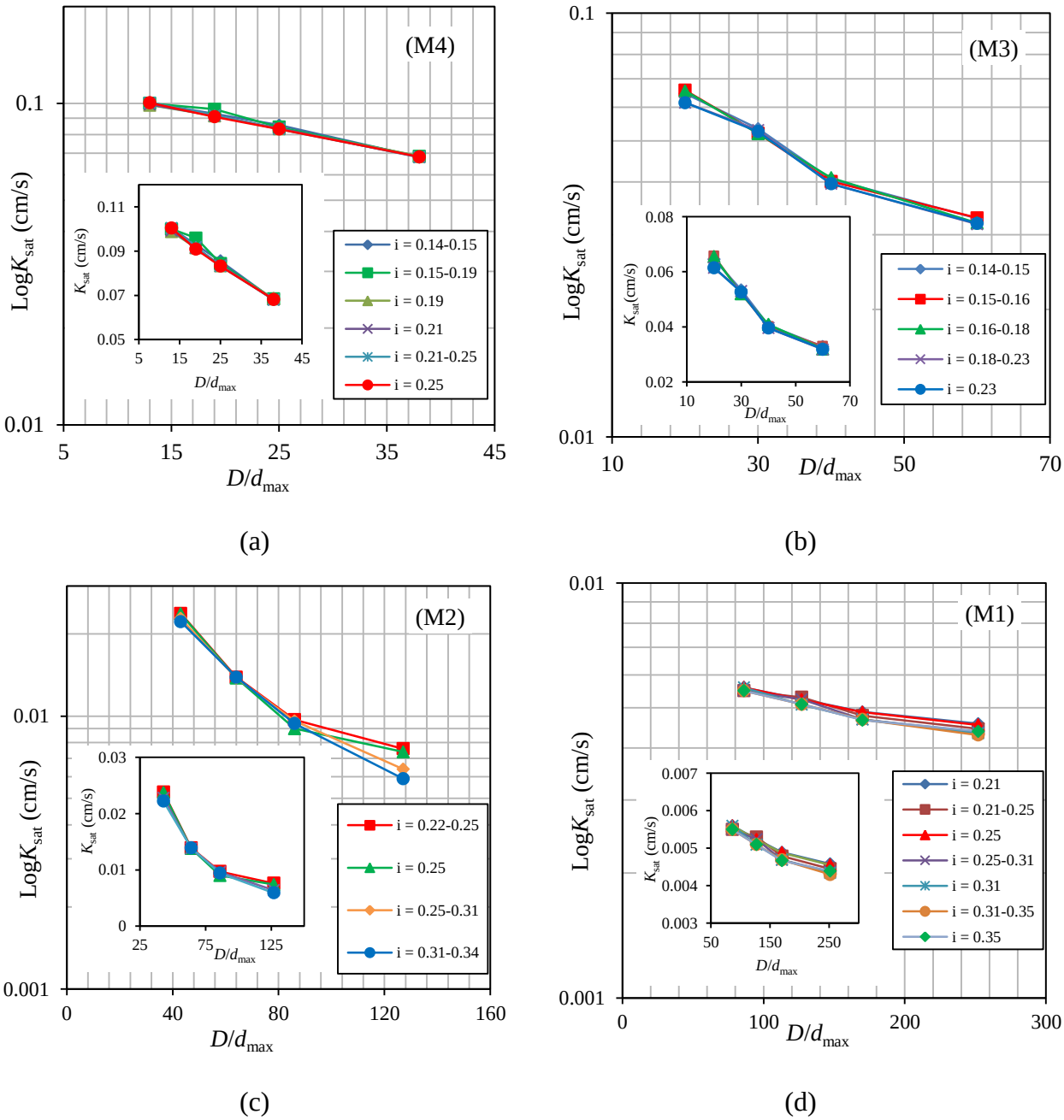

Figure 8.8 Variations of measured K_{sat} as a function of D/d_{max} at different hydraulic gradients, obtained for (a) M4, (b) M3, (c) M2 and (d) M1

8.3 Discussion

This paper presents the influence of the D/d_{max} ratio on the saturated hydraulic conductivity of coarse granular materials. The results indicate that the minimum required D/d_{max} ratio of 12 of ASTM is too small for constant head permeability tests to avoid any SSE. A value of 200 is recommended as the minimum required D/d_{max} ratio to eliminate SSE for constant head permeability tests. This value was proposed as a compromise between the accuracy and laboratory test convenience by considering its plausible value between 170 and 252 based on the test results of M1. Strictly, the recommendation remains valid for the tested material M1 under the tested density. More experimental work is necessary to test the validity of this recommendation by using more different materials tested under varying conditions.

Even with the minimum required D/d_{max} ratio of 12 of ASTM, it is already a big challenge to prepare specimens with coarse granular materials like gravel, rockfill and waste rocks for permeability tests. With the recommended value of 200 as the minimum required D/d_{max} ratio, the challenge of obtaining large enough specimens becomes even more important. Tests where the oversized particles are removed using a scaling down technique are unavoidable. Several scaling down techniques exist. The four most popular methods are scalping, parallel, replacement and quadratic down techniques (Deiminiat et al., 2020; Ovalle et al., 2014; Deiminiat & Li, 2022). The scalping down technique has been used frequently over the years to prepare the specimen of permeability tests (e.g., Hernandez, 2007; Gaillot, 2007; Bourrel, 2008; Peregoedova, 2012; Cabalar & Akbulut, 2016; Essayad et al., 2018) even though its reliability continues to be investigated. More work is thus necessary to study the reliability of scaling down techniques by following the methodology presented in Deiminiat and Li (2022). Of course, this work can only be done by using large enough specimens in all permeability testing.

Since the K_{sat} can also be determined by falling head permeability tests or triaxial compression tests, experimental work is necessary to evaluate if the minimum required D/d_{max} ratio of 6 specified by ASTM D5084-16a for falling head permeability tests and by ASTM D4767-11 (reapproved 2020) for triaxial compression tests is large enough to eliminate the SSE by following the methodology presented in this study.

8.4 Conclusions

With the aim of obtaining a reliable measurement or estimation of the hydraulic conductivity of coarse granular materials like gravel, rockfill and waste rocks, an experimental study was performed to examine the influence of the specimen size with respect to this objective. The results showed that the minimum required D/d_{max} ratio of 12 of ASTM D2434-19 is too small to avoid any SSE in constant head permeability tests. Rather, the experimental results tend to show that a value of D/d_{max} between 170 and 252 should be large enough to avoid SSE. By considering the accuracy and the convenience of laboratory tests, a value of 200 is recommended as the minimum required D/d_{max} ratio to eliminate SSE in constant head permeability tests.

Acknowledgments

The authors acknowledge the financial support from the Natural Sciences and Engineering Research Council of Canada (NSERC RGPIN-2018-06902), Fonds de recherche du Québec–Nature et Technologies (FRQNT 2017-MI-202860), industrial partners of the Research Institute on Mines and the Environment (RIME UQAT-Polytechnique;). Noura El-Harrak and Patrick Berneche are gratefully acknowledged for their assistance in the laboratory work.

8.5 References

ASTM D4767-11. (2011). Standard Test Method for Consolidated Undrained Triaxial Compression Test for Cohesive Soils, *ASTM International*, West Conshohocken, PA, USA.

ASTM C127-15. (2015). Standard test method for relative density (specific gravity) and absorption of coarse aggregate. *ASTM International*, West Conshohocken, PA, USA.

ASTM C128-15. (2015). Standard Test Method for Relative Density (Specific Gravity) and Absorption of Fine Aggregate, *ASTM International*, West Conshohocken, PA, USA.

ASTM D5084-16a. (2020). Standard test methods for measurement of hydraulic conductivity of saturated porous materials using a flexible wall permeameter. *ASTM International*, West Conshohocken, PA, USA.

ASTM 2434. (2019). Standard Test Method for Permeability of Granular Soils (constant Head). *ASTM International*, West Conshohocken, PA, USA.

Aubertin, M., Mbonimpa, M., Jolette, D., Bussière, B., Chapuis, R. P., James, M., & Riffon, O. (2002). Stabilité géotechnique des ouvrages de retenue pour les résidus miniers: problèmes persistants et méthodes de contrôle. In *Défis & Perspectives: Symposium*.

Bourrel, S., (2008). *Caractérisation des propriétés hydrogéologiques de rejets miniers*. Chaire industrielle CRSNG Polytechnique - UQAT en environnement et gestion de rejets miniers. École Polytechnique de Montréal, Canada.

Cabalar, A. F., & Akbulut, N. (2016a). Effects of the particle shape and size of sands on the hydraulic conductivity. *Acta Geotechnica Slovenica*, *13*(2), 83-93.

Cabalar, A. F., & Akbulut, N. (2016b). Evaluation of actual and estimated hydraulic conductivity of sands with different gradation and shape. *SpringerPlus*, *5*(1), 1-16.

Chapuis, R. P., Gill, D. E., & Baass, K. (1989a). Laboratory permeability tests on sand: influence of the compaction method on anisotropy. *Canadian Geotechnical Journal*, *26*(4), 614-622.

Chapuis, R. P., Baass, K., & Davenne, L. (1989b). Granular soils in rigid-wall permeameters: method for determining the degree of saturation. *Canadian Geotechnical Journal*, *26*(1), 71-79.

Chapuis, R. P. (1992). Similarity of internal stability criteria for granular soils. *Canadian Geotechnical Journal*, 29(4), 711-713.

Chapuis, R. P. (2004). Predicting the saturated hydraulic conductivity of sand and gravel using effective diameter and void ratio. *Canadian Geotechnical Journal*, *41*(5), 787-795.

Chapuis, R. P. (2012). Predicting the saturated hydraulic conductivity of soils: a review. *Bulletin of Engineering Geology and the Environment*, *71*, 404-434.

Chapuis, R. P., Gatien, T., & Marron, J. C. (2019). How to improve the quality of laboratory permeability tests in rigid-wall permeameters: a review. *Geotechnical Testing Journal*, *43*(4), 1037-1056.

Dawood, I., Aubertin, M., Intissar, R., & Chouteau, M. (2011). A combined hydrogeological–geophysical approach to evaluate unsaturated flow in a large waste rock pile. In *Pan-Am CGS Geotechnical Conference, Toronto*, Canada.

Deiminiat, A., Li, L., Zeng, F., Pabst, T., Chiasson, P., & Chapuis, R. (2020). Determination of the shear strength of rockfill from small-Scale laboratory shear tests: A Critical Review. *Advances in Civil Engineering*, *2020*, 8890237.

Deiminiat, A., Li, L. & Zeng, F. (2022). Experimental study on the minimum required specimen width to maximum particle size ratio in direct shear tests. *CivilEng*, 3, 66-84.

Deiminiat, A., & Li, L. (2022). Experimental study on the reliability of scaling down techniques used in direct shear tests to determine the shear strength of rockfill and waste Rocks. *CivilEng*, *3*(1), 35-50.

Dorador, L., & Villalobos, F. A. (2020). Analysis of the geomechanical characterization of coarse granular materials using the parallel gradation method. *Obras y Proyectos*, 27, 50-63.

Duhaime, F., Chapuis, R. P., Bigras, A., Kara, R., & Demers, L. (2012). Laboratory permeability tests on rock-fill. *In Proceedings of the 65th Canadian Geotechnical Conference*, Winnipeg, Canada.

Essayad, K., Pabst, T., Chapuis, R. P., & Aubertin, M. (2018). An experimental study of tailings migration through waste rock inclusions. *Communication présentée à GeoEdmonton*, Edmonton, Canada.

Fala, O., Molson, J., Aubertin, M., & Bussière, B. (2005). Numerical modelling of flow and capillary barrier effects in unsaturated waste rock piles. *Mine Water and the Environment*, *24*(4), 172-185.

Fala, O., Molson, J., Aubertin, M., Bussière, B., & Chapuis, R. P. (2006). Numerical simulations of long term unsaturated flow and acid mine drainage at waste rock piles. In *Proceedings of the 7th International Conference on Acid Rock Drainage (ICARD)* (pp. 26-30).

Fetter, C. (2001). *Applied hdrogeology (4th ed.)*. New Jersey, USA: Prentice-Hall.

Freeze, R. & Cherry, J. (1979). *Groundwater*. Toronto, Canada: Prentice-Hall.

Gaillot, A. (2007). *Caractérisation des propriétés hydrogéologiques de rejets miniers. Rapport de stage*. Chaire industrielle CRSNG Polytechnique - UQAT en environnement et gestion de rejets miniers. École Polytechnique de Montréal, Montreal, Canada.

Gan, D., Yang, X., & Zhang, Y. (2019). Experimental analysis on permeability characteristics of iron tailings. *Mathematical Problems in Engineering*, 2019(6539846).

Hamidi, A., Azini, E., & Masoudi, B. (2012). Impact of gradation on the shear strength-dilation behavior of well graded sand-gravel mixtures. *Scientia Iranica*, *19*(3), 393-402.

Hatanaka, M., Uchida, A., & Takehara, N. (1997). Permeability characteristics of high-quality undisturbed sands measured in a triaxial cell. *Soils and Foundations*, *37*(3), 129-135.

Hernandez Orellana, A. M. (2007). *Une étude expérimentale des propriétés hydriques des roches stériles et autres matériaux à granulométrie étalée* (Master thesis, École Polytechnique de Montréal).

Krumbein, W. C., & Monk, G. D. (1942). Permeability as a function of the size parameters of unconsolidated sands. *Petroleum Transactions, American Institute of Mining Engineers*, 151, 153–163.

Loudon, A. G. (1952). The computation of permeability from simple soil tests. *Geotechnique*, *3*(4), 165-183.

Lowe, J. (1964). Shear strength of coarse embankment dam materials. *In Proc., 8th Int. Congress on Large Dams*, Paris: International Commission on Large Dams (Vol. 3, pp. 745-761).

Mavis, F. T., & Wilsey, E. F., (1937). *A study of the permeability of sand*. Iowa State University. Engineering Bulletin 7.

Mbonimpa, M., Aubertin, M., Chapuis, R. P., & Bussière, B. (2002). Practical pedotransfer functions for estimating the saturated hydraulic conductivity. *Geotechnical & Geological Engineering*, *20*(3), 235-259.

MotahariTabari, S., & Shooshpasha, I. (2021). Evaluation of coarse-grained mechanical properties using small direct shear test. *International Journal of Geotechnical Engineering*, *15*(6), 667-679.

Navfac, D. (1974). Design manual-soil mechanics, foundations, and earth structures. *US Government Printing Office, Washington, DC. US.*

Ovalle, C., & Dano, C. (2020). Effects of particle size–strength and size–shape correlations on parallel grading scaling. *Geotechnique Letters*, *10*(2), 191-197.

Peregoedova, A. (2012). *Étude expérimentale des propriétés hydrogéologiques des roches stériles à une échelle intermédiaire de laboratoire* (MSc thesis, École Polytechnique de Montréal, Montreal, Canada).

Rowe, R. K., Armstrong, M. D., & Cullimore, D. R. (2000). Particle size and clogging of granular media permeated with leachate. *Journal of Geotechnical and Geoenvironmental Engineering*, *126*(9), 775-786.

Sukkarak, R., Pramthawee, P., Jongpradist, P., Kongkitkul, W., & Jamsawang, P. (2018). Deformation analysis of high CFRD considering the scaling effects. *Geomechanics & Engineering*, *14*(3), 211-224.

Terzaghi, K. (1922). *Der Grundbruch an Stauwerken und Seine Verhütung*. Wasserkraft, 17, 445–449.

Vukovic, M., & Soro, A. (1992). *Determination of hydraulic conductivity of porous media from grain-size composition*. Littleton, Colo: Water Resources Publications.

Zeller, J., & Wullimann, R. (1957). The shear strength of the shell materials for the Go-Schenenalp Dam, Switzerland. In *4th International Conference on Soil Mechanics and Foundation Engineering* (Vol. 2, pp. 399-415).

CHAPTER 9 GENERAL DISCUSSION

The main purpose of this study is to identify some reliable methods that can be used to measure or evaluate the mechanical and hydraulic properties of waste rocks. This has been partly achieved through the realization of two specific objectives (SO):

SO 1 To identify a reliable scaling down technique that can be used to correctly determine the shear strength of coarse granular materials.

SO 2 To identify a minimum required D/d_{max} ratio to be large enough and determine hydraulic conductivity of coarse granular materials exempt of specimen size effect (SSE).

In order to achieve the first SO, the SSE on shear strength of coarse granular materials has been first investigated through experimental work. The experimental results showed that the minimum required specimen width to d_{max} ratio of 10 specified by ASTM D3080-D3080M-11 for direct shear tests is too small to avoid SSE. Rather, the minimum required ratio of 60 is recommended to ensure stable and reliable test results. This recommended ratio has been used to conduct a series of direct shear tests on samples prepared by following scalping and parallel scalding down techniques. The results further showed the validity of scalping technique and invalidity of parallel technique. A method has also been proposed to obtain reliable (without SSE) friction angle of coarse granular materials based on direct shear tests on not large enough specimens. Despite these interesting discoveries, it should be kept in mind that the laboratory tests were realized with available equipment on a limited number of materials under simple testing conditions. The experimental program presented in this thesis contains several limitations, including for instance:

- The specimen size effect has been studied by considering different specimen sizes while the reliability of scaling down techniques was evaluated by considering different d_{max} values. It is well known that the mechanical properties of geo-materials are also affected by particle shape, fine and gravel contents, median size and coefficient of uniformity, density, moisture content and normal stress. In addition, the source materials were limited to two types of waste rocks. It can be questionable if all the conclusions given in the thesis are general or only valid under the tested conditions with the tested materials. More works are necessary to see if the suggested minimum required W/d_{max} ratio of 60 for

direct shear tests and if the scalping scaling down technique is still valid for untested materials under different testing conditions.

- In this study, three shear boxes available in the Geotechnique Laboratory of Polytechnique Montreal were used to study the effect of specimen width (W) by keeping other influencing factors constant. All the shear tests were conducted on the specimens prepared by the same compactness and moisture content. The tests were applied to the specimens with the same normal stress levels and shear rate. The same gap size was left between the upper and lower shear boxes. The tested specimen thickness (T) meets the minimum required T/d_{max} ratio specified by ASTM D3080/D3080M-11. It is however unclear how the gap size left between the upper and lower shear boxes affects the test results. It is also unclear whether the minimum required specimen thickness over d_{max} (T/d_{max}) specified by ASTM D3080-D3080M-11 is large enough to avoid any SSE.
- In this study, the d_{max} values of field samples are very small due to the lack of large shear boxes in the Geotechnique Laboratory at Polytechnique Montreal. Larger shear boxes are desirable to test the validity of the minimum required W/d_{max} ratio of 60 with coarser granular materials.
- The invalidity of the parallel technique and validity of scalping technique were shown based on experimental results obtained on samples having quite small ranges of d_{max}. Philosophically, these results are necessary and sufficient to invalidate the generally accepted conclusion in which the parallel technique is reliable. More work is necessary to test if the scalping technique remains on different materials with larger d_{max} values. The reliability of replacement technique was not tested.
- The maximum normal stress used in direct shear tests is limited to 150 kPa due to the limitation of air compressor of largest available direct shear device. It is unclear if the conclusions given in the thesis still remain valid under larger normal stresses.
- Pile tests were performed by slowly pouring materials on the top and keeping the falling height of granular material close to zero. More work is necessary by pouring the material in a natural way and see if the repose angle of pile tests is always insensitive of pile size.

- Dry waste rocks were used to perform direct shear tests and pile tests. This was to remove any possible influences associated with apparent cohesion and to ensure the tested materials in both the direct shear tests and pile tests are in the loosest state, exempt any other influencing factors such as moisture content, density, loading rate (for the case of direct shear test). More experiential work can be necessary by considering different moisture contents and densities.

The second SO has been partly achieved through the experimental investigation on the specimen size effect and the minimum specimen diameter to d_{max} ratio for constant head permeability tests of coarse granular materials. Both the test program and experimental results are quite preliminary due to several limitations such as:

- The specimen size effect of constant head permeability tests has been studied by considering different column sizes with several samples of different d_{max} values. Only one tested material has a large enough range of D/d_{max} ratio, by which one can recommend a minimum required D/d_{max} ratio of 200 to avoid SSE. More tests with larger columns are necessary to obtain a more precise and more reliable value for the minimum required D/d_{max} ratio, by which the SSE can be eliminated during a constant head permeability test.
- It is well known that the hydro-mechanical properties of geo-materials depend on particle shape, fine and gravel contents, median size and coefficient of uniformity, relative density, and degree of saturation. More experimental works are necessary to take into account the influence of these influencing factors.
- More works are necessary to see if the minimum required D/d_{max} ratio of 200 for constant head permeability tests still remains valid for untested materials under different testing conditions.
- Once the minimum required D/d_{max} is identified, it can be used to identify which scaling down technique can be used to predict the K_{sat} of field materials.

Finally, it is important to make difference between a SSE study and a sensitivity analysis of certain physical parameters. The former aims at finding the reliable test methods, while the latter

is to see the effect of the influencing parameters on the test results. The latter is impossible as long as the former is not solved.

CHAPTER 10 CONCLUSIONS AND RECOMMENDATIONS

10.1 Conclusions

With the main objective of to evaluate the mechanical and hydraulic properties of waste rocks, this thesis started by an identification of a reliable scaling down technique that can be used to determine the friction angle and hydraulic conductivity of coarse particle materials like gravel, rock fill and waste rocks. This work was ended by the publication of two journal articles and submission of two journal articles. The main findings of this thesis are summarized as follows:

- An inappropriate methodology was used in previous studies to validate or invalidate a scaling down technique. The validity or invalidity of the scaling down techniques has never been correctly shown.
- The minimum required specimen width over maximum particle size (W/d_{max}) ratio specified by ASTM D3080/D3080M-11 for direct shear tests was invalidated by direct shear test results on coarse granular materials, while its validity to eliminate the specimens size effect (SSE) for fine particle materials had never been shown. As all the available shear test results on coarse granular materials were obtained by using the minimum required W/d_{max} ratio of 10 specified in ASTM D3080/D3080M-11, the conclusions based on these test results are reliable.
- For coarse granular materials, the laboratory tests performed in this study showed that a minimum required W/d_{max} ratio of 60 is large enough to eliminate the SSE and to obtain reliable direct shear test results.
- For fine particle materials, the requirement of ASTM D3080/D3080M-11 for specimen width equal to 50 mm automatically leads to a minimum W/d_{max} ratio of 50, which is quite close to the minimum required ratio recommended in this study (i.e. $W/d_{max} \geq 60$). The ASTM D3080/D3080M-11 can thus be used without problem.
- Applying the minimum requirements of ASTM D3080/D3080M-11 for granular materials with d_{max} larger than 1 mm may result in a W/d_{max} ratio much smaller than the identified minimum required W/d_{max} ratio of 60. The obtained friction angles can be inaccurate and probably overestimated.

- The friction angles of the scalping scaled down samples and parallel scaled down samples increase when d_{max} increases, although the particle shapes are not rounded. This trend is different from those reported in the literature probably because the applied normal stresses in this study are very small.
- The present study showed that the scalping technique is a good scaling down technique that can be used to obtain friction angles of the field materials.
- The present study showed that the application of parallel scaling down technique cannot guarantee a reliable prediction on the friction angle of field materials.
- The experimental results confirm once again that the repose angle of a granular material corresponds to the internal friction angle of the material obtained by direct shear tests at its loosest state.
- In this study, an equation was proposed to obtain reliable friction angle of coarse grain materials based on direct shear test results obtained by using not large enough specimens.
- It is interesting to note that the repose angle of pile tests is insensitive to the variation of pile size. If this observation is valid in all cases, the repose angle of large waste rocks piles can be obtained by performing small pile tests with the same materials.
- This study shows that the repose angle or the internal friction angle at the loosest state increases with d_{max}. This trend corresponds to what we observe in the practice with commonly observed slopes of dams, waste rock pile, sand dune, etc. But this is different from that shown in previous studies, which showed increasing friction angle for angular or sub-angular particle materials with increased d_{max}. Once again, this last was probably due to the very large confining pressures applied in the triaxial compression tests.
- The minimum required D/d_{max} ratio of 8 or 12 specified by ASTM D2434-19 for constant head permeability tests is too small to remove the SSE on the K_{sat} of granular materials.
- The present studuy showed that a value of D/d_{max} between 170 and 252 can be considered as large to avoid SSE. By considering the compromise between the accuracy and convenience of laboratory tests, a value of 200 is recommended as the minimum required D/d_{max} ratio to eliminate SSE in constant head permeability tests.

10.2 Recommendations

Despite the interesting outcomes presented in this thesis, more works are necessary. Below are some recommendations for future works:

- More experimental work with materials of different origins having different particle shapes, water content, density, percentage of fine and gravel contents and under different normal stresses are necessary. The results can be used to determine whether the suggested large enough specimen width over d_{max} ratio for direct shear tests and scalping scaling down technique as reliable technique are still valid for untested materials with different testing conditions.
- More experimental investigation with different shear boxes of varied thickness and constant width is necessary not only to verify the suggested W/d_{max} ratio by this study, but also to validate the minimum required T/d_{max} ratio of ASTM D3080/D3080M-19.
- More experimental work with larger shear boxes is necessary to validate the reliability of scalping technique for field materials with d_{max} values larger than 5 mm and to see if the conclusion given in this study remains valid. In addition, the reliability of the replacement technique can also be evaluated.
- The parallel scaled down samples have been prepared by applying a given ratio to the particle size distribution (PSD) curve of field sample to reduce the ranges of particle sizes. Approximations were made for the calculated sizes that are not matched with available sieves or particle sizes smaller than the minimum particle size of the field sample. A process for the preparation of parallel sample can be recommended as follow for the future works:
    - Calculate the scaled down ratio between the d_{max} of field sample and targeted d_{max};
    - Apply the ratio to the particle size ranges of the field sample;
    - Draw a PSD curve for the scaled down sample using the calculated particle sizes. Thus, the PSD curve is perfectly parallel to the PSD curve of the field sample in the semi-log plane;

- Determine the percentage by weigh of the available sieves.

- Due to the limited capacity of the air compressor, the maximum normal stress was 150 kPa. Additional direct shear tests with a larger capacity loading cell may be necessary to compare the conclusions drawn in this thesis to those obtained by applying larger normal stress levels.

- As the scaling down techniques are usually used for the specimen preparation of direct and triaxial shear tests, it is interesting to study the reliability of the scaling down technique by performing triaxial compression tests. However, it should be noted that the tested specimens used in triaxial compression tests must be large enough to avoid any SSE.

- The pile tests were performed by keeping the funnel completely close to the growing pile. More work is necessary by pouring the material in a more natural way or using other pile test methods to see if the repose angle is still insensitive to pile size. The validity of the proposed equation can also be tested.

- More work is necessary to study the reliability of scaling down techniques for permeability tests by following the methodology presented in Deiminiat and Li (2022). This investigation can only be accomplished when large enough specimens in all the permeability tests are used.

- More works are necessary to see if the minimum required D/d_{max} ratio of 200 for constant head permeability tests still remains valid for untested materials under different testing conditions. Once the minimum required D/d_{max} is identified, it can be used to identify which scaling down technique can be used to predict the K_{sat} of field material.

- Since the K_{sat} can also be determined by falling head permeability tests or triaxial compression tests, experimental work is necessary to evaluate if the minimum required D/d_{max} ratio of 6 specified by ASTM D5084-16a for falling head permeability tests and by ASTM D4767-11 (reapproved 2020) for triaxial compression tests is large enough to eliminate the SSE by following the methodology presented in this study.

REFERENCES

Abbas, S. M. (2011). *Behaviour of rockfill materials: based on nature of particles*. Saarbrücken, Germany: LAP Lambert Academic Publishing.

Adams, R., Ahfeld, D., & Sengupta, A. (2007). Investigating the potential for ongoing pollution from an abandoned pyrite mine. *Mine Water and the Environment*. (26), 2-13.

Alakayleh, Z., Clement, T. P., & Fang, X. (2018). Understanding the changes in hydraulic conductivity values of coarse-and fine-grained porous media mixtures. *Water*, *10*(3), 313.

Al-Hussaini, M. (1983): Effect of particle size and strain conditions on the strength of crushed basalt. *Canadian Geotechnique Journal*, *20*(4), 706-717.

Alonso, E. E., Tapias, M., & Gili, J. (2012). Scale effects in rockfill behaviour. *Géotechnique Letters*, *2*(3), 155-160.

Amirpour Harehdasht, S., Karray, M., Hussien, M. N., & Chekired, M. (2017). Influence of particle size and gradation on the stress-dilatancy behavior of granular materials during drained triaxial compression. *International Journal of Geomechanics*, *17*(9), 04017077.

Amirpour Harehdasht, S., Hussien, M. N., Karray, M., Roubtsova, V., & Chekired, M. (2018). Influence of particle size and gradation on shear strength–dilation relation of granular materials. *Canadian Geotechnical Journal*, *56*(2), 208-227.

AS 1289.6.2.2. (1998). Soil strength and consolidation tests-determination of the shear strength of a soil-direct shear test using a shear box. *Standards Australia*, Sydney, NSW, Australia.

Asadzadeh, M., & Soroush, A. (2009). Direct shear testing on a rockfill material. *Arabian Journal for Science and Engineering*, *34*(2), 379.

ASTM C29/C29M-17a. (2007). Standard test method for bulk density (unit weight) and voids in aggregate, *ASTM International*, West Conshohocken, PA, USA.

ASTM D4767. (2011). Standard test method for consolidated undrained triaxial compression test for cohesive soils. ASTM International. West Conshohocken, PA, USA.

ASTM D3080/D3080M. (2011). Direct shear test of soils under consolidated drained conditions. ASTM International. West Conshohocken, PA, USA.

ASTM D2850. (2015). Standard test method for unconsolidated-undrained triaxial compression test on cohesive soils. *ASTM International*. West Conshohocken, PA, USA.

ASTM C127-15. (2015). Standard test method for relative density (specific gravity) and absorption of coarse aggregate, *ASTM International*, West Conshohocken, PA, USA.

ASTM, C128-15. (2015). Standard Test Method for Relative Density (Specific Gravity) and Absorption of Fine Aggregate, *ASTM International*, West Conshohocken, PA, USA.

ASTM D2434. (2019). Standard test method for permeability of granular soils (Constant Head). *ASTM Standard*, PA, USA.

ASTM D5084-16a. (2016). Standard test methods for measurement of hydraulic conductivity of saturated porous materials using a flexible wall permeameter. *ASTM International*, PA, USA.

Aubertin, M., Bussière, B., Bernier, B., (2002). *Environnement et gestion des rejets miniers, Manuel sur cédérom*, Presses Internationales Polytechnique. Montreal, QC, Canada.

Aubertin, M., Mbonimpa, M., Jolette, D., Bussière, B., Chapuis, R. P., James, M., & Riffon, O. (2002). Stabilité géotechnique des ouvrages de retenue pour les résidus miniers: problèmes persistants et méthodes de contrôle. In *Défis & Perspectives: Symposium*.

Aubertin, M., Fala, O., Molson, J., Gamache-Rochette, A., Lahmira, B., Martin, V., Lefebvre, R., Bussière, B., Chapuis, R.P., Chouteau, M., & Wilson, G.W. (2005). Évaluation du comportement hydrogéologique et géochimique des haldes a stériles. *Symposium Rouyn-Noranda: L'Environnement et les Mines*, Rouyn-Noranda, Canada.

Ayres, B., Landine, P., Adrian, L., Christensen, D., & O'Kane, M. (2006). Cover and final landform design for the B-zone waste rock pile at Rabbit Lake Mine. *In Uranium in the Environment* (pp. 739-749). Springer, Berlin, Heidelberg.

Azam, S., Wilson, G. W., Herasymuik, G., Nichol, C. & Barbour, L. S. (2007). Hydrogeological behavior of an unsaturated waste rock pile: a case study at the Golden Sunlight Mine, Montana, USA. *Bulletin of engineering geology and the environment*, *66*(3), 259-268.

Azam, S., & Li, Q. (2010). Tailings dam failures: a review of the last one hundred years. *Geotechnical news*, *28*(4), 50-54.

Bagherzadeh, A., & Mirghasemi, A. A., (2009). Numerical and experimental direct shear tests for coarse grained soils. *Particuology*. 7, 83-91.

Barbour, S. L., Hendry, M. J., Smith, J. L., Beckie, R. D., & Wilson, G. W. (2001). *A research partnership program in the mining industry for waste rock hydrology*. University of Saskatchewan, Saskatchewan, Canada.

Bareither, C. A., Benson, C. H., & Edil, T. B. (2008). Comparison of shear strength of sand backfills measured in small-scale and large-scale direct shear tests. *Canadian Geotechnical Journal*, *45*(9), 1224-1236.

Barton, N., & Kjærnsli, B. (1981). Shear strength of rockfill. *Journal of the geotechnical engineering division*, *107*(7), 873-891.

Beakawi Al-Hashemi, H. M., & Baghabra Al-Amoudi, O. S. (2018). A review on the angle of repose of granular materials, *Powder Technology*, *330*, 397–417.

Bell, F. G. (1996). Dereliction: colliery spoil heaps and their rehabilitation. *Environmental & Engineering Geoscience*, *2*(1), 85-96.

Blight, G. (2010). *Geotechnical engineering for mine waste storage facilities*, The Netherlands: CRC Press/Balkema

Blijenberg, H. M. (1995). In-situ strength tests of coarse, cohesionless debris on scree slopes. *Engineering Geology*, *39*(3-4), 137-146.

Boakye, K. (2008). *Large in situ direct shear tests on rock piles at the Questa Min, Taos county, New Mexico* (Doctoral dissertation, New Mexico Institute of Mining and Technology).

Bolduc, l., & Aubertin, M. (2014). Numerical investigation of the influence of waste rock inclusions on tailings consolidation. *Canadian Geotechnical Journal*, *51*(9), 1021-1032.

Bourrel, S., (2008). *Caractérisation des propriétés hydrogéologiques de rejets miniers*. Chaire industrielle CRSNG Polytechnique - UQAT en environnement et gestion de rejets miniers. École Polytechnique de Montréal, Canada.

Brown, P. L., Logsdon, M. J., Vinton, B., Schofield, I., & Payne, K. (2014). Detailed characterisation of the waste rock dumps at the Kennecott Utah Copper Bingham Canyon Mine–Optionality for Closure. In *Proceedings of the Eighth Australian Workshop on Acid and Metalliferous Drainage. Adelaide* (pp. 1-12).

Bussière, B. (1999). *Étude du comportement hydrique de couvertures avec effets de barrières capillaires inclinées à l'aide de modélisations physiques et numériques*. École Polytechnique de Montréal. Montreal, QC, Canada.

BS 1377. (1990). Methods of test for soils for civil engineering purposes. Shear strength tests (total stress). Part 7. *British Standard Institution*, London, UK.

Cabalar, A. F., & Akbulut, N. (2016a). Effects of the particle shape and size of sands on the hydraulic conductivity. *Acta Geotechnica Slovenica*, *13*(2), 83-93.

Cabalar, A. F., & Akbulut, N. (2016b). Evaluation of actual and estimated hydraulic conductivity of sands with different gradation and shape. *SpringerPlus*, *5*(1), 1-16.

Cai, H., Wei, R., Xiao, J. Z., Wang, Z. W., Yan, J., Wu, S. F., & Sun, L. M. (2020). Direct shear test on coarse gap-graded fill: plate opening size and its effect on measured shear strength. *Advances in Civil Engineering*, *2020*.

Casagrande, A., & Albert, S. G. (1932). *Research on the shearing resistance of soils*, International Society for Soil Mechanics and Geotechnical Engineering, (pp. 85-97).

Casagrande, A. (1936). Characteristics of cohesionless soils affecting the stability of slopes and earth fills. *Journal of Boston Society of Civil Engineers*, *23*(1), 13-32.

Cerato, A. B., & Lutenegger, A. J. (2006). Specimen size and scale effects of direct shear box tests of sands. *Geotechnical Testing Journal*, *29*(6), 507-516.

Chang, W. J., & Phantachang, T. (2016). Effects of gravel content on shear resistance of gravelly soils. *Engineering Geology*, *207*, 78-90.

Chapuis, R. P., Gill, D. E., & Baass, K. (1989a). Laboratory permeability tests on sand: influence of the compaction method on anisotropy. *Canadian Geotechnical Journal*, *26*(4), 614-622.

Chapuis, R. P., Baass, K., & Davenne, L. (1989b). Granular soils in rigid-wall permeameters: method for determining the degree of saturation. *Canadian Geotechnical Journal*, *26*(1), 71-79.

Chapuis, R. P. (2004). Predicting the saturated hydraulic conductivity of sand and gravel using effective diameter and void ratio. *Canadian Geotechnical Journal*, *41*(5), 787-795.

Chapuis, R. P. (2012). Predicting the saturated hydraulic conductivity of soils: a review. *Bulletin of Engineering Geology and the Environment*, *71*, 404-434.

Chapuis, R. P., Weber, S., & Duhaime, F. (2012). Discussion of "Intrinsic permeability of materials ranging from sand to rock-fill using natural air convection tests". *Canadian Geotechnical Journal*, *49*(11), 1319-1322.

Chapuis, R. P., Weber, S., & Duhaime, F. (2015). Permeability test results with packed spheres and non-plastic soils. *Geotechnical Testing Journal*, *38*(6), 950-964.

Charles, J. A. (1973). *Correlation between laboratory behaviour of rockfill and field performance, with particular reference to Scammonden Dam* (Doctoral Dissertation, University of London, London, UK).

Charles, J. A., & Watts, K. S. (1980). The influence of confining pressure on the shear strength of compacted rockfill. *Geotechnique*, *30*(4), 353-367.

Clayton, C.R.I., Abbireddy, C.O.R., & Schiebel, R. (2009). A method of estimating the form of coarse particulates. *Geotechnique*, *59*(6), 493-501.

Cooling, L. F., Smith, D. B., & Subcomerpre. (1936). Egineering research. Institution reseahc committee on earth-pressures. The shearing resistance of soils. *Journal of the Institution of Civil Engineers*, *3*(7), 333-343.

Das, B.M. (1983). *Advanced soil mechanics*, New York, McGraw-Hill Book Company.

Das, B. M. (2008). *Advanced soil mechanics* (Vol. 270). New York: Taylor & Francis.

Deiminiat, A., Li, L., Zeng, F., Pabst, T., Chiasson, P., & Chapuis, R. (2020). Determination of the shear strength of rockfill from small-Scale laboratory shear tests: A Critical Review. *Advances in Civil Engineering*, *2020*(8890237).

Deiminiat, A., & Li, L. (2022). Experimental study on the reliability of scaling down techniques used in direct shear tests to determine the shear strength of rockfill and waste Rocks. *CivilEng*, *3*(1), 35-50.

Donaghe, R., & Townsend, F. (1976). Scalping and replacement effects on the compaction characteristics of earth-rock mixtures. *In Soil Specimen Preparation for Laboratory Testing: ASTM Special Technical Publication, 599, 248-277.*

Donaghe, R. T., & Torrey, V. H. (1985). Strength and deformation properties of earth-rock mixtures. *US Army Corps of Engineers*, AD-A160 701.

Dorador, L., Anstey, D., & Urrutia, J. (2017). Estimation of geotechnical properties on leached coarse material. In *70 th Canadian Geotechnical Conference, GeoOttawa*, Ottawa, Canada.

Dorador, L., & Villalobos, F. A. (2020a). Scalping techniques in geomechanical characterization of coarse granular materials. *Obras y Proyectos*, (28).

Dorador, L., & Villalobos, F. A. (2020b). Analysis of the geomechanical characterization of coarse granular materials using the parallel gradation method. *Obras y Proyectos*, *27*, 50-63.

Douglas, K. (2002). *The shear strength of rock masses* (Doctoral Dissertation, University of New South Wales. Australia).

Dudgeon, C. R., (1966). An experimental study of the flow of water through coarse granular media. *La Houille Blanche*, (7), 785-801.

Dudgeon, C.R., 1967. Wall effects in permeameters. *Journal of the Hydraulics Division, ASCE, 93*(HY5), 137–148.

Duhaime, F., Chapuis, R. P., Bigras, A., Kara, R., & Demers, L. (2012). Laboratory permeability tests on rock-fill. *In Proceedings of the 65th Canadian Geotechnical Conference*, Winnipeg, Canada.

Earley, D., Kidd, D. A., Shelley, T., Walder, I., & Salvas, E. A. (2003). Slope stability of leached copper stockpiles. *In Talings and Mine Waste'03* (pp. 121-130).

Eriksson, N., & Destouni, G. (1997). Combined effects of dissolution kinetics, secondary mineral precipitation and preferential flow on copper leaching from mining waste rock, *Water Resources Research*, *33*(3), 471-483.

Essayad, K., Pabst, T., Chapuis, R. P., & Aubertin, M. (2018). An experimental study of tailings migration through waste rock inclusions. *Communication présentée à GeoEdmonton*, Edmonton, Canada.

Eurocode 7. (2007). Geotechnical design - Part 1: General rules: EN 1997-1. *The European Union Per Regulation*, Brussels, Belgium.

Fakhimi, A., Boakye, K., Sperling, D. J., & McLemore, V. T. (2007). Development of a modified in situ direct shear test technique to determine shear strength parameters of mine rock piles. *ASTM Geotechnical Testing Journal*, *31*(3), 269-273.

Fakhimi, A., Nunoo, S., Van Zyl, D., & McLemore, V. T. (2012). The effect of material scalping and water content on the shear strength of Questa mine materials. *In 46th US Rock Mechanics/Geomechanics Symposium. American Rock Mechanics Association*, Chicago, Illinois, USA.

Fakhry, A. A. & LaMoreaux, P. E. (2004). *Field methods for geologists and hydrogeologists*. New York: Springer.

Fala, O., Molson, J., Aubertin, M., Dawood, I., Bussière, B., & Chapuis, R. P. (2013). A numerical modelling approach to assess long-term unsaturated flow and geochemical transport in a waste rock pile. *International Journal of Mining, Reclamation and Environment, 27*(1), 38-55.

Feng, G., & Vitton, S. J. (1999). Laboratory determination of compaction criteria for rockfill material embankments. In *International Conference on Soil Mechanics and FOundation Engineering* (pp. 485-488).

Ferdosi, B., James, M., & Aubertin, M. (2015). Effect of waste rock inclusions on the seismic stability of an upstream raised tailings impoundment: a numerical investigation. *Canadian Geotechnical Journal, 52*(12), 1930-1944.

Fragaszy, R. J., Su, J., Siddiqi, F. H., & Ho, C. L. (1992). Modeling strength of sandy gravel. *Journal of Geotechnical Engineering*, *118*(6), 920-935.

Franzini, J. B. (1968). Wall effects in permeameters [Discussion] *Journal of the Hydraulics Division*. *In ASCE* (Vol. 94, pp. 1148-1150).

Freeze, R. A., & Cherry, J. A. (1979). *Groundwater*. Toronto, Canada: Prentice-Hall.

Frost, R. J. (1973). Some testing experiences and character. *In Evaluation of Relative Density and Its Role in Geotechnical Projects Involving Cohesionless Soils: A Symposium Presented at the Seventy-Fifth Annual Meeting, American Society for Testing and Materials*, Los Angeles, California (Vol. 523, p. 207).

Fumagalli, E. (1969). Tests on cohesion less materials for rockfill dams, *Journal of Soil Mechanics and Foundation Engineering, ASCE, 95*(1), 313-330.

Gan, D., Yang, X., & Zhang, Y. (2019). Experimental analysis on permeability characteristics of iron tailings. *Mathematical Problems in Engineering*, 2019(6539846).

Gaillot, A. (2007). *Caractérisation des propriétés hydrogéologiques de rejets miniers. Rapport de stage*. Chaire industrielle CRSNG Polytechnique - UQAT en environnement et gestion de rejets miniers. École Polytechnique de Montréal, Montréal, Canada.

Gomez, B. W., Dewoolkar, M. M., Lens, J. E., & Benda, C. C. (2014). Effects of fines content on hydraulic conductivity and shear strength of granular structural backfill. *Transportation Research Record, 2462*(1), 1-6.

Goodrich, E. P. (1904). Lateral Earth Pressures and Related Phenomena. *Transactions of the American Society of Civil Engineers*, *53*(2), 272-304.

Gupta, A. K. (2009). Triaxial behaviour of rockfill materials. *Electronic Journal of Geotechnical Engineering*, *14*(Bund. J), 1-18.

Gupta, A. K. (2016). Effects of particle size and confining pressure on breakage factor of rockfill materials using medium triaxial test. J*ournal of Rock Mechanics and Geotechnical Engineering*, *8*(3), 378-388.

Hall, E. B. (1951). A triaxial apparatus for testing large soil specimens. *ASTM*, 106, 152-161.

Hall, E. B., & Gordon, B. B. (1963). Triaxial testing with large-scale high pressure equipment. Laboratory Shear Testing of Soils, 361, 315-328.

Hall, E. B., & Smith, T. (1971). Special Tests for Design of High Earth Embankments on US-101. *Highway Research Record*, (345).

Hamidi, A., Azini, E., & Masoudi, B. (2012). Impact of gradation on the shear strength-dilation behavior of well graded sand-gravel mixtures. *Scientia Iranica*, *19*(3), 393-402.

Hassani, F., & Archibald J. H. (1998). *Mine backfill*. CIM, CD-ROM.

Hatanaka, M., Uchida, A., & Takehara, N. (1997). Permeability characteristics of high-quality undisturbed sands measured in a triaxial cell. *Soils and Foundations*, *37*(3), 129-135.

Hazen, A. (1892). Some physical properties of sand and gravel, with special reference to their use in filtration. Massachusetts State Board of Health, *24th annual report, Boston* (pp. 539–556).

Hawley, P.M. (2001). Site Selection, characterization, and assessment. In: W.A. Hustrulid, M.K. McCarter and D.J.A. van Zyl (Editors), *Slope Stability in Surface Mining: Society for Mining, Metallurgy, and Exploration, Inc (SME)*. Littleton (pp. 267-274).

Herasymuik, G.M. (1996). *Hydrogeology of a sulphide waste rock dump* (M.S. Thesis, University of Saskatchewan, Saskatoon, Saskatchewan, Canada).

Hernandez Orellana, A. M. (2007). *Une étude expérimentale des propriétés hydriques des roches stériles et autres matériaux à granulométrie étalée* (Master thesis, École Polytechnique de Montréal).

Hockley, D. E., Noel, M., Rykaart, E. M., Jahn, S., & Paul, M. (2003). *Testing of soil covers for waste rock in the ronneburg WISMUT mine closure*. Communication presented at 6th ICARD, Cairns, Australia.

Hossain, M. S., Parker, F., & Kandhal, P. S. (2000). Comparison and evaluation of tests for coarse aggregate particle shape, angularity, and surface texture. *Journal of Testing and Evaluation*, *28*(2), 77-87.

Hennes, R. G. (1952). The strength of gravel in direct shear. *Symposium on Direct Shear Testing of Soils, ASTM STP 131: American Society for Testing and Materials* (pp. 51-62).

Holtz, W., & Gibbs, H. J. (1956). Triaxial shear tests on pervious gravelly soils. *Journal of the Soil Mechanics and Foundations Division*, *82*(1), 1-22.

Holtz, R. D., & Kovacs, W. D. (1981). *An introduction to geotechnical engineering*, New York, USA: Prentice Hall.

Holtz, R. D., Kovacs, W. D., & Sheahan, T. C. (2011). *An introduction to geotechnical engineering*. Pearson, Upper Saddle River, NJ, 325.

Honkanadavar, N. P., Dhanote, S., & Bajaj, S. (2016). 161 Prediction of shear strength parameter for prototype alluvial rockfill material. *Indian Geotechnical Conference* IGC2016, Chennai, India.

Honkanadavar, N. P., Kumar, N., & Ratnam, M. (2014). Modeling the behavior of alluvial and blasted quarried rockfill materials. *Geotechnical and Geological Engineering*, *32*(4), 1001-1015.

Hribar, J., Dougherty, M., Ventura, J., & Yavorskyu, P. (1986). Large scale direct shear tests on surface mine spoil. *In Proceedings of international symposium on geotechnical stability in surface min*, AA Balkema, Calgary, Rotterdam (pp. 295-303).

Hu, W., Frossard, E., Hicher, P. Y., & Dano, C. (2010). Method to evaluate the shear strength of granular material with large particles. In *Soil Behavior and Geo-Micromechanics, GeoShanghai, Shanghai* (pp. 247-254).

Hu, W., Dano, C., Hicher, P.-Y., Le Touzo, J.-Y., Derkx, F. & Merliot, E. (2011). Effect of sample size on the behavior of granular materials. *Geotechnique*, *34*(3), 186-197.

Hutchinson, J. N., & Rolfsen, E. N. (1962). Large scale field shear box test and quick clay, *Geologie and Bauwesen*, *28*(1), 31 – 42.

Hvorslev, M. J. (1951). Time lag and soil permeability in ground water observations (No. 36). *Waterways Experiment Station, Corps of Engineering, US Army*.

Indraratna, B., Wijewardena, L. S. S., & Balasubramaniam, A. S. (1993). Large-scale triaxial testing of grey wacke rockfill. *Geotechnique, 43*(1), 37-51.

Indraratna, B., Ionescu, D., & Christie, H. D. (1998). Shear behavior of railway ballast based on large-scale triaxial tests. *Journal of Geotechnical and Geoenvironmental Engineering*, *124*(5), 439-449.

James, M. (2009). *The use of waste rock inclusions to control the effects of liquefaction in tailings impoundments* (Doctoral dissertation, Ecole Polytechnique de Montréal, Montréal, Canada).

James, M., Aubertin, M., Wijewickreme, D., & Wilson, G. W. (2011). A laboratory investigation of the dynamic properties of tailings. *Canadian Geotechnical Journal*, *48*(11), 1587-1600.

Jewell, R.A., & Wroth, C.P. (1987). Direct shear tests on reinforced sand. *Geotechnique*, 37(1), 53–68.

Kirkpatrick, W. M. (1965). Effects of grain size and grading on the shearing behaviour of granular materials. *In Proceedings of the sixth International Conference on Soil Mechanics and Foundation Engineering* (pp. 273-277).

Kolbuszewski, J., & Frederick, M. R. (1963). The significance of particle shape and size on the mechanical behaviour of granular materials. *In European Conference on Soil Mechanics and Foundation Engineering* (Vol. 1, pp. 253-263).

Kouakou, N. M., Cuisinier, O., & Masrouri, F. (2020). Estimation of the shear strength of coarse-grained soils with fine particles. *Transportation Geotechnics*, *25*, 100407.

Kresic, N. (1998). Quantitative solutions in Hydrogeology and Groundwater Modeling. Lewis Publishers, Florida.

Krumbein, W. C., & Monk, G. D. (1942). Permeability as a function of the size parameters of unconsolidated sands. *Petroleum Transactions, American Institute of Mining Engineers*, 151, 153–163.

Kutzner, C. (2020). *Grouting of rock and soil*. London, UK: Taylor & Francis Group.

Lambe, T., & Whitman, R. (1969). *Soil mechanics*. New York, NY, USA: John Wiley & Sons.

Leps, T. M. (1970). Review of shearing strength of rockfill. *Journal of Soil Mechanics & Foundations Division*, *96*(4), 1159-1170.

Leslie, D. (1963). Large scale triaxial tests on gravelly soils. *In Proc. of the 2nd Pan-American Conference on Soil Mechanic and Foundation Engineering, Brazil* (Vol. 1, pp. 181-202).

Lewis, J. G. (1955). Shear strength of rock fill. *New Zealand Engineering, 10*(11), 388-389.

Li, M. (2000). Unsaturated flow and transport observations in large waste rock columns. In *Proceedings Fifth International Conference on Acid Rock Drainage* (pp. 247-256).

Li, L., Ouellet, S., & Aubertin, M. (2009). A method to evaluate the size of backfilled stope barricades made of waste rock. *GeoHalifax*, Halifax, Canada (Vol. 1, p. 1).

Li, L., & Aubertin, M. (2011). Limit equilibrium analysis for the design of backfilled stope barricades made of waste rock. *Canadian Geotechnical Journal*, *48*(11), 1713-1728.

Linero, S., Palma, C., & Apablaza, R. (2007). Geotechnical characterization of waste material in very high dumps with large scale triaxial testing. *Paper presented at the Proceedings of International Symposium on Rock Slope Stability in Open Pit Mining and Civil Engineering*, Perth, Australia (pp. 59-75).

Loudon, A. G. (1952). The computation of permeability from simple soil tests. *Geotechnique*, *3*(4), 165-183.

Lowe, J. (1964). Shear strength of coarse embankment dam materials. *In Proc., 8th Int. Congress on Large Dams*, Paris: International Commission on Large Dams (Vol. 3, pp. 745-761).

Lucia, P. C. (1981). *Review of experiences with flow failures of tailings dams and waste impoundments*. Berkeley, US: University of California.

Maknoon, M. (2016). *Slope stability analyses of waste rock piles under unsaturated conditions following large precipitations* (Doctoral dissertation, Ecole Polytechnique, Montreal, Canada).

Marachi, N., Seed, H., & Chan, C. (1969). Strength characteristics of rockfill materials. *Seventh International Conference on Soil Mechanics and Foundation Engineering.*

Marachi, N. D., Chan, C. K. & Seed, H. B. (1972). Evaluation of properties of rockfill materials. *Journal of Soil Mechanics & Foundations Division*, *98*(1), 95-114.

Marescotti, P., Carbone, C., De Capitani, L., Grieco, G., Lucchetti, G., & Servida, D. (2008). Mineralogical and geochemical characterisation of open-air tailing and waste-rock dumps from the Libiola Fe-Cu sulphide mine (Eastern Liguria, Italy). *Environmental Geology*, *53*(8), pp. 1613-1626.

Marsal R. J. (1965). Research on the behavior of the granular material and rockfill samples. *Comision Federal de Electricidad*, Mexico.

Marsal, R. J. (1973). Mechanical properties of rockfill. *In: Hirschfeld RC, Poulos SJ (eds) Embankment-dam engineering, Casagrande volume. Wiley*, pp 109–200.

Marsal, R., & Fuentes de la Rosa, A. (1976). Mechanical properties of rockfill soil mixtures. *Paper presented at the Transactions of the 12th International Congress on Large Dams*, Mexico City (Vol. 1, pp. 179-209).

Marsland, A. (1971). The use of in-situ tests in a study of the effects of fissures on the properties of stiff clays. In *Proc. First Aust.-NZ Conf. on Geomechanics, Melbourne* (Vol. 1, pp. 180-189).

Martin, V., Aubertin, M., & Lessard, G. (2019). An assessment of hydrogeological properties of waste rock using infiltration tests and numerical simulations. *GeoStJohn's*.

Masch, F. D., & Denny, K. J. (1966). Grain size distribution and its effect on the permeability of unconsolidated sands. *Water Resources Research*, *2*(4), 665-677.

Matsuoka, H., & Liu, S. (1998). Simplified direct box shear test on granular materials and its application to rockfill materials. *Soils and Foundations*, 38(4), 275-284

Matsuoka, H., Liu, S. H., Sun, D., & Nishikata, U. (2001). Development of a new in situ direct shear test. *Geotechnical Testing Journal*, 24(1), 92-102.

Mavis, F.T., & Wilsey, E.F., (1937). *A study of the permeability of sand*. Iowa State University. Engineering Bulletin 7.

Mbonimpa, M., Aubertin, M., Chapuis, R. P., & Bussière, B. (2002). Practical pedotransfer functions for estimating the saturated hydraulic conductivity. *Geotechnical & Geological Engineering*, *20*(3), 235-259.

McCarter, M. K. (1990). Design and operating considerations for mine waste embankments. *Soc of Mining Engineering of Aime, Littleton* (pp. 890-899).

McLemore, V. T., Sweeney, D., Dunbar, N., Heizler, L., & Writer, E. P. (2009). Determining quantitative mineralogy using a modified MODAN approach on the Questa rock pile materials. *In Society of Mining, Metallurgy and Exploration Annula Convention, Denver* (pp. 9-20).

Mirzaeifar, H., Abouzar, A., & Abdi, M. R. (2013). Effects of direct shear box dimensions on shear strength parameters of geogrid-reinforced sand. In *66th Canadian geotechnical conference and the 11th joint CGS/IAH-CNC groundwater conference, Montreal* (pp. 1-6).

Montanari, D., Agostini, A., Bonini, M., Corti, G., & Del Ventisette, C. (2017). The use of empirical methods for testing granular materials in analogue modelling. *Materials*, 10, 635.

Mora, C. F., & Kwan, A. K. H. (2000). Sphericity, shape factor, and convexity measurement of coarse aggregate for concrete using digital image processing. *Cement and Concrete Research*, *30*(3), 351-358.

Morgan, G. C., & Harris, M. C. (1967). Portage mountain dam: II. Materials. *Canadian Geotechnical Journal*, *4*(2), 142-166.

Morin, K. A., Gerencher, E., Jones, C. E., & Konasewich, D. E. (1991). *Critical review of acid drainage from waste rock*. MEND Report 1.11.1.

MotahariTabari, S., & Shooshpasha, I. (2021). Evaluation of coarse-grained mechanical properties using small direct shear test. *International Journal of Geotechnical Engineering*, *15*(6), 667-679.

Moore, J. E. (2012). *A guide for site investigations and report preparation*. 2nd Edition ed. Boca Raton: CRC Press.

Nichols, R. S. (1986). Rock segregation in waste dumps. In Flow-through rock drains: *Proceedings of the International Symposium Convened at the Inn of the South*, Cranbrook, BC, Canada.

Nicks, J. E., Gebrenegus, T., & Adams, M. T. (2021). Interlaboratory Large-Scale Direct Shear Testing of Open-Graded Aggregates: Round One. In *IFCEE* (pp. 361-370).

Odong, J. (2007). Evaluation of empirical formulae for determination of hydraulic conductivity based on grain-size analysis. *Journal of American Science*, *3*(3), 54-60.

Ovalle, C., Frossard, E., Dano, C., Hu, W., Maiolino, S., & Hicher, P. Y. (2014). The effect of size on the strength of coarse rock aggregates and large rockfill samples through experimental data. *Acta Mechanica*, *225*(8), 2199-2216.

Ovalle, C., Linero, S., Dano, C., Bard, E., Hicher, P. Y., & Osses, R. (2020). Data compilation from large drained compression triaxial tests on coarse crushable rockfill materials. *Journal of Geotechnical and Geoenvironmental Engineering*, *146*(9), 06020013.

Oyanguren, P. R., Nicieza, C. G., Fernández, M. Á., & Palacio, C. G. (2008). Stability analysis of Llerin Rockfill Dam: An in situ direct shear test. *Engineering Geology*, *100*(3-4), 120-130.

Palmeira, E. M. & Milligan, G. W. E. (1989). Scale effects in direct shear tests on sand, *Proceedings of the 12th International Conference on Soil Mechanics and Foundation Engineering, Rio de Janeiro* (Vol. 1, pp. 739-742).

Pankaj, S., Mahure, N., Gupta, S., Sandeep, D., & Devender, S. (2013). Estimation of shear strength of prototype rockfill materials. *International Journal of Engineering*, *2*(8), 421-426.

Parsons, J. D. (1936). Progress report on an investigation of the shearing resistance of cohesionless soils. *Proceedings of the 1st International Conference on Soil Mechanics and Foundation Engineering* (Vol. 2, pp. 133-138).

Pearce, S., Lehane, S., & Pearce, J. (2016). Waste material placement options during construction and closure risk reduction—quantifying the how, the why and the how much. In *Mine Closure 2016: Proceedings of the 11th International Conference on Mine Closur* (pp. 691-706).

Pepin, G. (2009). *Évaluation du comportement géochimique de stériles potentiellement générateurs de drainage neutre contaminé à l`aide de cellules expérimentales in situ* (Mémoire de maîtrise. École polytechnique de Montréal, Université du Québec en Abitibi-Témiscamingue, Canada).

Peregoedova, A. (2012). *Étude expérimentale des propriétés hydrogéologiques des roches stériles à une échelle intermédiaire de laboratoire* (MSc thesis, École Polytechnique de Montréal, Montreal, Canada).

Pinto, N. L. D. S., Filho, P. L. M., & Maurer, E. (1985). Foz do Areia Dam\= Design, Construction, and Behaviour. *Concrete Face Rockfill Dams\= Design, Construction, and Performance*, 173-191.

P'kla, A., & Ayite, y. m. x. d. (2020). Comparative analysis of Broukou and Kpasside clay soils permeability coefficient measured from porchet and variable load pemeameter tests. *Annals of the Faculty of Engineering Hunedoara*, *18*(2), 127-133.

Potvin, Y., Thomas, E., & Fourie, A. (2005). *Handbook on mine fill*. Perth, Autaralia: Australian Centre for Geomechanics.

Powers, M. C. (1953). A new roundness scale for sedimentary particles. *Journal of Sedimentary Research*, *23*(2), 117-119.

Ramamurthy, T. (2004). A geo-engineering classification for rocks and rock masses. *International Journal of Rock Mechanics and Mining Sciences*, *41*(1), 89-101.

Rao, S. V., Bajaj, S., & Dhanote, S. (2011). Evaluations of strength parameters of rockfill material for Pakaldul hydroelectric project, Jammu and Kashmir—a case study. In *Proceedings of the 2011 Indian Geotechnical Conference*, Kochi, India (pp. 991-994).

Rathee, R. K. (1981). Shear strength of granular soils and its prediction by modeling techniques. *Journal of Institution of Engineers*, 62, 64-70.

Ren, Xingwei, ZHAO, Yang, DENG, & Qinglu, et al. (2016). A relation of hydraulic conductivity—void ratio for soils based on Kozeny-Carman equation. *Engineering geology*, 213, 89-97.

Rose, H. E. & Rizk, A. (1949). Further researches in fluid flow through beds of granular materials. *Proceedings – Institution of Mechanical Engineers*, 160, 493–511.

Rousé, P. (2014). Comparison of methods for the measurement of the angle of repose of granular materials. *Geotechnical Testing Journal*, *37*(1), 164-168.

Rowe, R. K., Armstrong, M. D., & Cullimore, D. R. (2000). Particle size and clogging of granular media permeated with leachate. *Journal of Geotechnical and Geoenvironmental Engineering*, *126*(9), 775-786.

Saberian, M., Li, J., Perera, S. T. A. M., Zhou, A., Roychand, R., & Ren, G. (2021). Large-scale direct shear testing of waste crushed rock reinforced with waste rubber as pavement base/subbase materials. *Transportation Geotechnics*, *28*, 100546.

Saleh-Mbemba, F., Aubertin, M., & Boudrias, G. (2019). Drainage and consolidation of mine tailings near waste rock inclusions. In *Sustainable and Safe Dams Around the World* (pp. 3296-3305).

Salimi, S. N., Yazdanjou, V., & Hamidi, A. (2008). Shape and size effects of gravel grains on the shear behavior of sandy soils. *In Landslides and Engineered Slopes. From the Past to the Future*, (pp. 491-496). CRC Press.

Santamarina, J. C., & Cho, G. C. (2001). Determination of critical state parameters in sandy soils—simple procedure, *Geotechnical Testing Journal, 24*(2), 185–192.

Santamarina, J. C., & Cho, G. C. (2004). Soil behaviour: The role of particle shape. In Advances in geotechnical engineering: *The Skempton conference: Proceedings of a three day Conference on Advances in Geotechnical Engineering*, Organised by the Institution of Civil Engineers and held at the Royal Geographical Society, London, UK, (pp. 604-617).

Scarpelli, G., & Wood, D. M. (1982). Experimental observations of shear patterns in direct shear tests. In *IUTAM Deformation and Failure of Granular Materials Conference* (pp. 473-483).

Schulze-Makuch, D., Carlson, D. A., Cherkauer, D. S., & Malik, P. (1999). Scale dependency of hydraulic conductivity in heterogeneous media. *Groundwater*, *37*(6), 904-919.

Seif El Dine, B., Dupla, J. C., Frank, R., Canou, J., & Kazan, Y. (2010). Mechanical characterization of matrix coarse-grained soils with a large-sized triaxial device. *Canadian Geotechnical Journal*, *47*(4), 425-438.

Selig, E. T., & Roner, C. J. (1987). Effects of particle characteristics on behavior of granular material. *Transportation Research Record*, (1131).

Sharma, V. M., Venkatachalam, K., & Roy, A. (1994). Strength and deformation characteristics of rockfill materials. *In Proceeding of the International Conference on Soil Mechanics and Foundation Engineering* (pp. 959-962).

Shepherd, R. G., (1989). Correlations of permeability and grain size. *Ground water, 27*(5), 633-638.

Sivakugan, N., Rankine, K., & Rankine, R. (2006). Permeability of hydraulic fills and barricade bricks. *Geotechnical and Geological Engineering, 24*(3), 661-673.

Skempton, A. W. (1958). Arthur Langtry Bell (1874 – 1956) and his contribution to soil mechanics. *Geotechnique, 8*(4), 143-157.

Slichter, C.S., 1898. *Theoretical investigation of the motion of ground waters*. In: 19th Annual Report. US Geology Survey, 2, 295–384.

Somerton, C.W., Wood, P., 1988. Effects of walls in modeling flow through porous media. *Journal of Hydraulic Engineering, 114*(12), 1431–1448.

Statham, I. (1974). The relationship of porosity and angle of repose to mixture proportions in assemblages of different sized materials. *Sedimentology, 21*(1), 149-162.

Stibinger, J. (2014). *Examples of determining the hydraulic conductivity of soils, theory and applications of selected basic methods*. University Handbook on Soil Hydraulics, Purkyně University in Ústí n. Labem.

Stormont, J. C., & Farfan, E. (2005). Stability evaluation of a mine waste pile. *Environmental & Engineering Geoscience, 11*(1), 43-52.

Svensson, A. (2014). *Estimation of hydraulic conductivity from grain size analyses* (Master thesis, Chalmers University of Technology: Gothenburg, Sweden).

Tachie-Menson, S. (2006). *Characterization of the acid-Producing potential and investigation of its effect on weathering of the Goathill North Rock Pile at the Questa Molybdenum Mine, New Mexico* (Doctoral dissertation, New Mexico Institute of Mining and Technology).

Takada, N. (1993). Mikasa's direct shear apparatus, test procedures and results. *Geotechnical Testing Journal, 16*(3), 314-322.

Tardif-Drolet, M., Li, L., Pabst, T., Zagury, G. J., Mermillod-Blondin, R., & Genty, T. (2020). Revue de la réglementation sur la valorisation des résidus miniers hors site au Québec. *Environmental Reviews*, *28*(1), 32-44.

Taylor, D. W. (1948). *Fundamentals of soil mechanics*. New York, US: John Wiley & Sons.

Terzaghi, K. (1925). Principles of soil mechanics: III. Determination of permeability of clay. *Engineering News Records*, *95*(21), 832–836.

Terzaghi, K. V. (1936). The shearing resistance of saturated soils and the angle between the planes of shear. In *First International Conference on Soil Mechanics* (Vol. 1, pp. 54-59).

Terzaghi, K., & Peck, R.B. (1948). *Soil mechanics in engineering practice*. New York, USA: John Wiley and Sons, Inc.

Todd, D. & Mays, L. (2005). *Groundwater hydrology (3d ed.)*. John Willey & Sons, Inc.

Tombs, S. G. (1969). *Strength and deformation characteristics of rockfill* (Doctoral Thesis, Imperial College London, London, UK).

Torrey III, V. H., & Donaghe, R. T. (1991). *Compaction characteristics of earth-rock mixtures*. Army Engineer Waterways Experiment Station Vicksburg MS Geotechnical Lab.

Unified Facilities Criteria (UFC). (2022). *Soil mechanics (DM 7.1)*. Retrieved from https://www.wbdg.org/FFC/DOD/UFC/ufc_3_220_10_2022.pdf.

US Army Corps Engineers, (1965). *Laboratory soil testing*. Technical Report, EM 1110-2-1906.

Valenzuela, L., Bard, E., Campana, J. & Anabalon, M. (2008). High waste rock dumps - challenges and developments. Rock Dumps 2008 — A. Fourie (ed). *Australian Centre for Geomechanics*, Perth, ISBN 978-0-9804185-3-8.

Valentin, R., Sardini, P., Mazurier, A., Regnault, O., & Descostes, M. (2016). Effective porosity measurements of poorly consolidated materials using non-destructive methods. *Engineering Geology*, 205, 24–29.

Vallerga, B., Seed, H., Monismith, C., & Cooper, R. (1957). Effect of shape, size, and surface roughness of aggregate particles on the strength of granular materials. *In Road and Paving Materials*: ASTM International.

Varadarajan, A., Sharma, K. G., Abbas, S. M., & Dhawan, A. K. (2006). The role of nature of particles on the behavior of rockfill material. *Soils and Foundations*, *46*(5), 569-584.

Varadarajan, A., Sharma, K. G., Venkatachalam, K., & Gupta, A. K. (2003). Testing and modeling two rockfill materials. *Journal of Geotechnical and Geoenvironmental Engineering*, *129*(3), 206-218.

Vasistha, Y., Gupta, A. K., & Kanwar, V. (2013). Medium triaxial testing of some rockfill materials. Electronic *Journal of Geotechnical Engineering*, *18*(D), 923-964.

Venkatachalam, K. (1993). *Prediction of mechanical behavior of rockfill materials* (Doctoral Dissertation, Indian Institute of Technology).

Verdugo, R. & De la Hoz, K. (2006). Strength and stiffness of coarse granular soils. Soil Stress-Strain Behavior: Measurement, Modeling and Analysis, *Geotechnical Symposium in Roma* (PP. 243-252).

Vukovic, M., & Soro, A. (1992). *Determination of hydraulic conductivity of porous media from grain-size composition*. Littleton, Colo: Water Resources Publications.

Wang, Y., Shao, S., & Wang, Z. (2019). Effect of particle breakage and shape on the mechanical behaviors of granular materials. *Advances in Civil Engineering*, *2019*(7248427).

Wickland, B. E., & Wilson, G. W. (2005). Self-weight consolidation of mixtures of mine waste rock and tailings. *Canadian Geotechnical Journal*, *42*(2), 327-339.

Williams, D.J. (2000). Assessment of embankment parameters. *Proceedings Slope Stability in Surface Mining. SME. Denver, CO* (pp. 275-284).

Williams, D. J., & Walker, L. K. (1983). *Laboratory and field strength of mine waste rock*, Research Report No. CE 48, University of Queensland. Australia.

Williams, D.J. & Rohde, T.K. (2008). Rainfall infiltration into and seepage from rock dumps—a review, *Australian Centre for Geomechanics*, Perth (pp. 79-89).

Wilson, G. (2000). Embankment hydrology and unsaturated flow in waste rock. *Slope stability in surface mining. Society for Mining Metallurgy*, *305*.

Wu, P. K., Matsushima, K., & Tatsuoka, F. (2008). Effects of specimen size and some other factors on the strength and deformation of granular soil in direct shear tests. *Geotechnical Testing Journal*, *31*(1), 45-64.

Xu, Y. (2018). Shear strength of granular materials based on fractal fragmentation of particles. *Powder Technology*, *333*, 1-8.

Xu, Y., Williams, D. J., Serati, M., & Vangsness, T. (2018). Effects of scalping on direct shear strength of crusher run and crusher run/geogrid interface. *Journal of Materials in Civil Engineering*, *30*(9), 04018206.

Xu, X., Fall, M., Alainachi, I., & Fang, K. (2019). Characterisation of fibre-reinforced backfill/rock interface through direct shear tests. *Geotechnical Research*, *7*(1), 11-25.

Xue, Z. F., Cheng, W. C., Wang, L., & Song, G. (2021). Improvement of the shearing behaviour of loess using recycled straw fiber reinforcement. *KSCE Journal of Civil Engineering*, 1-17.

Yaghoubi, E., Arulrajah, A., Yaghoubi, M., & Horpibulsuk, S. (2020). Shear strength properties and stress–strain behavior of waste foundry sand. *Construction and Building Materials*, *249*, 118761.

Yang, P., Li, L., Aubertin, M., Brochu-Baekelmans, M., & Ouellet, S. (2017). Stability analyses of waste rock barricades designed to retain paste backfill. *International Journal of Geomechanics*, *17*(3), 04016079.

Yang, G., Jiang, Y., Nimbalkar, S., Sun, Y., & Li, N. (2019). Influence of particle size distribution on the critical state of rockfill. *Advances in Civil Engineering*, *2019*.

Yu, X., Ji, S., & Janoyan, K. D. (2006). Direct shear testing of rockfill material. In *Soil and Rock Behavior and Modeling* (pp. 149-155).

Zeller, J., & Wullimann, R. (1957). The shear strength of the shell materials for the Go-Schenenalp Dam, Switzerland. In *4th International Conference on Soil Mechanics and Foundation Engineering* (Vol. 2, pp. 399-415).

Zahran, K., & Naggar, H. E. (2020). Effect of sample size on TDA shear strength parameters in direct shear tests. *Transportation Research Record*, *2674*(9), 1110-1119.

Zhai, Y., Li, L., & Chapuis, R. P. (2021a). Analytical, Numerical and Experimental Studies on Steady-State Seepage Through 3D Rockfill Trapezoidal Dikes. *Mine Water and the Environment*, *40*(4), 931-942.

Zhai, Y., Yang, P., & Li, L. (2021b). Analytical solutions for the design of shotcreted waste rock barricades to retain slurried paste backfill. *Construction and Building Materials*, *307*, 124626.

Zhang, Z. L., Xu, W. J., Xia, W., & Zhang, H. Y. (2016). Large scale in situ test for mechanical characterization of soil rock mixture used in an embankment dam. *International Journal of Rock Mechanics and Mining Sciences*, *86*, 317-322.

Zhang, Z., Sheng, Q., Fu, X., Zhou, Y., Huang, J., & Du, Y. (2020). An approach to predicting the shear strength of soil-rock mixture based on rock block proportion. *Bulletin of engineering Geology and the Environment*, *79*(5), 2423-2437.

Ziaie Moayed, R., Alibolandi, M., & Alizadeh, A. (2017). Specimen size effects on direct shear test of silty sands. *International Journal of Geotechnical Engineering*, *11*(2), 198-205.

Zięba, Z. (2017). Influence of soil particle shape on saturated hydraulic conductivity. *Journal of Hydrology and Hydromechanics*, *65*(1), 80.

Zolkov, E., & Wiseman, G. (1965). Engineering properties of dune and beach sands and the influence of stress history. *In Proc. of Sixth Int. Conference on Soil Mechanics and Foundation Engineering* (Vol. 1, pp. 134-138).

APPENDIX A – ADDITIONAL RESULTS RELATED TO CHAPTER 5

A.1. Specimen preparation with the same void ratio

In order to prepare the specimens of mini, small and large shear boxes with the same loose state, the following steps are followed:

1- Shear box dimensions are measured and the volumes of the boxes are calculated.

$V_{mini} = 0.038 \times 0.038 \times 0.045 = 6.5E-05\ m^3$

$V_{small} = 0.06 \times 0.06 \times 0.045 = 0.000162\ m^3$

$V_{large} = 0.3 \times 0.3 \times 0.18 = 0.0162\ m^3$

2- G_s of all samples are estimated by following ASTM C128-15 as shown in Table A.1.

3- A known portion taken from one sample (for example d_{max} = 5 mm) is slowly poured into the large shear box using a scoop to fill the box to the edge and obtain a loose specimen.

4- Using the mass of the material, volume of the shear box and G_s, density and e_{max} of the specimen are calculated.

M_s: Mass of the material = 23.5 kg

G_s = 2.65

$\rho_w = 998\,\frac{kg}{m^3}$

$\rho_s = M_s/V_{box}$ = 1450 Kg/m^3

$$e_{\max} = \frac{G_s \times \rho_w}{\rho_s} - 1 = \frac{2.65 \times 998}{1450} - 1 = 0.8$$

5- The e_{max} value is then used to obtain the precise required mass of the specimens for the mini and small shear boxes.

$M_s = (V_{box} \times (G_s \times \rho_w))/(e_{max} + 1)$

Required M_s for mini shear box:

M_s = 0.000065 × (2.65 × 998)/ (0.8+1) = 0.095 kg = 95 gr

Required M_s for small shear box:

$M_s = 0.000162 \times (2.65 \times 998)/ (0.8+1) = 0.238$ kg = 238 gr

6- The same procedure was repeated for all the samples. Table A.1 shows the required masses of all the samples of WR 1 and WR 2.

Table A.1 G_s and the required masses of all the samples for WR 1 and WR 2

d_{max} (mm)	G_s		M_s (gr)					
			38 mm × 38 mm × 45 mm		60 mm × 60 mm × 45 mm		300 mm × 300 mm × 180 mm	
	WR 1	WR 2	WR 1	WR 2	WR 1	WR 2	WR 1	WR 2
0.85	2.81	2.78	94.6	98.2	235.9	244.8	23586.5	24476.1
1.19	2.72	2.71	94.5	98.4	235.6	245.3	23563.6	24526.3
1.4	2.68	2.67	94.6	100.3	239.5	250.0	23947.8	25002.3
2.36	2.73	2.69	94.4	99.9	235.2	249.0	23524.5	24901.7
3.36	2.68	2.71	94.1	101.2	234.7	252.3	23468.1	25231.0
5.0	2.65	2.73	95.7	100.2	238.5	249.9	23850.0	24986.4
6.0	2.59	2.72	94.5	102.8	256.2	247.6	23571.9	25618.6

A.2. Effects of shear length scale

This section presents the macroscopic evidences of progressive failures observed in the stress ratio curves of the tested materials made of WR 1 (see Figure 5.4). Figure A.1 shows the shear stress ratios (τ/σ) obtained using mini, small and large shear boxes at a normal stress of 150 kPa against applied shear strain.

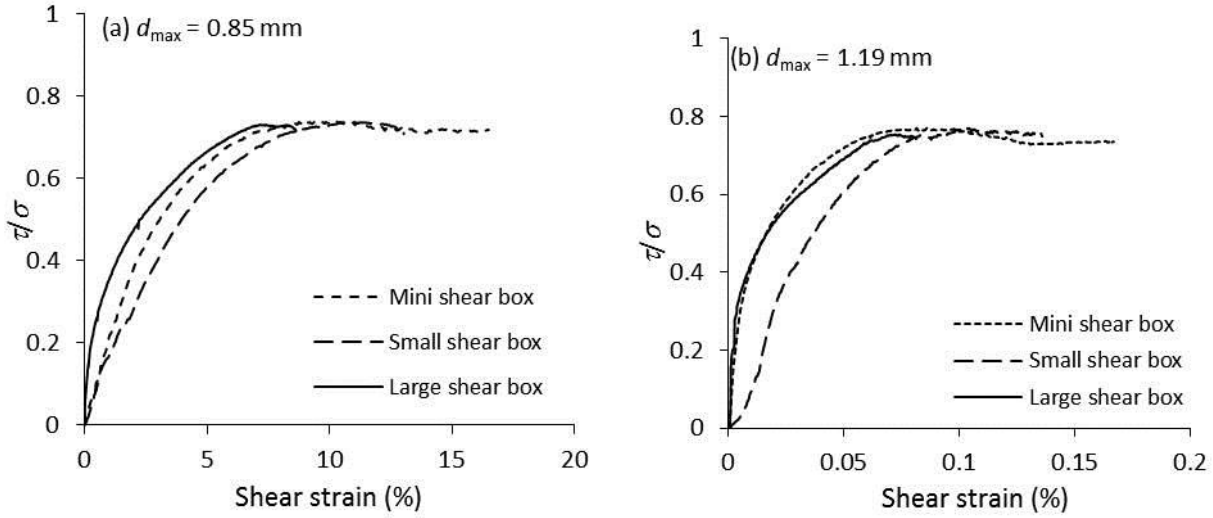

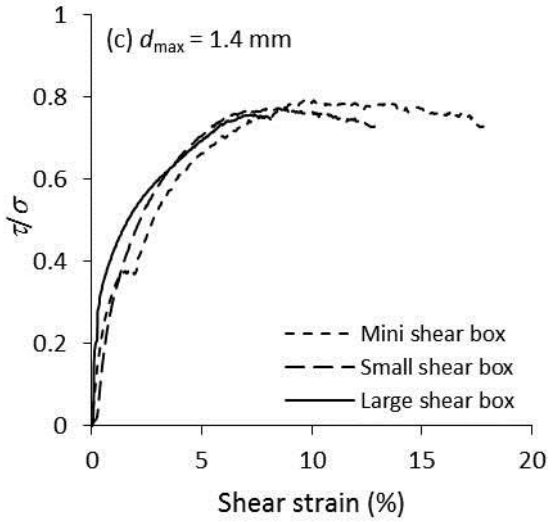
(c) d_{max} = 1.4 mm
τ/σ
Shear strain (%)
Mini shear box
Small shear box
Large shear box

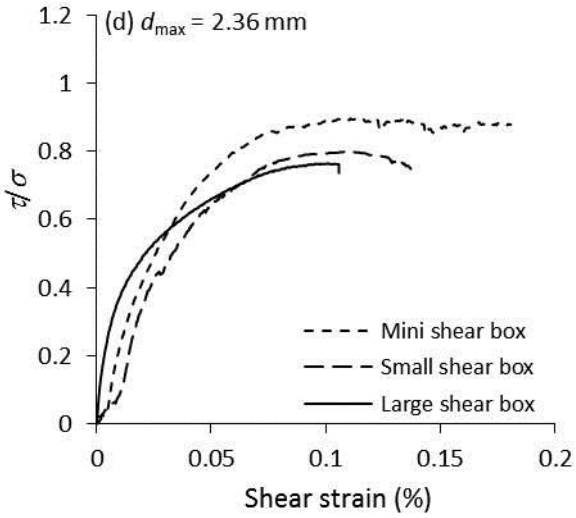
(d) d_{max} = 2.36 mm
τ/σ
Shear strain (%)
Mini shear box
Small shear box
Large shear box

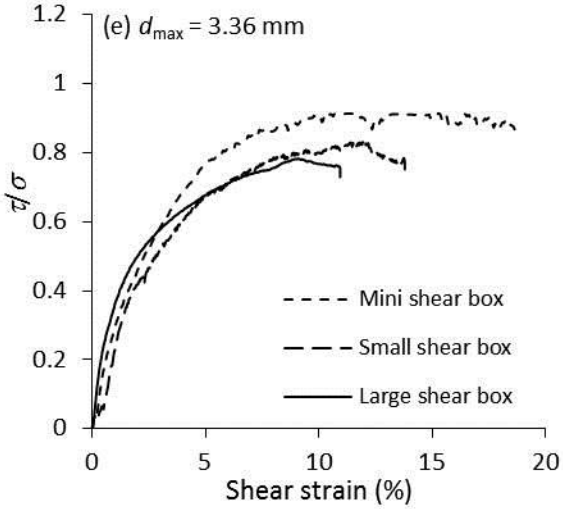
(e) d_{max} = 3.36 mm
τ/σ
Shear strain (%)
Mini shear box
Small shear box
Large shear box

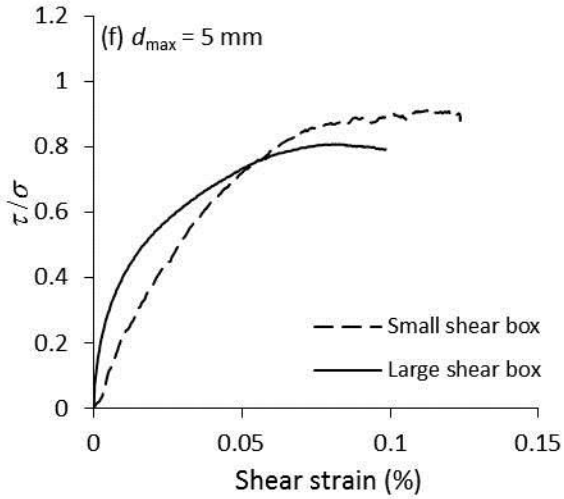
(f) d_{max} = 5 mm
τ/σ
Shear strain (%)
Small shear box
Large shear box

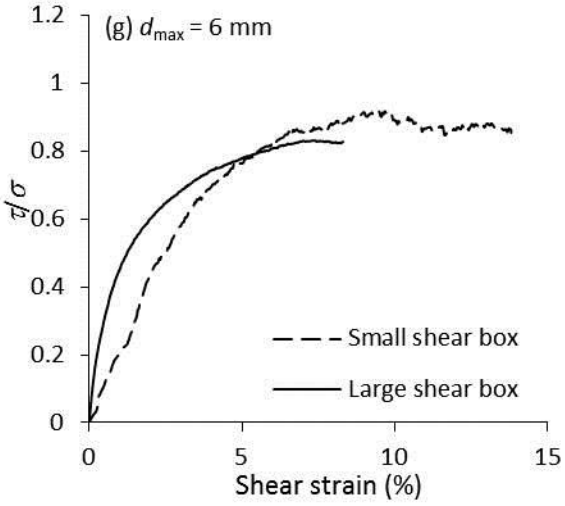
(g) d_{max} = 6 mm
τ/σ
Shear strain (%)
Small shear box
Large shear box

Figure A.1 Stress ratio (τ/σ) versus applied shear strain at a normal stress of 150 kPa obtained by mini, small and large shear boxes for the materials made of WR 1

As shown in Figures A.1a to A.1c for the fine particle materials, the peak stress ratios obtained by the mini, small and large shear boxes are almost identical and it is interesting to find that the peak shear ratios occur almost in the same shear strain. However, as it is seen in Figures A.1d to A.1g, the peak stress ratio decreases when the specimen size or the shear box size increases. More importantly, the shear strain at the peak stress ratio increases significantly as the specimen size decreases. This observation may be explained by the fact that when the specimen size is large enough, the influence of individual particles is diminished and the shearing resistance is gradually mobilized along the shear band, resulting in progressive failure. When the specimen size is very small, however, the influence of individual particles near the shear plane ameliorates in terms of shearing and dilation, which prevent the shear band from completely advancing into the specimen, resulting in local failure and overestimation of the shear strength.

APPENDIX B – ADDITIONAL RESULTS RELATED TO CHAPTER 6

B.1. Scalping scaled down samples

Tables B.1 and B.2 show portions of different particle sizes of field samples and scaled down samples prepared by applying the scalping technique for M1 and M3 and M2, respectively.

Table B.1 Portion distributions of field samples and scalped down samples for M1 and M3

Range of particle sizes	**Portion (%)**				
	d_{max} = 5 mm	**3.36 mm**	**2.36 mm**	**1.4 mm**	**1.19 mm**
3.36 – 5 mm	30.3				
2.36 – 3.36 mm	22.0	31.6			
1.40 – 2.36 mm	10.4	15.0	21.9		
1.19 – 1.40 mm	2.9	4.1	6.0	7.7	
0.85 – 1.19 mm	12.3	17.7	25.8	33.1	35.9
0.63 – 0.85 mm	8.0	11.5	16.8	21.5	23.3
0.315 – 0.63 mm	2.5	3.6	5.3	6.7	7.3
0.16 – 0.315 mm	1.8	2.5	3.7	4.7	5.1
0.08 – 0.16 mm	5.4	7.8	11.4	14.6	15.8
< 0.08 mm	4.3	6.2	9.1	11.6	12.6

Table B.2 Portion distributions of field samples and scalped down samples for M2

Range of particle sizes	**Portion (%)**				
	d_{max} = 5 mm	**3.36 mm**	**2.36 mm**	**1.4 mm**	**1.19 mm**
3.36 – 5 mm	23.8				
2.36 – 3.36 mm	18.1	26.3			
1.40 – 2.36 mm	10.7	12.4	16.0		
1.19 – 1.40 mm	5.2	5.5	7.2	9.9	
0.85 – 1.19 mm	11.3	16.0	19.3	19.8	23.6
0.63 – 0.85 mm	9.1	9.5	18.1	24.0	25.1
0.315 – 0.63 mm	4.7	8.2	12.3	12.4	13.7
0.16 – 0.315 mm	4.5	5.9	8.2	10.1	10.3
0.08 – 0.16 mm	6.7	8.8	11.0	14.1	14.9
< 0.08 mm	5.9	7.4	8.0	9.8	12.4

B.2. Parallel scaled down samples

To prepare the scaled down samples by applying parallel technique to the field samples, one has to first determine the ratio between d_{max} of the field sample and the required d_{max} of scaled down samples. Then, the ratio is applied to the field sample PSD curves to scale down the particle sizes

of the field samples and obtain the parallel scaled down samples. Table B.3 presents the ratios calculated for the scaled down samples with different d_{max} values.

Table B.3 The ratio of N calculated for scaled down samples prepared by applying parallel technique to the field sample PSD curve

Sample	**d_{max} (mm)**	**N = d_{max} of field sample/d_{max} of scaled down sample**
Field sample	5.0	-----
Parallel scaled down sample	3.36	5/3.36 = 1.49
	2.36	5/2.36 = 2.12
	1.4	5/1.4 = 3.57
	1.19	5/1.19 = 4.2

Tables B.4 to B.6 show the calculated and selected ranges of particle sizes of the scaled down samples prepared by applying parallel technique for M1, M2 and M3.

The calculated particle sizes are obtained by using the ratio of N (Equation 6.1) and the PSD curve of the field samples (Figure 6.2). When the calculated particle sizes can not be obtained due to the availability of the specific sieve numbers, the selected particle sizes are used.

Table B.4 Calculated and selected particle sizes of parallel scaled down sample with d_{max} = 2.36 mm for field samples M1, M2, and M3

Range of particle sizes of field sample	**Range of particle sizes of parallel scaled down sample**		**Portion (%)**	
	Calculated	**Chosen**	**M1 and M3**	**M2**
3.36 – 5 mm	1.59 – 2.36 mm	1.4 – 2.36 mm	30.3	23.8
2.36 – 3.36 mm	1.11 – 1.59 mm	1.19 – 1.4 mm	22.0	18.1
1.40 – 2.36 mm	0.66 – 1.11 mm	0.63 – 1.19 mm	10.4	10.7
1.19 – 1.40 mm	0.56 – 0.66 mm	0.56 – 0.63 mm	2.9	5.2
0.85 – 1.19 mm	0.40 – 0.56 mm	0.42 – 0.56 mm	12.3	11.3
0.63 – 0.85 mm	0.30 – 0.40 mm	0.315 – 0.42 mm	8.0	9.1
0.315 – 0.63 mm	0.15 – 0.30 mm	0.16 – 0.315 mm	2.5	4.7
0.16 – 0.315 mm	0.075 – 0.15 mm	0.08 – 0.16 mm	1.8	4.5
0.08 – 0.16 mm	0.038 – 0.075 mm	0.038 – 0.08 mm	5.4	6.7
< 0.08 mm	< 0.038 mm	< 0.038 mm	4.3	5.9

Table B.5 Calculated and selected particle sizes of parallel scaled sample with d_{max} = 1.4 mm for field samples M1, M2, and M3

Range of particle sizes of field sample	**Range of particle sizes of parallel scaled down sample**		**Portion (%)**	
	Calculated	**Chosen**	**M1 and M3**	**M2**

3.36 – 5 mm	0.94 – 1.4 mm	1.0 – 1.4 mm	30.3	23.8
2.36 – 3.36 mm	0.66 – 0.94 mm	0.63 – 1.0 mm	22.0	18.1
1.40 – 2.36 mm	0.39 – 0.66 mm	0.42 – 0.63 mm	10.4	10.7
1.19 – 1.40 mm	0.33 – 0.39 mm	0.35 – 0.42 mm	2.9	5.2
0.85 – 1.19 mm	0.24 – 0.33 mm	0.25 – 0.35 mm	12.3	11.3
0.63 – 0.85 mm	0.176 – 0.24 mm	0.18 – 0.25 mm	8.0	9.1
0.315 – 0.63 mm	0.09 – 0.176 mm	0.09 – 0.18 mm	2.5	4.7
0.16 – 0.315 mm	0.045 – 0.09 mm	0.045 – 0.09 mm	1.8	4.5
0.08 – 0.16 mm	0.022 – 0.045 mm	0.022 – 0.045 mm	5.4	6.7
< 0.08 mm	< 0.022 mm	< 0.02 mm	4.3	5.9

Table B.6 Calculated and selected particle sizes of parallel scaled down sample with d_{max} = 1.19 mm for field samples M1, M2, and M3

Range of particle sizes of field sample	**Range of particle sizes of parallel scaled down sample**		**Portion (%)**	
	Calculated	**Chosen**	**M1 and M3**	**M2**
3.36 – 5 mm	0.79 – 1.19 mm	0.80 – 1.19 mm	30.3	23.8
2.36 – 3.36 mm	0.56 – 0.79 mm	0.56 – 0.80 mm	22.0	18.1
1.40 – 2.36 mm	0.33 – 0.56 mm	0.35 – 0.56 mm	10.4	10.7
1.19 – 1.40 mm	0.28 – 0.33 mm	0.28 – 0.35 mm	2.9	5.2
0.85 – 1.19 mm	0.20 – 0.28 mm	0.21 – 0.28 mm	12.3	11.3
0.63 – 0.85 mm	0.15 – 0.20 mm	0.16 – 0.21 mm	8.0	9.1
0.315 – 0.63 mm	0.075 – 0.15 mm	0.08 – 0.16 mm	2.5	4.7
0.16 – 0.315 mm	0.038 – 0.075 mm	0.038 – 0.08 mm	1.8	4.5
0.08 – 0.16 mm	0.019 – 0.038 mm	0.02 – 0.038 mm	5.4	6.7
< 0.08 mm	< 0.019 mm	< 0.02 mm	4.3	5.9

B.3. Details on specimen preparation with the same density

In order to prepare the specimens of scaled down samples with the same loose density as that of the field sample, the following steps are followed.

1- Shear box dimensions are measured and the volume of the box is calculated.

$$V_{box} = 0.3 \times 0.3 \times 0.18 = 0.0162\ m^3$$

2- G_s of field samples and scaled down samples are estimated by following ASTM C128-15 as shown in Table B.7.

3- A known portion taken from a field sample (for example M1) is slowly poured into the shear box using a scoop to fill the box to the edge and obtain a loose specimen.

4- Using the mass of the material, volume of the shear box and G_s, density and the e_{max} of the specimen are calculated.

M_s: Mass of M1 = 26.9 kg

G_s = 2.65

$$\rho_w = 998 \frac{kg}{m^3}$$

$\rho_s = M_s/V_{box}$ = 1665 Kg/m^3

$$e_{max} = \frac{G_s \times \rho_w}{\rho_s} - 1 = \frac{2.65 \times 998}{1665} - 1 = 0.59$$

5- The e_{max} value of the field sample (M1) is then used to obtain the precise required mass of the scaled downs samples obtained by applying scaling down techniques on M1 for the same shear box.

$$M_s = (V_{box} \times (G_s \times \rho_w))/(e_{max} + 1)$$

6- The same procedure was followed for the field samples of M2 and M3. Table B.7 shows the masses of the field and scaled down samples.

Table B.7 G_s values and the required masses of the field samples and the scaled down samples for M1, M2 and M3

Sample	d_{max} **(mm)**	***Gs***			M_s **(kg)**		
		M1	**M2**	**M3**	**M1**	**M2**	**M3**
Field sample	5.0	2.65	2.72	2.73	26.9	25.9	26.9
Scalping scaled down samples	3.36	2.68	2.70	2.71	27.3	25.8	26.4
	2.36	2.73	2.69	2.73	28.2	25.9	26.3
	1.4	2.68	2.68	2.68	27.3	26.0	26.3
	1.19	2.72	2.70	2.71	27.7	26.3	26.2
Parallel scaled down samples	3.36	2.70	2.75	2.69	27.5	26.2	26.3
	2.36	2.65	2.61	2.68	27.0	25.3	26.3
	1.4	2.67	2.67	2.73	27.2	25.8	26.3
	1.19	2.69	2.71	2.70	27.4	26.3	26.4

B.4. Typical results of direct shear tests

Figure B.1 shows the shear stress - displacement curves of the scaled down samples with different d_{max} prepared by applying scalping and parallel techniques to the field samples of M1, M2 and M3, obtained with medium and large shear boxes.

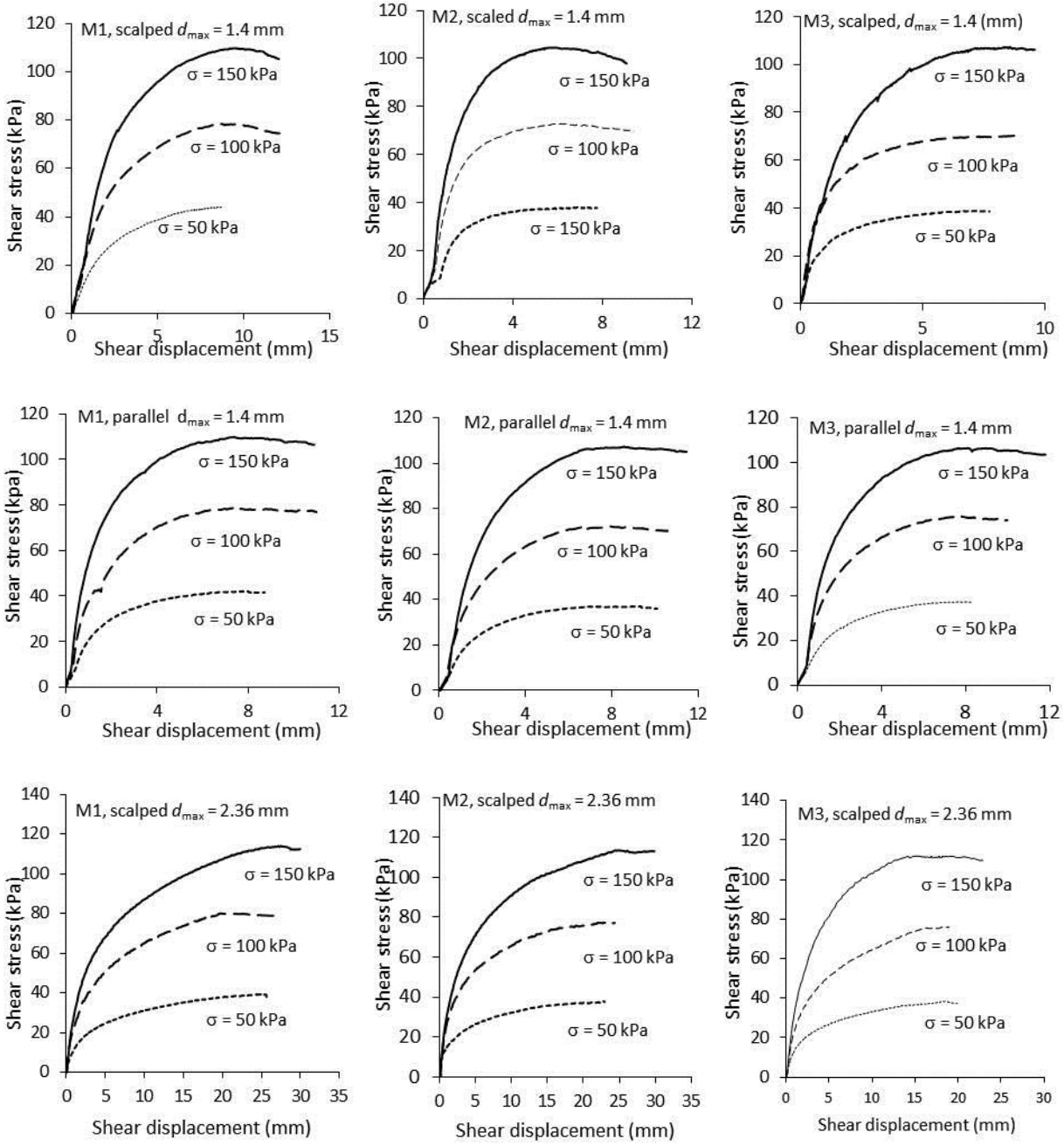

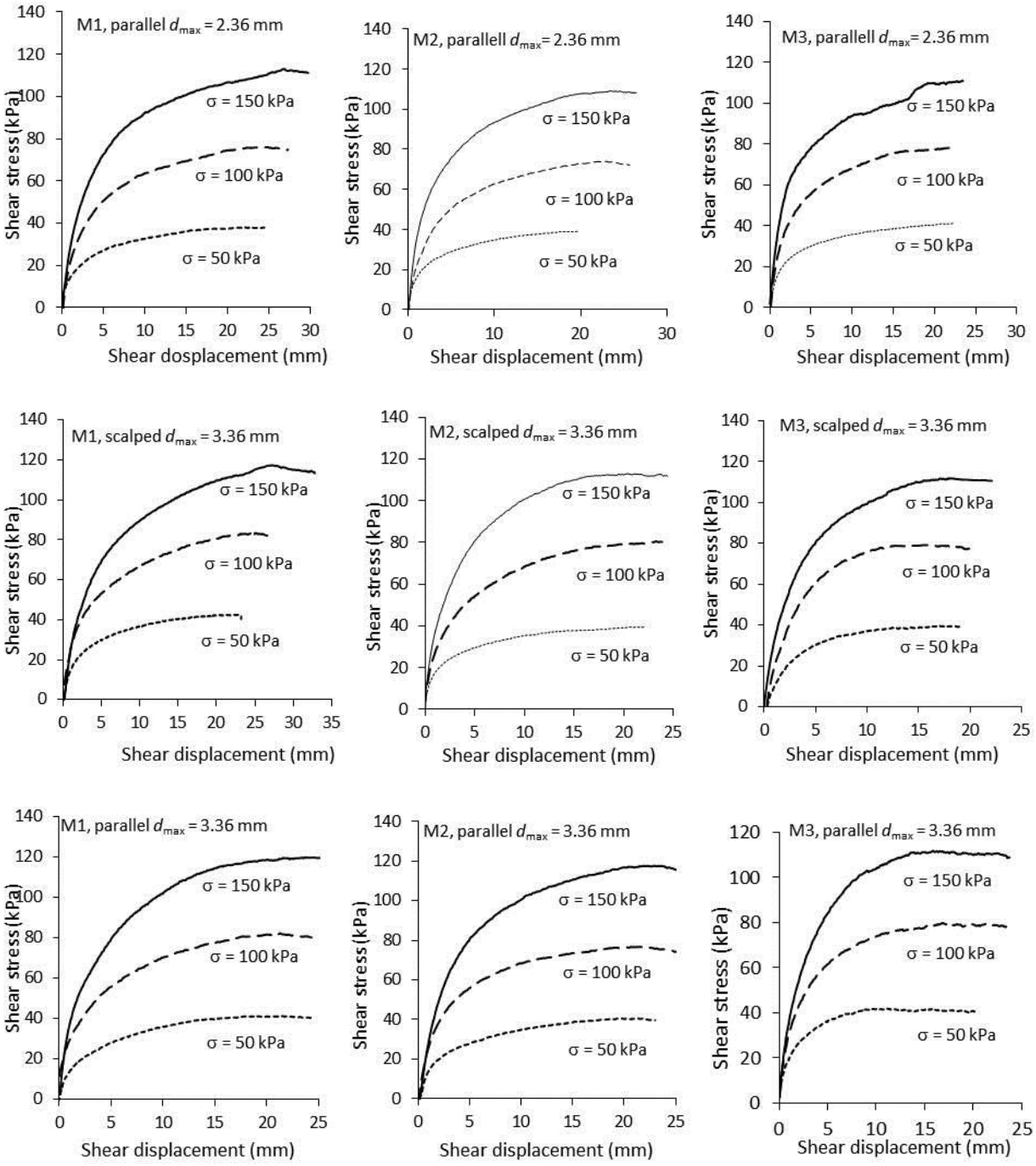

Figure B.1 Shear stress - shear displacement curves of scaled down samples with different d_{max} values prepared by applying scalping and parallel techniques for M1, M2, and M3, respectively

APPENDIX C – ADDITIONAL RESULTS RELATED TO CHAPTER 7

C.1. Typical results of direct shear tests

Typical results of direct shear tests are plotted in Figure C.1 as the variations of shear stress with shear displacement for M2, M4, M6 and M8.

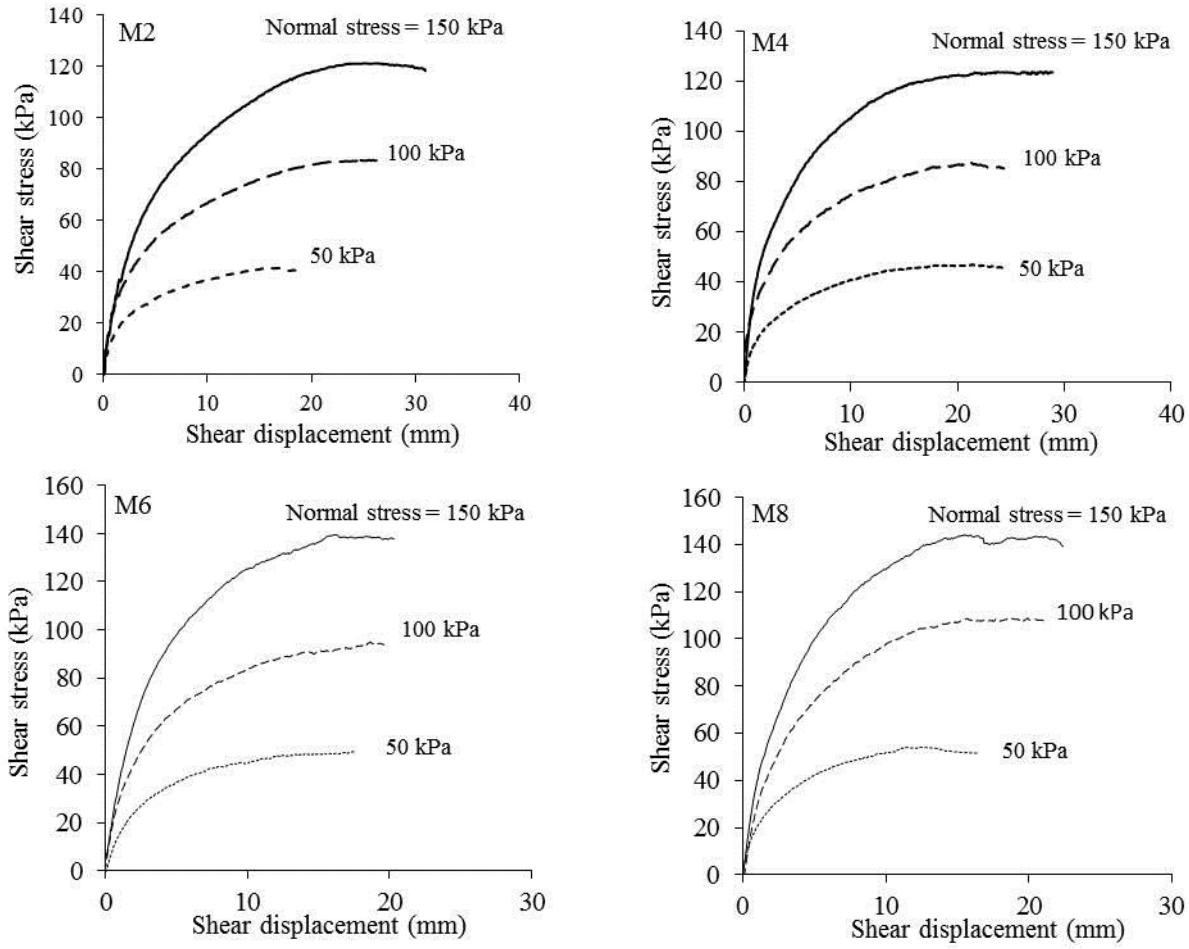

Figure C.1 Shear stress - displacement curves of M2, M4, M6 and M8 at three normal stresses

C.2. Pile size effect

Table C.1 shows the pile measurements and the repose angles determined for M1, M3, M5 and M7. Pile tests were repeated 3 times for each material. So, 192 measurements were obtained in total for the four materials.

Table C.1 The measurements and repose angles obtained by the pile tests for M1, M3, M5 and M7, h_p: pile height, d_p: bottom diameter of the pile and r: bottom radios of the pile

Material	d_{max} **(mm)**	(h_p) **(mm)**	h_p/d_{max}	$d_p/2$ *(mm)*	r/d_{max}	ϕ_{pt} **(°)**
M1	5	38.1	8	46.0	9	39.6
		54.0	11	65.5	13	39.5
		73.0	15	88.5	18	39.5
		101.6	20	123.5	25	39.4
		117.0	23	142.5	29	39.4
		127.0	25	155.0	31	39.3
		152.4	30	185.0	37	39.5
		165.1	33	200.0	40	39.5
		177.8	36	215.5	43	39.5
		185.0	37	222.5	45	39.7
		203.2	41	247.5	50	39.4
		228.6	46	275.0	55	39.7
		254.0	51	307.5	62	39.6
		279.4	56	337.5	68	39.6
		295.3	59	358.5	72	39.5
M1	5	38.1	8	46.5	9	39.3
		54.0	11	66.0	13	39.3
		73.0	15	89.0	18	39.4
		101.6	20	123.5	25	39.4
		117.0	23	141.0	28.2	39.7
		127.0	25	155.0	31	39.3
		152.4	30	182.5	37	39.9
		165.1	33	200.0	40.0	39.5
		177.8	36	214.0	43	39.7
		185.0	37	224.5	45	39.5
		203.2	41	246.5	49	39.5
		228.6	46	277.5	56	39.5
		254.0	51	309.0	62	39.4
		279.4	56	335.0	67	39.8

		311.2	62	376.5	75	39.6
M1	5	38.1	8	46.6	9	39.3
		54.0	11	66.5	13	39.1
		73.0	15	88.5	18	39.5
		101.6	20	123.5	25	39.4
		117.0	23	142.0	28.4	39.5
		127.0	25	153.5	30.7	39.6
		152.4	30	184.0	36.8	39.6
		165.1	33	202.5	40.5	39.2
		177.8	36	215.0	43.0	39.6
		185.0	37	222.5	44.5	39.7
		203.2	41	243.5	49	39.8
		228.6	46	275.0	55	39.7
		254.0	51	309.0	62	39.4
		279.4	56	337.5	68	39.6
		308.0	62	373.5	75	39.5
M3	9.5	47.6	5	57.5	6	39.6
		69.9	7	83.0	9	40.1
		82.6	9	97.5	10	40.3
		98.4	10	117.5	12	40.0
		114.3	12	136.5	14	39.9
		130.2	14	157.5	17	39.6
		142.9	15	172.5	18	39.6
		158.8	17	190.0	20	39.9
		184.2	19	222.5	23	39.6
		209.6	22	249.5	26	40.0
		235.0	25	278.5	29	40.2
		260.4	27	310.0	33	40.0
		285.8	30	342.5	36	39.8
		311.2	33	375.0	39	39.7
		336.6	35	398.5	42	40.2
M3	9.5	47.6	5	56.0	6	40.4
		69.9	7	83.0	9	40.1

		82.6	9	97.0	10	40.4
		98.4	10	115.5	12	40.4
		114.3	12	134.0	14	40.5
		130.2	14	156.0	16	39.8
		142.9	15	170.0	18	40.0
		158.8	17	188.5	20	40.1
		184.2	19	217.5	23	40.3
		209.6	22	245.0	26	40.5
		235.0	25	279.0	29	40.1
		260.4	27	312.5	33	39.8
		285.8	30	339.0	36	40.1
		311.2	33	365.0	38	40.4
		336.6	35	400.0	42	40.1
M3	9.5	47.6	5	56.5	6	40.1
		69.9	7	83.5	9	39.9
		82.6	9	99.0	10	39.8
		98.4	10	115.5	12	40.4
		114.3	12	135.0	14	40.3
		130.2	14	153.5	16	40.3
		142.9	15	171.0	18	39.9
		158.8	17	188.0	20	40.2
		184.2	19	220.0	23	39.9
		209.6	22	251.0	26	39.9
		235.0	25	281.0	30	39.9
		260.4	27	310.0	33	40.0
		285.8	30	335.0	35	40.5
		311.2	33	366.0	39	40.4
		336.6	35	395.0	42	40.4
M5	19	41.3	2	47.0	2	41.3
		60.3	3	68.5	4	41.4
		85.7	5	97.5	5	41.3
		114.3	6	130.0	7	41.3
		142.9	8	162.5	9	41.3
		168.3	9	192.5	10	41.2
		193.7	10	221.0	12	41.2

		219.1	12	250.0	13	41.2
		244.5	13	278.5	15	41.3
		257.2	14	291.0	15	41.5
		269.9	14	307.5	16	41.3
		298.5	16	341.5	18	41.2
		320.7	17	366.0	19	41.2
		346.1	18	395.0	21	41.2
		368.3	19	420.0	22	41.2
		381.0	20	432.5	23	41.4
		400.1	21	455.0	24	41.3
M5	19	41.3	2	47.0	2	41.3
		60.3	3	69.0	4	41.2
		85.7	5	98.0	5	41.2
		114.3	6	130.0	7	41.3
		142.9	8	162.5	9	41.3
		168.3	9	191.0	10	41.4
		193.7	10	221.0	12	41.2
		219.1	12	249.0	13	41.3
		244.5	13	278.5	15	41.3
		257.2	14	291.5	15	41.4
		269.9	14	307.5	16	41.3
		298.5	16	341.5	18	41.2
		320.7	17	367.5	19	41.1
		346.1	18	396.0	21	41.2
		371.5	20	425.0	22	41.2
		381.0	20	435.0	23	41.2
		400.1	21	455.0	24	41.3
M5	19	41.3	2	47.0	2	41.3
		60.3	3	69.0	4	41.2
		85.7	5	97.5	5	41.3
		114.3	6	131.0	7	41.1
		142.9	8	161.5	9	41.5
		168.3	9	190.5	10	41.5
		193.7	10	220.0	12	41.4
		219.1	12	250.0	13	41.2
		244.5	13	279.0	15	41.2
		257.2	14	292.5	15	41.3
		269.9	14	307.5	16	41.3
		298.5	16	341.0	18	41.2
		320.7	17	365.0	19	41.3

		346.1	18	395.0	21	41.2
		371.5	20	421.5	22	41.4
		381.0	20	432.5	23	41.4
		400.1	21	452.5	24	41.5
M7	25	38.1	1.5	43.0	2	41.5
		60.3	2	67.5	3	41.8
		85.7	3	96.5	4	41.6
		104.8	4	118.0	5	41.6
		120.7	5	136.0	5	41.6
		155.6	6	175.0	7	41.6
		190.5	8	214.0	9	41.7
		254.0	10	284.0	11	41.8
		263.5	11	294.0	12	41.9
		298.5	12	336.0	13	41.6
		320.7	13	360.5	14	41.7
		346.1	14	388.0	16	41.7
		368.3	15	415.0	17	41.6
		400.1	16	450.0	18	41.6
		428.6	17	481.0	19	41.7
		444.5	18	500.0	20	41.6
		498.5	20	562.5	23	41.5
M7	25	38.1	2	43.1	2	41.5
		60.3	2	68.0	3	41.6
		85.7	3	97.0	4	41.5
		104.8	4	118.5	5	41.5
		120.7	5	136.0	5	41.6
		155.6	6	175.0	7	41.6
		190.5	8	214.0	9	41.7
		254.0	10	285.0	11	41.7
		263.5	11	297.5	12	41.5
		298.5	12	336.0	13	41.6
		320.7	13	360.0	14	41.7
		346.1	14	389.0	16	41.7
		368.3	15	415.0	17	41.6
		400.1	16	447.0	18	41.8
		428.6	17	480.0	19	41.8
		444.5	18	497.5	20	41.8
		498.5	20	559.0	22	41.7
M7	25	38.1	2	43.1	2	41.5
		60.3	2	68.0	3	41.6
		85.7	3	97.0	4	41.5

		104.8	4	118.0	5	41.6
		120.7	5	136.5	5	41.5
		155.6	6	175.0	7	41.6
		190.5	8	214.0	9	41.7
		254.0	10	285.0	11	41.7
		263.5	11	295.0	12	41.8
		298.5	12	335.0	13	41.7
		320.7	13	360.5	14	41.7
		346.1	14	389.0	16	41.7
		368.3	15	412.5	17	41.8
		400.1	16	452.5	18	41.5
		428.6	17	482.5	19	41.6
		444.5	18	499.0	20	41.7
		498.5	20	562.5	23	41.5

APPENDIX D – ADDITIONAL RESULTS RELATED TO CHAPTER 8

D.1. Verification of the saturation degree (S_r) according to the weight method of Chapuis et al. (1989)

The weight method proposed by Chapuis et al. (1989) was used in this study to obtain the degree of saturation of the specimens by the following equations. Table D.1 shows the calculations of the degree of saturations for all the samples.

$$M_s = M_2 - M_1 \quad (D.1)$$

where M_s is the mass of dry soil; $M_1$is the mass of the dry permeameter alone; M_2 is the mass of the dry permeameter filled with dry soil.

$$M_{ms} = M_{tot} - (M_e - V\rho_w) \quad (D.2)$$

where M_{ms} is the mass of moist soil; M_{tot} is the total mass of the system (permeameter and all fittings, filled); M_e is the mass of the permeameter filled with de-aired water; V is the total volume.

$$M_w = M_{ms} - M_s \quad (D.3)$$

where M_w is the mass of water in the soil specimen; ρ_s is the density of solid particles; G is ρ_s/ρ_w, the specific gravity of solid. The volume of voids in the specimen is:

$$V_v = V - \left(\frac{M_s}{\rho_s}\right) \quad (D.4)$$

And degree of saturation is estimated as following equation:

$$S_r = \frac{V_w}{V_v} = \frac{M_w}{\rho_w V_w} = \frac{M_{tot} - M_e + V\rho_w - M_s}{V\rho_w - (\frac{M_s}{G})} \quad (D.5)$$

An example of the calculations for the sample with d_{max} = 5 mm using small column	
Mass of the dry column with accessories, M_1 (gr)	3092.5
Mass of the column filled with de-aired water and accessories M_e (gr)	4336
Mass of the dry column filled with dry soil and accessories M_2 (gr)	5185
Total mass of the system including column and accessories, soil and	5665

water, M_{tot} (gr)	
Mass of the dry soil, M_s (gr)	2092.5
Mass of the moist soil, M_{ms} (gr)	2427.8
Mass of water in the specimen, M_w (gr)	335.3
Volume of voids in the specimen, V_v (cm^3)	340.1
Degree of saturation, S_r (%)	98

Table D.1 Measurements and calculations of the weight method for all the samples

Material	D/d_{max}	V_{tot} (cm^3)	M_1 (gr)	M_e (gr)	M_2 (gr)	M_{tot} (gr)	M_s (gr)	M_{ms} (gr)	M_w (gr)	V_v (cm^3)	S_r
M1, d_{max} = 1.19 mm	86	1094.4	3121.7	4243.5	5235.6	5595.0	2113.9	2445.9	331.9	342.1	0.97
	127	3893.0	6773.7	11281.7	14310.7	16112.0	7537.0	8723.3	1186.3	1210.8	0.98
	170	9949.3	13586	23744	32852.0	36050.0	19266.0	22255.3	2989.3	3093.1	0.96
	252	64998	69669	140669	195619	221300	125950	145629	19679	20175.9	0.97
M2, d_{max} = 2.32 mm	43	1094.4	3121.7	4243.5	5109.5	5459.3	1987.8	2310.2	322.4	331.6	0.97
	64	3893.0	6773.7	11281.7	13869.2	15638.0	7095.5	8249.3	1153.8	1174.4	0.98
	86	9949.3	13586	23744	31720.0	34852.0	18134.0	21057.3	2923.3	3001.4	0.97
	127	64998	69669	140669	187619	212600	117950	136929	18979	19737	0.96
M3, d_{max} = 5 mm	20	1094.4	3121.5	4243.5	5195.0	5558.0	2073.3	2408.9	335.6	342.7	0.98
	30	3893.0	6773.7	11281.7	13999.0	15858.5	7225.3	8469.8	1244.5	1273.2	0.98
	40	9949.3	13586	23744	32500.0	35762.0	18914.0	21967.3	3053.3	3091.5	0.96
	60	64998	69669	140669	192719	218600	123050	142929	19879	20382.3	0.97
M4, d_{max} = 8 mm	13	1094.4	3121.7	4243.5	5126.8	5517.6	2005.1	2368.5	363.4	373.1	0.97
	19	3893.0	6773.7	11281.7	13975.8	15855.0	7202.1	8466.3	1264.2	1302.3	0.97
	25	9949.3	13586	23744	32010.1	35466.0	18424.1	21671.3	3247.2	3321.9	0.98
	38	64998	69669	140669	189919	216900	120250	141229	20979	21742.6	0.96

D.2. Permeability test results

Sample M1 with d_{max} = 1.19 mm (smallest column)										
Diameter		**(cm)**	**10.2**	**Length (*L*)**		**(cm)**	**6.5**	**Area**	**(cm^2)**	**81.67**
Piezometers reading			**Head**	**Gradient**	**Water volume**	**Time**	**Debit**	**Temp.**	**Permeability**	**Permeability at 20°c**
Test	h_1	h_2	Δh	i	V	t	q	θ	k_θ	K_{20}
			(h_1-h_2)	$\Delta h/L$			V/t		$q\times L/(A\times\Delta h)$	
	(cm)	(cm)	(cm)		(cm^3)	(sec)	(cm^3/s)	(°c)	(cm/s)	(cm/s)
	0.1	0.1	0.1	0.0001	1	0.1	0.001	0.1	0.01E	0.01E
1	89.3	87.95	1.35	0.21	17	162.5	0.10	25	0.0062	0.0056

2	89.7	88.3	1.4	0.22	17	158.3	0.11	25	0.0061	0.0055
3	90.2	88.6	1.6	0.25	17	137.1	0.12	25	0.0062	0.0056
4	91	89.2	1.8	0.28	17	123.7	0.14	25	0.0061	0.0055
5	91.7	89.7	2	0.31	17	109.5	0.16	25	0.0062	0.0056
6	92.4	90.1	2.3	0.35	17	95.7	0.18	25	0.0061	0.0055
7	93.4	91	2.4	0.37	17	92.0	0.18	25	0.0061	0.0055
Hydraulic conductivity at 20°c					K_{20}		0.01E		(cm/sec)	0.00554

Sample M2 with d_{max} = 2.36 mm (smallest column)										
Diameter	**(cm)**	**10.2**	**Length (*L*)**		**(cm)**	**6.5**	**Area**	**(cm^2)**	**81.67**	
Piezometers reading		**Head**	**Gradient**	**Water volume**	**Time**	**Debit**	**Temp.**	**Permeability**	**Permeability at 20°c**	
Test	h_1	h_2	Δh	i	V	t	q	θ	k_0	K_{20}
			(h_1-h_2)	$\Delta h/L$			V/t		$q\times L/(A\times\Delta h)$	
	(cm)	(cm)	(cm)		(cm^3)	(sec)	(cm^3/s)	(°c)	(cm/s)	(cm/s)
	0.1	0.1	0.1	0.0001	1	0.1	0.001	0.1	0.01E	0.01E
1	84.1	83	1.1	0.17	150	430.5	0.35	22.5	0.0252	0.0243
2	85	83.6	1.4	0.22	150	345.0	0.43	22	0.0247	0.0238
3	85.5	83.8	1.7	0.25	150	285.2	0.53	22	0.0246	0.0237
4	87.1	85.2	1.9	0.29	150	265	0.57	22	0.0237	0.0228
5	88.3	86.3	2	0.31	150	255.1	0.59	22	0.0234	0.0225
6	88.9	86.7	2.2	0.34	150	235.0	0.64	22	0.0231	0.0222
7	89.4	87.05	2.35	0.36	150	215.2	0.70	22.5	0.0236	0.0225
8	90	87.5	2.5	0.38	150	200.7	0.75	22.5	0.0238	0.0227
9	90.5	87.85	2.65	0.41	150	200.2	0.75	22.5	0.0225	0.0215
Hydraulic conductivity at 20°c					K_{20}		0.01E		(cm/sec)	0.0229

Sample M3 with d_{max} = 5 mm (smallest column)										
Diameter	**(cm)**	**10.2**	**Length (*L*)**		**(cm)**	**6.5**	**Area**	**(cm^2)**	**81.67**	
Piezometers reading		**Head**	**Gradient**	**Water volume**	**Time**	**Debit**	**Temp.**	**Permeability**	**Permeability at 20°c**	
Test	h_1	h_2	Δh	i	V	t	q	θ	k_0	K_{20}
			(h_1-h_2)	$\Delta h/L$			V/t		$q\times L/(A\times\Delta h)$	
	(cm)	(cm)	(cm)		(cm^3)	(sec)	(cm^3/s)	(°c)	(cm/s)	(cm/s)
	0.1	0.1	0.1	0.0001	1	0.1	0.001	0.1	0.01E	0.01E
1	80.5	79.5	1	0.15	110	125.13	0.88	24	0.0700	0.0646
2	81.05	80	1.05	0.16	110	114.4	0.96	25	0.0729	0.0658
3	82.5	81.3	1.2	0.18	110	100.3	1.10	25	0.0727	0.0656

4	84.4	82.7	1.7	0.23	110	75.6	1.46	25	0.0681	0.0615
5	86.1	84.2	1.9	0.29	110	70.1	1.57	25	0.0657	0.0593
6	86.7	84.7	2	0.31	110	63.95	1.72	25	0.0684	0.0618
7	87.9	85.7	2.2	0.34	110	55.86	1.97	25	0.0712	0.0643
8	88.9	86.4	2.5	0.38	110	49	2.24	25	0.0715	0.0641
9	89.8	87.2	2.6	0.40	110	45.73	2.41	25	0.0736	0.0665
Hydraulic conductivity at 20°c					K_{20}		0.01E		(cm/sec)	0.0637

Sample M4 with d_{max} = 8 mm (smallest column)										
Diameter		**(cm)**	**10.2**	**Length (*L*)**		**(cm)**	**6.5**	**Area**	**(cm^2)**	**81.67**
Piezometers reading			**Head**	**Gradient**	**Water volume**	**Time**	**Debit**	**Temp.**	**Permeability**	**Permeability at 20°c**
Test	h_1	h_2	**Δh**	i	V	t	q	θ	k_0	K_{20}
			(h_1-h_2)	$\Delta h/L$			V/t		$q\times L/(A\times\Delta h)$	
	(cm)	**(cm)**	**(cm)**		**(cm^3)**	**(sec)**	**(cm^3/s)**	**(°c)**	**(cm/s)**	**(cm/s)**
	0.1	**0.1**	**0.1**	**0.0001**	**1**	**0.1**	**0.001**	**0.1**	**0.01E**	**0.01E**
1	78.1	77.1	1	0.15	250	178.1	1.40	25.2	0.1117	0.1004
2	77.9	76.78	1.12	0.17	250	160	1.56	25.1	0.1110	0.1000
3	80.1	78.85	1.25	0.19	250	145.1	1.72	25.1	0.1097	0.0988
4	81	79.65	1.35	0.21	250	133.6	1.87	25.1	0.1103	0.0993
5	82.45	80.9	1.55	0.24	250	115.3	2.17	25	0.1113	0.1005
6	83.9	82.3	1.6	0.25	250	111.8	2.24	25	0.1112	0.0994
7	84.9	83	1.9	0.29	250	95.2	2.63	25	0.1100	0.0993
8	87	84.8	2.2	0.34	250	84	2.98	25.3	0.1077	0.0965
9	87.9	85.6	2.3	0.35	250	80.2	3.12	25.3	0.1079	0.0967
Hydraulic conductivity at 20°c					K_{20}		0.01E		(cm/sec)	0.0988

Sample M1 with d_{max} = 1.19 mm (small column)										
Diameter		**(cm)**	**15.1**	**Length (*L*)**		**(cm)**	**15.3**	**Area**	**(cm^2)**	**178.99**
Piezometers reading			**Head**	**Gradient**	**Water volume**	**Time**	**Debit**	**Temp.**	**Permeability**	**Permeability at 20°c**
Test	h_1	h_2	**Δh**	i	V	t	q	θ	k_0	K_{20}
			(h_1-h_2)	$\Delta h/L$			V/t		$q\times L/(A\times\Delta h)$	
	(cm)	**(cm)**	**(cm)**		**(cm^3)**	**(sec)**	**(cm^3/s)**	**(°c)**	**(cm/s)**	**(cm/s)**
	0.1	**0.1**	**0.1**	**0.0001**	**1**	**0.1**	**0.001**	**0.1**	**0.01E**	**0.01E**
1	90.5	87.35	3.15	0.21	17	87.0	0.20	21	0.0053	0.00522
2	91.5	87.95	3.55	0.23	17	76.0	0.22	21	0.0054	0.00530
3	92.2	88.3	3.9	0.25	17	69.9	0.24	21	0.0053	0.00524

4	92.8	88.6	4.2	0.27	17	65.0	0.26	21	0.0053	0.00524
5	93.9	89.2	4.7	0.31	17	59.7	0.28	21	0.0052	0.00509
6	94.8	89.7	5.1	0.33	17	55.0	0.31	21	0.0052	0.00510
7	95.5	90.1	5.4	0.35	17	52.0	0.33	21.5	0.0052	0.00504
Hydraulic conductivity at 20°c					K_{20}		0.01E		(cm/sec)	0.00517

Sample M2 with d_{max} = 2.36 mm (small column)										
Diameter	**(cm)**	**15.1**	**Length (*L*)**		**(cm)**	**15.3**	**Area**	**(cm^2)**	**178.99**	
Piezometers reading		**Head**	**Gradient**	**Water volume**	**Time**	**Debit**	**Temp.**	**Permeability**	**Permeability at 20°c**	
Test	h_1	h_2	**Δh**	i	V	t	q	θ	k_0	K_{20}
			(h_1-h_2)	$\Delta h/L$			V/t		$q\times L/(A\times\Delta h)$	
	(cm)	**(cm)**	**(cm)**		**(cm^3)**	**(sec)**	**(cm^3/s)**	**(°c)**	**(cm/s)**	**(cm/s)**
	0.1	**0.1**	**0.1**	**0.0001**	**1**	**0.1**	**0.001**	**0.1**	**0.01E**	**0.01E**
1	79.9	76.2	3.7	0.24	210	335.5	0.63	22.1	0.0145	0.0139
2	80.2	76.3	3.9	0.25	210	320.3	0.66	22.1	0.0144	0.0138
3	80.7	76.5	4.2	0.27	210	295.2	0.71	22	0.0145	0.0139
4	81.4	76.8	4.6	0.30	210	275.3	0.76	22	0.0142	0.0137
5	81.7	77	4.7	0.31	210	265.7	0.7904	22	0.0144	0.0138
6	82.9	77.9	5	0.33	210	248.1	0.85	22	0.0145	0.0139
7	83.5	78.3	5.2	0.34	210	240	0.88	21.9	0.0144	0.0139
8	84.2	78.7	5.5	0.36	210	230.1	0.91	21.9	0.0142	0.0137
9	84.6	78.9	5.7	0.37	210	225.3	0.93	21.9	0.0140	0.0135
10	84.6	78.8	5.8	0.38	210	217.2	0.97	21.9	0.0142	0.0138
Hydraulic conductivity at 20°c					K_{20}		0.01E		(cm/sec)	0.0138

Sample M3 with d_{max} = 5 mm (small column)										
Diameter	**(cm)**	**15.1**	**Length (*L*)**		**(cm)**	**15.3**	**Area**	**(cm^2)**	**178.99**	
Piezometers reading		**Head**	**Gradient**	**Water volume**	**Time**	**Debit**	**Temp.**	**Permeability**	**Permeability at 20°c**	
Test	h_1	h_2	**Δh**	i	V	t	q	θ	k_0	K_{20}
			(h_1-h_2)	$\Delta h/L$			V/t		$q\times L/(A\times\Delta h)$	
	(cm)	**(cm)**	**(cm)**		**(cm^3)**	**(sec)**	**(cm^3/s)**	**(°c)**	**(cm/s)**	**(cm/s)**
	0.1	**0.1**	**0.1**	**0.0001**	**1**	**0.1**	**0.001**	**0.1**	**0.01E**	**0.01E**
1	74.7	72.7	2.0	0.13	110	87.9	1.25	21.8	0.0535	0.0517
2	75.6	73.3	2.3	0.15	110	74	1.49	21.9	0.0552	0.0533
3	76.1	73.6	2.5	0.16	110	69.5	1.58	22.0	0.0541	0.0521
4	77.0	74.3	2.7	0.18	110	64.5	1.70	22.0	0.0540	0.0520
5	78.2	75.2	3.0	0.20	110	57.2	1.92	21.8	0.0548	0.0530

6	79.8	76.3	3.5	0.23	110	49.4	2.23	21.8	0.0544	0.0526
7	80.8	77.0	3.8	0.25	110	46.1	2.38	21.7	0.0536	0.0520
8	81.1	77.1	4	0.26	110	44.7	2.46	21.7	0.0526	0.0510
9	81.7	77.5	4.2	0.27	110	43.08	2.55	21.7	0.0520	0.0504
Hydraulic conductivity at 20°c					K_{20}		0.01E		(cm/sec)	0.0520

Sample M4 with d_{max} = 8 mm (small column)										
Diameter		**(cm)**	**15.1**	**Length (*L*)**		**(cm)**	**15.3**	**Area**	**(cm^2)**	**178.99**
Piezometers reading			**Head**	**Gradient**	**Water volume**	**Time**	**Debit**	**Temp.**	**Permeability**	**Permeability at 20°c**
Test	h_1	h_2	Δh	i	V	t	q	θ	k_0	K_{20}
			(h_1-h_2)	$\Delta h/L$			V/t		$q\times L/(A\times\Delta h)$	
	(cm)	(cm)	(cm)		(cm^3)	(sec)	(cm^3/s)	(°c)	(cm/s)	(cm/s)
	0.1	**0.1**	**0.1**	**0.0001**	**1**	**0.1**	**0.001**	**0.1**	**0.01E**	**0.01E**
1	112.9	110.6	2.3	0.15	210	75.26	2.79	25.4	0.1037	0.0928
2	114.8	112.4	2.4	0.16	210	69.73	3.01	25.4	0.1073	0.0959
3	116.95	114.1	2.85	0.19	210	61.55	3.41	25.4	0.1023	0.0915
4	118.45	115.2	3.25	0.21	210	53.95	3.89	25.4	0.1024	0.0916
5	123.35	119.8	3.55	0.23	210	49.23	4.27	25.4	0.1027	0.0919
6	125.0	121.2	3.8	0.25	210	46.48	4.52	25.4	0.1016	0.0909
7	127.3	123.0	4.3	0.28	210	41.0	5.1	25.4	0.1018	0.0910
8	130.5	125.4	5.1	0.33	210	36.1	5.8	25.4	0.0975	0.0872
9	133.9	128.4	5.5	0.36	210	33.3	6.3	25.4	0.0981	0.0877
Hydraulic conductivity at 20°c					K_{20}		0.01E		(cm/sec)	0.912

Sample M1 with d_{max} = 1.19 mm (medium column)										
Diameter		**(cm)**	**20.22**	**Length (*L*)**		**(cm)**	**8**	**Area**	**(cm^2)**	**320.95**
Piezometers reading			**Head**	**Gradient**	**Water volume**	**Time**	**Debit**	**Temp.**	**Permeability**	**Permeability at 20°c**
Test	h_1	h_2	Δh	i	V	t	q	θ	k_0	K_{20}
			(h_1-h_2)	$\Delta h/L$			V/t		$q\times L/(A\times\Delta h)$	
	(cm)	(cm)	(cm)		(cm^3)	(sec)	(cm^3/s)	(°c)	(cm/s)	(cm/s)
	0.1	**0.1**	**0.1**	**0.0001**	**1**	**0.1**	**0.001**	**0.1**	**0.01E**	**0.01E**
1	104.5	102.9	1.65	0.21	150	430.8	0.35	23.8	0.005261	0.004876
2	105.0	103.2	1.88	0.23	150	384.9	0.39	23.8	0.005167	0.004789
3	106.1	104.1	2	0.25	150	373.0	0.40	23.8	0.005012	0.004645
4	106.5	104.1	2.45	0.31	150	301.4	0.50	23.8	0.005063	0.004693
5	106.9	104.2	2.7	0.34	150	273.8	0.55	23.8	0.005058	0.004688
6	108.2	105.4	2.8	0.35	150	265.1	0.6	23.8	0.005037	0.004669

7	108.9	105.8	3.1	0.39	150	240.2	0.62	23.8	0.005021	0.004654
Hydraulic conductivity at 20°c					K_{20}		0.01E		(cm/sec)	0.00471

Sample M2 with d_{max} = 2.36 mm (medium column)										
Diameter		**(cm)**	**20.22**	**Length (*L*)**		**(cm)**	**8**	**Area**	**(cm^2)**	**320.95**
Piezometers reading			**Head**	**Gradient**	**Water volume**	**Time**	**Debit**	**Temp.**	**Permeability**	**Permeability at 20°c**
Test	h_1	h_2	Δh	i	V	t	q	θ	k_0	K_{20}
			(h_1-h_2)	$\Delta h/L$			V/t		$q\times L/(A\times\Delta h)$	
	(cm)	(cm)	(cm)		(cm^3)	(sec)	(cm^3/s)	(°c)	(cm/s)	(cm/s)
	0.1	**0.1**	**0.1**	**0.0001**	**1**	**0.1**	**0.001**	**0.1**	**0.01E**	**0.01E**
1	95.6	94.6	1.0	0.13	150	295.5	0.51	22.5	0.0119	0.0116
2	97.9	96.8	1.1	0.15	150	285.2	0.53	22.3	0.0112	0.0107
3	96.0	94.7	1.3	0.17	150	238.3	0.63	22.5	0.0113	0.0111
4	98.5	97.1	1.4	0.19	150	232.1	0.65	22.2	0.0108	0.0103
5	97.3	95.8	1.5	0.20	150	226.8	0.66	22.5	0.0103	0.0101
6	99.5	97.9	1.6	0.21	150	215.1	0.70	22.1	0.0102	0.0098
7	100.6	99.0	1.6	0.22	150	210.8	0.71	22.1	0.0101	0.0097
8	101.3	99.4	1.9	0.25	150	196.6	0.76	22.1	0.0094	0.0090
9	102.5	100.3	2.2	0.31	150	160.2	0.94	22.0	0.0099	0.0096
10	103.5	101.0	2.5	0.34	150	144.1	1.04	21.9	0.0097	0.0094
11	104.7	102.0	2.7	0.36	150	138.4	1.08	21.8	0.0094	0.0090
Hydraulic conductivity at 20°c					K_{20}		0.01E		(cm/sec)	0.0094

Sample M3 with d_{max} = 5 mm (medium colonne)										
Diameter		**(cm)**	**20.22**	**Length (*L*)**		**(cm)**	**8**	**Area**	**(cm^2)**	**320.95**
Piezometers reading			**Head**	**Gradient**	**Water volume**	**Time**	**Debit**	**Temp.**	**Permeability**	**Permeability at 20°c**
Test	h_1	h_2	Δh	i	V	t	q	θ	k_0	K_{20}
			(h_1-h_2)	$\Delta h/L$			V/t		$q\times L/(A\times\Delta h)$	
	(cm)	(cm)	(cm)		(cm^3)	(sec)	(cm^3/s)	(°c)	(cm/s)	(cm/s)
	0.1	**0.1**	**0.1**	**0.0001**	**1**	**0.1**	**0.001**	**0.1**	**0.01E**	**0.01E**
1	69.6	68.7	0.9	0.11	150	97.1	1.54	23.5	0.0435	0.0406
2	70.5	69.5	1.0	0.13	150	83.6	1.79	23.5	0.0438	0.0409
3	71.9	70.7	1.2	0.15	150	72.2	2.08	23.5	0.0435	0.0406
4	72.0	70.7	1.3	0.16	150	67.5	2.22	23.5	0.0429	0.0401
5	72.4	71.0	1.4	0.18	150	60.9	2.47	23.5	0.0439	0.0409
6	74.3	72.5	1.8	0.23	150	48.9	3.07	23.5	0.0425	0.0396
7	76.9	74.9	2.0	0.25	150	44.0	3.41	23.5	0.0425	0.0396

8	78.0	75.7	2.3	0.28	150	39.1	3.84	23.5	0.0425	0.0397
9	80.7	78.2	2.5	0.31	150	35.0	4.29	23.5	0.0427	0.0399
Hydraulic conductivity at 20°c					K_{20}		0.01E		(cm/sec)	0.0402

Sample M4 with d_{max} = 8 mm (medium column)										
Diameter	**(cm)**		**20.22**	**Length (*L*)**		**(cm)**	**8**	**Area**	**(cm^2)**	**320.95**
Piezometers reading			**Head**	**Gradient**	**Water volume**	**Time**	**Debit**	**Temp.**	**Permeability**	**Permeability at 20°c**
Test	h_1	h_2	Δh	i	V	t	q	θ	k_0	K_{20}
			(h_1-h_2)	$\Delta h/L$			V/t		$q\times L/(A\times\Delta h)$	
	(cm)	(cm)	(cm)		(cm^3)	(sec)	(cm^3/s)	(°c)	(cm/s)	(cm/s)
	0.1	0.1	0.1	0.0001	1	0.1	0.001	0.1	0.01E	0.01E
1	90.8	90.0	0.8	0.10	150	53.2	2.82	21.3	0.0879	0.0859
2	92.6	91.7	0.9	0.11	150	47.8	3.14	21.1	0.0869	0.0853
3	95.6	94.6	1.1	0.13	150	41.0	3.66	21.1	0.0869	0.0853
4	97.8	96.6	1.2	0.15	150	35.75	4.20	21.1	0.0872	0.0856
5	101.3	99.9	1.4	0.17	150	31.1	4.83	21.1	0.0860	0.0844
6	103.6	102.0	1.6	0.19	150	28.6	5.25	20.8	0.0845	0.0834
7	106.5	104.8	1.7	0.21	150	26.0	5.78	20.8	0.0847	0.0837
8	108.9	106.9	2.0	0.25	150	22.2	6.76	20.8	0.0842	0.0832
9	112.4	110.3	2.1	0.26	150	21.0	7.16	20.8	0.0850	0.0839
Hydraulic conductivity at 20°c					K_{20}		0.01E		(cm/sec)	0.0845

Sample M1 with d_{max} = 1.19 mm (large column)										
Diameter	**(cm)**		**30**	**Length (*L*)**		**(cm)**	**30**	**Area**	**(cm^2)**	**706.50**
Piezometers reading			**Head**	**Gradient**	**Water volume**	**Time**	**Debit**	**Temp.**	**Permeability**	**Permeability at 20°c**
Test	h_1	h_2	Δh	i	V	t	q	θ	k_0	K_{20}
			(h_1-h_2)	$\Delta h/L$			V/t		$q\times L/(A\times\Delta h)$	
	(cm)	(cm)	(cm)		(cm^3)	(sec)	(cm^3/s)	(°c)	(cm/s)	(cm/s)
	0.1	0.1	0.1	0.0001	1	0.1	0.001	0.1	0.01E	0.01E
1	117.5	111.3	6.2	0.21	150	223.0	0.67	21.1	0.004607	0.004522
2	118.9	111.8	7.1	0.24	150	198.0	0.76	21.1	0.004531	0.004448
3	119.5	112.1	7.4	0.25	150	188.0	0.80	21.1	0.004578	0.004494
4	120.5	112.2	8.3	0.28	150	173.0	0.87	21.1	0.004436	0.004355
5	120.8	112	8.8	0.29	150	160.0	0.94	21.7	0.004524	0.004386
6	121.6	112.3	9.3	0.31	150	153.0	0.98	21.7	0.004476	0.004340
7	122.8	113	9.8	0.33	150	145.0	1.03	21.7	0.004482	0.004346
8	124	113.5	10.5	0.35	150	137.0	1.09	21.7	0.004428	0.004293

Hydraulic conductivity at 20°c	K_{20}	0.01E	(cm/sec)	0.0044

Sample M2 with d_{max} = 2.36 mm (large column)										
Diameter		**(cm)**	**30**	**Length (*L*)**		**(cm)**	**30**	**Area**	**(cm^2)**	**706.50**
Piezometers reading			**Head**	**Gradient**	**Water volume**	**Time**	**Debit**	**Temp.**	**Permeability**	**Permeability at 20°c**
Test	h_1	h_2	**Δh**	i	V	t	q	θ	k_0	K_{20}
			(h_1-h_2)	$\Delta h/L$			V/t		$q\times L/(A\times\Delta h)$	
	(cm)	**(cm)**	**(cm)**		**(cm^3)**	**(sec)**	**(cm^3/s)**	**(°c)**	**(cm/s)**	**(cm/s)**
	0.1	**0.1**	**0.1**	**0.0001**	**1**	**0.1**	**0.001**	**0.1**	**0.01E**	**0.01E**
1	52.4	48.3	4.1	0.14	250	225.6	1.11	23.8	0.0115	0.0106
2	53.9	49.45	4.45	0.15	250	220.6	1.13	23.8	0.0108	0.0100
3	54.9	49.9	5	0.17	250	228.5	1.09	23.8	0.0093	0.0086
4	56.1	50.4	5.7	0.19	250	211.6	1.18	23.8	0.0088	0.0082
5	57.5	50.95	6.55	0.22	250	198.1	1.26	23.8	0.0082	0.0076
6	59.4	51.8	7.6	0.25	250	175.0	1.43	23.8	0.0080	0.0074
7	61	52.5	8.5	0.28	250	177.2	1.41	23.8	0.0070	0.0065
8	63.2	53.8	9.4	0.31	250	169.3	1.48	23.8	0.0067	0.0062
9	64.8	54.6	10.2	0.34	250	163.5	1.53	23.9	0.0064	0.0059
10	66.5	55.1	11.4	0.38	250	147.0	1.70	23.9	0.0063	0.0059
Hydraulic conductivity at 20°c					K_{20}		0.01E		(cm/sec)	0.0088

Sample M3 with d_{max} = 5 mm (large column)										
Diameter		**(cm)**	**30**	**Length (*L*)**		**(cm)**	**30**	**Area**	**(cm^2)**	**706.50**
Piezometers reading			**Head**	**Gradient**	**Water volume**	**Time**	**Debit**	**Temp.**	**Permeability**	**Permeability at 20°c**
Test	h_1	h_2	**Δh**	i	V	t	q	θ	k_0	K_{20}
			(h_1-h_2)	$\Delta h/L$			V/t		$q\times L/(A\times\Delta h)$	
	(cm)	**(cm)**	**(cm)**		**(cm^3)**	**(sec)**	**(cm^3/s)**	**(°c)**	**(cm/s)**	**(cm/s)**
	0.1	**0.1**	**0.1**	**0.0001**	**1**	**0.1**	**0.001**	**0.1**	**0.01E**	**0.01E**
1	99.2	95	4.2	0.14	250	76.2	3.28	21	0.0332	0.0326
2	99.9	95.5	4.4	0.15	250	71.9	3.48	21	0.0336	0.0330
3	100.6	95.9	4.7	0.16	250	67.6	3.70	21	0.0334	0.0329
4	101.5	96.4	5.1	0.17	250	64.3	3.89	21	0.0324	0.0318
5	102.6	97.1	5.5	0.18	250	59.0	4.24	21	0.0327	0.0322
6	103.3	97.4	5.9	0.20	250	55.0	4.55	21.5	0.0327	0.0318
7	104.5	98	6.5	0.22	250	50.0	5.00	21.5	0.0327	0.0318
8	105.5	98.6	6.9	0.23	250	47.0	5.32	21.9	0.0327	0.0319
Hydraulic conductivity at 20°c					K_{20}		0.01E		(cm/sec)	0.0323

Sample M4 with d_{max} = 8 mm (large column)										
Diameter		**(cm)**	**30**	**Length (*L*)**		**(cm)**	**30**	**Area**	**(cm^2)**	**706.50**
Piezometers reading			**Head**	**Gradient**	**Water volume**	**Time**	**Debit**	**Temp.**	**Permeability**	**Permeability at 20°c**
Test	h_1	h_2	**∆h**	i	V	t	q	θ	k_θ	K_{20}
			(h_1-h_2)	$\Delta h/L$			V/t		$q\times L/(A\times\Delta h)$	
	(cm)	**(cm)**	**(cm)**		**(cm^3)**	**(sec)**	**(cm^3/s)**	**(°c)**	**(cm/s)**	**(cm/s)**
	0.1	**0.1**	**0.1**	**0.0001**	**1**	**0.1**	**0.001**	**0.1**	**0.01E**	**0.01E**
1	98.5	94.3	4.2	0.14	400	55.1	7.26	23.5	0.0734	0.0685
2	99.5	95	4.5	0.15	400	52.0	7.69	23.5	0.0726	0.0677
3	100.2	95.5	4.7	0.16	400	49.3	8.11	23.5	0.0733	0.0684
4	100.9	95.9	5	0.17	400	46.2	8.66	23.5	0.0735	0.0686
5	101.8	96.4	5.4	0.18	400	43.0	9.30	23.5	0.0731	0.0682
6	102.9	97.1	5.8	0.19	400	39.4	10.15	24	0.0743	0.0686
7	103.6	97.4	6.2	0.21	400	37.2	10.75	24	0.0736	0.0680
8	105.4	98	7.4	0.25	400	31.1	12.88	24	0.0739	0.0682
Hydraulic conductivity at 20°c					K_{20}		0.01E		(cm/sec)	0.0683